Updates in Surgery

Giuseppe Spinoglio *Editor*

Robotic Surgery

Current Applications and New Trends

In collaboration with
Alessandra Marano
Giampaolo Formisano

Springer

Updates in Surgery

Giuseppe Spinoglio
Editor

Robotic Surgery

Current Applications and New Trends

In collaboration with
Alessandra Marano and Giampaolo Formisano

Forewords by
Giorgio De Toma
Francesco Corcione

Springer

Editor
Giuseppe Spinoglio
Department of General and Oncologic Surgery
"SS. Antonio e Biagio" Hospital
Alessandria, Italy

In collaboration with
Alessandra Marano and Giampaolo Formisano

The publication and the distribution of this volume have been supported by the Italian Society of Surgery

ISSN 2280-9848
ISBN 978-88-470-5713-5 ISBN 978-88-470-5714-2 (eBook)

DOI 10.1007/978-88-470-5714-2

Springer Milan Dordrecht Heidelberg London New York

Library of Congress Control Number: 2014950061

Cover design: eStudio Calamar S.L.
Typesetting: Graphostudio, Milan, Italy

Springer-Verlag Italia S.r.l. – Via Decembrio 28 – I-20137 Milan
Springer is a part of Springer Science+Business Media (www.springer.com)

To Lorenzo Capussotti
An honest man
Master of surgery
Unforgotten friend

Foreword

The symbol of technical evolution, in the last few years, in general surgery is undoubtedly robotic-assisted surgery. The introduction of this technique goes back a decade and as usually happens with advanced technologies, enormous steps forward have been made in the development of devices and equipment that is increasingly sophisticated and of reduced dimensions. A very significant impetus has been given to this kind of surgery by Prof. Giuseppe Spinoglio, who recently had the honor of being elected to the position of President to the *Clinical Robotic Surgery Association* in Chicago, a surgical society that is a key player of this specific branch, and so is forward looking and of relevance.

The hospital in which Prof. Spinoglio is Head of Department has become an internationally renowned point of reference for robotics in surgery, where all kinds of general surgery interventions are practiced, that can be treated through a minimally invasive approach. To Prof. Spinoglio's further credit is the energy devoted to create a European Training Center to inform and train younger surgeons in this particular type of surgery. This present text has been carefully edited by him and will certainly have an undeniable worth for Italian surgeons and will be of great didactic value for the youngest amongst them.

Rome, September 2014

Giorgio De Toma
President, Italian Society of Surgery

Foreword

Throughout the ages, there have always been men gifted with visions that in time proved to almost be foresight. By way of example, at the end of the 15th century, Da Vinci had already imagined the helicopter and the parachute among other inventions, and Jules Verne conceived the submarine decades before the first model was built.

Keeping the above in mind, what happened much more swiftly in the world of surgery under our own eyes, is without comparison. If someone had told me 25 years ago (not 250) that I would have been performing surgical interventions, even challenging ones, by introducing a thin tube into an abdominal cavity filled with CO_2 while watching operations on a screen, I would have been flabbergasted. And if someone had predicted I would even be able to one day operate on a patient remotely, and follow each step of the intervention in full 3D HD on a flat screen, while maneuvering sophisticated instruments that are as articulate as a human hand, I would have taken the speaker as mad. Nevertheless all this proved to be true, and in a short time span of 25 years! It may thus easily be understood that the surgeon relies increasingly on technology, to the point of being dependent of it. Robotic-assisted surgery is the latest and most demanding technological development in the operating room and, leaving aside all considerations arising from correct surgical indications and the still critical cost-benefit analysis, it surely represents a possibility of improvement that surgeons cannot disregard.

Even robotics evolves at a stunning pace, almost on a daily basis: after the older robots that were made available 15 years ago, nowadays devices are incredibly more practical and efficient. Further mention could be made of the monotrocar, surgical sealants and dissection devices, robotic suturing, imaging systems for lymphatic and vascular diagnosis and intervention, and many others.

All this should be a cause for reflection from the clinical and scientific point of view, before Isaac Asimov's dream can come true in the surgical sphere as well: "A robot may not injure a human being, or, through inaction, allow one to come to harm…"

I am thus very pleased to introduce this work that has very rightly been assigned to a friend and colleague Giuseppe Spinoglio, one of the Italian surgeons most devoted and committed in this specific field of surgery in recent years, acquiring an undisputed and internationally renowned competence.

To be aware of the latest technological innovations in robotics, to know the correct related clinical applications, how the new devices work and to be informed of all associated issues is an important function of professional growth that should not be missed, and reading this monograph will certainly enrich our knowledge and supply a most welcome update on one of the most revolutionary aspects of modern surgery.

Naples, September 2014

Francesco Corcione
Department of Laparoscopic and Robotic Surgery
"Azienda Ospedaliera dei Colli" - Monaldi Hospital
Naples, Italy

Preface

Robotics entered the lives of humans more than fifty years ago, with the technology being applied to engine construction.

In medicine, the use of robotics was established in the early 2000s with the dissemination of the outcomes of the nerve-sparing prostatectomy for cancer. In urology, and later in gynecology, robotics has achieved an immediate and favorable response and subsequent widespread usage. On the other hand, in general surgery its application was limited initially to procedures with a high degree of difficulty that could especially benefit from the advantages of the robotic suturing. Only at the end of the first decade of the 2000s, was robotics continuously applied to colorectal and digestive surgery, especially by Korean and Italian surgeons.

The da Vinci® System of Intuitive Surgical Inc. is the only robotic platform existing today and has undergone several evolutions from 1998 to present: standard three and four-arm, S™ HD, Si™ HD (including Si™ -e) and the newest Xi™ .

The complex nature of the setup of the first models and the feature of working in fixed and narrow surgical fields has hampered its routine use in general surgery. Indeed, while its users consider the robotic system as a revolutionary innovation, the opponents emphasize costs, time-consuming procedures and the lack of clinical evidence when compared to laparoscopy. Many of the issues related to the robotic setup and its time-spending applications have been overcome by the technical characteristics of the new models and by the standardization of surgical procedures, similar to what happened to surgery after the pioneering phase.

Regarding robotic benefits, three different types of problems can be identified:

1. Robotics has been applied to general surgery for little more than five years and for less time with a standardized technique: randomized clinical trials with adequate follow-up providing sound data are expected to be available in approximately ten years, as occurred with the CLASSIC and COLOR studies for oncological outcomes.
2. About 3,000 da Vinci® systems of different generations are currently installed worldwide and less than 2,000 are applied in general surgery for different procedures: in such conditions, it is difficult to collect a large enough sample to be compared with single laparoscopic procedures. Comparative studies on

short-term outcomes have been published to date but they have been performed on small series.

3. In robotic surgery, as occurred with other approaches, there is a learning curve. The number of robotic-experienced surgeons is a small percentage of those who have decided to implement it: this specific issue makes it hard to recruit homogeneous centers involved in studies (the same surgeon may be very experienced in laparoscopic techniques but not in robotic ones).
   Nevertheless, the following main issues need to be underlined:
   - To date, robotics technology has advantages over other present techniques that are absolutely clear. Its superiority over an action performed manually results mainly in the 3DHD vision, up to 10× magnification, the EndoWrist® instruments with seven degrees of freedom and the intuitive motion.
   - In every part of the world, surgeons who had the patience and perseverance to overcome the learning curve have not abandoned robotic surgery.
   - Surgeons who are not convinced of the advantages of robotic surgery are sticking to their opinion, as for the reasons mentioned above, these benefits cannot be demonstrated as yet.

The purpose of this book is to spread the robotic surgical technique for standardized procedures with the most recent updates. Since Italian surgeons were among the pioneers of this surgery, I had the pleasure of hosting in this volume both experiences of the finest ones and those of surgeons who have spread robotics abroad (i.e. Profs. Enrico Benedetti, Pier Cristoforo Giulianotti and Alessio Pigazzi). I sincerely thank President Giorgio De Toma and all SIC's Board for entrusting me with the lecture at the 116th SIC Congress and the subsequent writing of this book, with a focus on innovation, even when it is still questioned. Finally, I would like to thank my assistants for their sound collaboration, mainly Alessandra Marano and Giampaolo Formisano: without them, this book would never have been completed.

Alessandria, September 2014 Giuseppe Spinoglio

Contents

Acknowledgements

The volume editor and the publisher gratefully acknowledge the educational contribution offered by ab medica S.p.A., and wish to thank Intuitive Surgical®, Inc., for granting permission for the use of operating room setup and trocar lay-out images.

Contributors

Stefano Amore Bonapasta General Surgery Unit, "Misericordia" Hospital, Grosseto, Italy

Mario Annecchiarico Department of Oncology, Division of Oncological and Robotic General Surgery, Careggi University Hospital, Florence, Italy

Andrea Avanzolini General, Gastrointestinal, and Minimally Invasive Surgery Unit, "G.B. Morgagni – L. Pierantoni" Hospital, Forlì, Italy

Francesca Bazzocchi General, Gastrointestinal, and Minimally Invasive Surgery Unit, "G.B. Morgagni – L. Pierantoni" Hospital, Forlì, Italy

Enrico Benedetti Department of Surgery, Division of Transplantation, University of Illinois Hospital and Health Sciences System, Chicago, IL, USA

Paolo Pietro Bianchi Minimally Invasive Surgery Unit, European Institute of Oncology, Milan, Italy

Francesco Mario Bianco Division of General, Minimally Invasive and Robotic Surgery, University of Illinois, Chicago, IL, USA

Vivek Bindal Division of General, Minimally Invasive and Robotic Surgery, University of Illinois, Chicago, IL, USA

Raul M. Bosio Department of Surgery, University of California Irvine, Irvine, CA, USA

Luciano Casciola Minimally Invasive Surgery Unit, Casa di Cura Città di Roma, Rome, Italy

Graziano Ceccarelli Department of Surgery, Division of General Surgery, "San Francesco" Hospital, Nuoro, Italy

Giovanni Colli General Surgery Unit, "Sant'Agostino-Estense" New Hospital, Baggiovara (MO), Italy

Andrea Coratti Department of Oncology, Division of Oncological and Robotic General Surgery, Careggi University Hospital, Florence, Italy

Despoina Daskalaki Division of General, Minimally Invasive and Robotic Surgery, University of Illinois, Chicago, IL, USA

Timothy F. Feldmann Department of Surgery, University of California Irvine, Irvine, CA, USA

Giampaolo Formisano Department of General and Oncologic Surgery, "SS. Antonio e Biagio" Hospital, Alessandria, Italy

Marzio Frazzoni General Surgery Unit, "Sant'Agostino-Estense" New Hospital, Baggiovara (MO), Italy

Domenico Garcea General, Gastrointestinal, and Minimally Invasive Surgery Unit, "G.B. Morgagni – L. Pierantoni" Hospital, Forlì, Italy

Raquel Garcia-Roca Department of Surgery, Division of Transplantation, University of Illinois Hospital and Health Sciences System, Chicago, IL, USA

Pier Cristoforo Giulianotti Division of General, Minimally Invasive and Robotic Surgery, University of Illinois, Chicago, IL, USA

Davide Gozzo General Surgery Unit, "Sant'Agostino-Estense" New Hospital, Baggiovara (MO), Italy

Hoonbaen Jeon Department of Surgery, Division of Transplantation, University of Illinois Hospital and Health Sciences System, Chicago, IL, USA

Luca Matteo Lenti Department of General and Oncologic Surgery, "SS. Antonio e Biagio" Hospital, Alessandria, Italy

Alessandra Marano Department of General and Oncologic Surgery, "SS. Antonio e Biagio" Hospital, Alessandria, Italy

Fabio Melandro Department of General and Oncologic Surgery, "SS. Antonio e Biagio" Hospital, Alessandria, Italy

Gianluigi Melotti General Surgery Unit, "Sant'Agostino-Estense" New Hospital, Baggiovara (MO), Italy

Igor Monsellato Minimally Invasive Surgery Unit, European Institute of Oncology, Milan, Italy

Barbara Mullineris General Surgery Unit, "Sant'Agostino-Estense" New Hospital, Baggiovara (MO), Italy

Casimiro Nigro Department of Surgery, Tor Vergata University, Rome, Italy

Jose Oberholzer Department of Surgery, Division of Transplantation, University of Illinois Hospital and Health Sciences System, Chicago, IL, USA

Francesca Pagliardi Department of General and Oncologic Surgery, "SS. Antonio e Biagio" Hospital, Alessandria, Italy

Alberto Patriti Department of Surgery, Division of General, Minimally Invasive and Robotic Surgery, "San Matteo degli Infermi" Hospital, Spoleto (PG), Italy

Wanda Petz Minimally Invasive Surgery Unit, European Institute of Oncology, Milan, Italy

Micaela Piccoli General Surgery Unit, "Sant'Agostino-Estense" New Hospital, Baggiovara (MO), Italy

Alessio Pigazzi Department of Surgery, University of California Irvine, Irvine, CA, USA

Fabio Priora Department of General and Oncologic Surgery, "SS. Antonio e Biagio" Hospital, Alessandria, Italy

Ferruccio Ravazzoni Department of General and Oncologic Surgery, "SS. Antonio e Biagio" Hospital, Alessandria, Italy

Nazareno Smerieri General Surgery Unit, "Sant'Agostino-Estense" New Hospital, Baggiovara (MO), Italy

Giuseppe Spinoglio Department of General and Oncologic Surgery, "SS. Antonio e Biagio" Hospital, Alessandria, Italy

Vincenzo Trapani General Surgery Unit, "Sant'Agostino-Estense" New Hospital, Baggiovara (MO), Italy

Ivo Tzvetanov Department of Surgery, Division of Transplantation, University of Illinois Hospital and Health Sciences System, Chicago, IL, USA

Richard van Hillegersberg Department of Surgery, University Medical Center, Utrecht, The Netherlands

Michele Varoli General Surgery Unit, "Sant'Agostino-Estense" New Hospital, Baggiovara (MO), Italy

Giulia Veronesi Division of Thoracic Surgery, European Institute of Oncology, Milan, Italy

History of Robotic Surgery

1

Giuseppe Spinoglio, Alessandra Marano, Fabio Priora, Fabio Melandro, and Giampaolo Formisano

1.1 Introduction

The history of telerobotic surgery involves a revolutionary approach to minimally-invasive surgery. The concept of "telemanipulation" or "telepresence" emerged in the 1940s and was first used to describe the sensation that a person is in one location while being in another. It was driven by the need for certain complex tasks to be performed by machines in hazardous and unhealthy environment for human beings, such as the bottom of the ocean or in outer space. In Robert Heinlein's 1942 science fiction, entitled "Waldo", the lead character, Waldo Farthingwaite-Jones, was born frail and unable to lift his own body weight. Heilnlein describes a glove and harness device that allowed Waldo to control a powerful mechanical arm by simply moving his hand and fingers.

About eight or nine years after the abovementioned publication, these kinds of remote manipulators – popularly known as "Waldoes" – were developed in the real world by Raymond Goertz, an early pioneer in the field of robotics.

His first master/slave robotic arm was used to handle radioactive material while working for the Atomic Energy Commission at Argonne National Laboratory. However, significant progress in telepresence and robotic activity was only achieved in the 1980s because of major advancements in microelectronics and computing.

At the same time, we were seeing significant advancement in the surgical field. The first laparoscopy (minimally invasive surgery) was also being conducted. Specifically, an endoscope-like device was developed and the emergence of the charge coupled device (CCD) – needed for digital imaging, video electronics and display technologies – began to revolutionize the field of sur-

G. Spinoglio (✉)
Department of General and Oncologic Surgery, "Ss. Antonio e Biagio" Hospital, Alessandria, Italy
e-mail: giuseppe.spinoglio@gmail.com

G. Spinoglio (Ed), *Robotic Surgery: Current Applications and New Trends*, Updates in Surgery
DOI: 10.1007/978-88-470-5714-2_1,

gery and led to laparoscopic techniques for minimally invasive surgery. This culmination of technological advancements led to the first laparoscopic appendectomy by German gynaecologist Dr. Kurt Semm [1] and to the first reported laparoscopic cholecystectomy in 1987 by French surgeon Dr. Philippe Mouret [2]; actually, the first laparoscopic cholecystectomy was performed in 1985 by German surgeon Erich Mühe [3].

Soon after these landmark operations, laparoscopic technology and techniques continued to gain popularity into the 1990s. However, the tools being used for manual laparoscopy only worked well for relatively simple surgical procedures that involved the removal of tissue and basic tissue closure. Sophisticated mechanisms, such as staplers and other tissue closure devices were developed but still did not allow laparoscopic techniques to gain traction in more complex surgical procedures.

Though, in the strict sense of the word, the robotic systems developed for surgical applications are not actually "robots" but remote "performers" that work using the master-slave style, robotic telepresence was beginning to flourish at the same time laparoscopy was experiencing limitations. Many institutions recognized a potential opportunity to blend minimally invasive surgery (MIS) with robotics to overcome the limitations of laparoscopic surgery. The goal was to make MIS an option for even complex procedures with help from computers and mechanics.

The first robot-assisted surgical procedure was performed in 1983 with the use of "Arthrobot", which was designed to assist in orthopedic procedures. Later on, a transurethral resection of the prostate and standard prostatectomy were carried out in London with the PUMA (Programmable Universal Machine for Assembly) and the SARP (Surgeon-Assistant Robot for Prostatectomy) systems, respectively. Further development on SARP led to the creation of PROBOT, URobot and SPUD, which are abbreviation for "Prostate Robot", "Urology Robot" and "Surgeon Programmable Urological Device", respectively [4–6].

The first application of robotics in abdominal surgery dates back to 1993, when Yulin Wang succeeded in developing the first FDA-approved robotic device for use in general surgery. The system, Automated Endoscopic System for Optimal Positioning (AESOP) [7], consisted of a table-mounted articulating arm that was used to control the movements of the camera during laparoscopic surgery. Originally the AESOP was manipulated by hand or foot controls, but the later version was capable of utilizing voice commands and incorporated voice control of the endoscope and OR room lights.

The introduction in 2001 of the ZEUS system (Computer Motion Inc.) represented the real step towards the modern concept of robotically-assisted laparoscopic surgery. This platform allowed the surgeon to control a robotic slave device that was docked to the patient remotely from a console.

The ZEUS robotic system had a camera arm that was voice controlled (AESOP System), along with two other operating arms that provided four degrees of freedom and were able to hold a variety of instruments that were telemanipulated with joysticks from the surgical console. The software that inter-

faced the surgeon console with the robotic arms allowed tremor filtration and motion scaling by a factor of 2–10. The surgical field was visualized through a regular two-dimensional screen or through polarized glasses that allowed for three-dimensional images. This system was used for the first time in a full laparoscopic procedure for fallopian tube anastomosis at the Cleveland Clinic in 1998 [8] and for coronary bypass by Reichenspurner in 1999 [9].

In 2001, Jacques Marescaux utilized the ZEUS system to perform a robot-assisted cholecystectomy on a patient in Strasbourg, France, who was 4000 km away from the surgeon in New York [10]. This procedure, nicknamed "Operation Lindbergh", gave an impressive demonstration of telepresence in surgery.

In almost a parallel path, another group of researchers in California set about to develop a surgical robotic system for civilian use and founded Intuitive Surgical International in 1995: this group was eventually able to develop the first FDA-approved fully robotic system for application in laparoscopic surgery with licensed technologies from MIT, IBM and SRI International.

1.2 Da Vinci® Surgical System

1.2.1 Introduction

The design of the da Vinci® is the result of a long developmental process which integrated many ideas and technologies to produce an intuitive and functional surgical platform. The original project of the US Department of Defense was started with the aim of providing injured soldiers with a frontline surgical suite controlled by surgeons operating from a safe remote location. Although impractical at the time, the ultimate goal of the surgical platform was to produce a reliable system which would deliver the benefits of minimally invasive surgery to patients while preserving the benefits of the open approach to surgeons. The technology specifically aimed to address port-access limitations in dexterity, intuitiveness, visualization and ergonomics through advances in telepresence, telemanipulation and stereoscopic capture.

Animal trials started in 1996 and clearly demonstrated the promise of seven-degrees-of-freedom manipulators as well as the need for a mobile patient-side cart. The next major innovation was called "Mona" and featured exchangeable sterile components, which allowed human trial to proceed in 1997. In December 1998, the first commercial version of the da Vinci® system was delivered to the Leipzig University Heart Center in Germany.

Refinement of the original da Vinci® design continued with the addition of a fourth arm and with the expansion of instrument families.

The da Vinci® S™ and da Vinci® Si™ (released in 2009, Fig. 1.1) represent an evolution of the first generation system and are currently available on the market. Nowadays, moreover, access to the latest da Vinci® technology and future innovation is available in an upgradable three-arm configuration: the da Vinci®

Fig. 1.1 da Vinci® Si™ Surgical Platform. (© 2014 Intuitive Surgical, Inc.)

Fig. 1.2 da Vinci® Xi™ Surgical Platform. (© 2014 Intuitive Surgical, Inc.)

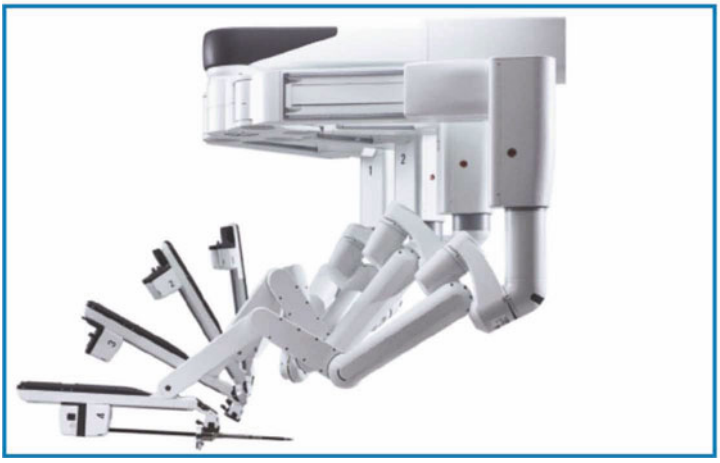

Fig. 1.3 da Vinci® Xi™ boom-mounted arms. (© 2014 Intuitive Surgical, Inc.)

Si-e™ System has been designed to deliver da Vinci® core functionality, providing a flexible and economical solution for many robotic-assisted procedures.

The latest product interaction is the fourth generation of the da Vinci® system (Xi™, Fig. 1.2, 1.3), which features improvements to the vision, control system and functionality.

1.2.2 Da Vinci® System Overview

The da Vinci® system is designed to represent the natural extension of the surgeon's eyes and hands and its motion capabilities are intended to mimic those of its human operator, as in open surgery.
The shared core technology of all systems offers the following distinguished features:

- physical separation of the surgeon from the patient by operating at an ergonomic console rather than at the patient's side, with less fatigue;
- EndoWrist® technology: robotic instruments provide seven degrees of freedom with intuitive control (compared with five degrees of freedom for standard laparoscopic instruments), which replicates the experience of open surgery by preserving natural eye-hand-instrument alignment (in contrast with standard laparoscopy);
- three-dimensional stereoscopic HD images with magnification (up to 10x);
- complete tremor filtering and motion scaling.

All systems consist of three main components: the surgical console, the patient cart and the vision cart.

The **surgical console** is the workplace of the robotic surgeon and contains the following core elements: master controllers, stereo viewer, touchpad for system configuration, left-side pod for ergonomic controls, right side pod for power and emergency stop, and a foot-switch for operative mode selection and energy devices activation.

The masters are built essentially like a human arm, with a wrist portion and the elbow/shoulder joints for positioning: the wrist portion moves the instrument tip in the surgical field, while the more proximal joints orient the instrument to the desired location. The master controllers also possess finger clutches, which decouple the joystick from the control of the corresponding instrument to allow for ergonomic repositioning during surgery.

The stereoviewer provides the 3D image of the operative field to the surgeon, including extended instruments and system information. The touchpad is the main control interface for system functions: it provides system status, instrument arm selection and control selections.

The **patient cart** has the primary function to support the operative arms and the camera arm. It contains five main components: the setup joints, instrument arms, camera arm, EndoWrist® instruments and an endoscope.

The setup joints enable movements of the instrument and camera arm to position them for sterile draping by the scrub nurse and docking of the system to the patient by the bedside assistant after trocar placement and correct table positioning according to the procedure. Clutch buttons are used by the assistant to free the setup joints, both for cart docking and arm repositioning, if needed, during the procedure. To ensure patient safety, any actions of the patient-side assistant should always preclude the telepresence of the robotic surgeon.

EndoWrist® instruments are installed onto the instrument arms after the

patient cart is docked. Most instruments are capable of seven degrees of freedom and about 90° of articulation in the wrist (distal) joint. Many different instruments and energy devices (monopolar, bipolar, ultrasonic, radiofrequency) are available with a diameter of 8 mm. A selection of 5 mm instruments is also available for use with smaller access ports.

The instruments are made by the following elements:

- a tip that represents the effector of a specific surgical task;
- an EndoWrist® articulating joint (with the exception of some instruments, as required by the underlying technology, i.e., Harmonic ACE®);
- a shaft that represents the rotating arm of the instrument and through movement are transferred from the robotic arm to the wristed tips;
- release levers for the instrument's removal;
- instrument housing that engages with the sterile adapter of the robotic arm.

The da Vinci® endoscope provides a three-dimensional high-definition imaging system. It is available with either a straight (0°) or angled (30°) tip and with a shaft diameter of 8.5 mm or 12 mm. In keeping with the anthropomorphic concept, the endoscope contains two separate optical channels and focusing elements, and the camera head contains two separate cameras. When displayed on two monitors to the left and right eye of the surgeon, a true and natural three-dimensional image is achieved.

The **vision cart** includes the image processing and vision equipment, a 24 inches touch screen monitor (touch screen not available on the Si-e™ system) for the bedside assistant and system settings, and adjustable shelves for other surgical devices such as insufflators and electrosurgical generators. The vision cart is the system's central connection point where all auxiliary equipments and audiovisual connections are routed.

A comparison between the different da Vinci® Surgical Systems (S™/Si-e™/Si™) currently available on the market is shown in Table 1.1.

1.2.3 da Vinci® Xi™ System

The recently designed da Vinci® Xi™ combines the advantages of a boom-mounted system with the flexibility of a mobile platform. This hybrid architecture enables placement of the surgical cart at any position around the patient while allowing unobstructed and fast four-quadrant anatomical access, with smaller and lighter arms with an extended range of motion if compared to previous versions.

Docking is facilitated by a laser-targeting system. The new endoscope is easier to handle and to use: draping, calibration and white balance are no longer required. It can be mounted on every robotic arm improving the procedure's flexibility and provides a crystal clear 3D HD visualization of the operative field.

The da Vinci® Xi™ has recently obtained FDA clearance for clinical use in the United States and CE mark for sale in Europe. Additional technologies (FireFly™ imaging system, EndoWrist® vessel Sealer and EndoWrist® stapler)

Table 1.1 da Vinci® Model Side-by-Side Comparison

Technology Details	da Vinci® S™	da Vinci® Si-e™	da Vinci® Si™
Four Arms	√	*upgradable*	√
3D HD Vision	√	√	√
Enhanced 3D HD Vision		√	√
Intuitive® Motion	√	√	√
EndoWrist® Instrumentation	√	√	√
Ergonomic Console	√	√	√
Upgraded Surgeon Console		√	√
Dual Console Capability		*upgradable*	√
Fast, Foolproof Setup	√	√	√
Cross-Quadrant Access	√	√	√
Interactive Video Displays	√	*upgradable*	√
OR Integration			√
Fluorescence Imaging Compatible		*upgradable*	√
Single-Site™ Technology		√	√

have been also FDA cleared for the da Vinci® Xi™ system, while CE mark is expected to be obtained in the near future. The Single-Site™ technology will be designed and integrated into a completely innovative platform.

1.3 Additional Evolving Technologies

1.3.1 Single-Site™ Platform

The Single-Site™ da Vinci® Si™ platform (Intuitive Surgical Inc., Sunnyvale, CA, USA) has been developed in 2011 in an effort to overcome some technical drawbacks of single incision laparoscopic surgery (SILS). Indeed, even if promising outcomes of this technique have been described [11], the most reported limitations of SILS are that the parallel placement of the surgical instruments and the surgeon's hands create internal and external conflicts that not even some strategic expedients could completely solve [12]. Moreover, there is poor surgical exposure and the loss of the triangulation, that is commonly considered the basis of a good and accurate manipulation in laparoscopic surgery.

The Single-Site™ port is made of silicone and thanks to its flexible shape can be easily and safely inserted into the abdominal wall through a nearly 2.5 cm incision down to the level of the fascia. The presence of a target anatomy arrow indicator optimizes its correct position and so the correct triangulation is achieved in order to work in an unobstructed surgical field. Moreover, the five marked lumens on the port provide guidance for proper setup and remote center placement.

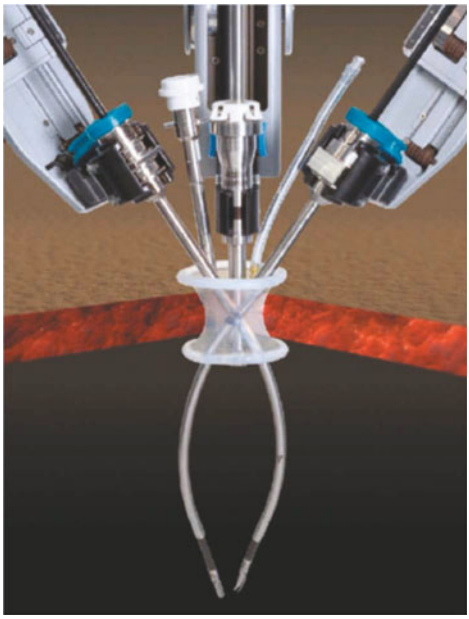

Fig. 1.4 da Vinci® Si™ Single-Site™ Surgical Platform. Curved cannulae are inserted through the silicone port. (© 2014 Intuitive Surgical, Inc.)

Three out of these five lumens are straight and are designed for the 8.5 mm 3D HD endoscope, the insufflation adaptor and the 5 mm assistant port, respectively. The two more lateral lumens are curved and cross in the midline of the Single-Site™ port (remote center) with the outlet holes on the opposite side of entry: the semi-rigid instrument that enters the abdomen from the left reaches the operative field on the right and vice versa. The curved 5 mm robotic cannulae are inserted into these channels so that the instrument arms outside the body wall are separated, maximizing the range of motion and minimizing potential internal and external crowding (Fig. 1.4).

Indeed, thanks to the abovementioned Single-Site™ configuration, the instruments and the camera, crossed within the port, use remote center technology to avoid cannula collisions, arm interferences and port-site movement. Subsequently the da Vinci® system software automatically detects and re-associates the user's hands with the instrument tips to create intuitive movement through crossed cannulae. At the end, the triangulation is restored and the correct hand/instrument correlation is obtained with the da Vinci® software.

The placement of the remote center at the level of the abdominal wall and the curvature of the cannulae guarantees an optimal focal distance of work allowing the instruments to converge correctly on the anatomical target. If the target is closer or further away to the optimum focus it will be necessary to advance or retract the cannulae. These modifications can firstly cause an incorrect positioning of the remote center and secondly produce excessive stress on the port and on the abdominal wall resulting in improper working of the instruments and loss of CO_2.

Additionally, if the instruments come out too far from the cannulae to reach a distant target, during the lateral traction they could overly flex with a potentially bullwhip effect. These issues can be mitigated by using one of the two sets of robotic curved cannulae of different lengths (250 mm or 300 mm). However, nowadays, the main drawback of this innovative platform is represented by the absence of the EndoWrist® technology, as in traditional robotic instruments.

To date, the da Vinci® Single-Site™ platform is made up of the following components:

- Single-Site™ accessories: Single-Site™ Port (with insufflation tubing and stopcock), a 8.5 mm endoscope cannula for the introduction of Intuitive Surgical Fluorescence or Basic three-dimensional high-definition endoscope (30° or 0°), two fixed-shape 5 mm curved cannulae (250 mm or 300 mm length) with flexible blunt obturator, a 5 mm and a 10 mm straight accessory cannula for insertion of manual laparoscopic instruments with corresponding flexible obturator, an 8 mm semi-rigid blunt obturator (250 mm and 300 mm length), a dock assist tool;
- Single-Site™ semi-rigid instruments: Maryland dissector, crocodile grasper, fundus grasper, cadiere forceps, curved scissors, monopolar cautery hook, Hem-o-Lok® clip applier, Hem-o-lok® ML clips (Weck®), suction irrigator, curved needle driver and bipolar Maryland;
- EndoWristed Single-Site™ needle driver is expected to be put on the market in the near future.

1.3.2 FireFly™ Imaging System

In 2011, a new optical system has been developed and integrated into the da Vinci® Surgical System. It is capable of emitting laser light that is close to infrared light with the ability to switch with dedicated commands at the console between white light and near-infrared (NIR) light view in real time, thus offering the opportunities to perform fluorescence-guided surgery thanks to the properties of the Indocyanine Green (ICG) vital dye [13] (Fig. 1.5).

ICG has been widely used for the study of blood flow and microcirculation for more than 40 years. It binds to plasma proteins when injected in the blood stream and reaches all the organs and body regions. Its routine use has widely spread through different specialties (cardiac surgery, neurosurgery, ophthalmology, hepatology, etc.) thanks to its excellent tolerability, few side effects, extremely low toxicity and few allergic reactions; the optimal dose range is between 0.1 and 0.5 mg/kg and should not exceed 2 mg/kg.

The ICG has the ability to absorb light in the NIR wavelengths between 600 and 900 nm. If its molecules are excited with infrared laser light, they emit a very intense fluorescent signal. At the frequency of 780 nm, it is possible to suppress the exciting laser light through dedicated filters in order to detect only the fluorescent signal.

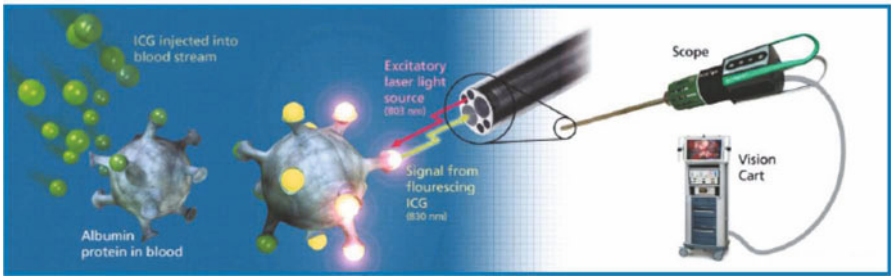

Fig. 1.5 Indocyanine Green Near-Infrared Fluorescence for the da Vinci® Si™ System. (© 2014 Intuitive Surgical, Inc.)

After intravenous injection, in a time interval that lies between 5 and 50 s, ICG reaches the arterial and venous vessels. After about one minute, it reaches the kidney where it remains for about 20 min; after about two minutes, it is eliminated via the bile by the liver without being subject to enterohepatic recirculation. The persistence in the liver and in extrahepatic bile ducts, before excretion is completed, is approximately 1–2 h.

When injected intradermally, subcutaneously, subserosally or submucosally, ICG is drained through the network of lymphatic vessels; it reaches the first lymph nodes (sentinel lymph nodes) and the locoregional lymph nodes after 10–20 min and 1–2 h, respectively. It is still detectable at time intervals between 24 and 48 h.

There are different fields of application of fluorescence in robotic general surgery that include: fluorescent cholangiography, evaluation of bowel stumps perfusion and lymph node mapping/sentinel lymph node biopsies. These procedures will be discussed in Chapter 19.

1.3.3 New Devices

- The EndoWrist® One™ vessel sealer is a single-use, sterile instrument with independent sealing and cutting functions and a dual-hinged jaw. It bears the CE mark and is cleared in the US for bipolar coagulation and mechanical transection of vessels up to 7 mm in diameter and tissue bundles that fit in the jaws of the instrument. It is cleared for commercial distribution in the US for use with the da Vinci® Si™ and Xi™ Surgical System and the ERBE VIO 300 D electrosurgical generator (identified by a label on the front bezel). Like other da Vinci® instruments, it features fully-wristed architecture and can be activated from the surgeon console. The single-use EndoWrist® One™ vessel sealer comes with an integrated cable and requires a proprietary and dedicated upgrade mounted to the vision cart of the da Vinci® Si™ System (ERBE VIO 300 D) that controls and activates the instrument and the

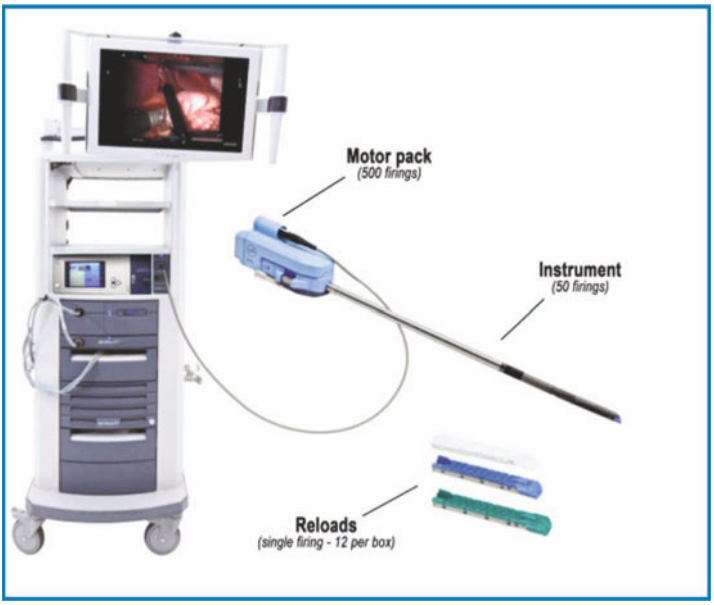

Fig. 1.6 EndoWrist® Stapler 45. (© 2014 Intuitive Surgical, Inc.)

EndoWrist® Stapler 45 too. The generator is integrated in the vision cart of the new da Vinci® Xi™ system.

- The EndoWrist® Stapler 45 (Fig. 1.6) is an endoscopic 45 mm stapler FDA cleared for use with the da Vinci® Si™ and Xi™ systems. CE mark for the Xi™ system is still pending. It is fully controlled from the surgeon console and provides fully-wristed articulation and features SmartClamp® feedback: this software detects if the instrument jaws are adequately closed on the target tissue based on each color of reload. The stapler guarantees a full cone of articulation with 108° total side-to-side, 54° total up-and-down for precise positioning around vital structures and access in deep spaces, such as the pelvis. Additionally, thanks to a complete distal tip stability, it minimizes the tremor experienced with positioning, clamping and firing of handheld staplers.
- Advanced Robotic Ultrasound Technology™ (ART™ BK Medical ApS, MA, USA) is a system that provides a curved linear probe (ProART™ Robotic Transducer) that is introduced through a standard trocar and it is designed to fit ProGrasp™ for maximum surgeon control. It guarantees a unique "real time" 3D visualization with a mobile, plug-free and maneuverable system with easy plug-and-play DVI for seamless integration of images with TilePro™. It is worth remembering that TilePro™ is a multi-input display system integrated into the da Vinci® platform: it allows the surgeon to visualize the operative field along with up to two additional digitalized information.

1.4 Conclusions

Robotic surgery was born to extend the frontiers of minimally invasive surgery. New robotic platforms are emerging for use in different surgical specialties and distinct new features will enable more procedures to be performed with the help of a computer-enhanced system. Additional technologies will be developed into currently existing or new platforms to hold the promise of becoming the central workstation of surgical care. However, although robotic surgery is growing, concerns regarding the high costs involved still exist and the market is yet to be fully matured.

References

1. Semm K (1983) Endoscopic appendectomy. Endoscopy 15:59–64
2. Mouret P (1991) From the first laparoscopic cholecystectomy to the frontiers of laparoscopic surgery: the future prospectives. Digestive surgery 8:124–125
3. Mühe E (1991) Laparoscopic cholecystectomy, late results. Langenbecks Arch Chir Suppl Kongressbd 416-423
4. Davies BL, Hibberd RD, Coptcoat MJ, Wickham JE (1989) A surgeon robot prostatectomy–a laboratory evaluation. J Med Eng Tech 13:273–277
5. Ho G, Ng WS, Teo MY et al (2001) Computer-assisted transurethral laser resection of the prostate (CALRP): theoretical and experimental motion plan. IEEE transactions on bio-medical engineering 48:1125–1133
6. Ho G, Ng WS, Teo MY et al (2001) Experimental study of transurethral robotic laser resection of the prostate using the LaserTrode lightguide. J Biomed Optics 6:244–251
7. Unger SW, Unger HM, Bass RT (1994) AESOP robotic arm. Surg Endosc 8:1131
8. Falcone T, Goldberg J, Garcia-Ruiz A et al (1999) Full robotic assistance for laparoscopic tubal anastomosis: a case report. J Laparoendoscop Adv Surg Tech A 9:107–113
9. Reichenspurner H, Damiano RJ, Mack M et al (1999) Use of the voice-controlled and computer-assisted surgical system ZEUS for endoscopic coronary artery bypass grafting. J Thorac Cardiovasc Surg 118:11–16
10. Marescaux J, Leroy J, Gagner M et al (2001) Transatlantic robot-assisted telesurgery. Nature 413:379–380
11. Qadan M, Curet MJ, Wren SM (2014) The evolving application of single-port robotic surgery in general surgery. J Hepatobiliary Pancreat Sci 21:26–33
12. Leblanc F, Champagne BJ, Augestad KM et al (2010) Single incision laparoscopic colectomy: technical aspects, feasibility, and expected benefits. Diagn Ther Endosc 2010:913216
13. Marano A, Priora F, Lenti LM et al (2013) Application of fluorescence in robotic general surgery: review of the literature and state of the art. World J Surg 37:2800–2811

Part I

Neck and Thoracic Surgery

Transaxillary Thyroidectomy and Parathyroidectomy

2

Micaela Piccoli, Barbara Mullineris, Davide Gozzo, Nazareno Smerieri, and Casimiro Nigro

2.1 Procedure Overview

In the last ten years, minimally invasive approaches have increased their applications in neck surgery.

The minimally invasive surgery can be distinguished in two groups:

- **direct cervical approach**: minimally invasive video-assisted thyroidectomy (MIVAT) [1] or endoscopic technique with an anterior approach carried out by Gagner and Cougard or with a lateral approach described by Henry and Inabnet [2–5];
- **indirect or extracervical approach** [6–8]: endoscopic techniques outside the neck region through a chest, axillary, or combined axillary-breast access, described for the first time by two Japanese surgeons, Ikeda and Takami in 1999 [2, 9].

Some of these techniques are totally gasless, such as the robotic transaxillary access; others are performed with gas insufflation. However, endoscopic procedures are limited by video camera platform instability, straight endoscopic instruments, two-dimensional imaging and a difficult manipulation of the anatomical structures. In the last years, some Asiatic surgeons have attempted to incorporate surgical robots in thyroid surgery, reducing the limitations of conventional endoscopy: improving freedom of motion through the use of multi-articulated instruments; providing the surgeon with an ergonomically perfect position at the robotic console; providing a three-dimensional, stable, magnified imaging; enabling the surgeon to perform minute, precise movements and allowing the dampening of physiologic tremors [10]. Prof. W.Y. Chung, from South Korea, in

M. Piccoli (✉)
General Surgery Unit, "Sant'Agostino-Estense" New Hospital, Baggiovara (MO), Italy
e-mail: m.piccoli@ausl.mo.it

G. Spinoglio (Ed), *Robotic Surgery: Current Applications and New Trends*, Updates in Surgery
DOI: 10.1007/978-88-470-5714-2_2,

2007, performed the first robot-assisted transaxillary thyroidectomy [10].

The birth and the development of this new technique, in a well-defined geographical area, depends on epidemiological reasons. The incidence of thyroid carcinoma is elevated in Korea, especially in young women; a well-organized thyroid screening allows the identification of suspicious thyroid nodules at an early stage. Furthermore, many young women do not want to have a neck scar after surgery, because hypertrophic scars are common in Asian people and also because of religion and cultural Asian belief. Robotic facelift thyroidectomy and transoral robotic thyroidectomy [11] are the last suggested approaches in thyroid surgery.

2.2 Patient Positioning

Under general endotracheal anesthesia, the patient is placed in the supine position with the neck slightly extended; the arm on the axillary access side is raised upon the head and positioned in such a way as to minimize the distance from the axilla to the anterior neck. The position of the arm is checked before the general anesthesia in order to avoid any wrong position that could favor an injury of the brachial plexus. The contralateral arm, with venous access, is placed along the body. Another support is placed near the head in order to avoid any lateral movements during the procedures (Fig. 2.1). A bladder catheter could be positioned only at the beginning of the experience, due to the more time consuming procedures.

The axillary access is chosen according to the side of:

- target parathyroidectomy;
- thyroid lobe to be removed in the case of a lobectomy;
- the larger nodule, in the event of a total thyroidectomy.

Fig. 2.1 Patient positioning

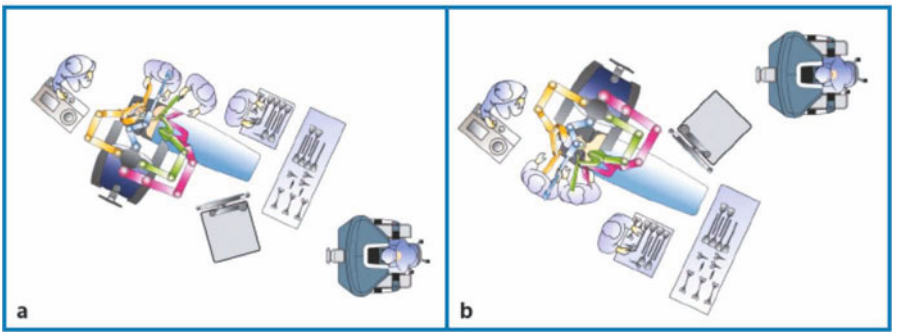

Fig. 2.2 **a** Left axillary access. **b** Right axillary access. (© 2014 Intuitive Surgical, Inc.)

2.3 Robot Positioning

The da Vinci® Si™ robot is docked contralaterally to the axillary access (Fig. 2.2a, b). Three arms are generally sufficient for lobectomy and parathyroidectomy; four arms are needed, however, for total thyroidectomy.

2.4 Procedure

The procedure is divided into three steps:

- Step 1 – transaxillary subcutaneous tunnel creation: flap or working space time
- Step 2 – robot position in the operative field or docking time
- Step 3 – thyroidectomy/target parathyroidectomy procedure or console time.

2.4.1 Step 1 (Working Space Time)

A 4–5 cm skin incision is made in the axilla, following the lateral edge of the major pectoralis muscle; the subplatysmal skin flap from the axilla to the anterior neck area is dissected over the anterior surface of the pectoralis major muscle using laparoscopic instruments (such as the Johann grasper and monopolar hook), under endoscopic vision with a 30° camera. The endoscopic vision instead of direct vision (used by Korean surgeons), allows all the surgical team to follow the creation of the flap, reducing the learning curve of this step. An external retractor – the so called "Modena Retractor" (CEATEC® Medizintechnik) – is used from the beginning to create the flap. A suction tube is directly connected to the retractor's blade in order to avoid field fogging. The myocutaneous flap is raised until the sternal and clavicular heads of the sternocleidomastoideum muscle (SCM) are visualized; then the dissection continues through the two SCM branches. During this time, care must be taken not to cause thermal burns on the overlying skin. The "Modena retractor" is reposi-

tioned beneath both the sternal branch of the SCM and the strap muscles and the thyroid is discovered.

The omohyoid muscle is the superior landmark; behind it, there is the upper thyroid pole. Care must be taken not to damage the internal jugular vein that is the first main venous vessel that appears in the operative field. The contralateral strap muscles are identified and raised if a total thyroidectomy must be performed.

2.4.2 Step 2 (Docking Time)

The robot is positioned in the operative field and three robotic arms are introduced all through the axillary incision: 30° optic, Harmonic curved shears (5 mm) and ProGrasp forceps (8 mm). In the case of the three robotic arms technique, only two arms are introduced in the incision: endoscope and Harmonic shears (the operation is conducted without the help of the ProGrasp). The fourth (or the third in case of three robotic arms technique) robotic arm is inserted through an independent incision at the inferior part of the axillary incision for the Maryland forceps. (Fig. 2.3a, b; Fig. 2.4a, b). During the operation, the Maryland forceps and Harmonic shears are interchangeable.

2.4.3 Step 3 (Console Time)

The operation proceeds in the same manner as conventional open thyroidectomy with a surgeon sitting at the console and a surgeon sitting at the operating table. All vessel dissections are performed using the Harmonic shears. The middle thyroid vein is identified and dissected. The upper pole of the thyroid is drawn downward and medially using the ProGrasp or Maryland forceps; superior thyroid vessels are identified and individually divided close to the thyroid gland to avoid injury of the external branch of the superior laryngeal nerve. The inferior thyroid artery (ITA), the recurrent laryngeal nerve (RLN) and the parathyroid glands are identified. The ITA is then divided close to the thyroid gland, and the whole cervical course of the RLN is traced. The thyroid lobe is dissected from the trachea and resected with the isthmus. The resected specimen is extracted through the axillary skin incision. During these procedures, the surgeon, at the table, checks the correct positioning of the robotic arms, cleans the camera when it is necessary, uses a suction laparoscopic device to clean the operative field and, with the same instrument, performs movements which widen the operating field. Contralateral lobectomy is performed using the same method with medial traction of the thyroid. The identification of contralateral RLN is the real difficult time of this procedure. After the identification of the contralateral RLN, its whole cervical course is traced. During this procedure, using the laparoscopic suction device, a soft traction on the trachea is performed in order to obtain a better vision

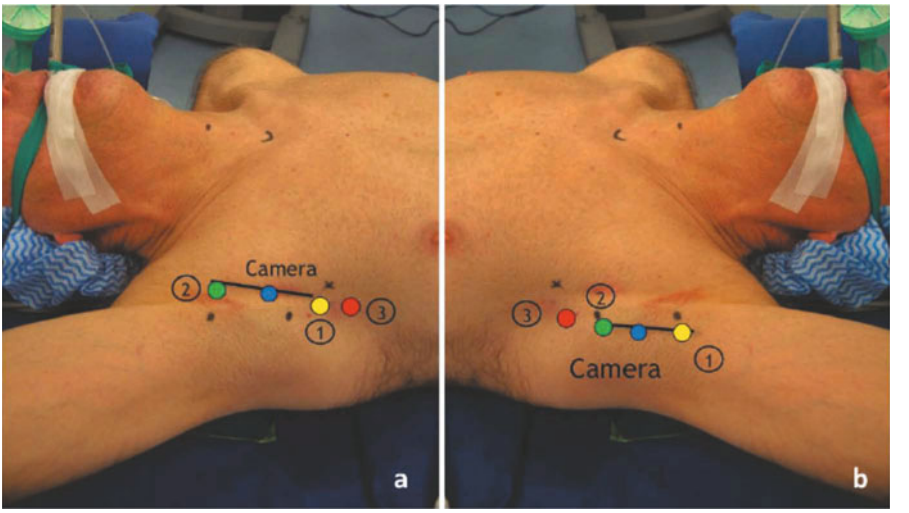

Fig. 2.3 **a** Right axillary access with four arms. **b** Left axillary access with four arms

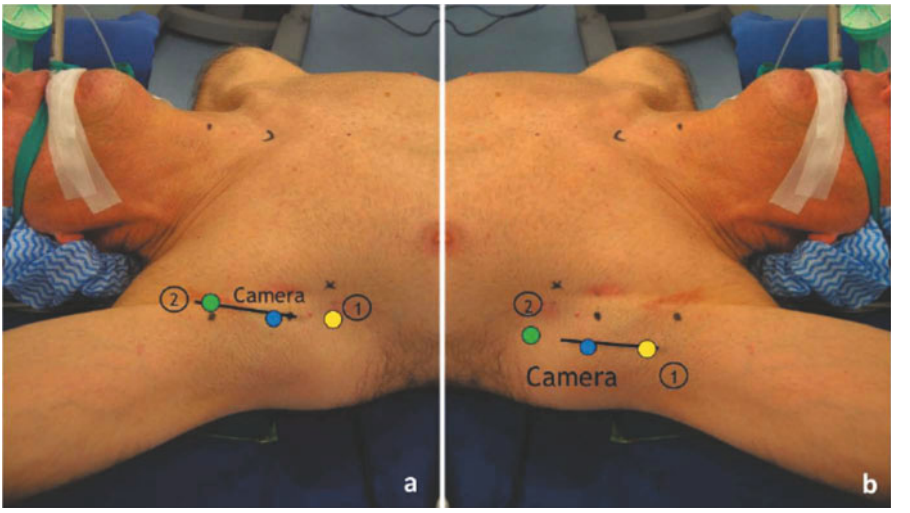

Fig. 2.4 **a** Right axillary access with three arms. **b** Left axillary access with three arms

of the RLN. At this time also the contralateral thyroid lobe is resected and extracted through the axillary skin incision. In the case of parathyroidectomy, the thyroid gland is turned medially and, with cautious dissection, the parathyroid adenoma is identified, than circumferentially dissected and excised. The venous bleeding is checked with the Valsalva maneuver. A closed suction drain is inserted through the separate incision under the axillary skin incision. The robotic arms are removed and the wound is cosmetically closed. The small incision scar in the axilla is completely covered when the arm is in its natural position.

2.5 Indications and Contraindications

Benign and malignant thyroid lesions could be treated with this approach: benign tumors not larger than 5 cm, follicular neoplasms, Graves' disease, well-differentiated thyroid cancer and early-stage medullary cancer. When initially gaining experience, it is better to treat T_1N_0 and N_{1a}. The current indications are: all stages except N_{1b} posteriorly located, T_3, T_{4a}, and T_{4b} [12].

In the case of lack of experience, it is better to avoid thyroiditis and Graves' disease. Other contraindications are: previous neck or breast surgery and/or neck radiotherapy. The presence of a pacemaker in the major pectoralis region is a contraindication to perform the flap at that side, too. Other contraindications could be shoulder arthrosis and previous shoulder surgery that does not allow the required arm extension.

The body mass index (BMI) is another important parameter. The working space is more difficult in patients who have a BMI > 30. If the distance between the axilla and the sternal notch is more than 15 cm, it would be difficult to perform the tunnel creation of Step 1. The procedures that may be possible to perform with the robotic technique are: lobectomy, loboisthmectomy, subtotal/near total/total thyroidectomy and target parathyroidectomy, following the ATA guidelines [10].

The central compartment node dissection (CCND), is feasible and it is also possible to perform a laterocervical neck dissection that importantly avoids the scar on the neck [12, 13].

2.6 Perioperative and Postoperative Complications

It is possible to divide complications in two categories: intraoperative and postoperative.

Intraoperative complications include thermal burns on the overlying skin; bleeding from the external jugular vein or from the internal jugular vein, during the flap time; or bleeding from the carotid artery, RLN injury, tracheal lesions, esophageal lesions, thoracic duct lesion, during the console time.

Postoperative complications include bleeding, permanent or transient RNL palsy, permanent or transient ipocalcemia, infection, seroma, anterior chest wall paresthesia, brachial plexus lesions, Horner syndrome.

Between all the complications, only two are really new: thermal burns and brachial plexus lesion. Cases of esophageal and tracheal perforation after open thyroidectomy are described in the literature while only very few cases of tracheal lesions are reported during robot-assisted endoscopic thyroidectomy (all conservatively treated). Only some cases of jugular vein lesions (which the authors were able to control without any consequences), and one case of esophageal perforation are reported in the literature.

2.7 Personal Experience

From September 2010 to May 2014, 191 patients underwent robot-assisted thyroidectomies (only four endoscopic, due to robotic technical problems) and five target parathyroidectomies using a unilateral transaxillary approach. The indications were: benign tumor, not larger than 5 cm; follicular neoplasm from FNAB; Graves' disease, well-differentiated thyroid cancer and parathyroid adenoma. The final pathologies were: 107 nodular hyperplasia, 25 follicular adenoma, 11 Hurtle adenoma, 2 diffuse hyperplasia, 38 differentiated thyroid carcinoma, 13 thyroid totalization (12 free thyroid tumor tissue and 1 contralateral microcarcinoma), 5 parathyroid adenoma. The median size of the dominant thyroid nodule was 28.6 mm (range: 5–60). Mean total operative time (from the end of induction of anesthesia to the completion of skin closure) was 160.2 min for total thyroidectomy (TT) and 115.1 min for lobectomy (LT). The mean time required to create the working space was 63.8 min (30–180 min), to dock the robot was 14.9 min (4–60 min). The mean console time was 53.7 min (10–135 min): mean LT, 39.0 min; mean TT, 77.1 min.

These intraoperative complications have been observed: two burns skin lesions, one external jugular vein lesion, and one internal jugular vein lesion, all resolved without conversion. As regards postoperative complications: 7 temporary RLN injury (3.5%), 27 transient hypocalcemia (13.7%), 6 transient ipsilateral arm paralysis (1 brachial plexus injury), 4 seromas (only one treated by percutaneuos aspiration), 1 subcutaneous tunnel infection, 4 postoperative hematoma: 2 conservatively treated and 2 reoperated. Median hospital stay is 2.0 days (1–15).

2.8 Conclusions

The robotic gasless transaxillary thyroidectomy is feasible and safe if performed by a surgeon skilled in endocrine and robotic surgery. Robotic thyroid and parathyroid surgery is often associated with longer operation time than conventional open/endoscopic surgery but with same outcomes in surgical completeness and safety. Compared to the conventional cervical approach, robotic neck surgery is associated not only with excellent cosmetic results, but also with reduced postoperative neck discomfort (pain, decreased voice and swallowing). Furthermore, another advantage is that the robotic surgery improves ergonomics and has a shorter learning curve than open or endoscopic surgery [13–15].

Prospective, controlled randomized studies with long-term follow-up are needed.

References

1. Miccoli P, Berti P, Bendinelli C et al (2000) Minimally invasive video-assisted surgery of the thyroid: a preliminary report. Langenbeck's Arch Surg 385:261–264
2. Slotema ET, Sebag F, Henry JF (2008) What is the evidence for endoscopic thyroidectomy in the management of benign thyroid disease? World J Surg 32:1325–1332
3. Cougard P, Osmak L, Esquis P et al (2005) Endoscopic thyroidectomy. A preliminary report including 40 patients. Ann Chir 2005 130:81–85
4. Henry JF, Sebag F (2006) Lateral endoscopic approach for thyroid and parathyroid surgery. Ann Chir 131:51–56
5. Inabnet WB III, Jacob BP, Gagner M (2003) Minimally invasive endoscopic thyroidectomy by a cervical approach. Surg Endosc 17:1808–1811
6. Cho YU, Park IJ, Choi KH et al (2007) Gasless endoscopic thyroidectomy via an anterior chest wall approach using a flap-lifting system. Yonsei Med J 48:480–487
7. Sasaki A, Nakajima J et al (2008) Endoscopic thyroidectomy by the breast approach: a single institution's 9-years experience.World J Surg 32:381–385
8. Koh YW, Kim JW, Lee SW, Choi EC (2009) Endoscopic thyroidectomy via a unilateral axillo-breast approach without gas insufflation for unilateral benign thyroid lesion. Surg Endosc 23:2053–2060
9. Ikeda Y, Takami H, Sasaki Y et al (2000) Endoscopic resection of thyroid tumors by the axillary approach. J Cardiovasc Surg 41:791–792
10. Kang SW, Chung W Y, Park C S et al (2009) Robot-assisted endoscopic surgery for thyroid cancer: experience with the first 100 patients. Surg Endosc 23:2399–2406
11. Richmon JD, Pattani KM, Benhidjeb T, Tufano RP (2011) Transoral robotic-assisted thyroidectomy: a preclinical feasibility study in 2 cadavers. Head Neck 33:330–333
12. Lee J, Yun JH, Nam KH et al (2011) Perioperative clinical outcomes after robotic thyroidectomy for thyroid carcinoma: a multicenter study. Surg Endosc 25:906–912
13. Lee J, Lee JH, Nah KY et al (2011) Comparison of endoscopic and robotic thyroidectomy. Ann Surg Oncol 18:1439–1446
14. Li X, Massasati SA, Kandil E et al (2012) Single incision robotic transaxillary approach to perform parathyroidectomy. Gland Surg 1:169–170
15. Lee J, Chung WY (2013) Robotic surgery for thyroid disease. Eur Thyroid J 2:93–101

Zenker Diverticulum Treatment

3

Gianluigi Melotti, Micaela Piccoli, Nazareno Smerieri, Barbara Mullineris, and Giovanni Colli

3.1 Introduction

Zenker's diverticulum (ZD), first observed by Ludlow in 1769 [1], became widely known after it was described by Zenker and von Ziemssen [2] in 1878. The anatomy of ZD was described in detail by Killian in 1908.
The place of origin of the diverticulum is posteriorly located in the midline, where the oblique fibers of the inferior pharyngeal constrictor, and the transverse cricopharyngeal fibers delimit a triangular space of relative weakness, the so called Killian's triangle.

ZD is a relatively rare pathology, with an annual incidence of about two cases per 100,000 people [3], occurring most often in men between the seventh and eighth decade of life. A variety of open and endoscopic surgical approaches for the treatment of ZD have been described.

The transaxillary gasless robotic access to the thyroid was first described by Kang et al. in 2009 [4, 5]. This kind of access to the neck has resulted in safe and precise procedures, with notable cosmetic and functional benefits as compared to the traditional open approach [6]. This chapter describes, for the first time, the author's technique of left transaxillary gasless robot-assisted endoscopic Zenker diverticulectomy and its applicability in the surgical management of cervical esophagus diseases.

M. Piccoli (✉)
General Surgery Unit, "Sant'Agostino-Estense" New Hospital, Baggiovara (MO), Italy
e-mail: m.piccoli@ausl.mo.it

G. Spinoglio (Ed), *Robotic Surgery: Current Applications and New Trends*, Updates in Surgery
DOI: 10.1007/978-88-470-5714-2_3,

3.2 Patient Positioning

Under general endotracheal anesthesia, the patient is positioned supine with the neck slightly extended, and the left arm is raised and positioned in such a way as to minimize the distance from the axilla to the anterior neck. This position is the same as for transaxillary robotic thyroidectomy (Figs. 3.1a, b).

3.3 Step-by-Step Review of the Surgical Technique

A 4–5 cm skin incision is made in the left axilla, following the lateral edge of the major pectoralis muscle; the subplatysmal skin flap from the axilla to the anterior neck area is dissected over the anterior surface of the pectoralis major muscle using reusable laparoscopic instruments (such us a Johann grasper or monopolar hook), under endoscopic vision with a 30° camera. An external retractor – the so called "Modena Retractor" (Ceatec Medizintechnik GMBH) – is used from the beginning to execute the flap (Fig. 3.2). The retractor is mounted at the operating table on the robot side, but all the adjustments are performed from the operation side: vertical height of the pillar, horizontal depth of the boom tube and blade angle. A suction tube was directly connected to the blade in order to avoid field fogging. The myocutaneous flap is raised until the sternal and clavicular heads of the sternocleidomastoideum (SCM) muscle are visualized; then the dissection continued through the two SCM branches. Next, the external retractor placed beneath the strap muscle is replaced with a larger one to maintain adequate working space.

After the creation of the working space and before the docking, the head is slightly turned on the right side. Then the da Vinci® Si robot is docked from the side of the bed, contra-lateral to the operative field. Three robotic arms are intro-

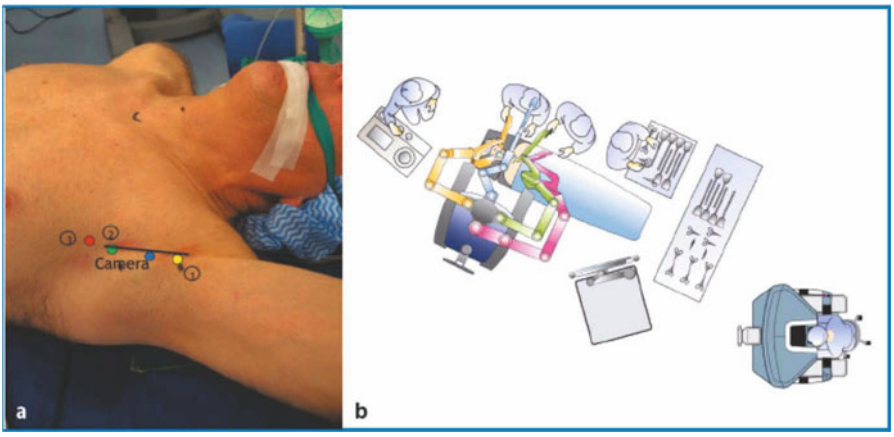

Fig. 3.1 **a** Patient positioning and trocar layout. 1, Harmonic curved shears; 2, ProGrasp™ forceps; 3, Maryland dissector. **b** OR setup (© 2014 Intuitive Surgical, Inc.)

duced all through the axillary incision: dual channel endoscope (central, down), Harmonic curved shears (right) and ProGrasp™ forceps (up). The fourth robotic arm is inserted through an independent incision in the inferior part of the axillary one, for Maryland dissector (left) (Fig. 3.1a). All vessel dissections are performed using the Harmonic curved shears. Under robotic guidance, the thyroid is drawn medially by the ProGrasp forceps in order to identify and spare the inferior thyroid artery and the inferior laryngeal nerve. It is necessary to cut the middle thyroid vein, and sometimes also the omohyoid muscle. The prevertebral fascia is identified, and the diverticulum can be isolated from its adhesion with the hypopharynx. The loose connective tissue surrounding the pouch is dissected to identify its neck on the posterior pharyngeal wall. This procedure must be carried out under esophagoscopic control. The neck of the diverticulum is fully exposed by tractioning the diverticulum to the left with the Maryland dissector. A complete myotomy must be performed, including the cricopharyngeal muscle and the first 5 cm of the circular layer of the cervical esophagus. The myotomy could be performed with a robotic monopolar hook allowing dissection and resection of the fibers, proceeding downward, starting from the upper esophageal sphincter. Then a surgical linear stapler (Endopath RTS-FLEX Endoscopic Articulating Linear Cutter 35 mm; Ethicon Endo-surgery, LLC) with a blue cartridge is inserted through the axilla and it is applied to the neck of the diverticulum, which is cut and sutured and then removed (Fig. 3.3).

Fig. 3.2 Videoassisted working space, using "Modena retractor" positioning

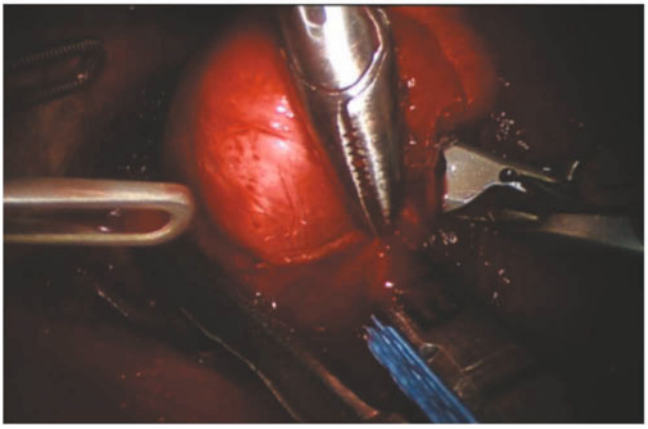

Fig. 3.3 Stapling device applied to the neck of the diverticulum

The complete diverticulum removal and its staple line could be checked endoscopically. A suction-type drain is left in place until the X-ray examination is performed. Intravenous broad-spectrum antibiotics are administered only perioperatively.

3.4 Literature Evidence

Treatment options for a Zenker diverticulum include open surgery, flexible endoscopic and rigid endoscopic therapy. Based on current evidence, traditional open surgery is suitable for all kinds of diverticula, providing satisfactory long-term outcomes, although with a significant incidence of complications including mediastinitis, recurrent laryngeal nerve injury, esophageal stricture, fistula, esophageal perforation, hematoma, wound infection, pneumonia and even death, with a 11% median incidence of major morbidity [1]. It also needs general anesthesia.

Rigid endoscopic treatment can be done under general anesthesia and hyperextension of the neck. It might be technically difficult when the diverticular septum cannot be well exposed. Flexible endoscopic therapy can be conducted without general anesthesia or neck hyperextension; however it is only suitable for selected patients.

The poor quality of current evidence renders it difficult to establish a sound conclusion for the optimal treatment of ZD [3, 7, 8]. Actually there is not strong evidence for a gold standard technique.

3.5 Personal Experience

Eight consecutive patients underwent surgery for symptomatic ZD from July 2013 to April 2014 in our Department. All the patients were treated with a left

transaxillary robotic approach. The median age was 70.3 years, seven patients were male and one female. The preoperative work-up included a barium swallow, which allowed determination of the diverticulum size and location and upper gastrointestinal endoscopy, and was mandatory to rule out malignancy.

An X-ray check with an oral soluble contrast swallow study was carried out 4 days after the operation. In the absence of leakage, oral feeding was administered to the patient and the patient could be discharged. Patients were scheduled for a clinic visit 5 days after discharge, and after 1 month a barium swallow study was performed.

The mean diameter of the ZD, on preoperative barium swallow, was 4.25 cm (range: 3–9 cm). The mean time for setting up the working space was 66 minutes (range 40–90 min.), the mean docking time was 12.8 min. (range 6–23 min.) and the mean robotic time 85.1 minutes (range 60–115 min). The mean hospital stay was 7 days. There were no conversions to open cervicotomy, no transient or definitive left recurrent nerve palsies. There was only one postoperative leak, which was conservatively treated and fully recovered. There was no evidence of persistence or recurrence at the postoperative, although short, follow-up.

3.6 Conclusions

The results of this technique show that the left transaxillary robotic approach is a safe and effective surgical procedure in the treatment of any kind of ZD. This procedure cannot be considered a cosmetic treatment, as ZD mostly occurs in men between the seventh and eighth decade of life, but the advantage offered by the da Vinci® Si™ surgical robot system is a three-dimensional field of view and a more accurate sense of perspective. Moreover, the magnification of target structures, made possible by the system, facilitates the preservation of the recurrent laryngeal nerve, thus preventing both transient and definitive left recurrent nerve palsy, and spares the esophageal mucosa during the myotomy, reducing the incidence of postoperative leakage.

It is also worth considering that the robot system incorporates features for hand-tremor filtration, fine motion scaling, negative motion reversal (allowing minute and precise tissue manipulation); in conjunction with the ergonomically designed console, they help decrease the surgeon's fatigue.

The robotic assisted transaxillary Zenker's diverticulectomy is a procedure that requires experience in performing the flap and, due to the rarity of this pathology, the only way for the surgeon to complete the learning curve is to perform robotic transaxillary thyroid surgery; so this procedure can be attempted only by surgeons well versed in neck robotic surgery, and skilled in esophageal diseases surgery.

Open diverticulectomy has low but significant adverse events, including mediastinitis, recurrent laryngeal nerve injury, esophageal stricture, fistula, esophageal perforation, hematoma, wound infection, pneumonia and even death.

Various techniques have been described for rigid and flexible endoscopic treatment of ZD. Despite overall good results, follow-up has been often inadequate [2, 3] and technical refinements are still in progress to avoid adverse events [7, 8].

The robot-assisted transaxillary Zenker's diverticulectomy is a technically demanding procedure. According to our preliminary data, this procedure appears safe and effective.

However, our results need to be confirmed in larger cohorts of patients and further randomized controlled studies comparing this technique with rigid and flexible endoscopic diverticulotomy.

References

1. Dzeletovic I, Ekbom DC, Baron TH (2012) Flexible endoscopic and surgical management of Zenker's diverticulum. Expert Rev Gastroenterol Hepatol 6:449–466
2. Law R, Katzka DA, Baron TH (2014) Zenker's diverticulum. Clin Gastroenterol Hepatol. doi:10.1016/j.cgh.2013.09.016
3. Yuan Y, Zhao Y-F, Hu Y, Chen L-Q (2013) Surgical treatment of Zenker's diverticulum. Dig Surg 30:214–225
4. Kang SW, Jeong JJ, Yun JS et al (2009) Robot-assisted endoscopic surgery for thyroid cancer: experience with the first 100 patients. Surg Endosc 23:2399–2406
5. Kang SW, Lee SC, Lee SH, Lee KY, Jeong JJ, Lee YS, Nam KH, Chang HS, Chung WY, Park CS (2009) Robotic thyroid surgery using a gasless, transaxillary approach and the da Vinci S system: the operative outcomes of 338 consecutive patients. Surgery 146:1048–1055
6. Lee S, Ryu HR, Park JH (2011) Excellence in robotic thyroid surgery: a comparative study of robot-assisted versus conventional endoscopic thyroidectomy in papillary thyroid microcarcinoma patients. Ann Surg 253:1060–1066
7. Huberty V, El Bacha S, Blero D et al (2013) Endoscopic treatment for Zenker's diverticulum: long-term results (with video). Gastrointest Endosc 77:701–707
8. Manno M, Manta R, Caruso A et al (2014) Alternative endoscopic treatment of Zenker's diverticulum: a case series (with video). Gastrointest Endosc 79:168–170

Thoracic Surgery

4

Giulia Veronesi

4.1 Procedure Overview

Video-assisted thoracic surgery (VATS) is a minimally invasive approach with several advantages over open thoracotomy for resectable lung cancer [1, 2]. However VATS use is limited because the instruments are rigid and difficult to use, and vision is limited. Robot technology appears to overcome these limitations as the robotic arms are more comfortable to use, and allow more precise, flexible and intuitive movements. This, combined with high-definition three-dimensional vision, renders operations easier for the surgeon, with probably a shorter learning curve than for VATS [3, 4].

Retrospective studies demonstrate that robot-assisted lobectomy is feasible and safe [3–6]; limited long-term data indicates that oncological radicality is similar to that of open/VATS approaches [2], although randomized controlled trials are not available. The few available papers on robotic resection of mediastinal lesions describes the procedure as safe and effective [7].

High capital and running costs [8], limited availability of robotic systems, and long operating times are important disadvantages of robotic thoracic surgery. Only one company is currently producing robotic systems (Intuitive Surgical) and entry of competitor companies should drive down costs. Further studies are required to assess the quality of life, morbidity, oncological radicality, and cost effectiveness.

G. Veronesi (✉)
Division of Thoracic Surgery, European Institute of Oncology, Milan, Italy
e-mail: giulia.veronesi@ieo.it

G. Spinoglio (Ed), *Robotic Surgery: Current Applications and New Trends*, Updates in Surgery
DOI: 10.1007/978-88-470-5714-2_4, © Springer-Verlag Italia 2015

4.2 Patient Positioning, Robot Positioning and System Docking

The patient is positioned in a lateral decubitus position with the arms in front of the face as in Figs. 4.1b and 4.1c. The operating table should ideally fold down at the level of the fifth intercostal space, to lower the level of the hips; alternatively a pillow can be placed under the chest. The patient is intubated with a double lumen endotracheal tube. The operation starts with the introduction of the high-definition endoscope through the port at the level of the seventh intercostal space in the anterior axillary line (Fig. 4.1a). Under endoscopic control, the utility incision is made through the fourth or fifth intercostal space. In long-limbed patients, use of the fifth intercostal space may make it easier to reach the diaphragm and the lower ligament.

Entry port positioning is standard for all lobectomies and segmentectomies (Fig. 4.1a), although on the left the endoscope port may moved 2 cm posteriorly compared to the right side inorder to avoid the heart obscuring hilar structures. Furthermore, if CO_2 insufflation is required (obese patients and small cavities), the utility incision for specimen removal is made at the end of the procedure, and in a lower position than normal – just above the diaphragm. The robot is positioned behind the patient's head, 20–30° off the midline (Figs. 4.1b and 4.1c). Docking requires 5–10 minutes, starting with the endoscope arm, followed by the two posterior arms, and then the anterior arm through the utility incision.

For mediastinal lesions the patient is positioned in a semilateral decubitus position with the preferred side (usually left) above. The arms are positioned along the side of the body. The room setup is described in Figs. 4.2b and 4.2c for the left and right approach.

Three ports are used (Fig. 4.2a): fifth intercostal space in the middle axillary line (submammary sulcus), fifth intercostal paramediastinic site, and third intercostal space at the anterior axillary line. A 30° endoscope is used, introduced via the central port. Lifting of the chest wall with the endoscope helps enlarge the chest cavity; CO_2 insufflation (8–10 mmHg) is also used. In some cases a right approach is used depending on the position of the lesion or surgeon preference.

4.3 Step-by-Step Review of Critical Elements of the Procedure

4.3.1 Lobectomy

An anterior approach lobectomy using four robotic arms is described. The resection begins by isolating hilar elements using a hook (or Maryland bipolar forceps) and two forceps. The hook is manipulated by the right robotic arm introduced through the utility port for right lung lobectomies, or the posterior eighth

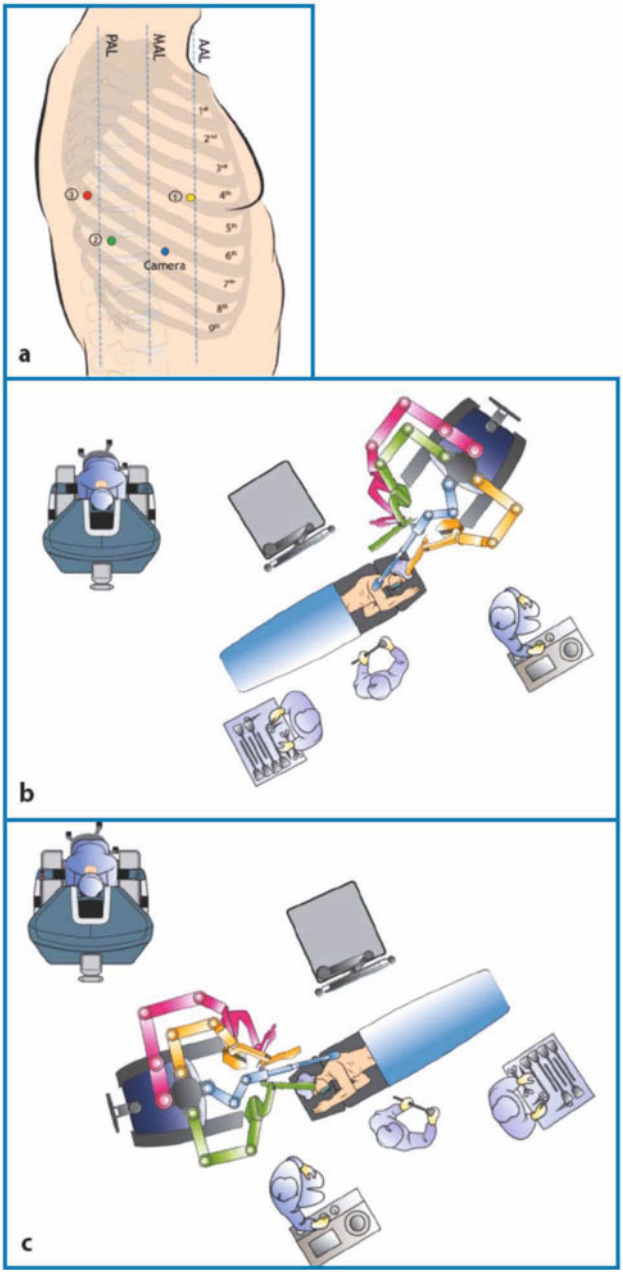

Fig. 4.1 **a** Positions of entry ports for right lobectomy. **b, c** OR setup for right (b) and left (c) lung resection. (© 2014 Intuitive Surgical, Inc.)

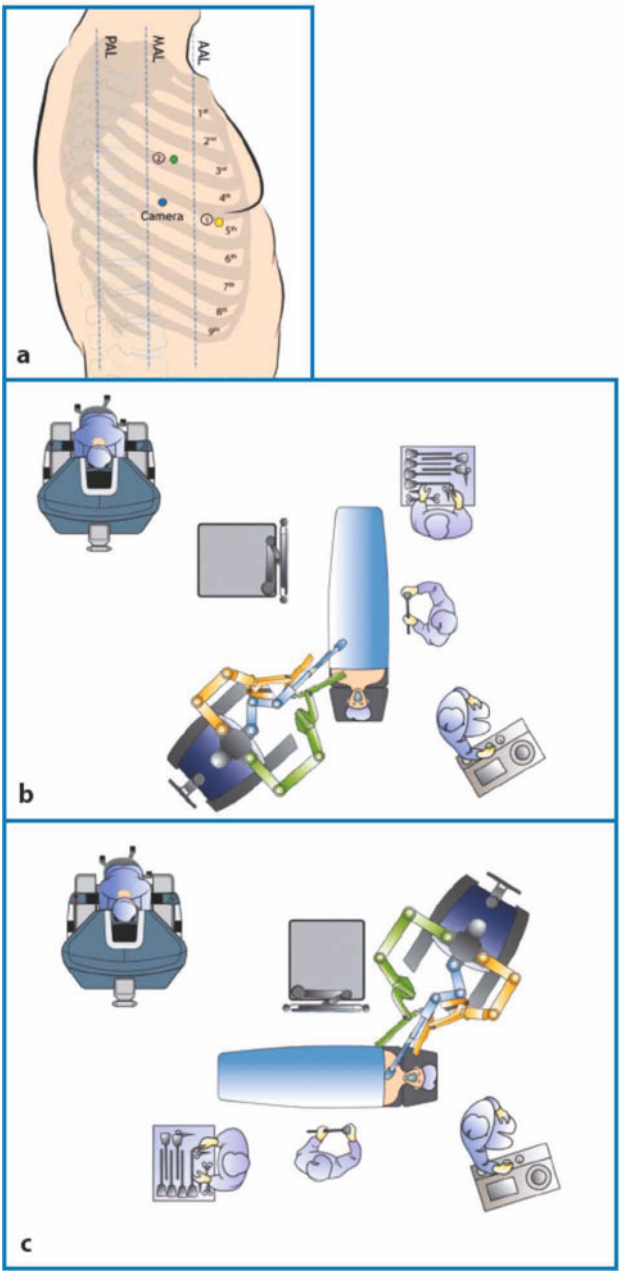

Fig. 4.2 **a** Port placement for resection of anterior mediastinal lesions. **b** OR setup for right approach to anterior mediastinal lesions. **c** OR setup for left approach to anterior mediastinal lesions. (© 2014 Intuitive Surgical, Inc.)

intercostal port for left-side lobectomies. One of the forceps (fourth robotic arm) is used to retract the lung and expose the structures. The other forceps are manipulated by the left robotic arm and used to grip structures during dissection: it is introduced through the utility thoracotomy for left-side lobectomies or the posterior eighth intercostal space for right-side lobectomies. When a hilar vessel or bronchus is ready to be surrounded with a vessel loop and stapled, a third pair of forceps is introduced (substituting the hook). The vessels and bronchus are sectioned with a stapler introduced by the assistant surgeon through the utility incision for upper lobes and through the posterior port after removing the robotic arm for lower lobes. The pulmonary vein is usually the first structure to be exposed and divided. If the lesion is in the right upper lobe, vein division is followed by exposure of the pulmonary artery branches and sectioning, and then bronchus exposure and sectioning. Anterior and posterior parenchyma division is completed with an EndoStapler (fissureless technique). If the lesion is in the right lower lobe, the sequence is usually: vein, artery, fissures and bronchus. If the anterior fissure is incomplete it can be completed after bronchus stapling. When performing a middle lobectomy, the most favorable sequence is vein, bronchus, artery.

For the left upper lobe, after pulmonary vein sectioning, the first mediastinal artery is exposed and transected to allow for the introduction of the stapler for bronchus sectioning. The posterior and lingular arteries are then isolated and stapled or cut between Hem-o-lok® clips, and the lobe is removed.

Left lower lobectomy starts with vein exposure and transection, followed by the artery and bronchus. Incomplete fissures are usually completed with an EndoGIA introduced by the assistant through one of the ports. The lobe is extracted through the anterior utility thoracotomy using an EndoCatch.

4.3.2 Segmentectomy

For suspected primary lung cancer but no preoperative diagnosis, a VATS wedge resection with frozen section examination may be performed to confirm malignancy before proceeding to segmentectomy. However, if possible this phase should be avoided as intersegmental planes can be disrupted by the atypical resections. For centrally located cancers, the operation proceeds directly to anatomical segmentectomy. Pulmonary artery and vein branches are divided with a Hem-o-lok® or a stapler; bronchi and parenchyma are divided with the stapler, which is introduced by the assistant. Dissection is usually performed with Cadière forceps in one hand and hook in the other. A spatula with monopolar cautery or a bipolar tool (Maryland) in the right hand can be used as an alternative to hook cautery. Fibrin glue is used to control parenchyma air leakage when required.

For right upper lobe dorsal segmentectomy, the first step is dissection of the interlobar portion of the pulmonary artery so as to identify the posterior ascend-

ing segmental artery, to the dorsal upper lobe, and the lower lobe apical segmental artery. The ascending branch is then cut between Hem-o-lok® clips. The upper lobe is pulled anteriorly with the forceps on the fourth arm and the bronchial tree is isolated to expose the upper lobe and intermediate bronchus. The dissection continues by identifying the branch to the dorsal segment, which is encircled and divided by the stapler. When visible, the segmental vein is divided between Hem-o-lok® clips. The segmentectomy is completed by dividing the parenchyma between the dorsal and apical segments with a stapler. The resected specimen is extracted in an Endobag through the anterior utility incision.

For right upper lobe anterior segmentectomy, the mediastinal pleura is completely incised anteriorly from the middle lobe vein to the truncus arteriosus. The anterior segmental vein is isolated and divided; the anterior segmental artery coming from the lower truncus arteriosus is isolated and divided. The anterior portion of the horizontal fissure is completed with the endovascular stapler, and the anterior segmental bronchus is isolated and divided. The remaining segmental fissures are divided with staplers, and the segment is removed.

For right lower lobe upper segmentectomy, if performed from posterior to anterior, the sequence of hilar structure transection is vein, bronchus, artery; when the approach is from the fissure, the sequence is artery, bronchus, vein. The posterior to anterior technique is described: with the lung retracted anteriorly, the pulmonary ligament is divided, and the lower pulmonary vein dissected bluntly to expose the lower lobe apical segmental vein. After division of the vein, the bronchus is exposed with the lung still retracted anteriorly. The lower lobe apical segmental artery is then identified in the fissure and stapled (or clipped with Hem-o-lok® clips). Lastly, the parenchyma is transected using a stapler introduced through the anterior utility incision.

For right lower lobe basilar segmentectomy, the sequence is vein, artery, bronchus. The lung is first retracted posteriorly, the lung ligament is transected, and the vein branch is isolated and divided. The next step is to identify the segmental artery within the fissure, which is then cut by a stapler. The bronchus is then isolated and divided by a stapler followed by parenchyma division with an articulated stapler.

Left lower lobe trisegmentectomy with lingual sparing proceeds in the sequence vein, upper artery, bronchus, ventral artery, dorsal artery. The procedure starts with blunt dissection of the upper pulmonary vein. The main branch is isolated from lingular branch and divided by the stapler. This is followed by gentle dissection of the artery to the upper segment (one or two branches). The culmen bronchus is than isolated and divided by the stapler. One or more ventral and dorsal branches are then isolated and cut after Hem-o-lok® clipping. Fissure division is the last step.

The sequence for lingual segmentectomy is artery, vein, bronchus. The artery in the fissure is first exposed so as to identify the lingular artery, which is then divided between Hem-o-lok® clips or with stapler. The segmental vein is isolat-

ed and divided between Hem-o-lok® clips while the bronchus is divided by a stapler. Fissure division is the last step.

The techniques for superior segmentectomy and basilar segmentectomy of the lower left lobe are similar to those for right-side segmentectomies.

4.3.3 Mediastinal Lymph Node Dissection

Radical lymph node dissection can be performed before or after lobectomy, but suspicious lymph nodes are usually removed before lobectomy. The technique is similar to that used in open surgery. The paratracheal lymph nodes on the right side are removed first, usually avoiding division of the azygos vein. The mediastinal pleura, between the superior vena cava and the azygos vein, is then incised and the lymph nodes, together with the fatty soft tissue of the paratracheal region are removed en bloc using the hook and forceps. Sometimes a PK system, UltraCision, is used in patients with large quantities of mediastinal fat or enlarged lymph nodes.

The nodes of the subcarinal station are removed after resection of the pulmonary ligament and retraction of the lung toward the anterior mediastinum to expose the posterior mediastinum. The bronchial arteries can usually be avoided since visibility is generally good, if not they are coagulated and a clip is not usually required. Fibrin sealant (Tissucol, Baxter) may be used at lymphadenectomy sites to reduce lymphorrhea, but is rarely required; sealant may also be applied to the bronchial stump and fissure surface, to reduce air leakage. Absorbable hemostatic agent is applied, and a single 28Ch pleural drain is emplaced at the end of the operation.

4.3.4 Resection of Anterior Mediastinal Lesions

The stereoendoscope is introduced through the central port of the fifth intercostal space. The forceps for the right hand, and hook for the left hand, are introduced under endoscopic visual control. Radical thymectomy begins by incising the mediastinal pleura above the phrenic nerve. The lower part of the thymus and mediastinal fat are dissected moving toward the apical region. The anonymous vein is best isolated from the right side where the subclavian vein is clearly visible. Intercostal mammary vessels are spared and mark the boundary of the anterior chest wall incision. Radical extended thymectomy is usually performed en bloc with mediastinal fat tissue. The fatty tissue of the superior poles, pericardium, and brachiocephalic truncus is removed. Hook cautery or ultracision is used for the dissection and a Cadière forceps for retraction. The boundaries of the resection are the diaphragm below, the thyroid above, and the phrenic nerves laterally. The small veins are controlled with monopolar cautery or ultracision. Large vessels are clipped. The controlateral pleura can be left intact if the lesion

is small; for larger tumors the contralateral pleura can be opened to remove all the mediastinal tissue without injury to the phrenic nerve, which is identified and spared. The specimen is removed through the parasternal incision, which may sometimes require enlargement. A single 28Ch chest tube is emplaced via the same port.

4.3.5 Postoperative Care

Intensive care is not normally necessary. Patients are typically awakened in the operating room soon after surgery has been completed and are then brought to the ward. Chest X ray and blood tests are done in the immediate postsurgical period. Patients are mobilized and start pulmonary rehabilitation (for those who have undergone lung surgery) on the first postoperative day; the vesical catheter is removed on the same day if diuresis is adequate (>30 cc/h) and there are no other contraindications. The drain is removed when less than 350–400 cc has accumulated over the preceding 24 hours, and air leaks are absent. Discharge is possible on the same day as the drain removal (third postoperative day at the earliest). In the event of prolonged air leakage, a Heimlich valve is attached to the chest tube, and discharge planned for the fifth postoperative day in the absence of further contraindications.

4.4 Advantages, Limitations and Relative Contraindications

Robotic thoracic surgery is still relatively new, but sufficient experience has accumulated to justify considering it as the future of minimally invasive surgery. Nevertheless, the claimed advantages of robotic surgery – high-definition stereoscopic view, improved dexterity due to more degrees of movement of the instuments, lack of the instrument fulcrum effect that occurs with VATS, tremor filtration, and greater surgeon comfort – have not been shown to produce superior clinical outcomes, so data supporting these perceived benefits are urgently required. The high capital and running costs [7], together with the requirement for the entire operating team to learn a new set of skills, have slowed down the adoption of robotic systems. Although it may be easier for the surgeon to learn robotic thoracic surgery than VATS, team learning may be longer and more difficult. Other disadvantages of robotic systems are the lack of tactile feedback with an inability to feel small lung nodules. However robotic technology is evolving quickly and the use of robotic thoracic surgery increased more than in any other surgical discipline in 2012–2013. Our own experience with the da Vinci® Surgical System (Intuitive Surgical) suggests that about 20 operations are required, for a surgeon experienced in open thoracic surgery (but not VATS), to achieve competence in robotic lobectomy [9]. Available data on complications, number of lymph nodes removed, and patient survival are encouraging, [3–6, 9,

10] supporting the safety and oncological radicality of the robotic approach to lobectomy in lung cancer patients.

There are a number of variations in surgical technique. We use a four-arm approach – three robot arms and the utility incision [1]. Some surgeons use only three arms [5]; others make the utility incision at the end of the procedure because they insufflate the chest cavity with CO_2 [5, 6]. The position of the utility incision varies with surgeon preference. Other teams use a hybrid robot-VATS approach [11].

In these cases, the robot is used for vascular, hilar, and mediastinal dissection, followed by VATS lobectomy.

The radicality of minimally invasive approaches to mediastinal lymph node dissection has long been debated [2]. Extent of pathologic nodal upstaging can be a surrogate for the completeness of node dissection and the quality of surgery. Wilson et al. [12] determined the rate of hilar (pN_1) nodal upstaging in 303 patients with stage I non-small-cell lung cancer, who underwent robotic surgery for their disease, and compared them historic hilar upstaging rates for VATS, and thoracotomy. They found that nodal upstaging following robotic resection appeared superior to VATS and comparable to thoracotomy, suggesting that the completeness of node dissection by robotic surgery is similar to that obtained by open surgery. In a study by our group [3], the median number of lymph nodes removed from patients undergoing lobectomy did not differ between robotic and open lobectomy, again suggesting that node dissection is reassuringly complete with the robotic approach.

Literature data on robotic mediastinal surgery are limited. Rea et al. [13] reported on 33 thymectomies performed on myasthenia gravis patients. Total thymomectomy is often necessary to obtain long-lasting or permanent remission of muscle weakness in patients with myasthenia gravis and thymoma. More controversially it is also used on myasthenic patients without thymoma. The study concluded that robotic thymectomy was safe and effective, with complete remission or much improved symptomatology in 92% of the series. The advantages of the left-sided approach were emphasized, but it was considered that long-term follow-up was essential to confirm benefit. Ruckert et al. [14] compared traditional monolateral VATS with a robotic approach for thymectomy myasthenia gravis patients. Duration of surgery, rate of conversion and morbidity were similar in the two groups, however patients receiving robotic surgery had a higher rate of complete remission that was attributed to more complete removal of thymus tissue with the robotic approach.

The largest published experience to date on robotic thymectomy is a study that assessed early and late results in patients with early-stage (Masaoka I or II) thymoma, treated at four European centers between 2002 and 2011 [7]. Seventy-nine patients of median age 57 years received left-sided (82.4%), right-sided (12.6%), or bilateral (5%) robotic surgery. Forty-five (57%) had myasthenia gravis. The mean operating time was 155 minutes and median hospital stay was 3 days. The median resected tumor diameter was 3 cm (range: 1–12 cm). After

Table 4.1 Summary of results of major publications (>30 cases) on robotic lung resections (lobectomies and segmentectomies)

Study [Reference]	Year	N. Patients	Mean operating time (min)	Mean postoperative stay (days)	Postoperative complications (%)	Mortality (%)	Conversions (%)
Robotic lobectomy/segmentectomy with utility incision at the beginning and no CO_2							
Melfi et al. [10]	2004	107	220	5	NA	1	NA
Gharagozloo et al. [11]	2009	100	216	4	21	3	13
Veronesi et al. [3]	2010	54	224	4.5	20	0	9.4
Park et al. [4]	2011	325	210	5	25	NA	8
Veronesi et al. [9]	2011	91	213	5	20	0	10
Robotic lobectomy/segmentectomy without utility incision at the beginning and with CO_2							
Dylewski et al. [5]	2011	165/35	90	3	26	0	1.5
Cerfolio et al. [6]	2011	106/16	132	2	27	0	10

NA, not available

a median follow-up of 40 months, 74 patients were alive and five had died (four from non-thymoma causes and one of disseminated intrathoracic recurrence). Five-year survival was 90% comparing favorably with historical results.

It is important to remove all thymic tissue when performing thymectomy in myasthenic patients in order to maximize the chance of long-term remission. When using a unilateral approach, identification of the contralateral phrenic nerve is a key landmark for ensuring maximum removals of thymic tissue.

Waegner et al. [15] used fluorescence imaging with indocyanine green during right robotic thymectomy to assist with identification of the contralateral phrenic nerve. The technique consists of bolus iv injection of indocyanine green solution. The robot visual system is switched to fluorescent mode and a fluorescence response in mediastinal blood vessels is observed about 10 seconds after the injection. The contralateral phrenic nerve was thus identified as it runs parallel to the pericardiophrenic neurovascular bundle, which shows up as fluorescent. It was found that the contralateral pericardiophrenic neurovascular bundle was visualized in 80% of patients from a left pleural view, rarely from a mediastinal view, and never distal to the aortopulmonary window. The authors concluded that this technology had the potential to maximize thymic tissue resection using the unilateral approach, while reducing operating time and nerve injury.

References

1. Boffa D, Kosinski AS, Paul S et al (2012) Lymph node evaluation by open or video-assisted approaches in 11,500 anatomic lung cancer resections. Ann Thorac Surg 94:347–353
2. Whitson SS, Groth SJ, Duval SJ, Swanson MA (2008) Maddaus Surgery for early-stage non-small cell lung cancer: a systematic review of the video-assisted thoracoscopic surgery versus thoracotomy approaches to lobectomy. Ann Thorac Surg 86:2008–2016
3. Veronesi G, Galetta D, Maisonneuve P et al (2010) Four-arm robotic lobectomy for the treatment of early-stage lung cancer. J Thorac Cardiovasc Surg 140:19–25
4. Park BJ, Melfi F, Mussi A et al (2011) Robotic lobectomy for non-small cell lung cancer (NSCLC): long-term oncologic results. J Thorac Cardiovasc Surg 143:383–389
5. Dylewski MR, Ohaeto AC, Pereira JF (2011) Pulmonary resection using a total endoscopic robotic video-assisted approach. Semin Thorac Cardiovasc Surg 23:36–42
6. Cerfolio RJ, Bryant AS, Skylizard L, Minnich DJ (2011) Initial consecutive experience of completely portal robotic pulmonary resection with 4 arms. J Thorac Cardiovasc Surg 142:740–746
7. Marulli G, Rea F, Melfi F et al (2012) Robot-aided thoracoscopic thymectomy for early-stage thymoma: a multicenter European study. J Thorac Cardiovasc Surg 144:1125–1130
8. Barbash GI, Glied SA (2010) New technology and health costs – the case of robot assisted surgery. N Engl J Med 363:701–704
9. Veronesi G, Agoglia B, Melfi F et al (2011) Experience with robotic lobectomy for lung. Innovations (Phila) 6:355–360
10. Melfi FM, Ambrogi MC, Lucchi M, Mussi A (2005) Video robotic lobectomy. Multimed Man Cardiothorac Surg doi: 10.1510/mmcts.2004.000448
11. Gharagozloo F, Margolis M, Tempesta B et al (2009) Robot-assisted lobectomy for early-stage lung cancer: report of 100 consecutive cases. Ann Thorac Surg 88:380–384
12. Wilson JL, Louie BE, Cerfolio RJ et al (2014) Prevalence of nodal upstaging during robotic lung resection in early stage non-small cell lung cancer. Ann Thorac Surg 97:1901–1907
13. Rea F, Marulli G, Bortolotti L et al (2006) Experience with the "da Vinci" robotic system for thymectomy in patients with myasthenia gravis: report of 33 cases. Ann Thorac Surg 81:455–459
14. Rückert JC, Swierzy M, Ismail M (2011) Comparison of robotic and nonrobotic thoracoscopic thymectomy: a cohort study. J Thorac Cardiovasc Surg 141:673–677
15. Wagner OJ, Louie BE, Vallières E et al (2012) Near-infrared fluorescence imaging can help identify the contralateral phrenic nerve during robotic thymectomy. Ann Thorac Surg 94:622–625

Part II

Upper Gastrointestinal Surgery

Esophagectomy for Cancer

5

Richard van Hillegersberg

5.1 Procedure Overview

Minimally invasive esophagectomy (MIE) for patients with esophageal cancer was designed to reduce surgical trauma, resulting in lower rates of morbidity and mortality. MIE has been shown to decrease the blood loss, reduce postoperative complications and shorten hospital stay, with comparable oncologic results [1].

In 2003 the robot-assisted minimally invasive esophagectomy (RAMIE) was developed at UMC Utrecht [2].

5.2 Patient Positioning

The patient is positioned in the left lateral decubitus position, tilted 45° toward the prone position. This semi-prone position keeps the lung out of the operating field. The operating table is flexed, lowering the legs and upper thorax (the patient is positioned with the xyphoid above the pivoting point of the table). This extends the thorax and widens the intercostal space for introducing trocars.

5.3 Robot Positioning and Docking

The bedside cart is brought to the table from the dorsocranial side of the patient (Fig. 5.1).

R. van Hillegersberg (✉)
Department of Surgery, University Medical Center,
Utrecht, The Netherlands
e-mail: r.vanhillegersberg@umcutrecht.nl

G. Spinoglio (Ed), *Robotic Surgery: Current Applications and New Trends*,
Updates in Surgery
DOI: 10.1007/978-88-470-5714-2_5, © Springer-Verlag Italia 2015

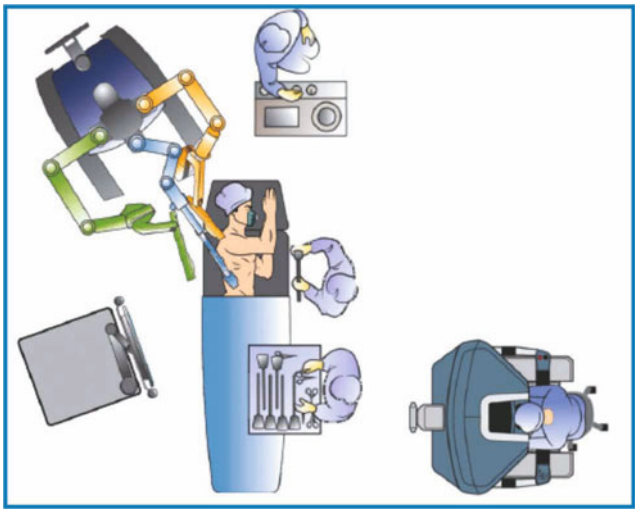

Fig. 5.1 OR Setup. The patient is in left lateral position, toward 45 prone. The robot is docked from the dorsocranial side. (© 2014 Intuitive Surgical, Inc.)

5.4 Trocar Placement

Before incision, the right lung is desufflated after double lumen tube intubation. A 10-mm camera port is placed at the sixth intercostal space, posterior to the posterior axillary line. Under vision, two 8-mm robot-ports are placed just anterior to the scapular rim in the fourth intercostal space and more posterior in the ninth intercostal space. These ports are used for the monopolar thermal hook at arm 1 and Cadiere forceps at arm 2. Two thoracoscopic ports are used in the fifth and seventh intercostal spaces just posterior to the posterior axillary line. These ports are used for conventional thoracoscopic assistance such as suction, traction, and clipping (Fig. 5.2). CO_2 insufflation of the thoracic cavity with 6 mmHg permits excellent vision, without the need for retracting the lung from the operative field. In the case of a noncompliant lung, a retractor can be used.

5.5 Step-by-Step Review of Critical Elements of the Procedure

After division of any pulmonary adhesions and when a proper overview of the operating field is achieved, the right pulmonary ligament is divided. The parietal pleura is dissected at the anterior side of the esophagus from the diaphragm up to the azygos arch. The azygos arch is carefully ligated with robotic Hem-o-lok® ligation clips in arm 1. (Fig. 5.3). Then dissection of the parietal pleura is continued above the aortic arch for a bilateral paratracheal lymph node dissection (Fig. 5.4). The right vagal nerve is dissected just above the level of the carina. Right paratracheal lymph nodes (2R and 4R) are dissected over the superior

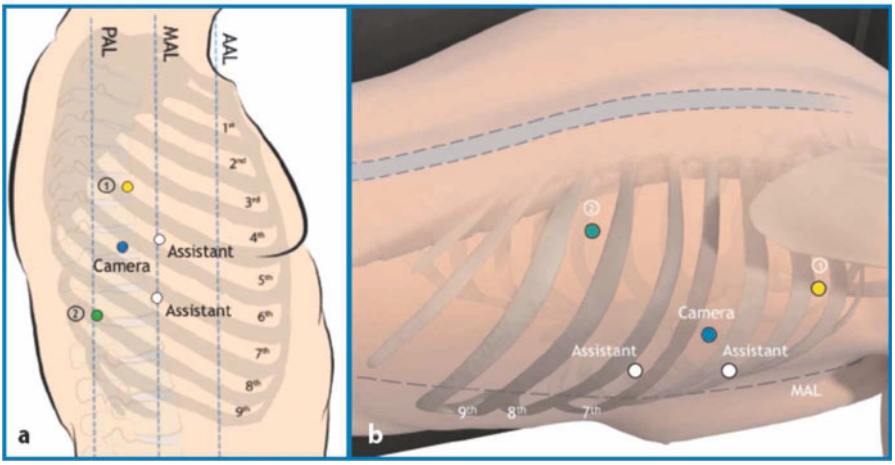

Fig. 5.2 **a** Port position. Robotic arms 1 (*yellow*), 2 (*green*) and camera (*blue*). Two assisting ports (*white*). **b** Port position. Robotic arms 1 (*yellow*), 2 (*green*) and camera (*blue*). Two assisting ports (*white*). (© 2014 Intuitive Surgical, Inc.)

caval vein up to the level of the right subclavian artery and vein (Fig. 5.5). Left paratracheal lymph nodes (2L and 4L) are dissected along the left pleura and left recurrent nerve, that runs just at the tracheal rim. Often the left carotid artery is visualized. Subsequently, the parietal pleura is dissected at the posterior side of the esophagus, cranially to caudally, along the azygos vein toward the diaphragm, including the thoracic duct. At the level of the diaphragm, the thoracic duct is clipped with a 10-mm endoscopic clipping device (Endoclip™ II; Covidien, Mansfield, Massachusetts, USA) to prevent postoperative chylous leakage.

At the level of the diaphragm, a Penrose drain is placed around the esophagus to provide traction by the assistant, facilitating esophageal lifting off the pericardium and pulmonary veins. The esophagus is then resected en bloc with the periesophageal (station 8) mediastinal lymph nodes and the thoracic duct from the diaphragm up to the thoracic inlet. The aorta is completely exposed and aortoesophageal vessels are identified and clipped with Endoclip by the assisting surgeon. Finally the aortopulmonary window (station 5), subcarinal nodes (station 7) are dissected. The subcarinal nodes are very fragile and bleed easily, therefore first the nodes are dissected along the carinal cartilage and then the surrounding fascia is dissected, preventing grasping of the nodes. A 24-Fr chest tube is placed, and the lung is insufflated under direct vision.

After completion of the robot-assisted thoracoscopic esophageal mobilization, the patient is put in the supine position. An 11-mm camera port is introduced left paraumbilically, and an 11-mm working port is placed at the left midclavicular line at the umbilical level. A 5-mm working port is placed more cra-

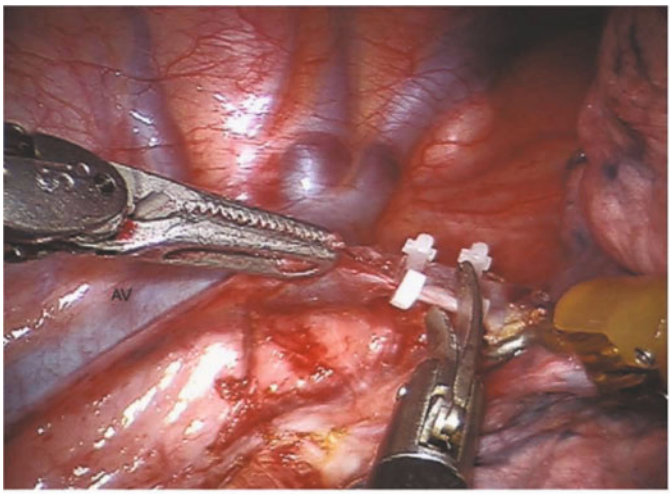

Fig. 5.3 Division of the Azygos vein over the esophagus

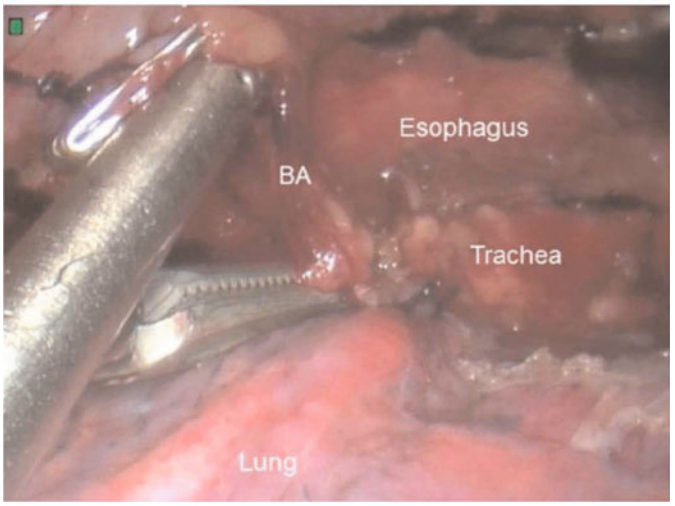

Fig. 5.4 Identification and dissection of a bronchial artery (*BA*) at the level of the crossing azygos vein after dissection of the vein

nially at the right midclavicular line. A 5-mm assisting port is placed in the left subcostal area, and a 12-mm port is placed pararectally right for the liver retractor. The abdomen is insufflated to a carbon dioxide pressure level of 15 mmHg.

The hepatogastric ligament is opened. The greater and lesser curvatures are dissected with ultrasonic harmonic scalpel (Harmonic Ace®, Ethicon Endosurgery, Johnson&Johnson, New Brunswick, New Jersey, USA). The hiatus is opened, and the distal esophagus is dissected from the right and left crus. The carbon dioxide pressure level is reduced to 6 mmHg to avoid excessive intrathoracic pressure and a chest tube is placed in the left pleural sinus. Dissection and lymphadenectomy

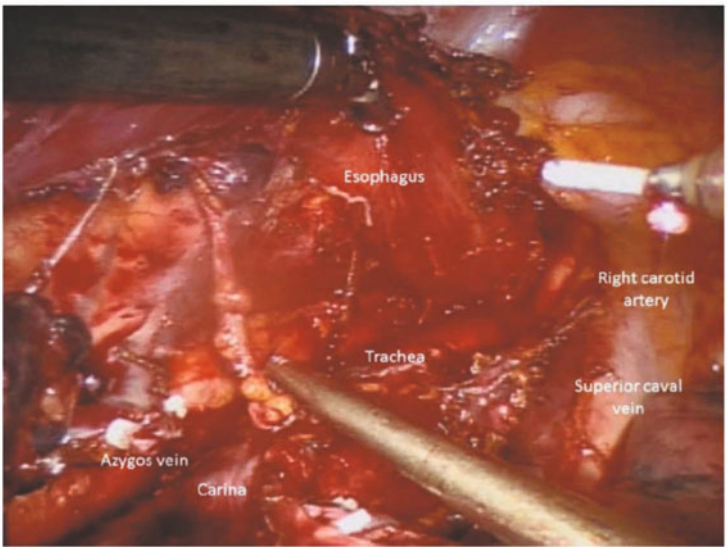

Fig. 5.5 Excellent view of thoracic inlet

then continues around the celiac trunk. The left gastric artery and vein are then transected at their origin with Hem-o-lok® ligation clips (Teleflex Medical , NC, US). Abdominal lymphadenectomy includes lymph nodes surrounding the left gastric artery and the lesser omental lymph nodes.

The cervical esophagus is mobilized through a left-side longitudinal neck incision along the sternocleidoid muscle. No formal cervical lymph node dissection is carried out, but cervical lymph nodes are dissected if lymph node metastases are suspected macroscopically during the cervical phase of esophagectomy. The esophagus is dissected and a cord is attached to the proximal part of the specimen to enable pull-up of the gastric conduit along the anatomical tract of the esophagus.

The esophagus and surrounding lymph nodes are pulled into the abdomen under laparoscopic vision. A 7-cm transverse incision is made at the level of the left paraumbilical port for extraction of the specimen and stomach using a wound protector.

Outside the abdomen, a 5-cm-wide gastric tube is constructed with staplers (GIA TM 80, 3.8 mm; Covidien, Dublin, Ireland), and the stapled line is oversewn with 3-0 polydioxanone. Routine extracorporal oversewing was reintroduced as two serious complications occurred when the staple line was not oversewn [3].The specimen consisting of the esophagus and cardia of the stomach is sent for pathological examination. After the gastric tube has been pulled to the neck, a hand-sewn end-to-side esophagogastrostomy is performed in the neck using 3-0 polydioxanone single-layer running sutures. Excess gastric tubing is removed using a GIA stapler.

A feeding jejunostomy (Freka® FCJ-Set, Fresenius Kabi AG, Bad Homburg vd H., Germany) is placed at the level of the transverse incision.

5.6 Advantages, Limitations and Relative Contraindications (Personal Experience and Literature Outcomes)

Optimal treatment for esophageal cancer consists of transthoracic en bloc esophagectomy (TTE) with an extensive mediastinal lymph node dissection. This approach through thoracotomy is accompanied by significant morbidity, mainly consisting of cardiopulmonary complications. To reduce surgical trauma and morbidity of open transthoracic esophagectomy, less invasive surgical techniques such as transhiatal esophagectomy (THE) and minimally invasive esophagectomy (MIE) have been introduced.

Recent analyses of the MIE to date have shown a decreased operative blood loss, reduced complication rate and shorter hospital stay [1, 4, 5]. However, conventional endoscopic surgery has important limitations, such as a two-dimensional view, a disturbed hand-eye-coordination and limited degrees of freedom. Robotic systems have been developed to overcome these limitations [6]. During esophagectomy, the robotic platform enables the surgeon to perform an accurate mediastinal dissection of the esophagus en bloc with surrounding lymphatic tissue and mediastinal fat, often harboring metastatic disease. Robot-assisted minimally invasive esophagectomy (RAMIE) in conjunction with conventional laparoscopy has been shown to be technically feasible. Moreover, it provides sufficient oncological resection and is associated with low blood loss [2, 7]. The abdominal phase of the operation can also be performed robotically. In our experience this is easily feasible, however there are several drawbacks. The large area in the upper abdomen that needs to be dissected can often not be reached from a single docking position. Most importantly, the dissection of the greater curvature is difficult with robotic harmonic scissors as the articulation of the tip is lacking. We expect a much better performance with the Vessel sealer®. However, much care should be given not to damage the gastroepiploic vessels which supply the future gastric tube.

For the thoracic part, the left lateral decubitus position is preferred as conversion to thoracotomy is easily performed. When the robotic system is in place, access to the patient in case of emergency is limited. Therefore, the surgical team should be capable of rapidly removing the robot if required. This is not possible in the prone position.

Post-operatively, patients are transferred to the intensive care unit (ICU). After leaving the operating room, mechanical ventilation is continued briefly and the patients are usually extubated later that evening. After 1 day in the ICU, patients are transferred to a medium care (MC) ward.

Important for postoperative care are a nasogastric tube, feeding jejunostomy and an epidural catheter. The nasogastric tube is used for gastric decompression and to provide splinting in case of anastomotic dehiscence.

Appropriate patient selection is essential to a successful esophageal surgery program. Approximately 30–40% of esophageal cancer patients are eligible to undergo an esophagectomy with curative intent, taking into account tumor stage

and co-morbidity. The minimally invasive approach may offer a greater percentage of patients a potentially curative surgical resection. Patients with stage I–III disease, i.e., T1–T4a tumors, and no evidence of distant metastases are eligible to RAMIE [8].

With our growing experience, especially patients with tumors in the upper mediastinum and with paratracheal lymph node metastases were resected successfully with the thoracoscopic robotic approach (Fig. 5.5). These tumors are often in close contact with the upper mediastinal blood vessels (superior caval vein, carotid artery and subclavian artery and vein). The thoracic inlet is very difficult to reach with an open or conventional thoracoscopic approach. With the robot, this area can be reached without any limitations. This extends the operative and potentially curative options in these specific groups of patients substantially. A recent report of a Korean group shows that a very extensive complete paratracheal lymph node dissection can be performed with the robot [9].

5.7 Results of RAMIE

Following our initial report of RAMIE in 2009, we analyzed the following consecutive series of 108 patients until 2011. Esophageal dissection was completed thoracoscopically in 88 patients. Conversion to thoracotomy was necessary in 12 patients due to: bulky adhesive tumor in the mediastinum (4); bleeding that could not be controlled thoracoscopically (4); insufficient collapse of the right lung (2); or inadequate thoracoscopic trocar position (2). Conversion to a transhiatal procedure was necessary in 9 patients due to: insufficient collapse of the right lung (6); inadequate thoracoscopic port position (1); pleural adhesions (1); or enlarged right cardiac atrium (unusual anatomy) (1). Conversion of the laparoscopic abdominal phase was required in 3 patients due to bleeding that could not be controlled laparoscopically (1), locally advanced tumor requiring total gastrectomy with colonic interposition (1) or very low position of the greater curvature (1). There was a significant decrease in the percentage of conversions between the first 54 and second 54 patients (13 (24%) vs. 7 (13%) respectively; $p < 0{\cdot}001$).

The median set up time for the robot was 17 minutes (range 5–91). The median duration of the total procedure was 381 minutes (range 264–550). The thoracoscopic phase (88 patients) had a median duration of 175 minutes (range 108–241). There was a significant decrease in thoracoscopic operative time between the first 44 and second 44 patients who completed the thoracic phase thoracoscopically (199 min versus 166 min respectively; $p < 0{\cdot}001$).

We found a high percentage (95%) of radical resections despite the high rate of T3 tumors (78%) and only 64% neoadjuvant therapy. A median of 26 dissected lymph nodes were retrieved. Follow-up was at least 25 months with a median follow-up of 34 months. Median disease-free survival was 21 months and median overall survival was 29 months, with a 5-year overall survival of 40%. The percentage of in-hospital pulmonary infections after RAMIE in our series

was 34% (unpublished data).

Our results from robot-assisted esophagectomy are in concordance with a recently published systematic review [10]. This systematic review included 9 articles (130 cases) describing robot-assisted esophagectomy. It was concluded that robot-assisted esophagectomy was a feasible and safe technique. In terms of short-term oncological outcomes, RAMIE was at least equivalent to the open transthoracic approach for esophageal cancer. The systematic review strongly emphasized the need for well conducted randomized controlled trials including long-term survival to prove the superiority of robot-assisted minimally invasive thoracolaparoscopic esophagectomy over open transthoracic esophagectomy. Therefore, we initiated the ROBOT trial (ClinicalTrial.gov Identifier: NCT01544790) to compare RAMIE with open transthoracic esophagectomy. Results from this randomized controlled trial are to be expected in 2016 [11].

References

1. Luketich JD, Pennathur A, Awais O et al (2012) Outcomes after minimally invasive esophagectomy: review of over 1000 patients. Ann Surg 256:95–103
2. van Hillegersberg R, Boone J, Draaisma WA et al (2006) First experience with robot-assisted thoracoscopic esophagolymphadenectomy for esophageal cancer. Surg Endosc 20:1435–1439
3. Boone J, Rinkes IH, van Hillegersberg R (2006) Gastric conduit staple line after esophagectomy: to oversew or not? J Thorac Cardiovasc Surg 132:1491–1492
4. Biere SS, van Berge Henegouwen MI, Maas KW et al (2012) Minimally invasive versus open oesophagectomy for patients with oesophageal cancer: a multicentre, open-label, randomised controlled trial. Lancet 379:1887–1892
5. Verhage RJ, Hazebroek EJ, Boone J, van Hillegersberg R (2009) Minimally invasive surgery compared to open procedures in esophagectomy for cancer: a systematic review of the literature. Minerva Chir 64:135–146
6. Ruurda JP, Draaisma WA, van Hillegersberg R et al (2005) Robot-assisted endoscopic surgery: a four-year single-center experience. Dig Surg 22:313–320
7. Kernstine KH (2004) Robotics in thoracic surgery. Am J Surg 188: 89S–97S
8. Boone J, Schipper ME, Moojen WA et al (2009) Robot-assisted thoracoscopic oesophagectomy for cancer. Br J Surg 96:878–886
9. Kim DJ, Park SY, Lee S et al (2014) Feasibility of a robot-assisted thoracoscopic lymphadenectomy along the recurrent laryngeal nerves in radical esophagectomy for esophageal squamous carcinoma. Surg Endosc 28:1866–1873
10. Clark J, Sodergren MH, Purkayastha S et al (2011) The role of robotic assisted laparoscopy for oesophagogastric oncological resection; an appraisal of the literature. Dis Esophagus 24:240–250
11. van der Sluis PC, Ruurda JP, van der Horst S et al (2012) Robot-assisted minimally invasive thoraco-laparoscopic esophagectomy versus open transthoracic esophagectomy for resectable esophageal cancer, a randomized controlled trial (ROBOT trial). Trials 13:230

Anti-reflux Procedures and Cardioesophagomyotomy

6

Gianluigi Melotti, Vincenzo Trapani, Marzio Frazzoni, Michele Varoli, and Micaela Piccoli

6.1 Anti-reflux Procedures

6.1.1 Introduction

Currently, gastroesophageal reflux disease (GERD) is defined as a condition that develops when the reflux of gastric contents into the esophagus leads to troublesome symptoms and/or complications [1]. In Western countries, GERD is the most common chronic disease in the adult population with a 20% prevalence. The typical reflux syndrome includes heartburn and regurgitation. Barrett's esophagus is the most dreaded complication of GERD, occurring in 2% of the general adult population: it predisposes sufferers to esophageal adenocarcinoma, the fastest growing cause of cancer mortality in Western countries [2]. No more than 20% of patients with typical reflux symptoms have erosions of the esophageal mucosa at endoscopic examination, i.e. have erosive reflux disease. The vast majority of patients with the typical reflux syndrome have normal endoscopic findings: those responding to proton pump inhibitor (PPI) therapy have nonerosive reflux disease whereas those with PPI-refractory typical symptoms should undergo 24 h impedance-pH monitoring to discriminate between PPI-refractory GERD and functional heartburn [3, 4]. PPIs provide rapid symptomatic relief in up to 80% of patients with the typical reflux syndrome, transforming the vast majority of acid refluxes into less toxic weakly acidic refluxes. However, typical GERD symptoms recur within 1 year in more than 90% of patients after PPI-withdrawal, in many of them within few days: thus, many patients become PPI-dependent and surgical therapy has been regarded as a treatment option for these patients [5].

M. Piccoli (✉)
General Surgery Unit, "Sant'Agostino-Estense" New Hospital, Baggiovara (MO), Italy
e-mail: m.piccoli@ausl.mo.it

G. Spinoglio (Ed), *Robotic Surgery: Current Applications and New Trends*, Updates in Surgery
DOI: 10.1007/978-88-470-5714-2_6, © Springer-Verlag Italia 2015

Currently, laparoscopic fundoplication is considered the standard surgical treatment for GERD because it affords persistent relief of heartburn in 90% of PPI-responsive patients at 20-year follow-up [6, 7]. Up to 20% of patients fail to respond, either partially or completely, to PPI therapy at standard and even high dosages. Given the high efficacy of laparoscopic fundoplication in curing PPI-responsive GERD, it is the only treatment modality currently recommended for overcoming PPI failures [5].

Before surgical intervention, a firm diagnosis of GERD is required, particularly in patients with endoscopy-negative heartburn. Currently, impedance-pH monitoring is the gold-standard preoperative reflux test; it must always be preceded by esophageal manometry to rule out severe esophageal motility disorders [5].

6.1.2 Procedure Overview

In 1991, Dallemagne [8] described the laparoscopic technique for the Nissen fundoplication. The laparoscopic approach had a lot of benefits over the traditional open approach, including improved cosmesis, reduced morbidity, decreased hospital stay, decreased respiratory complications, and faster recovery.

The Nissen fundoplication, consisting of a total (360°) wrap, is the most commonly performed anti-reflux operation. Despite general reflux alleviation, dysphagia and gas bloating are the primary causes of dissatisfaction after Nissen fundoplication. In order to reduce the postoperative dysphagia and gas bloating, a variety of procedures in which the fundus is only partially wrapped have been proposed, including the Toupet fundoplication, consisting of a posterior (270°) wrap, and the Dor fundoplication, consisting of an anterior (180°) wrap. Similar efficacy on heartburn/regurgitation and reflux parameters but less dysphagia and gas bloat have been reported when the Toupet fundoplication has been compared with the Nissen fundoplication [9, 10]: it should be noted, however, that with both techniques the fundoplication was performed by fixing the wrap to the anterior wall of the esophagus. The Nissen procedure can also be carried out without anchoring the fundoplication: no wrap slipping, negligible gas bloating, and cumulative incidence of postoperative dysphagia quite similar to that reported with the Toupet procedure, in conjunction with normal reflux parameters and sustained symptom remission in the vast majority of cases have been found with this technique [11, 12]. To prevent postoperative dysphagia, other key technical issues must be considered, including division of the short gastric vessels whenever deemed necessary in order to adequately mobilize the esophagus and to make the fundoplication tension-free, and insertion of a 52-Fr bougie into the esophagus during construction of the wrap.

Robot-assisted surgery was developed to overcome the limitations of laparoscopic technology and to expand the benefits of minimal invasive surgery. The first report of robot-assisted fundoplication was published by Meininger in 2001 [13] and its use has been increasing since then.

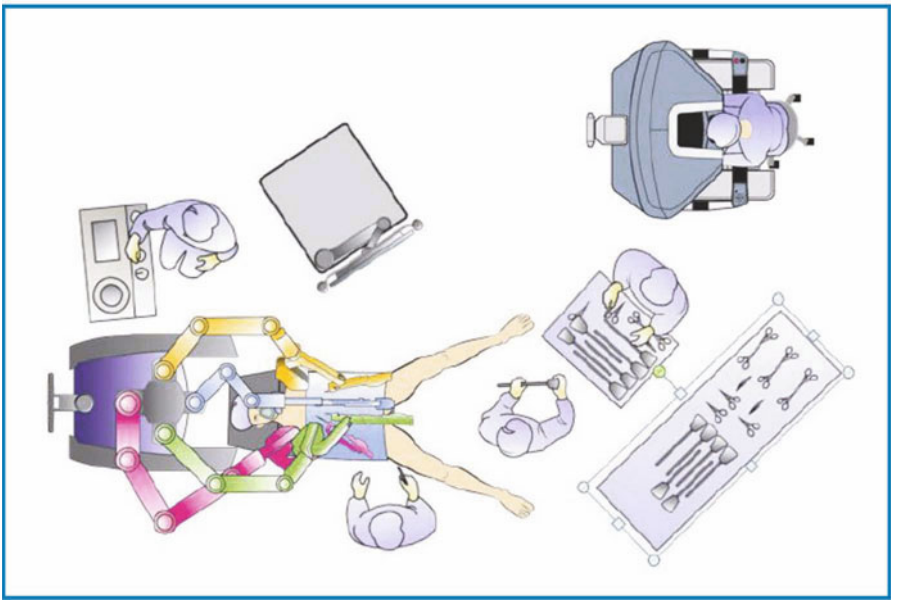

Fig. 6.1 OR Setup. (© 2014 Intuitive Surgical, Inc.)

6.1.3 Patient Positioning

After satisfactory induction of general endotracheal anesthesia, the patient is placed in the semi-lithotomy position (head up approximately 30°), legs spread.

6.1.4 Robot Positioning and Docking

The patient-side cart is positioned at the head of the patient and it includes four robotic arms; the vision system is at the left side of the bed, and the surgeon console is distant from the bed, but in the same operating room (Fig. 6.1).

6.1.5 Trocar Placement

After a 12 mmHg pneumoperitoneum is created with a Veress needle in the left hyphocondrium, four robotic trocars (one 12-mm disposable for the camera, three 8-mm reusable) are inserted as shown in Fig. 6.2.

The first trocar (12 mm for camera) is placed about 3 cm to the left of the umbilicus, approximately two finger-breadths above the umbilicus. Two 8-mm trocars are placed in the right and left upper quadrant in the mid-clavicular line for two operative robotic arms. One 8-mm trocar, inserted about two finger-breadths below the costal margin in the right anterior axillary line, is used for the third robotic arm

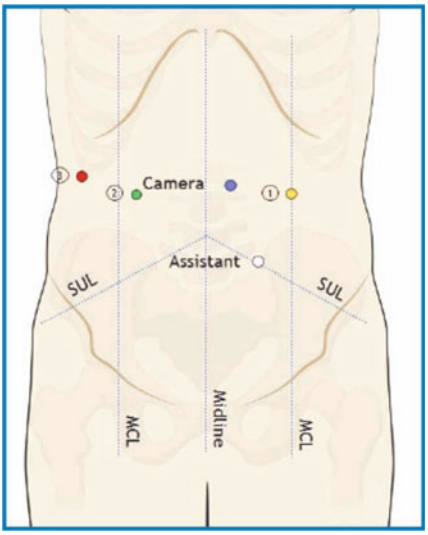

Fig. 6.2 Trocar positioning. (© 2014 Intuitive Surgical, Inc.)

to retract the liver. A 5–11 mm assistant port is placed about 2 cm under the umbilical line, between the midline and the mid-clavicular line, in the left side. The setup of the robot is usually performed by the assistant at the bedside.

6.1.6 Critical Elements of the Procedure

The operative technique performed by robot is essentially the same as described by Dallemagne [14] and Cadière [15] for the laparoscopic approach. The main differences are in the trocar position (as shown before). Operative robotic arms perform the same procedure that is made by a surgeon's arms in a laparoscopic technique.

The assistant surgeon sits between the patient legs and uses the assistant port to insert instruments (clip-applier, stitches, scissors, etc). The whole dissection can be carried out utilizing monopolar cautery by a hook dissector with a full degree of articulation. A floppy 360° fundoplication is constructed using the anterior wall of the fundus. The division of the upper gastric vessels is usually necessary. The fundoplication is sutured neither to the esophagus nor to the diaphragm but is calibrated onto a 52 Fr bougie, which is inserted at the start of the procedure.

6.1.7 Advantages of Robot-assisted Laparoscopic Fundoplication

Two prospective randomized studies have compared robot-assisted and conventional laparoscopic fundoplication [16, 17]. In the study by Morino and co-workers [16], conventional or robot-assisted laparoscopic Nissen fundoplication

(LNF) was carried out by three expert surgeons: nonsignificant differences were found in the postoperative clinical outcome and in pH-metric parameters between the two groups of patients. In the study by Draaisma and co-workers [17], 25 patients treated with conventional LNF were compared to 25 patients treated with robot-assisted LNF: similar postoperative pH-metric results were found in the two groups of patients but the study detected a statistically significant difference of only 35% and the two surgical procedures were carried out by seven surgeons.

In a recent study comparing 44 patients who underwent robot-assisted laparoscopic fundoplication with 44 patients who underwent conventional laparoscopic fundoplication, at a 3-month postoperative follow-up no difference in terms of heartburn remission was found but normalization of acid reflux was detected significantly more frequently in patients treated with robotic surgery (100% vs. 86%, P =0.026) [18]. It should be noted that in this study all the interventions were carried out by the same surgeon. The potential advantages of robotic surgery include greater precision due to the anti-tremble filter, better vision as a result of the three-dimensional imaging of the surgical field, and reduced bleeding. Taken together, these advantages can explain these slightly but significantly better results after robot-assisted laparoscopic fundoplication in terms of postoperative acid reflux control. Currently, anti-reflux surgery is mainly advised for PPI-refractory GERD patients and alternatives of proven efficacy are not available [5]. Even a 14% gain in normalization of postoperative acid reflux parameters provided by the robot-assisted technique can be clinically relevant for PPI-refractory patients. It can be concluded that in centers where robot-assisted laparoscopic fundoplication is available, it should be preferred to the conventional technique in patients with PPI-refractory GERD.

6.2 Cardioesophagomyotomy

6.2.1 Introduction

Cardioesophagomyotomy is the standard surgical procedure currently recommended for achalasia. Achalasia is a rare primary motility disorder of the esophagus that affects one person in 100,000 per year and is characterized by the absence of esophageal peristalsis and incomplete relaxation of a frequently hypertensive lower esophageal sphincter (LES) in response to swallowing. Most patients present with dysphagia for solids and liquids and regurgitation of undigested food. Other common symptoms include chest pain, heartburn, weight loss, and nocturnal cough. The first diagnostic step is to rule out anatomical lesions by using endoscopy or radiology. In early stages, both endoscopy and radiology may be completely normal. Manometry represents the diagnostic gold standard with over 90% accuracy.

No treatment can restore muscular activity to the denervated esophagus and every treatment for achalasia is directed at reducing the gradient across the LES.

Treatment options include medical therapy, such as nitrates and calcium channel blockers; endoscopic therapy, such as pneumatic dilation or botulinum toxin injection; and operative cardioesophagomyotomy [19].

Botulinum toxin injection is safe but less effective than balloon dilation; it requires retreatment and leads to scar formation in the submucosal plane, which can result in a more difficult myotomy and greater rates of mucosal perforation (up to 30%) during dissection. It should be reserved for patients who are poor candidates for other more effective treatment options.

Currently, except for high-risk or elderly patients, pneumatic dilation or laparoscopic cardioesophagomyotomy with anterior fundoplication (Heller-Dor) represent the standard management for achalasia. Using a graded approach with increasing diameters of the polyethylene balloon dilator from 3.0 to 4.0 cm, up to a 93% response rate has been achieved during a follow-up period of up to 4 years with a relatively low perforation risk (3%). In a recent multicenter randomized trial, endoscopic dilation (up to three series of pneumatic dilations) and laparoscopic Heller-Dor had comparable success at two years: 92% for dilation and 87% for myotomy [20].

The robot-assisted cardioesophagomyotomy has been described for the first time by Horgan et al. in 2005 [21].

Recently, peroral endoscopic myotomy (POEM) has been introduced as a promising alternative to the current treatments [22]. Several open label studies have been published showing excellent short term results with only a few complications. However, there is currently insufficient evidence to perform POEM as routine achalasia treatment. Until the long-term efficacy data from randomized controlled trials are available, POEM should be restricted to centers participating in clinical trials.

6.2.2 Patient and Robot Positioning, Trocar Placement and Docking

This is described in Sections 6.1.3–6.1.5.

6.2.3 Critical Elements of the Procedure

The operative technique to perform a robot-assisted Heller-Dor procedure is essentially the same as described by Ancona et al. for the laparoscopic procedure [23]. The main differences are in the trocar position [21]. We usually insert an endoscope at the beginning of the surgical procedure, to detect the squamocolumnar junction as the landmark to start esophagomyotomy, to check the complete dissection of muscular fibers, and to identify possible microperforations of the mucosa and to assist the related suturing procedure. The same endoscope is used at the end of the procedure to calibrate the Dor fundoplication. Only the

anterior part of the esophagus is dissected, respecting the posterior attachments. The dissection and myotomy are carried by robotic articulated hook electrocautery that, thanks to the elimination of physiological tremor, allows a finest dissection with less bleeding.

6.2.4 Advantages of Robot-assisted Cardioesophagomyotomy

In a retrospective, multicenter study, esophageal perforations were more frequent after conventional laparoscopic (16%) than robot-assisted cardioesophagomyotomy (0%) [21]. These findings have been confirmed in a prospective, single-center study [24]. However, it must be acknowledged that perforations are immediately recognized and repaired using intracorporeal suturing techniques and a recent multicenter retrospective analysis concluded that robotic and laparoscopic cardioesophagomyotomy can be considered equivalent in terms of safety and efficacy [25].

References

1. Katz P, Gerson L, Vela M (2013) Guidelines for the diagnosis and management of gastroesophageal reflux disease. Am J Gastroenterol 108:308–328
2. Fitzgerald RC, Di Pietro M, Ragunath K et al (2014) British Society of Gastroenterology guidelines on the diagnosis and management of Barrett's oesophagus. Gut 63:7–42
3. Frazzoni M, Conigliaro R, Mirante VG et al (2012) The added value of quantitative analysis of on-therapy impedance-pH parameters in distinguishing refractory non-erosive reflux disease from functional heartburn. Neurogastroenterol Motil 24:141–e87
4. Frazzoni M, Manta R, Mirante VG et al (2013) Esophageal chemical clearance is impaired in gastro-esophageal reflux disease – A 24h impedance-pH monitoring assessment. Neurogastroenterol Motil 25:399–e295
5. Katz P, Gerson L, Vela M (2013) Guidelines for the diagnosis and management of gastroesophageal reflux disease. Am J Gastroenterol 108:308–328
6. Dallemagne B, Perretta S (2011) Twenty years of laparoscopic fundoplication for GERD. World J Surg 35:1428–1435
7. Engstrom C, Cai W, Irvine T et al (2012) Twenty years of experience with laparoscopic antireflux surgery. Br J Surg 99:1415–1442
8. Dallemagne B, Weerts JM, Jehaes C et al (1991) Laparoscopic Nissen fundoplication: preliminary report. Surg Laparosc Endosc 3:138–143
9. Broeders JA, Bredenoord AJ, Hazebroek EJ et al (2012) Reflux and belching after 270 degree versus 360 degree laparoscopic posterior fundoplication. Ann Surg 255:59–65
10. Koch OO, Kaindlstorfer A, Antoniou SA et al (2013) Comparison of results from a randomized trial 1 year after laparoscopic Nissen and Toupet fundoplications. Surg Endosc 27:2383–2390
11. Frazzoni M, Conigliaro R, Melotti G (2011) Reflux parameters as modified by laparoscopic fundoplication in 40 patients with heartburn/regurgitation persisting despite PPI therapy. A study using impedance-pH monitoring. Dig Dis Sci 56:1099–1106
12. Frazzoni M, Piccoli M, Conigliaro R et al (2013) Refractory gastroesophageal reflux disease as diagnosed by impedance-pH monitoring can be cured by laparoscopic fundoplication. Surg Endosc 2013; 27:2940–2946

13. Meininger DD, Byhahn C, Heller K et al (2001) Totally endoscopic Nissen fundoplication with a robotic system in a child. Surg Endosc 11:1360
14. Dallemagne B (1999) Treatment of the gastroesophageal reflux syndrome. In Meinero M. Mouret Ph. Melotti G, (eds.): Laparoscopic surgery; the nineties. Masson, Milan pp. 251–260
15. Cadière GB (1995) Trattamento video-laparoscopico del reflusso gastro-esofageo-E.M.C. Roma Tecniche Chirurgiche-Addominale, 40189, p10
16. Morino M, Pellegrino L, Giaccone C et al (2006) Randomized clinical trial of robot-assisted versus laparoscopic Nissen fundoplication. Br J Surg 93:553–558
17. Draaisma WA, Ruurda JP, Scheffer RCH et al (2006) Randomized clinical trial of standard laparoscopic versus robot-assisted laparoscopic Nissen fundoplication for gastro-oesophageal reflux disease. Br J Surg 93:1351–1359
18. Frazzoni M, Conigliaro R, Colli G et al (2012) Conventional versus robot-assisted laparoscopic Nissen fundoplication. A comparison of postoperative acid reflux parameters. Surg Endosc 26:1675–1681
19. Stefanidis D, Richardson W, Farrell TM et al (2012) SAGES guidelines for the surgical treatment of esophageal achalasia. Surg Endosc 26:296–311
20. Boeckxstaens GE, Annese V, Bruley des Varannes S et al (2011) Pneumatic dilation versus laparoscopic Heller's myotomy for idiopathic achalasia. New Engl J Med 364:1807–1816
21. Horgan S, Galvani C, Gorodner MV et al (2005) Robotic-assisted Heller myotomy versus laparoscopic Heller myotomy for the treatment of esophageal achalasia: multicenter study. J Gastrointest Surg 9:1020–1030
22. Bredenoord AJ, Rosch T, Fockens P (2014) Peroral endoscopic myotomy for achalasia. Neurogastroenterol Motil 26: 3–16
23. Ancona E, Zaninotto G, Costantini M (2003) Miotomie Esofagee. In: Encycl Mèd Chir (Editions Scientifiques et Medicales Elsevier SAS, Paris) Tecniche Chirurgiche-Addominale, pp. 40–183
24. Huffmanm LC, Pandallai PK, Boulton J et al (2007) Robotic Heller myotomy: A safe operation with higher postoperative quality-of-life indices. Surgery 142:613–20
25. Shaligram A, Unnirevi J, Simorov A et al (2012) How does the robot affect outcomes? A retrospective review of open, laparoscopic, and robotic Heller myotomy for achalasia. Surg Endosc 26:1047–1050

Gastrectomy for Cancer

7

Andrea Coratti, Mario Annecchiarico, and Stefano Amore Bonapasta

7.1 Procedure Overview

The first experiences of robot-assisted gastrectomy (RAG) were published by Giulianotti et al. and Hashizume and Sugimachi in 2003 [1, 2].

Nowadays, the reported results are satisfactory in terms of surgical complications, mortality, conversion rate, length of hospital stay and oncological adequacy; no differences are demonstrated between patients who had robotic and laparoscopic gastrectomy (LG) [3–5].

Robotic surgery for gastric cancer has been demonstrated to overcome intrinsic limitations of conventional laparoscopic surgery thanks to the wristed instruments that allow seven degrees of freedom, the tremor-filter, the three-dimensional vision and the steady image, thus minimizing blood losses, surgical trauma and the improvement of surgeon's dexterity when fine manipulation is required. This can be especially helpful during maneuvers in restricted fields and around major vessels such as in extended lymphadenectomy. Robotic surgery allows the surgeon to reproduce routine D2-lymphadenectomy and to perform enlarged resections and complex reconstructions in the case of advanced disease [6, 7].

Minimally invasive surgery (MIS) can have an important role in the therapeutic strategy for advanced disease. However, to date, MIS is indicated for early gastric cancer but its oncologic safety for advanced gastric cancer remains controversial. Because of the short follow-up time of the major published series, the number of harvested lymph nodes and resection margins have been used as indicators of oncologic acceptability of robotic resection.

M. Annecchiarico (✉)
Department of Oncology, Division of Oncological and Robotic General Surgery, Careggi University Hospital, Florence, Italy
e-mail: mannecchiarico@hotmail.com

G. Spinoglio (Ed), *Robotic Surgery: Current Applications and New Trends*, Updates in Surgery
DOI: 10.1007/978-88-470-5714-2_7, © Springer-Verlag Italia 2015

According to the articles present in the up-to-date literature, RAG with limited lymphadenectomy is indicated for Stage 1a, while RAG with D2 lymphadenectomy is indicated for Stage 1b–2a. Mucosal and submucosal tumors, if eligible, are considered for endoscopic resection first [3, 8]. RAG for more advanced stages is the object of investigations and at present should be performed only in highly specialized centers.

We describe the technique of distal subtotal and total gastrectomy with D2 lymphadenectomy.

7.2 Patient Positioning

The patient is placed in the supine position on a split table. After placing the ports, the patient is moved to an about 15–20° reverse-Trendelenburg position. A nasogastric tube is inserted for gastric decompression.

7.3 Robot Positioning and Docking

The robotic cart is docked from the patient's head (Fig. 7.1a). Correct positioning of the robotic cart is fundamental because its **axis** must coincide with the working axis, coming from the opposite site.

Because the operating table cannot be changed once the robot has been docked, the height and slope of the operating table must be reconfirmed before the robot is docked.

7.4 Trocar Placement

The placement of the ports can be summarized as follows except for some minor variations between authors:

- Pneumoperitoneum of 12 mmHg is achieved with open or blind technique;
- The camera port is inserted in the periumbilical region;
- Under direct vision, three 8-mm robotic ports are placed, two in the upper abdomen at the anterior axillary line on the left (robotic arm, R1) and on the right (robotic arm, R3), and one at the right midclavicular line (robotic arm, R2). In addition, a 12-mm port for the assistant surgeon is placed between the R1 port and the camera port along the left midclavicular line (Fig. 7.1b). However, ports positioning can partially change due to the anatomy of the abdomen and depends on the procedure being performed (subtotal or total gastrectomy), especially for what concerns the camera port;
- The console surgeon controls R1 by the right master, while R2 and R3 are controlled switching the left master. R1 carries the cautery hook or harmonic scalpel for the dominant hand. R2 is used by the nondominant hand with

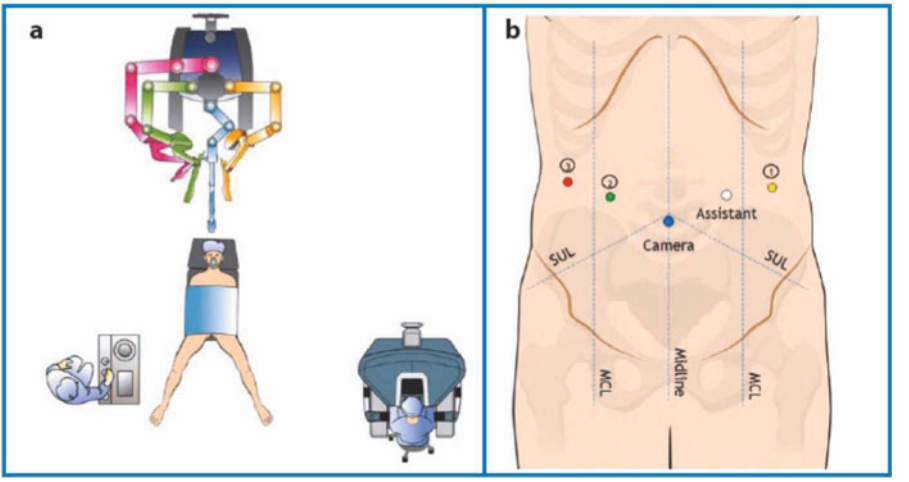

Fig 7.1 OR setup (a) and trocar placement (b). (© 2014 Intuitive Surgical, Inc.)

bipolar forceps. R3 is armed with a grasper and used for retraction and exposure;

- The assistant surgeon aids the console surgeon using the accessory port for aspiration/irrigation, for clip or stapler application and other additional maneuvers.

7.5 Step-by-Step Review of Critical Elements of the Procedure

7.5.1 Distal Subtotal Gastrectomy

7.5.1.1 Exploration

The abdominal cavity is explored in order to assess a definitive staging of disease. Diagnostic peritoneal lavage is performed routinely. Intraoperative ultrasound is performed only if hepatic metastases are suspected. Intraoperative endoscopy can be conducted to establish the location of the tumor and to mark the proximal resection margin.

After laparoscopic exploration, the robotic cart is docked as previously described.

7.5.1.2 Coloepiploic Detachment

A complete coloepiploic detachment is performed dissecting the avascular plane between great omentum and transverse colon. The dissection is extended toward the lower pole of the spleen and the right colonic flexure by using monopolar cautery and bipolar forceps. In case of fatty or obese patients, an advanced

energy device (robotic ultrasound dissector or other devices controlled by assistant surgeon) may be helpful during this surgical step.

Given the wideness of operative field, coloepiploic detachment may be performed even with conventional laparoscopy before docking the robotic arms.

7.5.1.3 Section of Left Gastroepiploic Vessels

The dissection is then continued to the more distal short gastric vessels, which are sectioned at their roots between bipolar coagulation and clips along with the left gastroepiploic vessels. Lymph nodes of stations 4sb and 4d are removed.

7.5.1.4 Section of Right Gastroepiploic and Gastric Vessels

The right gastroepiploic vessels are dissected en bloc with lymphatic tissue. Usually, preliminary exposure of the inferior pancreatic edge is a helpful trick in order to avoid incorrect planes of dissection. A second landmark is represented by the right colonic vein and the Henle's venous trunk: following these ones, the origin of right gastroepiploic vein is identified and sectioned between clips or ligatures. After this, a wide vision is achieved and the right gastroepiploic artery may be dissected safely and divided at its origin from the gastroduodenal artery. Lymph node station 6 is removed en bloc with gastroepiploic vessels. In case of pyloric tumor or lymphatic metastatic disease in station 6, the dissection is extended at the nodes of station 14v (Fig. 7.2a, b).

Finally, the pyloric vessels are identified and sectioned between clips or ligatures, removing the lymph nodes of station 5.

7.5.1.5 Duodenal Section

The duodenum is circumferentially dissected and transected about 2 cm distally to the pylorus, using an endoscopic linear stapler. The staple line of the duodenal stump is not reinforced by oversewing sutures; some stitches are put in case of bleeding.

7.5.1.6 Section of Left Gastric Vessels and Lymphadenectomy

The hepatogastric ligament is divided up to the right side of the cardia. The hepatic hilum and common hepatic artery are exposed by the retraction of the left lobe of the liver, using R3.

The lymph nodes are dissected by hook cautery and bipolar forceps by removing, en bloc, the lymphatic stations along the proper hepatic artery (12a), common hepatic artery (8a/p), celiac trunk (9), proximal splenic artery (11p), and origin of left gastric artery (7) (Fig. 7.2c, d).

The left gastric artery is usually sectioned at its origin between a ligature (proximal stump) and a clip; otherwise, it can be divided using a vascular stapler. A left hepatic artery arising from the left gastric artery may be found in the case of a gastrectomy. In the case of great size or in the absence of a left hepatic artery originating from the common hepatic artery, it should be preserved: the common trunk of the left gastric artery is exposed, the gastric branches are divi-

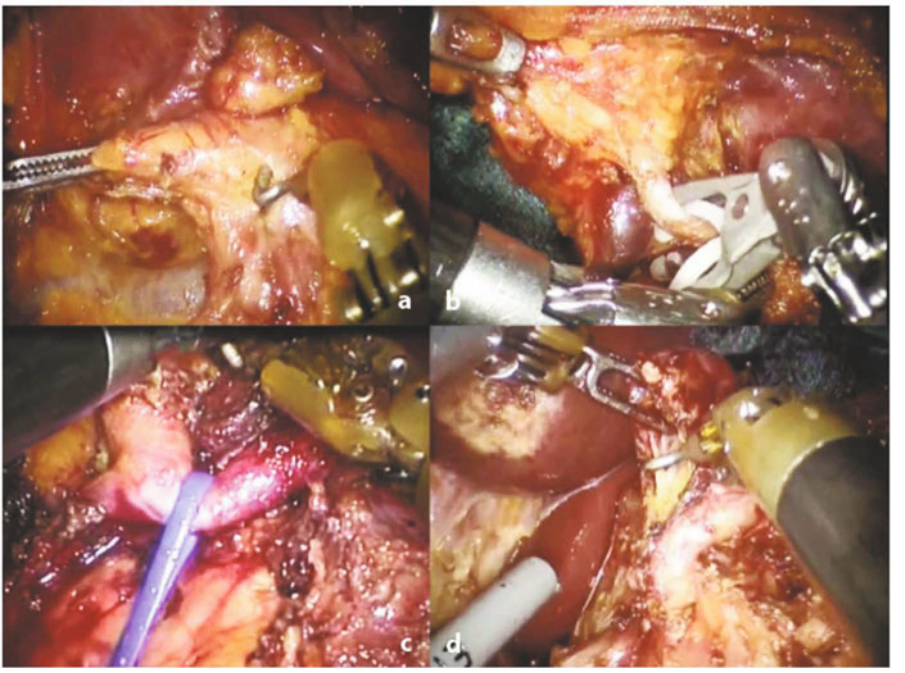

Fig. 7.2 Lymph node dissection. **a** Station 6. **b** Section of right gastroepiploic artery. **c** Retraction of hepatic artery by vessel loop. **d** Station 7

ded and the nodes of station 7 are removed. The left gastric vein is divided between clips or ties.

The gastropancreatic connective tissue is dissected up to esophagogastric junction along the lesser curvature and the lymphatic nodes of station 1–3 (along the right cardia and lesser curvature) are removed.

7.5.1.7 Gastric Transection

Once lymphadenectomy is completed, the stomach is divided at its proximal third by the assistant surgeon, using an articulated linear stapler. The specimen (including stomach, omentum and lymphatic tissue) is placed into a large endoscopic bag and retrieved through a mini-laparotomy (performed on a suprapubic site or enlarging a 12 mm port-site).

7.5.1.8 Reconstruction

The digestive continuity is restored by intra-corporeal gastrojejunal anastomosis (GJA) on a Roux-en-Y jejunal loop. In elderly patients, a Billroth II GJA is usually preferred. In both cases, the jejunal loop is transposed with antecolic reconstruction.

A mechanical GJA is carried out with a side-to-side fashion, on the posterior

wall of the stomach, using a linear stapler. The gastroenterostomy is closed by running absorbable suture. A hand-sewn GJA is an interesting option in case of difficult application of linear stapler, as in case of very small remnant gastric fundus. Whichever technique is used, anastomosis is always tested by injection of methylene blue via the gastric tube.

In the case of GJA on Roux-en-Y, the enteroenterostomy is performed intracorporeally using a linear stapler, or extracorporeally through a left side mini-laparotomy performed for the specimen retrieval. Finally, a drain is placed near the duodenal stump.

7.5.2 Total Gastrectomy

The surgical steps are the same as for distal gastrectomy, except for the following: division of the short gastric vessels and dissection along the gastro-splenic ligament, extent of lymphadenectomy, restoring of the digestive continuity.

7.5.2.1 Section of Short Gastric Vessels

The gastrosplenic ligament is sectioned and all short gastric vessels are divided: the hemostasis is ensured by clips and bipolar forceps (or advanced energy devices). The lymphatic station 4sa is removed and the gastric fundus is mobilized.

7.5.2.2 Lymphadenectomy

In order to achieve a correct D2 lymphadenectomy, the dissection is extended removing the nodes on the distal splenic artery (station 11d) and the splenic hilum (station 10); the spleen is preserved, unless there is massive lymphatic metastasis of the hilum or direct infiltration of the organ.

The lymphatic dissection is enlarged to remove the nodes on the left side of the cardia (station 2).

7.5.2.3 Esophageal Transection

The distal esophagus is exposed to achieve a safe resection margin and a good stump for the anastomosis. The cardia is closed with a loop and the distal esophagus is divided by robotic scissors.

7.5.2.4 Reconstruction

A long Roux-en-Y is made extracorporeally through the left-side mini-laparotomy. The esophagojejunal anastomosis (EJA) can be fashioned both with a circular stapler or robot-assisted hand-sewing technique.

Up to a year ago, we mainly performed mechanical EJA. To fashion this anastomosis, a purse string is carried out on the esophageal stump by robotic hand-sewn technique; the anvil of a 25 mm or 29 mm circular stapler is inserted into the esophageal stump, and the purse string is closed (Fig. 7.3c, d). The circular stapler is then inserted into the jejunal loop and introduced inside the abdomen

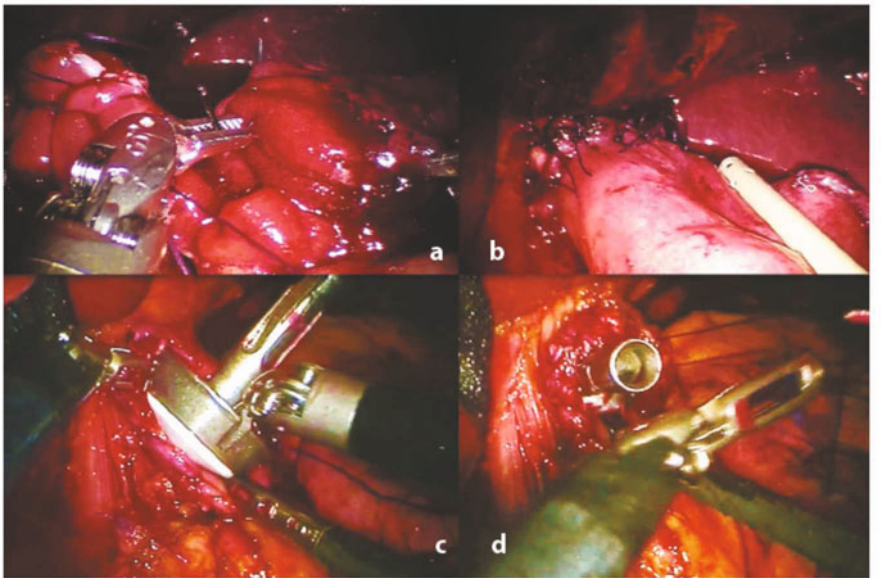

Fig. 7.3 Esophagojejunostomy. Hand-sewn end-to-side esophagojejunostomy (**a**, **b**); insertion of the anvil into the esophageal stump and closure of the purse string (**c**, **d**)

through the left-side mini-laparotomy; it can be facilitated by the application to the mini-laparotomy of a hand-port device. When the stapler is inside the abdominal cavity and the pneumoperitoneum is re-established, the end-to-side EJA is performed with standard laparoscopic control. The stump of jejunal loop is closed by a linear stapler.

More recently, we have introduced a technique of hand-sewn end-to-side EJA with Roux-en-Y reconstruction. After the division of the esophagus, the mucosa is approached to the muscular layer of the proximal esophageal stump with absorbable 4.0 or 5.0 stitches. The EJA is then carried out with two 3.0 absorbable running sutures (posterior and anterior plane); in the case of a small esophageal stump, the anterior suture is performed by interrupted stitches (Fig. 7.3a, b).

In both techniques, the anastomosis is always tested by injecting methylene blue via the gastric tube.

Two drains are placed near the duodenal stump and the EJA, respectively.

7.6 Advantages, Limitations and Outcomes of Robotic Gastrectomy

7.6.1 Technical Aspects

Robotic technology can overcome most of the drawbacks of conventional laparoscopy. It provides the surgeon with an advanced system for viewing and

manipulation, and the physiologic tremor is eliminated using a computerized mechanical interface. The magnified, three-dimensional, high-definition vision and the stability of the camera platform make the robotic console similar to a surgical microscope, enhancing the skill of surgeons in performing difficult dissections and suturing techniques [6, 7]. Articulate endoscopic instruments provide seven degrees of freedom to reproduce the movements of the human hand inside the abdominal cavity, with coaxial alignment of the eyes, hands, and tool tip image [8]. Furthermore, the robotic console reduces ergonomic discomfort, enabling the surgeon to maintain a comfortable position for many hours if needed. The intrinsic advantages of the da Vinci® Surgical System can be helpful in making easier lymph node dissection and intracorporeal anastomosis.

During a radical gastrectomy, the operating field ranges from the first jejunal loop to the celiac trunk, or esophageal hiatus in cases of total gastrectomy. The nature of this operating field (particularly in obese or long-limbed patients) can require more accessory ports and a switch between camera and surgical tools to optimize the working conditions. In robotic surgery, it is possible to lift up the abdominal wall ("tent effect") using the laparoscopic gasless procedure. This simple maneuver, performed by the camera arm and 30° endoscope, provides good vision even with low pressure of pneumoperitoneum, gains some degrees in the angle of vision and provides an excellent view up to the celiac trunk and esophageal hiatus [6].

7.6.2 D2-Lymphadenectomy

Since there is a risk of understaging of patients diagnosed with early gastric cancer at preoperative workup, surgery with D2-lymphadenectomy is considered the optimal option for resectable gastric cancer, for the therapeutic role as well as for the prognostic significance of the extended lymphadenectomy [7]. This is also our opinion and part of the policy followed in our in clinical practice.

It is widely accepted that D2 lymph node dissection is the more critical part of the minimally invasive gastrectomy procedure for gastric cancer. Although laparoscopic D2-lymphadenectomy is feasible and safe, with similar results to the open technique in terms of average number of harvested lymph nodes and postoperative outcomes, the diffusion of this procedure has been limited to only a few advanced MIS centers. The anatomic complexity of the vascular structures, the technical limits of the conventional laparoscopic instrumentation, and the lack of a steady image, can make this procedure quite complex even for minimally invasive well-trained surgeons.

The technical advantages offered with robotic surgery can help to standardize minimally invasive D2-lymphadenectomy and enable surgeons to perform this procedure routinely in their clinical practice [7].

The robotic system makes easier the dissection of difficult lymphatic areas, namely stations 7–12a and 14v, which represent the "hot point" in conventional laparoscopy.

The removal of station 14v is controversial. Originally part of the D2-lymphadenectomy for tumors of the lower third, this station has since been excluded in the latest edition of Japanese Classification. However, the removal of station 14v can still be beneficial in cases of macroscopic metastasis of lymph nodes in station 6. Furthermore, if dissection of the infrapyloric area is started from station 14v, a good exposure of the pancreas can be obtained before approaching station 6. This technique can reduce the amount of mistakes of dissection plane, particularly in obese patients. Another difficult area to dissect is the splenic hilum. By using the robotic system, the surgeon can perform a correct spleen-preserving dissection thus reducing the likelihood of mistakes of plane and the risk of bleeding [6, 7, 9].

Additionally, the enhanced three-dimensional vision and the high precision of the robotic movements allow an optimal identification of vascular anomalies, such as an accessory left hepatic artery coming from the left gastric artery, and permits the dissection of the lymphatic tissue surrounding the main trunk.

7.6.3 Oncological Safety

Given the short follow-up times, the numbers of harvested lymph nodes and the resection margin are used as indicators of oncological adequacy. Most authors report a mean number of nodes superior to 30 that are in-line with the recommended standard for conventional open D2-lymphadenectomy. In their recent meta-analysis including a total of 7200 patients (663, RAG; 1236, LG; 5301, open gastrectomy (OG)), Hyun et al. [10] reported that the number of retrieved lymph nodes with RAG was similar to that for LG and OG, even with a subgroup analysis matched for the extent of lymphadenectomy and type of gastrectomy. Likewise, in the meta-analysis from Xiong et al. [3], there were no differences observed in the number of nodes retrieved between the RAG and LG procedures.

The majority of studies reported free resection margins at pathological examination in 100% of cases following RAG [7, 9]. This likely reflects an accurate preoperative selection of cases, with prevalence for early versus advanced stages. In our experience, intraoperative endoscopy can be useful to confirm the location of the gastric lesion and to evaluate the adjacent mucosa.

Currently, there is no significant data available in terms of long-term oncological results and survival in robotic gastric surgery. The longest follow-up to date was reported by Pugliese et al. [11], with a mean observation of 53 months. According to their data, there are not significant differences in 5-year survival between LG and RAG.

MIS plays an important role in the therapeutic strategy for advanced disease offering a less aggressive procedure that can help to reduce the time between

surgery and postoperative chemotherapy. Moreover, faster recovery can increase the number of patients able to receive adjuvant chemotherapy. Some authors reported that all histologically-proven N+ patients who underwent RAG, started adjuvant treatment without any surgery-related delay within 30 days of surgery [7]. In this context, RAG can play an important role in allowing the surgeon to reproduce routine D2-lymphadenectomy, to perform complex resections at other organs (including the pancreas, liver, and colon) and to provide precise minimally invasive reconstruction. Multicenter, randomized, controlled trials and long-term follow-up evaluation are needed to definitively establish the oncological adequacy of RAG.

7.6.4 Digestive Restoration

In several studies, it has been reported that digestive restoration was performed extracorporeally through the same mini-laparotomy used for specimen removal [9, 10]. This hybrid-open technique was used both in gastrojejunostomy and gastroduodenostomy following distal gastrectomy, as well as in esophagojejunostomy following total gastrectomy. This approach is possible for patients with a very low BMI, indeed the technique of extracorporeal anastomosis is primarily used by Eastern surgeons. In cases with high BMI, it is very difficult to perform an extracorporeal anastomosis, unless an incision larger than that for a mini-laparotomy is used. Other disadvantages of extracorporeal anastomosis are the lack of appropriate vision and the excessive traction put on the viscera, which make the application of stapling devices potentially difficult and dangerous. This is why other authors described an intracorporeal digestive restoration using a linear stapler for GJA and a circular stapler for EJA [1, 7]. Extracorporeal anastomosis may negate the potential minimally invasive surgical approach, especially for obese patients, and the intracorporeal techniques appear to be the preferred solution. The robotic system, moreover, permits full hand-sewn ("robot-sewn") technique of anastomosis. All reconstructions, including Roux-en-Y jejunal limb, EJA, GJA, or even gastroduodenal anastomosis, can be fully carried out by the intracorporeal robot-sewn method.

In our present clinical practice we always perform intracorporeal anastomosis: mechanical side-to-side GJA after distal gastrectomy, and hand-sewn end-to-side EJA after total gastrectomy. The hand-sewn anastomosis is achievable thanks to the ability of the robotic system to provide the surgeon with the necessary tools to perform precise sutures even in deep and narrow spaces.

7.6.5 Perioperative Outcomes

7.6.5.1 Hospital Stay

Most studies reported similar results for postoperative short-term outcomes after

RAG compared with LG: no differences were found in time to start mobilization and time to resume diet [6, 10]. The hospital stay is shorter in patients undergoing RAG than in those having LAG, but such a difference is not statistically significant [3, 8]. Hospital stay for RAG is significantly shorter than OG in all series [10].

7.6.5.2 Operative Time

The mean operating time is commonly longer in robotic surgery than in conventional laparoscopy or open surgery. This finding has been reported as the most consistent in the meta-analysis from Hyun et al. [10]. Only one series, excluding the procedures completed during the initial RAG learning period, reported a similar operating time for RAG and LG (234 vs. 220 min) [4]. Robotic surgery needs additional setup procedures, including preparing and docking, which often require less than 20 minutes [10, 11]. Both setup time and operative time decrease with the progressive experience of the surgical team [1, 4, 7].

Compared with LAG, robotic surgery increases the shift from extracorporeal to intracorporeal anastomosis, which is known to be a more consuming time technique. Furthermore, robotic surgery is typically associated with a more meticulous dissection than conventional laparoscopy, particularly along the vessels and during the lymphadenectomy [6].

7.6.5.3 Blood Loss

The robotic platform is very helpful in reducing blood loss even in major and complex surgical procedures.

First, it is due to the fact that the robotic system allows an extremely accurate dissection, especially in the case of extended lymphadenectomies. Furthermore, in the case of major bleeding by vascular injury the robotic control of hemostasis is much easier than in conventional laparoscopy. In this situation, the surgeon has direct control of the vision and he can use three surgical tools for clamping and suturing. Moreover, the surgeon also has an assistant who maintains the operating field clean using sponge, suction, and irrigation. It is impossible to reproduce these same working conditions during conventional laparoscopy [6]. The articulation of the endowrist permits free ligation and suturing in the narrow abdominal cavity with few limitations in the movement of the instruments [2]. In a comparative study among OG, LG, and RAG, Kim et al. [5] reported that the estimated blood loss in the robotic group was significantly lower than in the open and laparoscopic groups. The same result was reported in the meta-analysis from Xiong et al. [3].

A perfect dissection and a better control of bleeding can result in a reduction of perioperative transfusions and better long-term oncological results [6].

7.6.5.4 Complications

In their series of 5839 patients (4542 OG, 861 LAG and 436 RAG), Kim and colleagues [12] found that overall rates of complications, reoperation and mor-

tality were similar between the three groups. Postoperative ileus and intestinal obstruction, as well as intra-abdominal fluid collections and abscesses, occurred more frequently after open surgery, while anastomotic leakage was significantly more common after minimally invasive approach (LG, 2.1%; RAG, 2.3%; OG, 1.1%; P = 0·017). The authors hypothesized that the higher rate of leaks in LG and RAG may be associated with the limited tactile feedback or differences in staple-line reinforcement. Indeed, almost all anastomoses were made using staplers and the staple lines were always reinforced by over-sewing sutures during OG, whereas reinforcement was not performed in laparoscopic and robotic procedures.

In the meta-analyses from Hyun [10] and Xiong [3], the complication rate and mortality rate does not differ significantly between RAG, LG and OG.

Conversion to open surgery is critical because converted patients have higher complication rates and worse oncological outcomes. The conversion rate does not differ significantly between LG and RAG [3].

7.6.6 Cost Analysis

Improvements in technology and widespread multidisciplinary use could lead to lower charges, but prompt reduction of costs in the near future is harder to achieve and it is certainly a big limit. A shorter hospital stay for LG and RAG compared with OG could offset the increased operation costs.

Anyway, a detailed analysis of cost is still lacking.

7.7 Conclusions

The most convincing indications for robotic surgery are procedures that involve a small, deep, fixed operating field or where MIS requires extreme accuracy, fine dissection and endoscopic suturing [1]. Therefore, the major technical advantages of the robot-assistance in gastric surgery may be appreciated during lymph node dissection, bleeding control, intracorporeal reconstruction, enlarged resections and complex reconstructions. Finally, the learning curve and reproducibility of RAG seem to be shorter and more feasible than with conventional laparoscopy.

For these reasons, robotics has the potential to contribute to a standardization and major diffusion of MIS for the treatment of gastric cancer, making it a routine approach even in advanced stages. Hence, RAG could better integrate minimally invasive resection with neoadjuvant and adjuvant multimodal therapies.

Longer operation time, higher costs and oncologic equivalency to its counterparts are still unresolved issues, which need further development and investigation.

References

1. Giulianotti PC, Coratti A, Angelini M et al (2003) Robotics in general surgery: personal experience in a large community hospital. Arch Surg 138:777–784
2. Hashizume M, Sugimachi K (2003) Robot-assisted gastric surgery. Surg Clin North Am 83:1429–1444
3. Xiong B, Ma L, Zhang C (2012) Robotic versus laparoscopic gastrectomy for gastric cancer: a meta-analysis of short outcomes. Surg Oncol 21:274–280
4. Hyun MH, Lee CH, Kwon YJ et al (2013) Robot versus laparoscopic gastrectomy for cancer by an experienced surgeon: comparisons of surgery, complications, and surgical stress. Ann Surg Oncol 20:1258–1265
5. Kim MC, Heo GU, Jung GJ (2010) Robotic gastrectomy for gastric cancer: surgical techniques and clinical merits. Surg Endosc 24:610–615
6. Coratti A, Annecchiarico M, Di Marino M et al (2013) Robot-assisted gastrectomy for gastric cancer: current status and technical considerations. World J Surg 37:2771–2781
7. D'Annibale A, Pende V, Pernazza G et al (2011) Full robotic gastrectomy with extended (D2) lymphadenectomy for gastric cancer: surgical technique and preliminary results. J Surg Res 166:e113–120
8. Marano A, Hyung WJ (2012) Robotic gastrectomy: the current state of the art. J Gastric Cancer 12:63–72
9. Song J, Oh SJ, Kang WH et al (2009) Robot-assisted gastrectomy with lymph node dissection for gastric cancer: lessons learned from an initial 100 consecutive procedures. Ann Surg 249:927–932
10. Hyun MH, Lee CH, Kim HJ et al (2013) Systematic review and meta-analysis of robotic surgery compared with conventional laparoscopic and open resections for gastric carcinoma. Br J Surg 100:1566–1578
11. Pugliese R, Maggioni D, Sansonna F et al (2010) Subtotal gastrectomy with D2 dissection by minimally invasive surgery for distal adenocarcinoma of the stomach: results and 5-year survival. Surg Endosc 24:2594–2602
12. Kim KM, An JY, Kim HI et al (2012) Major early complications following open, laparoscopic and robotic gastrectomy. Br J Surg 99:1681–1687

Robotic Subtotal Gastrectomy: a Modified Korean Technique

8

Giuseppe Spinoglio, Giampaolo Formisano, Ferruccio Ravazzoni, Francesca Pagliardi, and Alessandra Marano

8.1 Procedure Overview

The robotic approach for the treatment of gastric cancer (GC) has been initially adopted mainly in Asia, where this malignant disease is more common than in Western countries and it is diagnosed at earlier stages thanks to a screening program. Among Asian countries, South Korea started to embrace the robotic technique in 2005 and now it has become one of the leading countries in robotic gastric cancer surgery. In this chapter we present our experience of robotic subtotal gastrectomy (RSTG) with D2 lymph node (LN) dissection for GC where the step-by-step procedure is based mostly on the technique of Dr Woo Jin Hyung [1].

8.2 Patient and Robot Positioning

The patient is secured in the supine position with both arms alongside the body and the legs are closed; a nasogastric tube is inserted during the anesthesiologist's preparation. The table is then placed in a 15° reverse-Trendelenburg position. The surgical cart is placed at the head side of the patient, the monitor to the right side of the patient and the assistant stands to the left of the table (Fig. 8.1a).

G. Spinoglio (✉)
Department of General and Oncologic Surgery,
"Ss. Antonio e Biagio" Hospital,
Alessandria, Italy
e-mail: giuseppe.spinoglio@gmail.com

G. Spinoglio (Ed), *Robotic Surgery: Current Applications and New Trends*,
Updates in Surgery
DOI: 10.1007/978-88-470-5714-2_8, © Springer-Verlag Italia 2015

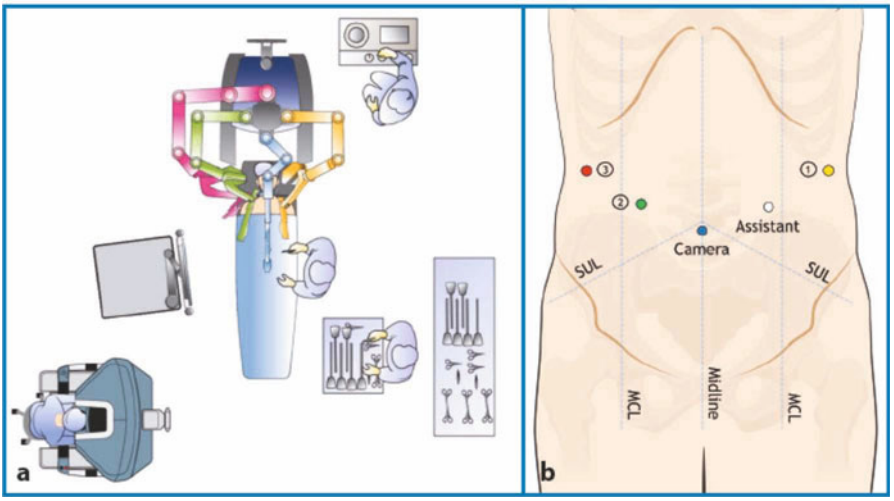

Fig. 8.1 Subtotal gastrectomy. **a** Overhead view of the OR setup. **b** Trocar layout. (© 2014 Intuitive Surgical, Inc.)

8.3 Trocar Placement

A 12 mmHg pneumoperitoneum is achieved with a small incision at Palmer's point in the left upper quadrant and a infraumbilical 12-mm camera port, for the 30° down scope is introduced.

Under direct visualization, trocars are inserted as follows (Fig. 8.1b):

- one 8 mm robotic trocar (arm No. 1: R1) 1 cm below the costal angle, as far lateral as possible on the patient's left side, for the bipolar forceps, Hot Shears™ (monopolar curved scissors), large needle driver, Hem-o-lok® clip applier. Port should be 1 cm above the level of the bowel when viewed internally from the scope;
- one 8 mm robotic trocar (arm No. 2: R2) 2–4 cm superior to umbilicus, at the same distance between the Instrument R3 and the camera port, for the ultrasonic shears;
- one 8 mm robotic trocar (arm No. 3: R3) 1 cm below the costal angle, as far lateral as possible on the patient's right side, for the ProGrasp™ forceps (alternatively Cadiere forceps). Port should be 1 cm above the level of the bowel when viewed internally from the scope;
- one 12 mm assistant's trocar, 1 cm superior to umbilicus, at the same distance between and 1–2 cm below a diagonal line from Instrument R1 and the camera port on patient's left side, for suction/irrigation, clip/stapler application or other maneuvers.

R1 and R2 trocar placement can be subject to minor adjustments according to the patient's body habitus, for instance in the case of larger patients, both trocar should be placed more medially and the R2 trocar should be higher in order

to achieve the correct angle with the ultrasonic shears to perform a complete LN dissection of station No. 11p.

8.4 Step-by-Step Review of Critical Elements of the Procedure

8.4.1 Exploration, Liver Retraction and Tumor Detection

After the laparoscopic exploration of the abdominal cavity to exclude the presence of metastatic disease, the left lobe of the liver is retracted toward the abdominal wall with a liver- suspension method [2].

The technique requires: two X-ray-detectable 5 × 5 cm gauze pads, one 90 cm 2-0 nylon monofilament with a 60 mm double straight taper needle and two plastic surgical clips (Hem-o-lok®, Weck; Teleflex Medical Europe Ltd). The gauze pads are folded in half, threaded with the 2-0 nylon suture, then both straight needles, with the attached suture-threaded gauze pads, are introduced into the abdominal cavity through the assistant's port.
One of the straight needles is brought out through the anterior abdominal wall, directly anterior to the middle of the left lobe of the liver.

The nylon suture is then secured to the pars condensa of the hepatogastric ligament with two Hem-o-lok® clips, after having divided the pars flaccida up to the right of the esophageal crus. The other straight needle is passed externally through the abdominal wall immediately to the right of the falciform ligament. While the assistant slowly pulls upward on the two sutures, the two gauze pads are brought together and stretched to cover the undersurface of the retracted liver. Finally, the two external sutures are tied together to rest on the external abdominal wall.

Originally, in the case of small or undetectable GC, portable plain radiography was performed to identify endoscopic metallic clips, applied just proximal to the tumor, during the preoperative upper endoscopy [3]. Actually, we use an ultrasound evaluation with a curved linear probe (ProART™ Robotic Transducer), which is introduced into the abdominal cavity through the assistant port. Once the tumor location is identified, the patient-side cart is moved next to the patient and the robot is docked, as previously described.

8.4.2 Left and Right Gastroepiploic Vessels Division

An omentectomy is performed using ultrasonic shears (R2) toward the lower pole of the spleen where the left gastroepiploic vessels are sectioned at their roots. Once entered into the lesser sac, coloepiploic detachment is continued toward the pylorus and the right gastroepiploic vessels are identified and ligated with clips (LN station No. 4sb, No. 4d). The dissection proceeds along the gastroduodenal artery to where it springs from the common hepatic artery (CHA).

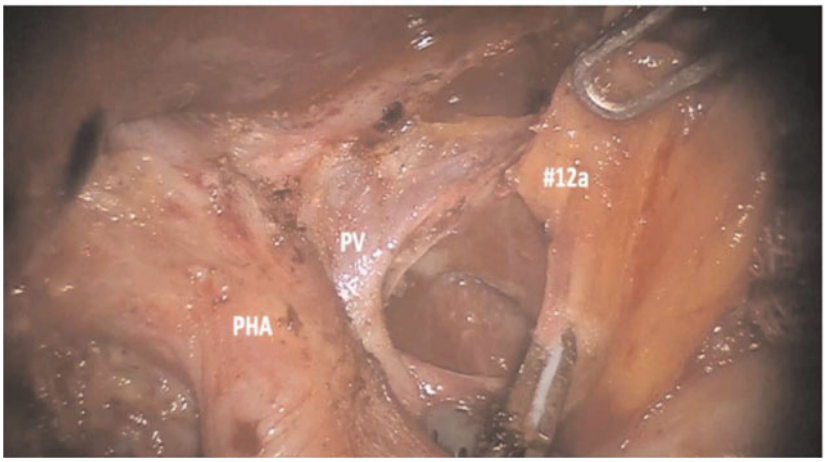

Fig. 8.2 Complete dissection of lymph node No. 12a around proper hepatic artery (*PHA*). The medial side of portal vein (*PV*) is pictured

8.4.3 Hepatoduodenal Ligament Dissection and Duodenal Transection

The lesser omentum is dissected and the right gastric artery is identified and divided between clips at its origin. The supra- and infrapyloric nodes (LN station No. 5, No. 6) are removed: in the case of a suspected metastatic LN at station No. 6, the dissection of LN station No. 14v might be of benefit to the patient. The duodenum, after being circumferentially cleared, is transected 2 cm distal to the pylorus using a 45 mm Endo-linear stapler inserted through the assistant port. The removal of LN station No. 12a is then carried out (Fig. 8.2).

8.4.4 Lymphadenectomy of the Suprapancreatic Area and Left Gastric Artery Ligation

The dissection continues by ablation with ultrasonic shears of LN station No. 8a (Fig. 8.3) and No. 9; during this step the left gastric vein is exposed and divided. Then, the left gastric artery is carefully transected at its root with clips and the soft tissues around it are retrieved for LN station No. 7 (Fig. 8.4). The splenic vessels are finally skeletonized with the removal of LN No. 11p.

8.4.5 Lesser Curvature Dissection and Proximal Gastric Resection

The retroperitoneal detachment of the stomach is completed along the lesser curvature up to the right esophageal crus together with the retrieval of LN station No. 3 and No. 1. Once the mobilization of the stomach is completed, the resec-

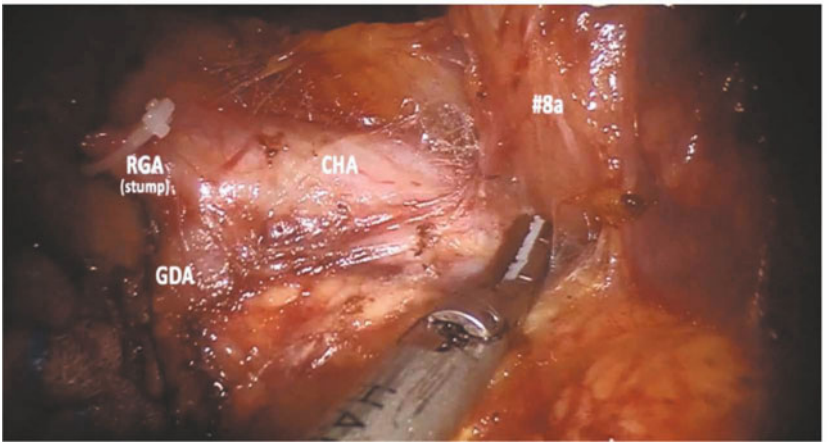

Fig. 8.3 Complete dissection of lymph node No. 8a around common hepatic artery (*CHA*). *GDA*, gastroduodenal artery; *RGA*, right gastric artery

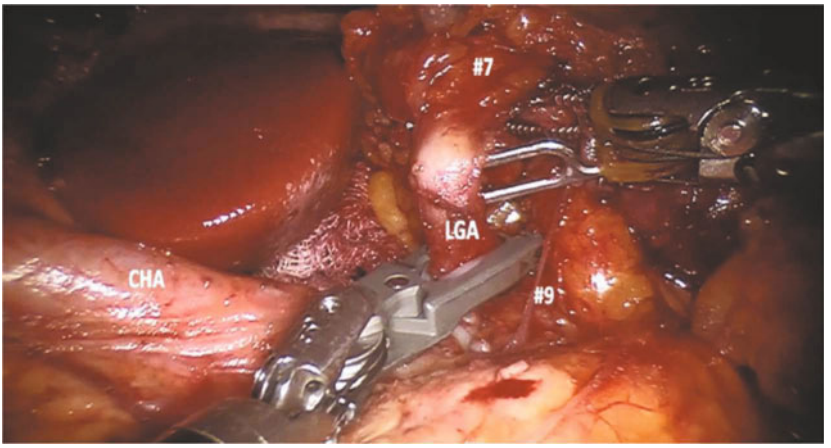

Fig. 8.4 Clipping of the left gastric artery (*LGA*) with removal of lymph nodes Nos. 7 and 9. *CHA*, common hepatic artery

tion is performed by the assistant using a 60 mm Endolinear stapler; the specimen is bagged intracorporeally and is placed on the right lobe of the liver.

8.4.6 Reconstruction

After the transection, a gastrotomy on the posterior wall of the stomach and then an enterotomy 15–20 cm away from the Treitz ligament are performed by means of ultrasonic dissection. A gastrojejunostomy is performed intracorporeally, using a 60 mm Endolinear stapler; the common entry hole for the anastomosis is closed with interrupted 3/0 PDS sutures. The robot is undocked; a suction drain is posi-

tioned close to the duodenal stump and finally the specimen is removed through a Pfannenstiel incision. The nasogastric tube is left in place and removed on POD 1.

8.5 Advantages

The main advantages of our technique are described as follows:

- **Use of ultrasonic shears in R2:** even if this device is nonwristed compared to other available robotic instruments and is generally controlled by the non-dominant left hand of the surgeon, we believe that this technical difference provides some potential advantages mainly during LN dissection including station Nos. 6, 14v, 8a, 9, 7, 12a, and 11p.
  The infrapyloric area and superior mesenteric vein (LN No. 6 and LN No. 14v) are considered the most frequent source of bleeding during surgery while the suprapancreatic lymphatic tissues (LN station Nos. 8a, 9, 7) are the second [4]. The dissection conducted with the ultrasonic shears around LN station No. 6, No. 12 and along the CHA from the right to the left-side of the patient is more intuitive and makes the lymphadenectomy better to be implemented. An adequate hemostasis is also achieved, especially in advanced GC stages.
  Indeed, during this phase, a good dissection plane can be followed along the CHA: the ultrasonic shears, controlled by the surgeon's left hand, reach the target anatomy tangentially from the patient's right side with a parallelism between the instrument tip and the vessel.
  An appropriate tension is provided by the instrument in R3, grasping the lymphatic tissue and the dissection continues with the ultrasonic shears in R2: its mobility is not limited by the pancreatic head and body thanks to its working angle.
  For LN station No. 11p, a dissection carried out in the aforementioned way aids the surgeon to perform a more accurate LN removal and vessels dissection, minimizing the intraoperative bleeding.
- **Liver retraction**: utilizing a 2/0 prolene suture and a gauze pad as a "sling" is a way to achieve complete exposure of the anterior surface of the hepatogastric ligament.
  The instrument in R3, free for dynamic use, can grasp and lift up the lymphatic tissue while the dissection of LN No. 8 and No. 12 is carried out by instruments in R1 and R2. The assistant port is also available for additional maneuvers.
- **Intraoperative identification of transection line**: in the case of small or undetectable GC, in order to avoid an intraoperative endoscopy, metal clips are placed on the greater and lesser gastric curvature to delineate the location of the transection when coordinated with the internal clips placed via preoperative endoscopy. Originally, we used to perform this double check with an intraoperative plain radiography; actually, we employ an intraoperative ultrasound assessment with a dedicated probe to detect the lesion, previously marked with clips.

8.6 Personal Experience

From March 2011 to April 2014, 26 patients affected by histologically-proven early and advanced GC, located in the distal stomach, underwent RSTG with D1-D2 lymphadenectomy, according to the recommendations of the Japanese Gastric Treatment Guidelines and Classification [5–7]. All surgeries have been performed with the da Vinci® Si HD Surgical System. The pathologic stage classification of the tumor was worked out according to AJCC Cancer Staging Manual-Seventh Edition [8].

All patient characteristics and perioperative outcomes are shown in Table 8.1. The console time averaged 190.3 ± 48.9 minutes (range: 150–350 minutes).

Table 8.1 Experience of our Institution of Robotic Subtotal Gastrectomy for Cancer

Variable	GC group (n=26)
Age (y), *mean ± SD*	67.7 ± 10.6
Gender (M/F) *n (%)*	17/9
BMI (kg/m²), *mean ± SD*	24 ± 3.8
Co-morbidity, *n (%)* Hypertension/COPD/CAOD/ CVD/History of previous tumor/Other*	 7 (26.9)/3 (11.5)/2 (7.6)/ 2 (7.6)/2 (7.6)/3 (11.5)
ASA score, *n (%)* I/II/III	 6 (23.1)/14 (53.8)/6 (23.1)
Extent of lymph-node dissection, *n (%)* D1/D2	 2 (7.6)/24 (92.3)
Console time (min), *mean ± SD*	190.3 ± 48.9
Intraoperative complications, *n (%)*	0 (0)
Liquid diet start (day), *mean ± SD*	2.9 ± 1.6
Hospital stay (days), *mean ± SD*	9.2 ± 2.9
Complications, *n (%)* None/Present Hyperamylasemia/Prolonged ileus/ Pneumonia	 19 (73.1)/7 (26.9) 1 (3.8)/2 (7.6)/4 (15.3)
Tumor location, *n (%)* middle third/ lower third	 7 (26.9)/19 (73.1)
Histology type, *n (%)* intestinal/diffuse/mixed type	 11 (42.3)/7 (26.9)/8 (30.7)
Grading, *n (%)*0/1/2/3	2 (7.6)/3 (11.5)/10 (38.4)/11 (42.3)
AJCC stage, *n (%)* 0/ IA/ IB/ IIA/ IIB/ IIIA/ IIIB	 2 (7.6)/4 (15.4)/4 (15.4)/1 (3.8)/5 (19.2)/3 (11.5)/7 (26.9)
Negative proximal margin, *n (%)*	26 (100)
Number of retrieved LNs, *mean ± SD*	29.5 ± 12.6

GC, gastric cancer; *BMI*, body mass index; *COPD*, chronic obstructive pulmonary disease; *CAOD*, coronary artery obstructive disease; *CVD*, cerebrovascular disease; *LN*, lymph nodes.
*Other, co-morbidity includes inflammatory bowel disease, diabetes and lithiasis of gallbladder

No intraoperative complications were observed; we registered one case of conversion (conversion rate 3.8%) due to a suspected infiltration of the diaphragmatic pillars.

Except for special contraindications, all patients were managed according to our fast track protocol: after a contrast swallow on postoperative day one, liquid diet was started (mean ± SD, 2.9 ± 1.6 days) and the mean hospital stay was 9.2 ± 2.9 days. One ASA III patient, affected by atherosclerotic cardiovascular disease, died on postoperative day 12 as a result of a myocardial infarction (3.8% mortality). Early postoperative complications occurred in 7 out of 26 (morbidity 26.9%): transient asymptomatic hyperamylasemia (1500 UI/mL), pneumonia, prolonged ileus occurred in one, two and four patients, respectively and were all medically treated. The 30-day readmission rate was 11.5%: three patients presented with abdominal fluid collection and so underwent ultrasound-guided drainage with complete remission.

A D1-lymphadenectomy was performed in two cases of early GC (7.7%); D2-lymphadenectomy was carried out in all the other stages (92.3%). The mean number of retrieved LNs was 29.5 ± 12.6. Proximal resection margins were tumor-free in all patients (100%). The mean follow-up time was 25 ± 10.8 months (range: 1–38 months) and was conducted on 22 out of 25 patients.

References

1. Hyung W, Woo Y, Noh S (2011) Robotic surgery for gastric cancer: a technical review. Journal of Robotic Surgery 5:241–249
2. Woo Y, Obama K, Son TI et al (2011) Minimizing hepatic trauma with a novel liver retraction method during robotic and laparoscopic gastric cancer surgery, a simple liver-suspension with gauze-suture technique. Int J Med Robotics Comput Assist Surg 7:56
3. Kim HI, Hyung WJ, Lee CR et al (2011) Intraoperative portable abdominal radiograph for tumor localization: a simple and accurate method for laparoscopic gastrectomy. Surg Endosc 25:958–963
4. Kim MC, Heo GU, Jung GJ (2010) Robotic gastrectomy for gastric cancer: surgical techniques and clinical merits. Surg Endosc 24:610–615
5. Japanese Gastric Cancer Association (1998) Japanese classification of gastric carcinoma – 2nd English edition. Gastric Cancer 1:10–24
6. Japanese Gastric Cancer Association (2011) Japanese classification of gastric carcinoma: 3rd English edition. Gastric Cancer 14:101–112
7. Japanese Gastric Cancer Association (2011) Japanese gastric cancer treatment guidelines 2010 (ver. 3). Gastric Cancer 14:113–123
8. Edge SB, Compton CC (2010) The American Joint Committee on Cancer: the 7th edition of the AJCC cancer staging manual and the future of TNM. Ann Surg Oncol 17:1471–1474

Part III

Hepatobiliopancreatic Surgery

Hepatic Resections

9

Alberto Patriti, Graziano Ceccarelli, and Luciano Casciola

9.1 Procedure Overview

Minimally invasive surgery of the liver (MIS) is growing worldwide. As many as 1677 minimally invasive liver resections were reported in Italy between 1 January 1995 and 28 February 2012 [1]. Meanwhile, the interest in robot-assisted liver resections (RALR) is rising.

The indications for MIS are similar to those for open liver resections as recently stated in the Louisville Statement Consensus Conference. Laparoscopic liver resections (LLR) were initially indicated for benign and peripherally located lesions [2]. In the last few years the number of laparoscopic complex liver resections has increased and even major hepatectomies and segmentectomies of the postero-superior (P-S) segments have been successfully performed [3]. Recently, robotics has been introduced in general surgery with the aim to overcome some of the limitations of traditional laparoscopy providing a greater maneuverability with a set of articulated instruments and a tridimensional vision. Since the first reports in 2008, a lot of case series and comparative studies were published showing the feasibility of robot-assisted minor and major liver resections. Potential advantages of robot-assistance include facilitating complex reconstructions (i.e., biliary and vascular anastomoses) and parenchyma-preserving resections of lesions located in P-S segments. Giulianotti et al. have demonstrated that robot-assisted major hepatectomies are safe and feasible even when a biliary reconstruction is required, such as in case of hilar cholangiocarcinoma [4]. In a recent study by our institution we showed

A. Patriti (✉)
Department of Surgery Division of General, Minimally Invasive, and Robotic Surgery, "San Matteo degli Infermi" Hospital, Spoleto (PG)
e-mail: albertopatriti@gmail.com

G. Spinoglio (Ed), *Robotic Surgery: Current Applications and New Trends*, Updates in Surgery
DOI: 10.1007/978-88-470-5714-2_9, © Springer-Verlag Italia 2015

the possibility given by the robot to preserve liver parenchyma even in the case of tumor location in the P-S segments or close to a major liver vessel [5]. In the present chapter, technical details of robot-assisted liver resection will be provided along with a discussion on the current clinical applications of robotics in hepatobiliary surgery.

9.2 Operating Room Setup, Patient and Trocar Positioning

Robot docking and patient position are of paramount importance to easily approach all the liver segments. When approaching anterior segments, segment 1 (Spiegel lobe) and major hepatectomies a reversed Trendelenburg supine patient position is optimal. The patient can be tilted to the left or to the right according to the site of the hemihepatectomy. The on-table surgeon stands between the legs and the scrub nurse and instruments are positioned lateral to the left leg. The trocars are generally positioned along a bowl-shaped line passing through the umbilicus.

For parenchyma-preserving resections of lesions located in the right postero-lateral sector (upper segment 6 and segment 7), the patient is rotated on the left flank in order to facilitate liver mobilization and inferior vena cava dissection. The camera port and the left-sided trocars should be placed as close as possible to the right costal margin, whereas the right trocar can be inserted in the inter-costal space between the 10^{th} and 11^{th} rib close to the scapular line. At this level the risk to accidentally injury the lung is very low and a direct access to the postero-lateral segments is provided.

For bilobar liver metastases with involvement of both anterior segments and S7–8, two options are equally effective: re-docking the robot and changing patient position according to the tumor location; and using a semi-left lateral patient position with the robot over the patient head. The latter is preferred in our institution since it does not require robot re-docking and changes of patient position during surgery which can cause possible contamination of the surgical field.

9.3 Ultrasound Exploration

Ultrasound exploration follows the same general rules of traditional laparoscopic liver surgery. The typical frequency range adopted for LIOUS is 5–10 MHz. Access for the US probe to the peritoneal cavity is achieved through 10 or 11 mm ports, which are usually the same ports used by the on-table surgeon for suction/irrigation and retraction. The supramesocolic space is instilled with saline solution until the space between the liver dome and the right diaphragm is completely filled in order to better explore the bare area of S7–8 and the hepa-

tocaval confluence. A first ultrasound exploration of the liver is performed before the robot is docked, and any other maneuver on the liver has been performed, to avoid artifacts. This first exploration is intended to allow the surgical staff to acquire a clear three-dimensional picture of liver vascular anatomy and lesion location. The examination is usually performed by contact scanning using the liquid film on the glissonian surface as a coupling agent. The hepatocaval confluence is usually visualized with the probe introduced through a right port and placed on S4a. Moving the probe between the diaphragm and the liver dome, the right hepatic vein is then identified. Portal bifurcation and right hepatic pedicles are visualized by positioning the transducer on S4b and moving it to the right side. The left portal pedicles and left hepatic vein are better identified from the left upper quadrant. Using the linear probe, exploration of the diaphragmatic margins of S7–8 is carried out placing the probe on the water surface created in the right sub-diaphragmatic area. Finally, the transection plane is outlined on the liver capsule with monopolar diathermy. When the robot is docked and resection begins, a continuous and meticulous ultrasound assessment of the transection margin is imperative due to the lack of tactile feedback.

9.4 Basic Maneuvers of Liver Surgery

9.4.1 The Pringle Maneuver and the Inflow Control

The Pringle maneuver is the easier and safer way to control the inflow but its use in laparoscopic surgery has been neglected for years. An ideal system for laparoscopic Pringle maneuver should be cost-effective, as user-friendly as to permit intermittent inflow occlusion during parenchymal transection and guarantee a fast vascular control in case of bleeding. The device for inflow occlusion set in our institution is composed of a 20 Fr chest tube, an umbilical tape and a plug used for occlusion of the Foley catheter [6].

The chest tube is inserted in the right upper abdominal quadrant and the umbilical tape is passed around the hepatoduodenal ligament with the use of an endowristed Cadiere forceps (Intuitive Surgical Inc., Sunnyvale, CA) or an articulated laparoscopic device (Endoflex). The umbilical tape is then exteriorized through the chest tube with the use of a 5-mm laparoscopic forceps. The chest tube is finally closed with the plug in order to avoid air loss. When inflow occlusion is needed the on-table surgeon removes the plug and pulls the umbilical tape. When the desired tape tension is achieved, the chest tube is closed with the plug.

For major hepatectomies individual dissection and control of portal and arterial pedicles is possible and greatly facilitated by endowristed instruments. Dissection is carried out as in open surgery with scissors or hook and a bipolar forceps (Fig. 9.1).

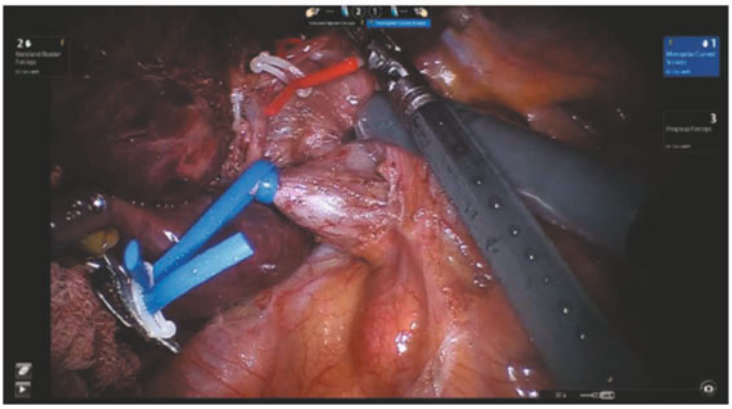

Fig. 9.1 Hilar dissection for right hepatectomy. The right portal vein is encircled and exposed

9.4.2 Parenchymal Transection

Two robotic devices are available for parenchymal transection. The Kelly clamp-crushing technique associated with an intermittent Pringle maneuver is considered the safer and more accurate method of parenchymal transection in open liver surgery. The major advantages of the Kelly clamp-crushing technique are the low costs and the ability to fragment the parenchyma, preserving the vascular structures that can be ligated and divided or preserving according to the resection plan. Using the endowristed PreCise™ bipolar forceps (Intuitive Surgical Systems, Sunnyvale, CA, USA) the parenchyma can be easily fragmented exposing the inner vessels as in open surgery. The on-table surgeon uses the forceps to perform the intermittent inflow occlusion, thereby allowing the console surgeon to focus his/her attention only on the transection line. The robotic clamp-crushing technique allows parenchymal preservation even for deeply located lesions, widening the indications for a minimally invasive approach to lesions in the P-S segments and those located close to major liver vessels. Hemostasis of small vessels is obtained with monopolar or bipolar cautery. To secure larger vessels on the transection line, we use Hem-o-lock® clips or ligatures with Vicryl® and Prolene®. The hepatic veins (HVs) are usually divided with the laparoscopic linear stapler or sutured with Prolene®. Biliostasis is assessed by observation and the bile leaks controlled with sutures as in open surgery.

The harmonic scalpel is the other device used to transect the liver. It can be used to cut and coagulate the liver or, by taking advantage of ultrasonic dissection, using it to fragment the liver parenchyma exposing the underlying vessels. The only drawback of this device is related to its four degrees of freedom making it ideal for straight-line resections (left and right hepatectomies) but less effective for parenchyma-preserving resections.

9.4.3 Liver Retraction

For resections on anterior segments, left lateral sectionectomy included, some stay sutures can be useful to retract the specimen using the fourth robotic arm or the assistant grasper. A vessel-loop held by the fourth arm around the left lobe can be used to stretch the parenchyma along the transection plane thus facilitating the effect of the Kelly clamp-crushing technique. For deeply located lesions or when the tumor is close to a major vessel the "corkscrew technique" can be reproduced. After identification of the lesion by inspection and intraoperative ultrasound, Glisson's capsule is marked with electrocautery 1–2 cm away from the tumor margin. According to the location of the tumor the marked area is anchored by stitches, with caution, in order to prevent the needle from entering the tumor. The suture is held together by clips and upward traction is performed, facilitating the transection of the parenchyma and correct identification of vascular and biliary structures. Parenchymal transection is performed with the monopolar shears for the first liver layer (1 cm from the Glisson capsule) and then with the Kelly clamp-crushing technique. For steady exposure of the parenchymal transection plane in major hepatectomies, the "rubber band technique" can be used. Two sterile rubber bands are introduced into the abdominal cavity. One end of each rubber band is anchored with stay sutures at the right and left resection margins. The other end is pulled outside using an EndoClose needle and fixed with appropriate tension.

9.5 Step-by-Step Review of Critical Elements of Hemihepatectomies and Bisegmentectomies

9.5.1 Right Hepatectomy

The patient is placed in mild reverse Trendelenburg position, with semi-left lateral decubitus and spread legs. The pneumoperitoneum is made using a Veress needle in the left upper quadrant, maintaining a pressure of 12 mmHg. Four trocars are placed for the robot, one in the right pararectal for the camera, two 8 mm trocars in the right flank and left pararectal, and another 8-mm trocar for the fourth arm in the left flank. Two additional 10-mm trocars are inserted to be used by the assistant (Fig. 9.2a). The OR setup in shown in Fig. 9.2b. Cholecystectomy is completed and the hepatic hilum is dissected using the monopolar hook in the right arm of the robot, and the bipolar forceps in the left. The right hepatic artery is the first element to be sectioned between ligatures or Hem-o-lock® clips. The right portal vein is exposed, looped and sectioned between Hem-o-lock® clips or 5-0 polypropylene suture.

The dissection and evaluation of the biliary tree requires special attention because sectioning will be made either at this time or later during the procedure, depending upon the location of the biliary bifurcation. Recent visualization technology with ICG (Indocyanine Green) fluorescence enables the evaluation of the

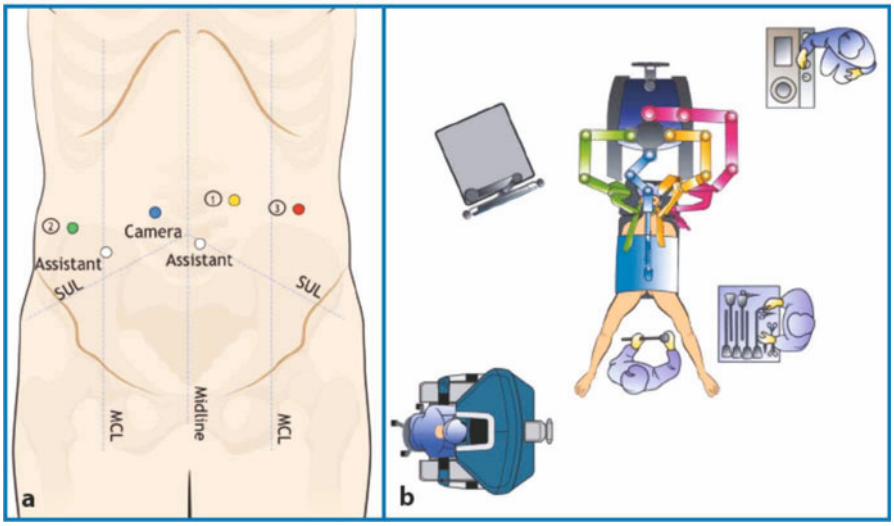

Fig. 9.2 **a** Trocar disposition for right hepatectomy. **b** OR setup for right and left hepatectomy. For left hepatectomy arm 3 is positioned on the opposite side. (© 2014 Intuitive Surgical, Inc.)

extrahepatic biliary tree without requiring any invasive procedure; this is due to the physical characteristics of ICG, which allows for unique hepatic metabolism and biliary excretion (Fig. 9.3). The right liver is retracted to the left using the fourth arm. The first step is to section the right triangular ligament, using the hook. The liver is gently retracted to the left while dissection proceeds to the bare area of the liver. At this point, the space between the vena cava and the liver is dissected in a caudal-to-cephalad direction, sectioning between Hem-o-lock® clips the accessory veins to segments 6 and 7. For a better hemostasis, polypropylene 5-0 sutures can be applied on the side of the vena cava. A hepatocaval dissection is then made up to the drainage of the RHV.

The ischemic delineation of the transection along Cantlie's line is marked following the section of the vascular vessels of the right liver. The monopolar hook can be used to mark this line and open the capsule of Glisson, although it is not mandatory. Prior to starting the transection, two stay sutures at the transection margins can be used for a better retraction. The transection is performed using the harmonic scalpel, closing gradually as ultrasonic energy is applied. The transection is performed in a caudal-to-cephalad direction. Once the vascular branches are crossing between right and left liver lobes, they are ligated or secured with Hem-o-lock® clips. The surgical specimen is then extracted in an endoscopic plastic bag, through a Pfannenstiel incision. The surgical hemostasis and the trocars' orifices are again evaluated and two closed Jackson-Pratt drains are left in place.

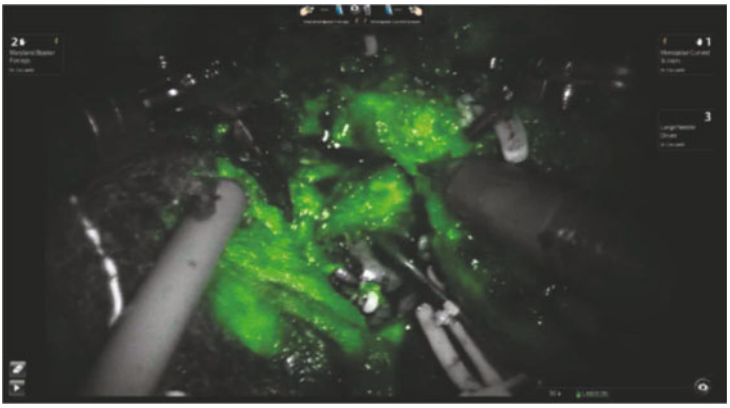

Fig. 9.3 ICG fluorescence highlighting the extrahepatic biliary tree during a right hepatectomy

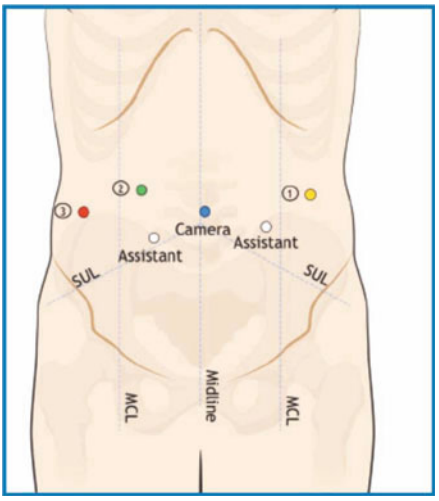

Fig. 9.4 Trocar disposition for left hepatectomy and left lateral sectionectomy. (© 2014 Intuitive Surgical, Inc.)

9.5.2 Left Hepatectomy

The patient is placed in mild reverse Trendelenburg position, with semi-right lateral decubitus and with spread legs. Patient's arms are either tucked along the body to avoid collision with robotic arms. The assistant stands in between the patient's legs.

The robot is docked directly over the head of the patient with two operating arms on the patient's right side.

A total of 5–6 ports are placed, replacing the specular shape of the trocar disposition of the right hepatectomy. Pneumoperitoneum is maintained at 12 mmHg (Fig. 9.4).

Surgery starts with visual exploration of the abdomen, followed by contact ultrasonography of the liver. As soon as resectability is confirmed, the left lobe

is freed from its surrounding peritoneal and diaphragmatic attachments. Next, the hepatoduodenal ligament is exposed by retracting upward and cephalad, the gallbladder is grasped with Cadiere forceps driven by robotic arm 3. Left hepatic artery and portal vein are dissected and divided between ligatures, as previously described. After vascular isolation of the portal triad supplying the left hepatic lobe, a vascular demarcation along the parenchymal transection plane becomes evident.

Parenchymal transection is carried out using bipolar forceps or the harmonic scalpel and monopolar curved scissors. During this phase, Cadiere forceps in robotic arm 3 may be used to retract the specimen, to allow optimal alignment of the transection line with robotic scissors, or to control hemorrhage on the remnant by compression.

HVs are sealed and divided intraparenchymally using an endoscopic stapler armed with a vascular cartridge. The stapler is usually inserted through the 12 mm assistant's port since the alignment between the device and the target hepatic vein is usually optimal

The specimen is removed in an endoscopic bag through a Pfannestiel incision. Before completing the operation the raw surface of the liver is carefully inspected. Bile leaks and bleeding sites are individually sealed by suture ligature. Two closed Jackson-Pratt drains are placed near the transection surface of the liver.

9.5.3 Left Lateral Sectionectomy

The patient is placed in mild reverse Trendelenburg position, with right lateral decubitus and with spread legs. Patient's arms are either tucked along the body to avoid collision with robotic arms. The assistant stands in between the patient's legs. The robot is docked directly over the head of the patient. Trocar disposition is the same as that used for left hepatectomy (Fig. 9.4). We generally encircle the liver pedicle for the Pringle maneuver in case of bleeding. A 2-0 stay suture is passed at the inferior border of segment 3 to retract the left lateral section to the left. The Rex fossa is therefore exposed. The falciform ligament is transected sparing the round ligament. After opening of the bare area of the hepatocaval confluence, the anterior and posterior layer of the left triangular ligament are sectioned with monopolar hook or scissors. Retracting the left lateral section to the left allows the pedicle of segment 3 (P3) to be identified. Sometimes a small bridge of parenchyma has to be separated before reaching the pedicle (the so called hepatic bridge). Liver transection is carried out with bipolar forceps in the left hand and a monopolar scissor in the right hand. Transection starts 5 mm to the left of the falciform ligament. The first portion of liver parenchyma is transected to allow a complete exposition of P3. The small arteries to S3 are identified and ligated with titanium clips or coagulated with bipolar forceps. P3 is finally encircled using the bipolar forceps and secured with Hem-o-lock® clips. After its transection parenchymal division is continued

till reaching the portal pedicle of segment 2 (P2), which is clipped and divided in the same way. The LHV is finally secured and divided with a single fire of an endovascular stapler. The specimen can be extracted through the umbilicus or a Pfannenstiel incision. Two closed suction Jackson-Pratt drains are placed near the transection surface of the liver.

9.6 Step-by-Step Review of Critical Elements of Segmentectomies and Sub-segmentectomies

For segmentectomies and sub-segmentectomies, the patient positioning and trocar placement should be individualized according to the tumor location. Pneumoperitoneum induction with the Verres needle can help to tailor trocar position limiting the use of an umbilical port to the cases where it is really necessary. Anatomical and nonanatomical liver resections of peripheral (segments 2, 3, 4b, 5, 6), superficial lesions is generally feasible and can be done with minimal morbidity and mortality rates. Pedicle clamping is optional or can be applied only in the case of bleeding and liver division can be performed with all the available transection devices. Generally three to four trocars disposed at the level of the umbilical line are adequate. For lesions located in the postero-lateral sector (upper segment 6, segments 7 and 8) the patient is rotated on the left flank in order to facilitate liver mobilization and inferior vena cava dissection, when necessary. The camera port and the left-sided trocars should be placed as close as possible to the right costal margin, whereas the right trocar can be inserted in the intercostal space between the 10th and 11th rib along the scapular line (Fig. 9.5). Due to the higher risk of bleeding, intermittent pedicle clamping

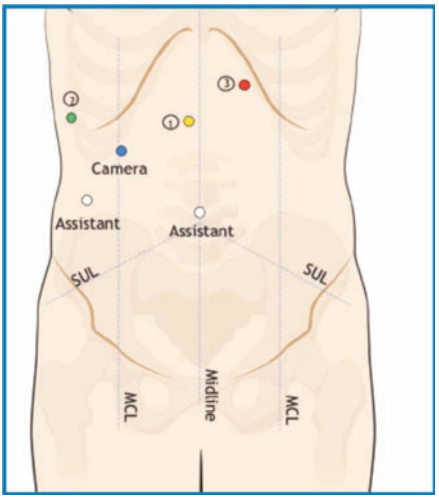

Fig. 9.5 Trocar layout for segments 7 and 8. The patient is tilted on the left flank and the right robotic trocar in inserted between the 10th and 11th rib. (© 2014 Intuitive Surgical, Inc.)

is advisable when approaching P-S segments. Careful ultrasonographic exploration with demarcation on the Glisson capsule of the right hepatic vein can avoid major bleeding during parenchymal transection. For deeply located lesions or when the tumor is close to a major vessel, even in case of lesions located in the anterior segments, the "corkscrew technique" can be useful. After identification of the lesion by inspection and intraoperative ultrasound, Glisson's capsule is marked with electrocautery 1–2 cm away from the tumor margin. According to the location of the tumor the marked area is anchored by stitches with caution in order to prevent the needle from entering the tumor. Metallic clips hold the suture together and upward traction is performed, facilitating the transection of the parenchyma and correct identification of vascular and biliary structures. The control of the surgical margin can be verified by intraoperative ultrasonography during parenchymal transection. Generally, small specimens can be extracted with an endoscopic bag through any port site, otherwise enlarging the umbilical port or rarely a Pfannenstiel incision could be necessary. Robot-assistance is particularly useful to perform parenchymal-preserving resections especially in the P-S segments and when the tumor is in contact with a portal branch or HV, and when both are close to the tumor mass. In fact, the endowristed instruments allow fine movements and complex transection planes reducing the discomfort coming from the use of rigid tools. The principles of patient and trocar positions in conventional laparoscopic surgery are applicable also for the robot-assisted approach. For liver surgery the robot is docked over the patient's head.

All liver resections should be guided by the ultrasound performed by the on-table surgeon. The console surgeon can view the ultrasound screen in picture-in-picture modality directing the dissection plane, which appeared as an echogenic line between the cut surfaces. Parenchyma is usually transected with the harmonic scalpel for straight-line resections. The Kelly clamp-crushing technique with the endowristed PreCise™ bipolar forceps (Intuitive Surgical Systems, Sunnyvale, CA, USA) is preferred for curved and angulated section lines and for tumor dissection close to a major liver vessel. Hemostasis of small vessels is obtained with monopolar or bipolar cautery. To secure larger vessels on the transection line, we use Hem-o-lock® clips or ligatures with Vicryl® or Prolene®. The HVs are usually divided with the laparoscopic linear stapler or sutured with Prolene®. Biliostasis is assessed by observation and the bile leaks controlled with sutures as in open surgery.

9.7 Indications and Results of Robot-assistance in Liver Surgery

To date, only a few reports have focused on robotics in liver surgery, the number of patients included is rather small and the majority of reviews are carried out on a retrospective basis [3, 5, 7]. Therefore there is still not good evidence

of a superiority of robotics over standard laparoscopy. Potential advantages of robot-assistance arising from these studies may include facilitating complex reconstructions (i.e., biliary and vascular anastomoses) and parenchyma-preserving resections of lesions located in the P-S segments. Giulianotti et al. have demonstrated that robot-assisted major hepatectomies are safe and feasible even when a biliary reconstruction is required, such as in case of hilar cholangiocarcinoma [8]. However, there are no studies comparing the outcome of robot-assisted and laparoscopic major hepatectomies. In a recent study by our institution, where every attempt is made for a parenchyma-preserving surgery, we showed the possibility given by the robot to preserve liver parenchyma even in the case of a tumor located in the P-S segments or close to a major liver vessel. In a total of 23 cases, 9 patients (47.8%) had liver nodules in the P-S segments, in three cases the tumor was in connection with a portal branch, in two cases with a hepatic vein and in one case with both vascular structures. Using robotics we performed, even in complex cases, the same parenchyma-preserving resections that we would have done in the open setting, thus avoiding carrying out major hepatectomies [3]. When comparing the two minimally invasive techniques, robotics allowed a more parenchymal preservation surgery in respect to laparoscopy [5].

Even if randomized controlled studies are still missing, robotic assistance could be attractive for those surgeons who want to perform a minimally invasive parenchyma-preserving surgery even in the case of lesions close to main liver vessels or located in segments 7, 8 or 1. As there are not randomized studies demonstrating the superiority of robotics over laparoscopy in major hepatectomies and anterolateral segment resections, the two approaches can be considered analogous. There are some evidences that applications of robotics in major hepatectomies could improve two phases of liver resection: hilar and hepatocaval confluence dissection [4]. This aspect gives the basis for prospective studies on the application of the da Vinci® system for liver resections requiring a meticulous vascular dissection and reconstruction. Nevertheless, if a program of robotic liver surgery is planned, even resections in the anterior segments should be considered in the first phase of the learning curve in order to gain expertise and the P-S segments and complex major hepatectomies can be safely approached when all the members of the staff are familiar with the robotic surgery features.

References

1. Aldrighetti L, Cipriani F, Ratti F et al (2013) The Italian experience in minimally invasive surgery of the liver: A national survey. In: Calise F, Casciola L (eds) – Minimally invasive surgery of the liver. Springer, Milan
2. Buell JF, Cherqui D, Geller DA et al (2009) The international position on laparoscopic liver surgery: The Louisville Statement, 2008. Annals of Surgery 250:823–830
3. Casciola L, Patriti A, Ceccarelli G et al (2011) Robot-assisted parenchymal-sparing liver surgery including lesions located in the posterosuperior segments. Surg Endosc 25:3815–3824

4. Giulianotti PC, Coratti A, Sbrana F et al (2010) Robotic liver surgery: Results for 70 resections. Surgery 149:29–39
5. Troisi RI, Patriti A, Montalti R, Casciola L (2013) Robot assistance in liver surgery: a real advantage over a fully laparoscopic approach? Results of a comparative bi-institutional analysis. Int J Med Robot 9:160–166
6. Patriti A, Ceccarelli G, Bartoli A, Casciola L (2011) Extracorporeal Pringle maneuver in robot-assisted liver surgery. Surg Laparosc Endosc Percutan Tech 21:e242–244
7. Tsung A, Geller DA, Sukato DC et al (2014) Robotic versus laparoscopic hepatectomy. Annals of Surgery 259:549–555
8. Giulianotti PC, Sbrana F, Bianco FM, Addeo P (2010) Robot-assisted laparoscopic extended right hepatectomy with biliary reconstruction. J Laparoendosc Adv Surg Tech A 20:159–163

Biliary Tract Tumors (Resection and Reconstruction)

10

Pier Cristoforo Giulianotti, Vivek Bindal, and Despoina Daskalaki

10.1 Classification

Bile duct tumors can be broadly classified into benign, premalignant and malignant tumors as per the histologic findings, and into intrahepatic and extrahepatic tumors based on their location [1]. Most of these tumors are malignant. Bile duct adenoma is the most common benign neoplasm of the bile ducts, though it is rare. Premalignant bile duct tumors include biliary intraepithelial neoplasia (BilIN) and intraductal papillary neoplasm of the bile duct (IPN-B). Cholangiocarcinoma (CC) is the commonest primary malignancy of the bile ducts [2]. It is predominantly adenocarcinoma (95% of cases), although other histologic types including squamous cell carcinoma, small cell carcinoma and sarcomas have been described.

CC can be classified as intrahepatic or peripheral, perihilar and distal depending on their location. The distal CC, if resectable, is treated by pancreaticoduodenectomy (described in next chapter). Perihilar CC, also called Klatskin tumor, accounts for 60% cases of extrahepatic CC [3]. It is a challenging situation, as it may require a formal hepatectomy with lymphadenectomy and reconstruction. We shall elaborate on these details in the sections below.

10.2 Surgical Treatment

R0 resection of the tumor offers the only possibility for long term survival and has been regarded as the gold standard for the treatment of resectable disease.

P. C. Giulianotti (✉)
Division of General, Minimally Invasive and Robotic Surgery,
University of Illinois, Chicago, IL, USA
e-mail: piercg@uic.edu

G. Spinoglio (Ed), *Robotic Surgery: Current Applications and New Trends*,
Updates in Surgery
DOI: 10.1007/978-88-470-5714-2_10, © Springer-Verlag Italia 2015

For Klatskin tumor, which forms the majority of cases, this may include extended hepatectomy, combined with complete extrahepatic bile duct resection and radical lymphadenectomy [4]. This aggressive surgical strategy has increased the rate of curative resection and long term survival for the patients harboring this disease [5]. There are many challenging technical complexities in this approach like inflow control, inclusion of caudate lobe and reconstruction with separate small caliber ducts. The feasibility and safety of laparoscopic techniques in liver resections have been reported, especially for anterior and lateral segments. However, the adoption of laparoscopy for biliary tumors has been restricted due to technical limitations and oncologic concerns [6].

Robotic surgery may help overcome certain limitations of laparoscopy and provide the minimally invasive advantage to these patients, who otherwise usually undergo extensive open surgery. The main challenges faced during these procedures are right lobe mobilization, hepatic hilum dissection, control of bleeding during parenchymal transection, and complex biliary reconstruction. The robotic platform provides many advantages which have been already well described. This helps the surgeon increase the precision of dissection while facilitating suturing in difficult situations. It also provides him with the ergonomic comfort in these long and challenging procedures so as to allow him to work to his full potential.

In all these advanced procedures, it is important to understand that with the use of a minimally invasive method, indications and patient selection for a procedure does not change. The fundamental principles of a safe R0 surgical resection and adequate lymphadenectomy should not be compromised. A low threshold for conversion to an open procedure should be kept if the goals of the operation cannot be accomplished safely by using minimally invasive technique.

10.2.1. Preoperative Assessment of Patient

One has to assess these patients for their performance status and fitness for major surgery that may include a partial hepatectomy. Chronic liver disease or portal hypertension generally makes these patients bad candidates for surgery. If there is any evidence of cholangitis, it should be treated with adequate drainage and antibiotics before surgery [2].

The main goal of the surgery is R0 resection with free proximal and distal margins, resection of tumor bed (including caudate lobe and vascular elements) and adequate lymphadenectomy. A complete resection with histologically negative resection margins is a very important criterion for long term survival in cholangiocarcinoma.

The criteria for unresectable disease are [7]:

- major comorbidities precluding safe surgery;
- metastatic disease;

- invasion of main portal vein or hepatic artery proximal to their bifurcation;
- bilateral invasion of portal vein or hepatic artery branches;
- bilateral involvement of hepatic ducts up to secondary radicles; and
- unilateral duct and/or vessel involvement with contralateral liver lobe atrophy.

Some of these restrictions can be overcome by techniques like portal venous embolization, which induces contralateral liver hypertrophy to increase the future remnant liver volume.

10.3 Procedure Overview

10.3.1 Patient Positioning and Docking

Under general anaesthesia, the patient is placed in the supine position with parted legs with approximately a 20° reverse-Trendelenburg tilt. The abdomen is cleaned and draped and an orogastric tube and urinary catheter are inserted. The assistant stands in between the legs. Pneumoperitoneum is achieved to 15 mmHg using a Veress needle at Palmer's point. A 10/12 mm trocar is placed in supraumbilical position (which is used as an assistant port in the operation). One optical and three da Vinci® trocars are placed as follows (Fig. 10.1a):

- optical (12 mm): in the right midclavicular line, approximately 10 cm from the assistant trocar, above the level of the umbilicus;
- R1: in the left midclavicular line approximately 10 cm away from the assistant trocar, above the level of umbilicus;
- R2: in right anterior axillary line, at least at 10 cm from the optical trocar;
- R3: in left anterior axillary line, used for retraction purpose.

The port placement needs to be adjusted based on the body habitus of the patient so as to prevent external arm collision and provide optimal exposure.

A diagnostic laparoscopy is done to look for any metastatic deposits or free fluid. If a suspicious deposit is seen, it is biopsied and sent for frozen examination to rule out metastatic disease. Any free fluid is sent for cytology to look for malignant cells. Intraoperative ultrasonography is performed to rule out any undetected metastatic deposits in the liver.

The da Vinci® patient cart is brought from the head of the patient, and the arms are docked to the placed ports. The third arm of the robot comes from the left side of the patient. To start the procedure, a monopolar hook is taken in R1, bipolar forceps in R2 and grasping forceps in R3. The assistant surgeon stands in between the legs for complementary maneuvers (i.e., suction, stapling, retraction, and laparoscopic ultrasonography). A sample OR setup for right extended hepatectomy for CC is depicted in Fig. 10.1b.

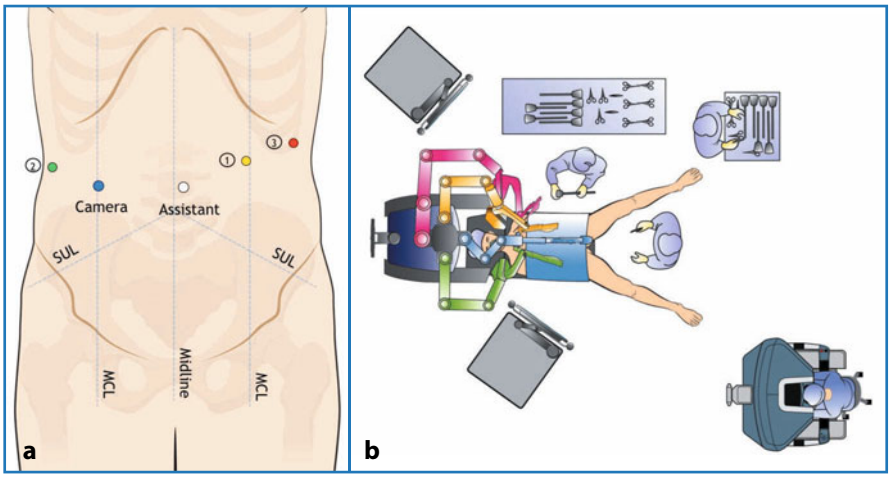

Fig. 10.1 Robotic-assisted right extended hepatectomy. **a** Port position. *SUL*, spino-umbilical line; *MCL*, midclavicular line; 1, 2, 3 represent positions for robotic arm 1, 2 and 3 respectively. **b** OR setup. (© 2014 Intuitive Surgical, Inc.)

10.3.2 Bile Duct Resection

Hepatic flexure of the colon is mobilized medially and caudally and a partial Kocher maneuver is performed. Dissection is commenced at the hepatic hilum while it is retracted using R3. If the gallbladder is in place, it is taken down keeping the cystic duct attached to the common bile duct (CBD). Indocyanine green fluorescence aids in the detection of CBD and any aberrant biliary anatomy. The CBD is dissected and transected distally at the superior border of pancreas, and the distal stump is oversewn. The distal margin is sent for frozen section, which if positive, calls for a pancreaticoduodenectomy with or without liver resection, as per disease location, spread and performance status of the patient. Now, the proximal bile duct is lifted up and dissection is continued to separate the hepatic artery and portal vein from the bile duct. Starting at the superior border of the pancreatic head, a lymphadenectomy along the common hepatic artery is performed. The origin of gastroduodenal artery is exposed. Generally, lymph node dissection in hepatoduodenal ligament is adequate. The fat and lymph nodes are resected en bloc with the bile duct. At the hilum, right and left hepatic ducts are dissected and encircled with vessel loops to aid in traction. If one can get proximal to the tumor, bile ducts are divided and margins are sent for frozen section to confirm R0 resection.

In case of Bismuth type III tumors, an extended right or left hepatectomy along with bile duct resection may be required for R0 resection. The detailed technique of these procedures is described below in separate sections.

Vascular resection and reconstruction may be required in case of portal venous or hepatic arterial involvement. This may be done only by experienced

surgeons and institutions with good perioperative results in such high risk procedures.

10.3.3 Reconstruction: Roux-en-Y Hepaticojejunostomy

For a Roux-en-Y hepaticojejunostomy, the attention is diverted to the submesocolic area in order to prepare the loop for reconstruction. A proximal jejunal loop is divided using a stapler, and a jejunojejunostomy is performed with a laparoscopic stapler to create a Roux loop. The distal loop is then brought into the right upper quadrant usually in a transmesocolic fashion. Here, an anastomosis between the bile duct and the loop is performed in end-to-side fashion, using 4-0, 5-0 or 6-0 PDS (Ethicon, Somerville NJ) depending on the diameter of the bile duct. A ductoplasty may be required if the bile duct diameter is small. We usually do a single layered anastomosis with half running layers of suture, one for the posterior and one for the anterior wall. Few interrupted stitches may be placed to reinforce the anastomosis. Sometimes, anterior layer has to be formed by interrupted stitches, in case of small diameter or thin walled ducts (Fig. 10.2). The possibility of doing microsurgical interrupted stitches is one of the main advantages of using robot. In order to decrease the tension of the anastomosis,

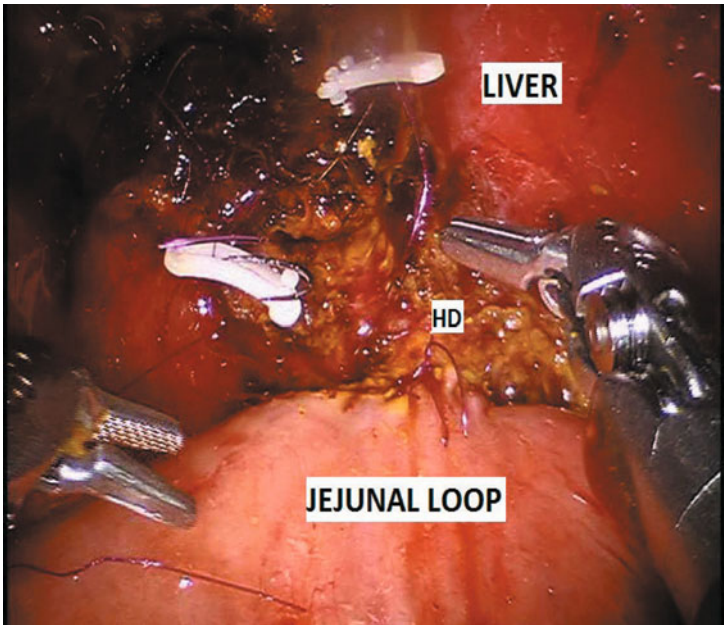

Fig. 10.2 Interrupted stitches to perform the anterior layer of hepaticojejunostomy. The interrupted sutures are held in position by clips. Use of robotic platform provides the distinct advantage of ability to perform microsurgical interrupted stitches in a minimally invasive environment. HD, hepatic duct

two stitches of Prolene 3-0 (Ethicon, Somerville, NJ, USA) are placed to fix the jejunal loop to the hilum.

Use of fibrin glue may be considered at the end of the anastomosis. At the end of the procedure, a drain may be left near the biliary anastomosis.

10.3.4 Extended Left Hepatectomy with Caudate Lobe Resection

Ports are placed as already described. A thorough diagnostic laparoscopy is done along with ultrasonography of the liver to rule out metastatic disease. The patient cart is docked and the operation starts by removing the gall bladder, while keeping the cystic duct intact. Indocyanine green fluorescence is used to identify the biliary anatomy and look for any variations. The CBD is completely dissected, tied and transected. The distal margin of CBD is sent for frozen section and the stump is oversewn with PDS sutures. Lymphadenectomy is performed along the hepatoduodenal ligament. The left hepatic artery is dissected, and before transection with a stapler, confirmed by a clamping test which leads to a change in color of the liver parenchyma on the left side. The left branch of the portal vein is then dissected, ligated and divided (Fig. 10.3). Parenchymal transection is done along the line of ischemia usually using ultrasonic shears. Habib™ (a bipolar radiofrequency device) or cavitational ultrasonic surgical aspirator (CUSA) may be used for parenchymal transection. Anterior and pos-

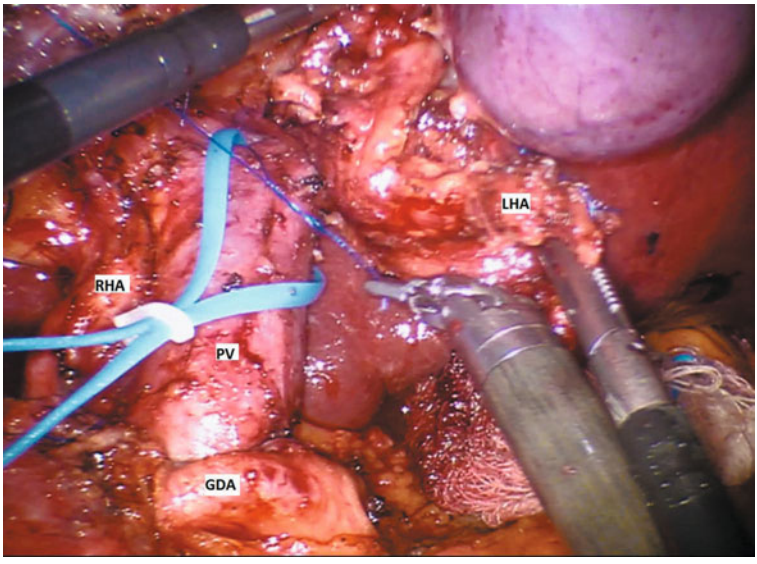

Fig. 10.3 Left branch of portal vein (*PV*) being ligated. The left hepatic artery (*LHA*) has been divided and lifted up. One can see the gastroduodenal artery (*GDA*) and right hepatic artery (*RHA*)

terior branches of right hepatic duct are dissected, transected and margins are sent for frozen section. The caudate lobe is dissected from the inferior vena cava. The parenchymal transection is completed and hemostasis confirmed. The reconstruction is done in a Roux-en-Y fashion. The Roux limb is created by stapled jejunojejunostomy (as described in Sect. 10.3.3) and it is brought cranially in a transmesocolic (sometimes retrogastric) fashion. Using 5-0 PDS, the two right ducts are connected to each other. An opening made in the Roux limb and a posterior layer of the anastomosis is performed using continuous suturing. An interrupted anterior layer is thrown and a few stitches are placed between liver and Roux limb so as to avoid undue tension on the anastomosis. Fibrin glue is used over the anastomosis and the raw surface of transected liver parenchyma. The specimen is retrieved in an Endobag usually through a Pfannensteil incision.

10.3.5 Extended Right Hepatectomy

Initially, the hepatic flexure of the colon is mobilized, and a partial Kocher maneuver is performed. Starting at the superior border of the pancreatic head, a lymphadenectomy of the common hepatic artery is performed, using a monopolar hook and bipolar forceps, to expose the origin of the gastroduodenal artery. The inferior aspect of segment IV is retracted upward by using the third robotic arm, and the CBD is dissected and sectioned at the superior border of the pancreatic head. The distal stump of the CBD is sutured, and a frozen section is sent to rule out neoplastic invasion. The right hepatic artery is dissected and divided at its origin from the proper hepatic artery. The left hepatic duct is transected at the left umbilical fissure and a frozen section is sent at this level as well. Following this, the right portal vein is dissected and divided between ligatures. The right liver lobe is mobilized from its peritoneal attachments. This is done by sectioning the falciform ligament and the anterior half of the coronary ligament, until the anterior side of the inferior vena cava (IVC) and the right hepatic vein is reached. The hepatorenal ligament and the right triangular ligament are divided by using a monopolar hook. The third arm is used to retract the inferior aspect of the right liver lobe upward. In this way, the right side of the IVC is exposed. The accessory hepatic vein is suture ligated and the dissection proceeds until the inferior aspect of the right hepatic vein is reached. After sectioning the bridge of parenchyma between segments IV and III, the parenchymal transection is carried out along the right aspect of the falciform ligament, by harmonic scalpel, starting at the anterior border of the liver. The recurrent vessels from the umbilical fissure to segment IV, middle hepatic and right hepatic veins are divided using staplers. The reconstruction is done as per the already described method. The specimen is retrieved in an Endobag.

10.4 Palliative Surgery

A vast majority of patients with cholangiocarcinoma have a surgically unresectable tumor at the time of diagnosis. The goal in these patients is palliation of symptoms using interventions with least morbidity and maximal efficacy [8, 9]. For distal CC, usually endoscopic stenting is the preferred modality, while for proximal CC, percutaneous methods with or without endoscopic interventions are helpful. In a limited number of situations, a surgical biliary and/or digestive bypass may be needed, but is associated with a high morbidity and mortality when done by open approach [10]. With the use of surgical robotics, we can provide minimally invasive advantage to these patients with a low morbidity [11].

10.5 Liver Transplantation

Orthotopic liver transplantation, in combination with multimodality therapy, is rarely an option in advanced tumors like those invading the portal vein, bilateral hepatic ducts and atrophic liver lobes. However, there are only a few studies on liver transplantation as a modality for treatment of cholangiocarcinoma. Also, because of the shortage of organs and poor outcomes, the indications of transplant are very limited and it cannot be considered as a standard form of therapy. In a few cases when transplant needs to be done, use of robotic platform can be an option for living donor hepatectomy [12].

10.6 Postoperative Outcomes

Surgery for bile duct tumors is associated with significant postoperative morbidity and mortality. The perioperative complications associated with the procedure are bile leak, hemorrhage, cholangitis, liver abscess, hepatic failure, organ space or superficial surgical site infections and respiratory complications.

Our experience included more than 150 cases of robotic hepaticojejunostomy for different indications, out of which 52.9% patients has had a previous hepatobiliary procedure, either open or laparoscopic. There was a 3.9% bile leak rate, 4% biliary stenosis rate and 3% cholangitis rate at 16.82±13.09 month follow-up. The variables which significantly increased the risk of complications after a minimally invasive bilioenteric anastomosis were iatrogenic bile duct injury and duct diameter ≤5 mm. These results are better placed than most of the studies with open and laparoscopic hepaticojejunostomy.

As per the literature, less than 50% of patients with cholangiocarcinoma are able to undergo a curative resection. The five-year survival rates are highly variable, ranging from 8 to more than 50%. The factors which predict a better outcome are negative margins on histopathology, no lymph nodal involvement, concomitant liver resection, well-differentiated tumors, papillary tumors and

lack of perineural invasion [13]. In general, the best outcomes are in patients who undergo R0 resection and this is the best predictor for five-year survival.

References

1. Joo I, Lee JM (2013) Imaging bile duct tumors: pathologic concepts, classification, and early tumor detection. Abdominal Imaging 38:1334–1350
2. Jarnagin W, Winston C (2005) Hilar cholangiocarcinoma: diagnosis and staging. HPB 7:244–251
3. Lazaridis KN, Gores GJ (2005) Cholangiocarcinoma. Gastroenterology 128:1655
4. Giulianotti PC, Sbrana F, Fransesco BM, Addeo P (2010) Robot-assisted laparoscopic extended right hepatectomy with biliary reconstruction. J Laparoendosc Adv Surg Tech 20:159–163
5. Ito F, Agni R, Rettammell RJ et al (2008) Resection of hilar cholangiocarcinoma: Concomitant liver resection decreases hepatic recurrence. Ann Surg 248:273–279
6. Simillis C, Constantinides VA, Tekkis PP et al (2007) Laparoscopic versus open hepatic resections for benign and malignant neoplasms—a meta analysis. Surgery 141:203–211
7. Whang EE, Duxbury M, Rocha FG; Zinner MJ (2013). Cancer of the gall bladder and bile ducts. In: Maingot R, Zinner M, Ashley SW, (eds.) Maingot's abdominal operations, 12th edn. McGraw-Hill Medical, New York
8. Date RS, Siriwardena AK (2005) Current status of laparoscopic biliary bypass in the management of non-resectable peri-ampullary cancer. Pancreatology 5:325–329
9. Smith AC, Dowsett JF, Russell RC et al (1994) Randomised trial of endoscopic stenting versus surgical bypass in malignant low bile duct obstruction. Lancet 344:1655–1660
10. Lesurtel M, Dehni N, Tiret E et al (2006) Palliative surgery for unresectable pancreatic and periampullary cancer: a reappraisal. J Gastrointest Surg 10:286–291
11. Buchs NC, Addeo P, Bianco FM et al (2011) Robotic palliation for unresectable pancreatic cancer and distal cholangiocarcinoma. Int J Med Robotics Comput Assist Surg 7:60–765
12. Giulianotti PC, Tzvetanov I, Jeon H et al (2009) Robot assisted right lobe donor hepatectomy. Transpl Int 25:e5–e9
13. Santibanes ED, Ardiles V (2012) High malignant biliary tract obstruction. In: Fischer JE, (ed.) Fischer's Mastery of Surgery. 6th ed. Lippincott Williams & Wilkins

Pancreatic Surgery for Cancer

11

Pier Cristoforo Giulianotti, Despoina Daskalaki, and Francesco Mario Bianco

11.1 Introduction

Pancreatic cancer is the fourth leading cause of cancer-related death in the United States, with more than 45,000 estimated new cases per year [1]. The only potentially curative treatment is surgery, but unfortunately only 10–20% of patients have a resectable disease at the time of diagnosis [2]. The most important factors that can improve the oncologic outcome after surgery are an adequate lymphadenectomy and a negative resection margin [3]. Even though the overall morbidity and mortality rates after pancreatic surgery have been progressively decreasing over the past twenty years, pancreas-related complications are still a major concern.

The last major innovation in pancreatic surgery has been the introduction of minimally invasive (MI) techniques [4–6]. Even though the rates of pancreatic fistula and delayed gastric emptying have not been proven to be lower with the MI approach, several other postoperative outcomes are in favor of these techniques: less blood loss and transfusion, less wound infections, shorter hospital stay, faster recovery and faster start of adjuvant treatment are all indisputable advantages of MI surgery [7, 8].

The laparoscopic approach to the pancreas has proved to be feasible and safe [9, 10]. However, while laparoscopic distal pancreatectomy has been widely adopted even for malignant disease, laparoscopic pancreaticoduodenectomy still remains relatively uncommon [11]. This is most likely due to the technical complexity of this procedure and the steep learning curve.

The introduction of robotic technology more than a decade ago, has slowly

P. C. Giulianotti (✉)
Division of General, Minimally Invasive and Robotic Surgery, University of Illinois, Chicago, IL, USA
e-mail: piercg@uic.edu

G. Spinoglio (Ed), *Robotic Surgery: Current Applications and New Trends*, Updates in Surgery
DOI: 10.1007/978-88-470-5714-2_11, © Springer-Verlag Italia 2015

but steadily revolutionized the field of MI surgery. Robot-assistance can overcome the limits of laparoscopy (two-dimensional imaging, rigid instrumentation and counter-intuitive movements) and expand the indications of the MI approach. With the robotic assistance, surgeons can recreate the open technique in a MI fashion, allowing for adequate oncologic resections. In a recent meta-analysis comparing robotic and open pancreatectomy [12], the authors concluded that robotic pancreatic resections are as efficient as open surgery not only for benign, but also for malignant disease.

11.2 Operative Technique

Our experience with robotic pancreatic resections started more than ten years ago and since then we have improved and standardized our technique. In our experience, the main advantages of the robot can be mostly appreciated during the uncinate process dissection, the lymphadenectomy and the reconstructive phase, in the case of pancreaticoduodenectomies; and in the spleen preservation, in the case of distal pancreatectomies [5, 6].

11.2.1 Step-by-Step Robotic Oncological Pancreaticoduodenectomy (PD)

The patient is placed supine, in a reverse-Trendelenburg position, slightly tilted to the left side. The robot is positioned at the patient's head. The assistant surgeon is placed between the patient's legs (Fig. 11.1).

We always start with a diagnostic laparoscopy, in order to exclude liver metastases or carcinomatosis.

The robotic trocars are placed as follows (Fig. 11.2):

- 12-mm camera port: placed in the right pararectal area (this allows optimal exposure of the superior mesenteric vein during the uncinate process dissection);
- 12-mm assistant port: placed in the periumbilical area;
- 8-mm port for the right robotic arm (R1): placed in the lower left hypochondriac region;
- 8-mm port for the left robotic arm (R2): placed medially in the right flank;
- 8-mm port for the fourth robotic arm (R3): placed laterally in the right flank (the fourth robotic arm is mainly used for retraction and exposure of tissues) when the patient body conformation is not too small;
- 5-mm assistant port: placed between the camera port and R2.

The procedure starts with the mobilization of the right colonic flexure. The lesser sac is opened and explored, in order to assess any tumor infiltration. The right colon is then mobilized up to the origin of the gastroepiploic vessels. The duodenum is exposed and the superior mesenteric vein (SMV) is identified at the root of the mesentery (evaluation of resectability).

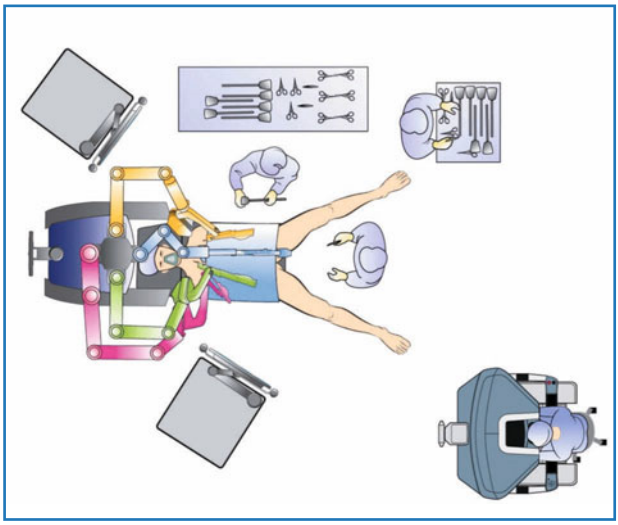

Fig. 11.1 OR setting for robotic pancreaticoduodenectomy. (©2014 Intuitive Surgical, Inc.)

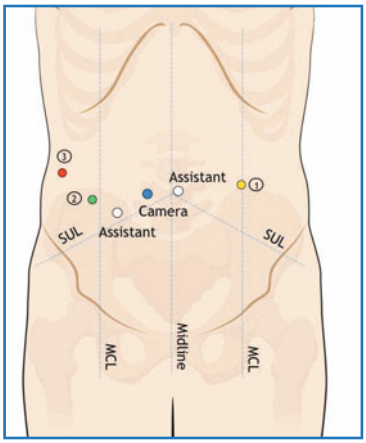

Fig. 11.2 Trocar placement for robotic pancreaticoduodenectomy. (© 2014 Intuitive Surgical, Inc.)

A wide Kocher maneuver is performed and continued up to the left lateral border of the aorta. The nodal tissue surrounding the portal vein, hepatic artery and common bile duct (CBD) is dissected and sent for permanent pathology.

The next step is the hepatic hilum dissection. At this point, the gall bladder is taken down (remains en bloc with the specimen by keeping the cystic duct intact) and the CBD is dissected and isolated. The common hepatic artery is identified, dissected and followed distally in order to identify the gastroduodenal artery that is then dissected, ligated and divided preferably in between sutures. At this point, the CBD can be transected and its proximal margin sent to pathology for frozen-section evaluation.

The pancreas is now exposed and the pancreatic neck is identified. The dissection continues along the inferior border of the pancreas in order to expose the SMV. The retropancreatic tunnel can be created at this point, paying attention not to disrupt any vascular branches.

Usually at this point we perform an intraoperative ultrasound in order to localize the mass and assess its relationship to the vessels.

The duodenum (or the stomach, depending on the type of pancreaticoduodenectomy) is now transected, using an Endostapler. The jejunum is also divided using a stapler device, distal to the Treitz ligament. At this point, the jejunum is retracted to the right, rotating the specimen. This maneuver facilitates exposure of the SMV and artery.

The pancreas is now completely dissected. Prolene® sutures are placed at the superior and inferior border of the pancreas as a way of anchoring and retracting it, prior to division of the gland. The parenchyma is now divided using the robotic ultrasonic shears (Intuitive Surgical, Sunnyvale, CA) being careful not to occlude the duct. A plastic stent is placed in the main pancreatic duct and secured with a stitch. The proximal margin of the pancreatic remnant is sent to pathology for frozen-section analysis.

The next step is the uncinate process dissection. The pancreas is lifted upward and rotated, facilitating the dissection from the SMV; the fourth robotic arm facilitates the retraction. The dissection begins distally, following the SMV upward (Fig. 11.3). The small jejunal branches are transected either with the robotic ultrasonic shears or between sutures. The value of robotic technology is particularly evident during this step of the procedure. The stability of the platform and the magnified vision, together with the EndoWrist® instruments, allow a precise dissection with minimal blood loss. Moreover, even in the case of bleeding, suturing can be performed like in open surgery, with less technical difficulty compared to laparoscopy.

After confirmation of the negative resection margins, the reconstructive phase of the operation can begin. In the case of a pylorus-preserving procedure, we prefer performing a dunking transgastric pancreaticogastrostomy (PG) (Fig. 11.4). The PG is performed by making an anterior gastrotomy and then pulling the pancreatic stump into the gastric cavity through a posterior gastrotomy. Once the pancreas is well mobilized (for at least 2 inches) inside the stomach, the sutures are placed and the anterior gastrotomy is closed with a running PDS suture. Attention must be made to the accurate hemostasis of the gastric mucosa, in order to avoid postoperative bleeding. The hepaticojejunostomy (HJ) and duodenojejunostomy are performed with a single loop of jejunum, with running PDS suture, or interrupted stitches in the case of a HJ with a small/normal CBD. In the case of the classical Whipple, without preservation of the pylorus, the jejunal loop is used for the pancreatic reconstruction. We usually prefer placing two drains, one near the PG and one near the HJ.

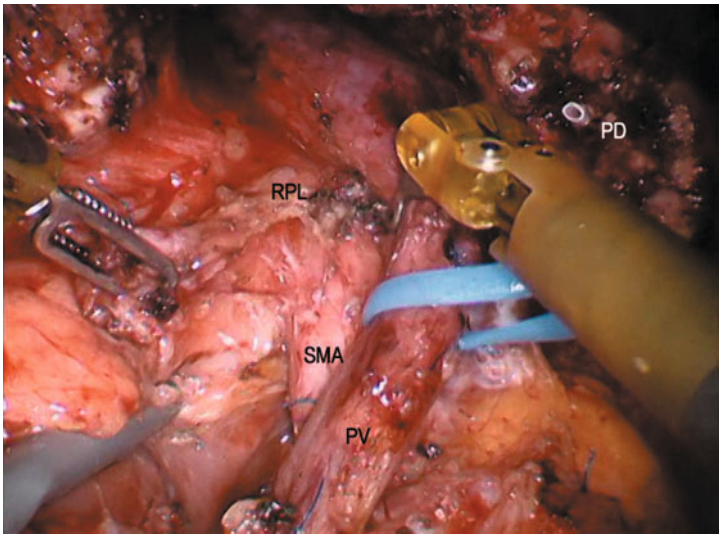

Fig. 11.3 Uncinate process dissection. The dissection follows the superior mesenteric vein caudal to cephalad. *SMV*, superior mesenteric vein; *SMA*, superior mesenteric artery; *RPL*, retroportal lamina; *PD*, pancreatic duct

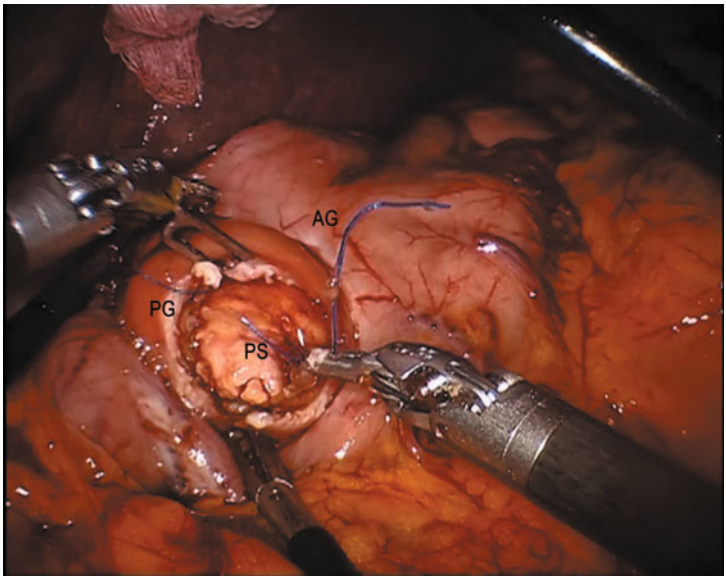

Fig. 11.4 Dunking transgastric pancreaticogastrostomy during the reconstructive phase of pancreaticoduodenectomy. An anterior gastrotomy is performed and the pancreatic stump is then pulled into the gastric cavity through a posterior gastrotomy. *PG*, posterior gastrotomy; *AG*, anterior gastrotomy; *PS*, pancreatic stump

After the reconstruction is completed, accurate hemostasis is performed. The specimen is placed in an Endobag and extracted through a Pfannenstiel incision, or through a previous incision, if present.

11.2.2 Robotic Distal Splenopancreatectomy (DSP)

Facilitating splenic preservation in distal pancreatectomy (DP) is one of the main advantages of using the robotic technique. But in case of pancreatic cancer, we require DSP for adequate lymphadenectomy to maintain the radical nature of the procedure.

Laparoscopy already has a clear and established role in DSP. The use of the robotic platform can be of benefit in the following steps of the procedure:

1. Better control of the vascular structures, especially when they are encased by the tumor. This allows performing more complex resections in a MI way;
2. More precise lymphadenectomy;
3. Major ability in performing multiorgan resections *en bloc*, if required.

11.2.2.1 Step-by-Step Robotic Distal Splenopancreatectomy

The patient positioning, trocar placement and docking are similar to the robotic PD. For this procedure, the 12 mm camera port is placed periumbilically, along the midline.

After a diagnostic laparoscopy, the procedure starts by dividing the gastrocolic ligament and entering the lesser sac, paying attention to preserve the gastroepiploic artery. The stomach is retracted upward and the pancreas is exposed. At this point, we perform an intraoperative ultrasound in order to localize the lesion and its relationship to the vessels and surrounding organs.

The dissection starts at the pancreatic neck. The SMV, splenomesenteric confluence and portal vein are identified and dissected. A retropancreatic tunnel is now created and a Penrose drain is placed around the pancreatic neck for retraction purposes. The splenic vessels are isolated and dissected. The splenic artery is ligated and divided first, followed by the splenic vein. In some cases, the splenic vessels can be divided together using an Endostapler. The dissection continues proximal to distal, toward the tail of the pancreas, or vice-versa, depending on the location of the mass. The inferior border of the pancreas is dissected from the mesocolon. The pancreatic gland is now mobilized and the parenchyma is transected with the use of the robotic ultrasonic shears. The transection line of the pancreatic stump is reinforced with prolene mattress sutures, being careful to include the Wirsung duct in order to minimize the risk of a pancreatic leak. The lateral attachments of the spleen are dissected and the whole specimen is removed en bloc with the pancreas. A drain is placed near the pancreatic remnant.

Hemostasis is accurately checked. The specimen is placed in an Endobag and extracted through a Pfannenstiel incision or through enlargement of a trocar site.

11.3 Innovations

11.3.1 Indocyanine Green Fluorescence (ICG)

We are currently using ICG fluorescence during all the hepatobiliopancreatic procedures. In the case of robotic PD, we use ICG for biliary identification during dissection of the hepatic hilum. During robotic DSP, ICG can be used for identification of the vascular anatomy and even the vascular pattern of the pancreatic lesion. It is useful in identification of neuroendocrine tumors of the pancreas as well.

11.3.2 New instruments

A robotic EndoWrist® stapler is available in the market; this allows the surgeon sitting at the console to control the device directly.

Integrated imaging is one of the most important innovations that will soon be available. The robotic console could allow integration of preoperative imaging that could be superimposed onto the intraoperative view and may even allow virtual-reality options. This would be an important step toward better training of robotic surgeons and patient safety.

11.4 Advantages, Limitations and Personal Experience

Pancreatic resections, especially pancreaticoduodenectomies, represent the most challenging procedures in general surgery. The robotic approach can solve some of the technical difficulties that are encountered during laparoscopic pancreatic surgery. The features of the robot (EndoWrist® instruments, magnified vision, stable platform, tremor filtering) allow meticulous dissection, even in narrow operative fields and precise suturing (like in open surgery), which leads to better and easier anastomosis and bleeding control. In the case of PD, the robotic approach allows a fine dissection of the uncinate process, extensive lymphadenectomy and precise reconstruction. Moreover, vascular resection and reconstruction is feasible, like in open surgery. In distal pancreatectomy, the laparoscopic approach is currently the gold-standard for benign and borderline malignant disease. The robotic technique allows a higher spleen preservation rate, in the case of benign disease and multiorgan resection en bloc, if needed [6]. Even though long-term follow-up results are still lacking, the oncologic principles of open pancreatic resection can be followed with the robotic approach.

In a recent metanalysis comparing robotic to open pancreatic surgery, the authors report that the overall complication rate is lower with the robot (absolute risk reduction 12%). Robotic surgery also demonstrated to have a significantly lower reoperation rate and lower positive margin rate [12]. These results are

encouraging and even though larger studies are needed, they open the way for wider acceptance of robotic technology in the pancreatic field. It is important to note that robotic pancreatic surgery should be performed by experienced robotic, hepatopancreatobiliary surgeons. The initial learning curve of a robotic surgeon, should include simpler procedures and then be followed by more complex operations, such as pancreatic resections.

Our experience with robotic pancreatic surgery started in 2000. Since then 115 cases of PD and 77 cases of DP, for different indications, have been performed by a single surgeon, in two different centers (Grosseto, Italy and Chicago, USA). The results of the series were presented in an oral communication at the 2013 Clinical Robotic Surgery Association Meeting (Washington DC). Out of 114 PDs, 66 were standard Whipple procedures and 48 were pylorus-preserving; the mean operative time was 443.5 min (including the docking time), with a mean estimated blood loss of 343 mL; the conversion-to-open rate was 13% and the postoperative morbidity (Clavien III/IV) rate was 24.7%; the mortality rate was 2.8%; the surgical indication was malignant disease in 70% of cases; a negative resection margin (R0) was achieved in more than 90% of cases, with a mean of 19.4 lymph nodes retrieved.

Of the 77 DPs, 41 included splenectomy and 36 were spleen-preserving (these last ones performed for benign disease); the intention-to-treat spleen-preservation rate was 97%; the mean operative time was 236 min (including the docking time), with a median estimated blood loss of 100 mL; the rate of clinically significant postoperative pancreatic fistula, grade B according to the ISGPF definition [13], was 12%; no grade C fistulas occurred in our series; the conversion-to-open rate was 5% and the mortality was nil; surgery was performed for malignant disease in 36% of the patients; the mean number of lymph nodes harvested was 10.3, with a 90% negative resection margin.

We should mention at this point that opting for a robotic approach in pancreatic surgery also has some limitations, especially for the less experienced surgeons that have yet to learn how to troubleshoot the potential problems that could arise by using the robotic system. The lack of tactile feedback represents a drawback, especially at the beginning of the learning curve. With experience though, the surgeon learns how to compensate by taking advantage of the excellent vision that the robotic system provides. Another limitation is the difficulty of performing multiquadrant surgery and the inability of changing the patient's position, once the robotic system is docked. This can be overcome by careful preoperative planning of the robot setting and a correct placement of the robotic trocars, in a way that collisions will be avoided. Also, all the advanced robotic procedures require a trained team of assistant surgeon and scrub nurse. As the main surgeon is separated from the patient while performing robotic surgery, the assistant surgeon has to be trained enough to help in performing difficult tasks and also to take care of any emergency situation that could arise during the procedure. The role of a trained scrub nurse and operating room technician is also very important in streamlining the conduct of the procedure and preventing any

wastage of time and resources. Thus, team work is the key to success in advanced robotic surgery.

References

1. Siegel R, Naishadham D, Jemal A (2013) Cancer statistics, 2013. CA: Cancer J Clin 63:11–30
2. Bilimoria KY, Bentrem DJ, Ko CY et al (2007) Validation of the 6th edition AJCC Pancreatic Cancer Staging System: report from the National Cancer Database. Cancer 110:738–744
3. Konstantinidis IT, Warshaw AL, Allen JN et al (2013) Pancreatic ductal adenocarcinoma: is there a survival difference for R1 resections versus locally advanced unresectable tumors? What is a "true" R0 resection? Annals of Surgery 257:731–736
4. Venkat R, Edil BH, Schulick RD et al (2012) Laparoscopic distal pancreatectomy is associated with significantly less overall morbidity compared to the open technique: a systematic review and meta-analysis. Annals of Surgery 255:1048–1059
5. Giulianotti PC, Sbrana F, Bianco FM et al (2010) Robot-assisted laparoscopic pancreatic surgery: single-surgeon experience. Surgical Endoscopy 24:1646–1657
6. Milone L, Daskalaki D, Wang X, Giulianotti PC (2013) State of the art of robotic pancreatic surgery. World J Surg 37:2761–2770
7. Kendrick ML (2012) Laparoscopic and robotic resection for pancreatic cancer. Cancer J 18:571–576
8. Kooby DA (2006) Laparoscopic surgery for cancer: historical, theoretical, and technical considerations. Oncology (Williston Park) 20:917–927
9. Jayaraman S, Gonen M, Brennan MF et al (2010) Laparoscopic distal pancreatectomy: evolution of a technique at a single institution. J Am Coll Surg 211:503–509
10. Kim SC, Song KB, Jung YS et al (2013) Short-term clinical outcomes for 100 consecutive cases of laparoscopic pylorus-preserving pancreatoduodenectomy: improvement with surgical experience. Surgical Endoscopy 27:95–103
11. Subar D, Gobardhan PD, Gayet B (2014) Laparoscopic pancreatic surgery: An overview of the literature and experiences of a single center. Best Pract Res Clin Gastroenterol 28:123–132
12. Zhang J, Wu WM, You L, Zhao YP (2013) Robotic versus open pancreatectomy: a systematic review and meta-analysis. Ann Surg Oncol 20:1774–1780
13. Bassi C, Dervenis C, Butturini G et al (2005) Postoperative pancreatic fistula: an international study group (ISGPF) definition. Surgery 138:8–13

Part IV

Lower Gastrointestinal Surgery

Right Colectomy for Cancer: Three-arm Technique

12

Domenico Garcea, Francesca Bazzocchi, and Andrea Avanzolini

12.1 Procedure Overview

The surgical use of robotic systems stems from a military medical research effort. Since then it has been applied to several surgical specialties as the technological reply to overcome the inherent limitations of laparoscopy [1]. To date, however, scientific evidence about the clinical advantages of robotic colonic surgery over laparoscopy is still lacking.

Though the main benefits are expected to be demonstrated in low anterior resections and different studies have been published [2], robotic right colectomy is an ideal procedure for starting the robotic learning curve: it could represent the operation used for training and is propaedeutic for other more complex procedures.

The robotic system may have several potential advantages in performing right colectomies since it facilitates:

- a more precise, meticulous dissection and lymphadenectomy along the superior mesenteric vein, especially in obese patients with short and heavy mesentery or with voluminous lymph nodes;
- suturing and undertaking intracorporeal anastomosis;
- the extraction of the specimen through optimally located minimal incisions;
- an ergonomic operative position for increased comfort with reduction of physical stress;
- less experienced surgeons to perform complex tasks with a minimally invasive approach.

F. Bazzocchi (✉)
General, Gastrointestinal, and Minimally Invasive Surgery Unit,
"G.B. Morgagni - L. Pierantoni" Hospital,
Forlì, Italy
e-mail: francesca.bazzocchi@ausl.fo.it

G. Spinoglio (Ed), *Robotic Surgery: Current Applications and New Trends*,
Updates in Surgery
DOI: 10.1007/978-88-470-5714-2_12, © Springer-Verlag Italia 2015

12.2 Patient Positioning

The patient is supine with the right side up and the arms alongside the body in order to avoid neurological injury. Security devices, such as belts and shoulder holders, guarantee body position during Trendelenburg and left-side tilting movements.

The gastric tube and urinary catheter are placed; an intermittent mechanical compression device is applied to both legs to prevent deep venous thrombosis. Final positioning will be adjusted according to the operative field exposure before docking.

12.3 Robot Positioning and Docking

The operative field can be identified as a triangle connecting the right costal margin, right anterior superior iliac spine and the camera port. The patient cart will be moved aligning the camera arm along the bisectrix of the camera port angle (with the arrow on the second joint of the camera arm within the blue marker).

After correct positioning of the camera arm is achieved, the cart can be locked without any further changing of patient and operating table position (Fig. 12.1).

12.4 Trocar Placement

We usually perform right colectomy with a three-arm technique. The ports are placed as follows:

- camera port (C), 10–12 mm: on a transverse umbilical line, 3–5 cm left paraumbilical;
- instrument arm 1 (R1), 8 mm: on the left midclavicular line, 5 cm below left costal margin;
- instrument arm 2 (R2), 8 mm: on the left midclavicular line, slightly above the bisiliac line;
- assistant port, 10–12 mm: placed 10 cm lateral to the camera port (used for stapling, ligation, retraction, suction and irrigation);
- assistant port, 5 mm: on the midline 3–5 cm below xiphoid process (used for retraction, suction and irrigation) (Fig. 12.2).

The ports are inserted under direct vision once a pneumoperitoneum of 11 mmHg is achieved by means of open laparoscopy and the abdominal cavity is explored; port placement can be modified according to patient size and anatomy. After port placement, the patient is placed in the Trendelenburg position with a left tilt.

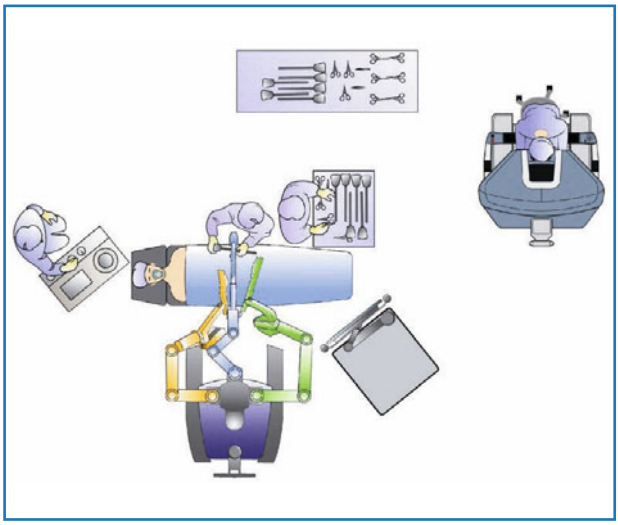

Fig. 12.1 OR setup (our technique). (© 2014 Intuitive Surgical, Inc.)

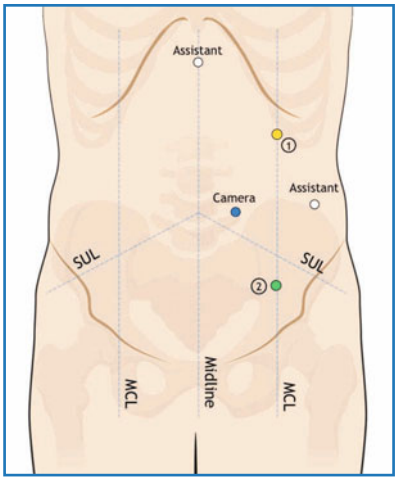

Fig. 12.2 Trocar placement (our technique). (© 2014 Intuitive Surgical, Inc.)

12.5 Step-by-Step Review of Critical Elements of the Procedure

The procedure begins laparoscopically in order to identify a tattoo, perform takedown of any adhesions and to rule out peritoneal or hepatic metastases. The greater omentum and the small intestine are moved toward the left upper quadrant of the abdomen thus exposing the cecum and terminal ileum as well as the

axis of the superior mesenteric vein: it represents the target and horizon of the operative field.

When the surgeon is sure about the feasibility of the procedure the robotic cart is docked. A medial to lateral approach is used. Sometimes in obese patients it is necessary to use a lateral to medial approach; an inferior to superior approach has also been described [3]. In order to avoid intraoperative complications, proper tractions and countertractions should be exerted by robotic and laparoscopic forceps to create an adequate exposure: the surgeon can better visualize the vascular anatomy and its variations, can avoid ureteral injuries and can execute a safe dissection along the correct planes without unnecessary bowel manipulation. The technique is described step-by-step.

12.5.1 Gastrocolic Ligament Dissection

The gastrocolic ligament is put in tension, divided and then dissected up to the right colic flexure so that the lesser sac and the duodenum are exposed. For neoplasms of the right colic flexure or proximal transverse colon, it is necessary to extend the dissection of the gastrocolic ligament toward the distal transverse colon, in order to facilitate the execution of the intracorporeal ileocolic anastomosis in the right side of the abdomen without changing the robotic docking. Moreover, in these neoplasms, it is mandatory to carry out the dissection of the gastrocolic ligament along the greater curve of the stomach rather than along the margin of the transverse colon, performing in this way the lymphadenectomy of the right gastroepiploic vessels.

12.5.2 Section of the Ileocolic Pedicle and of the Right Branch of the Middle Colic Pedicle

By retracting the mesocolon of the ascending colon anteriorly and laterally, it is possible to identify and lift up the ileocolic pedicle so that the peritoneum on each side is incised. The dissection is carried out along the avascular plane between Gerota's fascia posteriorly and Toldt's fascia anteriorly, up to the third and second duodenal portions, and the head of the pancreas superiorly and the right iliac vessels inferiorly. In this manner, two windows beside the ileocolic pedicle and lateral to the superior mesenteric vein are created. In this step, it is necessary to visualize the right ureter and gonadal vessels in order to avoid injuries. The ileocolic vein and artery and the right colic vessels (if present) are isolated and sectioned between large Hem-o-lok® (violet) clips at their origin. Now the assistant at the operating table lifts up the transverse colon with fenestrated forceps to visualize the middle colic pedicle and its branches. Depending on the tumor location, the surgeon can isolate and divide between the clips, the right branch, or the main trunk of the middle colic artery (Fig. 12.3).

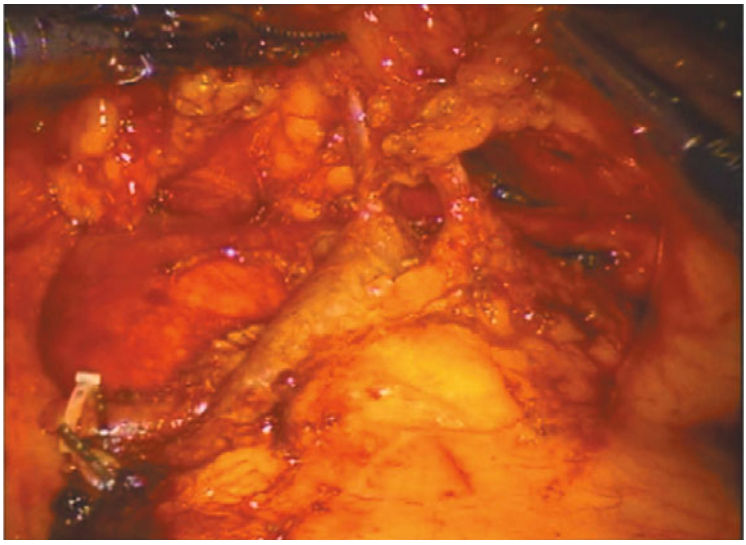

Fig. 12.3 Exposure of the superior mesenteric vein during lymphadenectomy

12.5.3 Mobilization of Right Colon

We continue with a medial to lateral dissection in the previously referred avascular plane. After cecum and ascending colon takedown is completed, the right colic flexure is fully mobilized.

12.5.4 Transection of Transverse Colon and Ileum

The transverse mesocolon is divided from its root to the colonic wall for final transection. The ileal mesentery is divided approximately 10–20 cm from the ileocecal valve. Marginal arteries will need to be controlled with clips or cautery. A linear articulated stapler with tri-staple technology is used by the assistant at the operating table for the transection of the transverse colon and ileum.

12.5.5 Intracorporeal Ileocolic Anastomosis

The ileum is approximated to the transverse colon in order to perform an intracorporeal isoperistaltic side-to-side anastomosis. With the use of the monopolar hook, we create the enterotomies through which the jaws of a linear stapler are inserted and fired. Now we put one stitch of suspension at the medial margin of

the mechanical suture and the bowel defect is closed with a two-layer running suture with an absorbable self-locking thread. The mesenteric defect is then closed with an absorbable suture.

The specimen extraction is carried out through a paraumbilical incision or a sovrapubic minilaparotomy with plastic wound protection.

12.6 Advantages, Limitations and Relative Contraindications (Personal Experience and Literature Outcomes)

The advantages of the robotic approach over standard laparoscopy are: a) a shorter learning curve; b) major precision in carrying out intracorporeal anastomoses; and c) a more accurate lymphadenectomy and dissection of the ileocolic and middle colic vessels, especially in obese patients or in patients with voluminous lymph nodes. On the other hand robotic procedures are associated with a significantly longer operative time, even if there are no differences in the estimated blood loss and early complication rates [3–7].

However, different factors can influence the abovementioned results: a) an intracorporeal anastomosis is usually performed in the robotic series and this is a time consuming technique; b) most of the clinical trials comparing robotic and laparoscopic outcomes have been performed by surgeons who had a greater experience with laparoscopic surgery whilst they were at the beginning of their robotic learning curve; c) for those surgeons who have skipped the laparoscopic step, a longer learning curve is necessary to standardize the robotic approach.

According to Spinoglio et al. [8], however, mean operative time decreases as team experience improves and other studies have demonstrated that robotic surgery has a shorter learning curve than laparoscopy [7].

Certainly, the robotic system greatly enables less experienced surgeons to perform an advanced minimally invasive procedure and permits a progressive improvement of the entire surgical team's skills. The robotic system may be a valid tool in carrying out an intracorporeal anastomosis [5, 8], though it is performed extracorporeally in some robotic series. [3, 9]. In our opinion, intracorporeal anastomosis avoids the risk of ileus caused by the mesenteric twisting during the extraction of the bowel and allows the surgeon to choose the optimal abdominal location to perform a small and cosmetic skin incision.

The robotic system improves the accuracy in vessel skeletonization and makes lymphadenectomy along the superior mesenteric vein easier, especially in the case of obese patients or voluminous lymph nodes. The mean number of retrieved nodes, reported in the systematic review by Fung, is 22.2. In our series (231 robotic colorectal resections), the mean number of harvested lymph nodes in right colectomies (91 cases) was 24.7; though controversies exist on the real value of higher lymph node counts, it may represent a measure of the quality of care of the robotic technique. Leak rate and 30-day mortality were 0%. Despite some skilled laparoscopic surgeons not recognizing the real value of the robotic

system in colectomies, we believe that the da Vinci® System may improve accuracy during lymphadenectomy and intracorporeal anastomosis. The high costs of robotic surgery represent the main limitation to the widespread diffusion of this technology. In order to reduce costs, we have chosen to use only three robotic arms and no more than three robotic instruments (monopolar hook, Maryland bipolar forceps, needle driver). Therefore, the approximate additional cost for a right colectomy is 2250 USD.

In conclusion, the robotic system improves the performance of the surgeon and allows to reproduce open procedures faithfully. Further studies comparing clinical and cost-effectiveness outcomes with laparoscopy are required to better assess the role of this technology in colorectal surgery.

References

1. Mirnezami AH, Mirnezami R, Venkatasubramanian AK et al (2010) Robotic colorectal surgery: hype or new hope? A systematic review of robotics in colorectal surgery. Colorectal Dis 12:1084–1093
2. Antoniou SA, Antoniou GA, Koch OO et al (2012) Robot-assisted laparoscopic surgery of the colon and rectum. Surg Endosc 26:1–11
3. Park SY, Choi GS, Park JS et al (2012) Robot-assisted right colectomy with lymphadenectomy and intracorporeal anastomosis for colon cancer: technical considerations. Surg Laparosc Endosc Percutan Tech 22:271–276
4. de Souza AL, Prasad LM, Park JJ et al (2010) Robotic assistance in right hemicolectomy: is there a role? Dis Colon Rectum 53:1000–1006
5. D'Annibale A, Pernazza G, Morpurgo E et al (2010) Robotic right colon resection: evaluation of first 50 consecutive cases for malignant disease. Ann Surg Oncol 17:2856–2862
6. Rawlings AL, Woodland JH, Vegunta RK et al (2007) Robotic versus laparoscopic colectomy. Surg Endosc 21:1701–1708
7. Fung AKY, Aly EH (2013) Robotic colonic surgery: is it advisable to commence a new learning curve? Dis Colon Rectum 56:786–796
8. Spinoglio G, Summa M, Priora F et al (2008) Robotic colorectal surgery: first 50 cases experience. Dis Colon Rectum 51:1627–1632
9. Zimmern A, Prasad L, Desouza A et al (2010) Robotic colon and rectal surgery: a series of 131 cases. World J Surg 34:1954–1958

Right Colectomy with Complete Mesocolic Excision: Four-arm Technique

13

Giuseppe Spinoglio, Alessandra Marano, Fabio Priora, Ferruccio Ravazzoni, and Giampaolo Formisano

13.1 Introduction

Minimally invasive surgery is gaining worldwide acceptance in the treatment of colonic cancer and the advantages over the traditional open approach are well known [1–3]. Unfortunately, during recent decades, the outcomes of patients after colon cancer resection have not improved to the same degree as for rectal cancer, whose treatment with total mesorectal excision (TME) is universally accepted as the standard of care. The complete mesocolic excision (CME), first reported by Hohenberger and colleagues in 2008 [4], seems to produce better long-term outcomes when compared to standard lymphadenectomy by following the same embryological-based principles introduced by Heald for rectal cancer more than 20 years ago [5]. However, well-conducted randomized studies are needed to confirm its efficacy.

Additionally, laparoscopic right colectomy with intracorporeal anastomosis is still considered by some surgeons as one of the most difficult procedures to perform [6] and radical lymphadenectomy with CME is technically challenging when performed with conventional laparoscopic instruments.

To date and to the best of our knowledge, few reports analyzing the safety and feasibility of laparoscopic CME for right-sided colonic malignancies exist in the literature [7–14]. No studies have focused selectively on the robotic approach.

This chapter describes the technical approach to robotic CME in right colectomy, including technical tips culminating from the author's nearly 10-year experience in robotic colonic surgery.

G. Spinoglio (✉)
Department of General and Oncologic Surgery,
"Ss. Antonio e Biagio" Hospital,
Alessandria, Italy
e-mail: giuseppe.spinoglio@gmail.com

G. Spinoglio (Ed), *Robotic Surgery: Current Applications and New Trends*,
Updates in Surgery
DOI: 10.1007/978-88-470-5714-2_13, © Springer-Verlag Italia 2015

13.2 Procedure Overview

The concept of CME stems from the knowledge of the embryological process of gut rotation and subsequent coalescence of fascial layers. The sharp dissection of the visceral fascial layer from the parietal one, both constituting the Toldt's fascia, results in a complete mobilization of the entire mesocolon covered by an intact visceral fascial layer on both sides: this allows the safe ligation of the supplying vessels (ileocolic, right colic if present and right branches of middle colic vessels) at their root. The procedure is full-robotic.

13.3 Patient Positioning

After induction of general anesthesia, a nasogastric tube and a urinary catheter are put in place. Antithrombotic prophylaxis with compressive elastic stockings is performed. The patient is placed on the operating room table in the supine position, with arms along the body and legs closed. After port placement has been completed, the table is placed in a Trendelenburg position with a slight angle (5–10°) and with a left tilt (5–10°). This position allows the small bowel to move aside under gravity and expose the right and transverse mesocolon. The head plate is tilted down (10–15°) to avoid facial soft-tissue injury from the robotic arm movement.

13.4 Trocar Placement

For optimal port placement, the superior mesenteric axis must be considered our "target" organ for CME. Figure 13.1a shows our trocar layout.

- The camera port is placed in the mid point of the left spinoumbilical line. This location in the left iliac fossa guarantees visualization of the entire right quadrant of the abdomen and the course of superior mesenteric axis.
- R1 is positioned 2–3 cm laterally to the left mid-clavicular line and 2–3 cm below the costal margin.
- R2 is placed on the midline and 2 cm above the symphysis pubis. The R1 and R2 trocars are used for dissection.
- R3 is located just below the xyphoid process and is used for retraction.
- The 15-mm assistant port is positioned between the camera port and R1 in the left flank. This port is used for suction/irrigation, clipping, stapling and additional retraction if necessary.

The distance between all ports should be at least 8 cm. We strongly recommend that the port locations are not changed and adapted according to the patient's body habitus. The umbilicus is always considered to be the midpoint between the xyphoid process and the pubis.

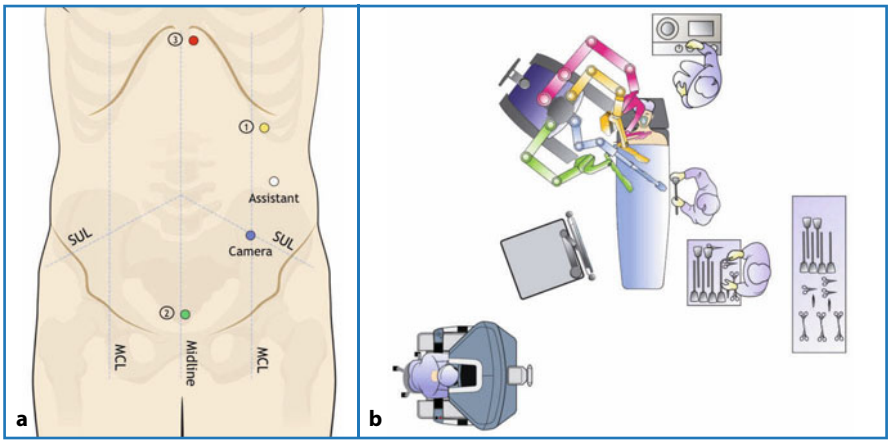

Fig. 13.1 Robotic right colectomy. **a** Trocar layout. **b** Overhead view of OR setup. (© 2014 Intuitive Surgical, Inc.)

13.5 Robot Positioning and Docking

The surgical cart is positioned at the patient's right hemithorax level with a 45° angle; the vision cart is on the right side of the surgical cart; and the robot arms are docked to the trocars. Figure 13.1b shows an overhead view of the recommended operating room setup for robotic right colectomy. The first assistant is on the patient's left side and the scrub nurse to the assistant's left.

13.6 Step-by-Step Review of Critical Elements of the Procedure

A 30° down endoscope is used. Monopolar curved scissors or a cautery hook are placed on arm 1 for dissection. Bipolar forceps and fenestrated Cadiere forceps are mounted on arm 2 and arm 3, respectively.

13.6.1 Step 1 – Mesocolic Exposure and Traction on the Superior Mesenteric Axis

The first important step is to achieve exposure of the right and transverse mesocolon. R2 and R3 trocars are used to keep the superior mesenteric axis in traction and the monopolar cautery hook/scissors in R1 are used for dissection.

13.6.2 Step 2 – Vascular Control with Complete Mesocolic Excision (Medial-to-Lateral Approach)

We routinely perform CME with a medial-to-lateral approach, primary exposure of the left anterior aspect of the superior mesenteric vein (SMV) and ligation of the vessels at their roots, avoiding the need of colonic detachment or Kocker maneuver as described by Hohenberger in open surgery. This strategy allows the complete removal of both visceral fascia layers of the right mesocolon, progressively exposing the root of the SMV in a caudal-to-cephalad direction.

The location of the camera port in the left iliac fossa guarantees visualization of the entire right quadrant of the abdomen and the course of the superior mesenteric axis, which is our "target" organ for CME. The trocar layout allows arm movement to be maximized and external collisions to be minimized without any difficulties in the far lateral and superior extension or the blind spots, with complete respect of optimal working, azimuth and elevation angles. After gentle cephalad traction on the transverse mesocolon, with the grasp in R3, the ileocolic vessels are identified and lifted up with R2; the peritoneum is then opened just below their prominence and along the left side of the anterior aspect of the SMV. Ileocolic vessels, right colic vessels (if present), right colic veins at their confluence with the Henle's sinus and the right branch of the middle colic artery can be easily and safely ligated at their roots along the right border of the superior mesenteric axis and at the Henle sinus (Fig. 13.2). Both the robotic clip applier (Hem-o-lok®, Weck) and the laparoscopic one (through the assistant port) can be used.

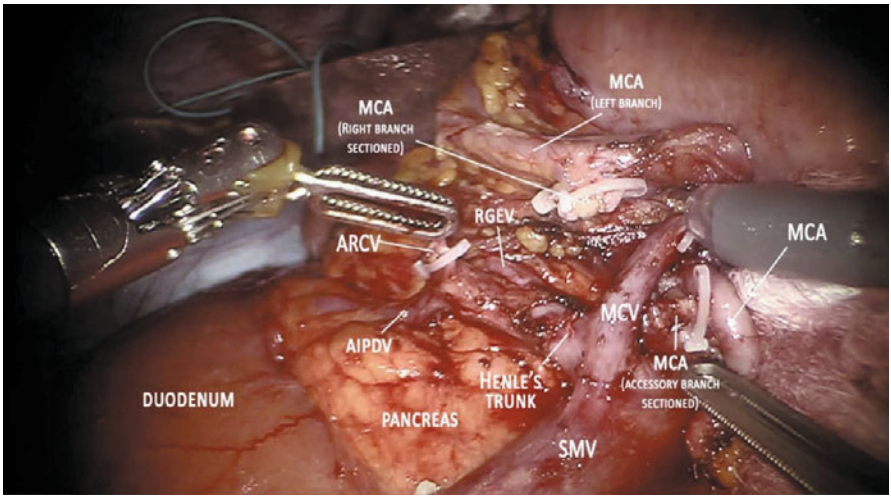

Fig. 13.2 Final view of the operative field after complete mesocolic excision. *MCA*, middle colic artery; *SMV*, superior mesenteric vein; *MCV*, middle colic vein; *RGEV*, right gastroepiploic vein; *ARCV*, accessory right colic vein; *AIPDV*, anterior inferior pancreaticoduodenal vein

A CME is performed by sharp dissection, exposing the duodenum and the pancreatic head. The right gonadal vessels and the right ureter are identified and preserved retroperitoneally. Cephalad dissection continues with the transverse mesocolic division from its root to the colon, which is transected with a linear stapler. When the hepatic flexure or the proximal transverse colon are involved (T3/T4/N+ tumors), en bloc resection of the right gastroepiploic lymphovascular chain is also performed close to the greater curvature of the stomach. The ileal mesentery is sectioned at the selected point with both monopolar and bipolar cautery devices and the skeletonized ileum is transected with a linear stapler. Both ileal and colonic stumps are evaluated for perfusion with ICG-NIR fluorescence imaging system and sectioned in a well-vascularized area. Complete coloparietal detachment is then performed; the specimen is inserted in a 15-mm Endobag, which is introduced through the assistant port and is subsequently placed in the right upper quadrant.

13.6.3 Step 3 – Ileocolic Intracorporeal Anastomosis and Specimen Extraction

The transverse colon and the ileum are approximated to choose the correct enterotomy sites, but no stay sutures are placed since they are not useful, in our opinion. Monopolar curved scissors in R1 are used to create enterotomies on the antimesenteric border of the ileum and the free taenia of the transverse colon. The monopolar device in R1 is then replaced with a needle driver. A 60-mm linear stapler is introduced through the assistant port to perform an isoperistaltic anastomosis and the enterotomies are subsequently closed with a robotically hand-sewn double-layer running suture (using absorbable monofilament barbed knotless sutures; V-Loc™ , Covidien). The mesenteric defect is also closed with a continuous suture to prevent internal hernias.

The specimen is then extracted into a plastic bag through a mini-Pfannenstiel incision performed at the suprapubic port site, avoiding any squeezing. The advantages of intracorporeal anastomosis are minimal colonic mobilization, limited chance for bowel and anastomotic twisting, and also the possibility to choose the specimen extraction site (according to the patient's history of prior abdominal surgery).

13.6.4 Step 4 – Wound Closure and Abdominal Re-exploration

Once the specimen is removed, the mini-laparotomy incision is closed and the pneumoperitoneum re-established for a final check of the operative field. No drain is routinely left in place. The trocars are removed under direct vision and all the sites greater than 8 mm in diameter are closed with absorbable sutures at the fascial level.

13.7 Advantages, Limitations and Relative Contraindications (Personal Experience and Literature Outcomes)

According to the retrospective and prospective published studies, robot-assisted right colectomy for cancer is technically safe and feasible and short-term postoperative outcomes are comparable to those of conventional laparoscopic surgery. Therefore, robotic assistance is not recommended by some authors [15] for right colectomy because of the higher costs involved, although experience with the robotic technique demonstrated considerably lower conversion rates, ranging from 0 to 4% [15–21], compared with 16.7–25% for laparoscopic colonic resections [1–3].

Table 13.1 Perioperative outcomes and pathological characteristics of robotic vs. laparoscopic right colectomy for cancer with complete mesocolic excision

	RRC (101 pts)	**LRC (101 pts)**	***p value***
Operating room time *(min)*			
Mean (SD)	279 (80)	236 (68)	*p<0.001*†
Range	135–540	95–465	
Conversion rate			
n (%)	0 (0)	7 (6.9)	*p=0.014*§
Length of stay			
Mean (SD)	7.9 (5.2)	7.9 (3.5)	*p=0.948*†
Range	4–37	4–19	
Time to return of bowel function *(days)*			
Mean (SD)	1.9 (1)	1.8 (0.8)	*p=0.563*†
Range	1–7	1–4	
Oral re-intake *(days)*			
Mean (SD)	1.3 (1.1)	1.1 (0.5)	*p=0.150*†
Range	1–9	1–4	
Harvested lymph nodes *(n)*			
Mean (SD)	28.2 (10.6)	30.4 (13.1)	*p=0.188*†
Range	13–66	12–74	
Specimen length *(cm)*			
Mean (SD)	35.2 (9.9)	36.2 (10.8)	*p=0.489*†
Range	21–70	20–88	
AJCC staging *(n)*			*p=0.088*‡
I	21	26	
II	38	28	
III	37	33	
IV	5	14	

Values are expressed as mean (SD=standard deviation) or n (%). *RRC*, robotic right colectomy; *LRC*, laparoscopic right colectomy; *AJCC*, American Joint Committee on Cancer; †Student's t test; ‡Pearson's chi-squared test; §Fisher's exact test

Table 13.2 Comparison of oncological outcomes

Study [Reference]	3-Y DFS	3-Y CRS	3-Y OS	3-Y LR	5-Y DFS	5-Y CRS	5-Y OS	5-Y LR	5-Y OS in converted pts
CLASSICC [1]	66.8%§	–	67.8%§	8.4%	56.4%§	–	57.9%§	10.1%§	49.6%§
COLOR [2]	74.2%§	–	81.8%§	–	66.5%§	–	73.8%§	8%§	–
COST [3]	83%§	–	85%§	–	80.2%§	–	77.1%§	–	–
Hohenberger et al. [4]	–	–	–	–	–	89.1%†	–	3.6%†	–
Our series	87.1%§ 91.1%‡	90.5%§ 93.7%‡	86%§ 91.2%‡	3.9%§ 1.9%‡	–	–	–	–	–

DFS, disease-free survival; *CRS*, cancer-related survival; *OS*, overall survival; *LR*, locl recurrence; § laparoscopic series; ‡ robotic series; † open series

To date, however, no robotic series directly addresses the issue of CME for right-sided colonic malignancies.

We recently conducted a retrospective analysis on prospectively collected data of 101 patients who underwent robotic right colectomy with CME at our institution between October 2005 and November 2013. The results of a consecutive contemporary series of 101 standard laparoscopic resections carried out with the same operative technique have been retrospectively analyzed. The groups were comparable in terms of baseline characteristics and we found only two statistically significant differences: the robotic series showed a lower conversion rate (0% vs. 6.9%; $p=0.014$) but longer operative times (279 min. vs. 236 min.; $p<0.001$) than the laparoscopic one (Table 13.1), thus confirming results from previously published studies. Anastomotic leak rate (1%) and reoperation rate (2%) were equal in both groups, as well as minor complication rates. The 3-year disease-free, cancer related and overall survival were 91.1%, 93.7% and 91.2% in the robotic group, respectively, and 87.1%, 90.5% and 86% in the laparoscopic series, respectively. Though encouraging and superior to the 3-year results from previous randomized studies (from 67.8% to 84.2%) [1–3], at least a 5-year follow-up is required (Table 13.2).

Robotic right colectomy with CME is feasible and safe. The inherent properties of the robotic system might eventually lessen the technical difficulties of vascular control, extended lymphadenectomy and intracorporeal anastomosis during right colonic resections, but longer operating room times are required. Nevertheless, scientific evidence about the clinical advantages of both the robotic approach and CME, if compared to laparoscopy and standard lymphadenectomy, is still insufficient at present to recommend their adoption in routine practice.

References

1. Jayne DG, Thorpe HC, Copeland J et al (2010) Five-year follow-up of the Medical Research Council CLASICC trial of laparoscopically assisted versus open surgery for colorectal cancer. Br J Surg 97:1638–1645
2. Fleshman J, Sargent DJ, Green E et al (2007) Laparoscopic colectomy for cancer is not inferior to open surgery based on 5-year data from the COST Study Group trial. Ann Surg 246:655–662
3. Buunen M, Veldkamp R, Hop WC et al (2009) Survival after laparoscopic surgery versus open surgery for colon cancer: long-term outcome of a randomised clinical trial. Lancet Oncol 10:44–52
4. Hohenberger W, Weber K, Matzel K et al (2009) Standardized surgery for colonic cancer: complete mesocolic excision and central ligation—technical notes and outcome. Colorectal Dis 11:354–364
5. Heald RJ (1988) The 'Holy Plane' of rectal surgery. J R Soc Med 81:503–508
6. Jamali FR, Soweid AM, Dimassi H et al (2008) Evaluating the degree of difficulty of laparoscopic colorectal surgery. Archives Surg 143:762–767
7. Bae SU, Saklani AP, Lim DR et al (2014) Laparoscopic-assisted versus open complete mesocolic excision and central vascular ligation for right-sided colon cancer. Ann Surg Oncol 21:2288–2294
8. Adamina M, Manwaring ML, Park KJ, Delaney CP (2012) Laparoscopic complete mesocolic excision for right colon cancer. Surg Endosc 26:2976–2980
9. Feng B, Ling TL, Lu AG et al (2013) Completely medial versus hybrid medial approach for laparoscopic complete mesocolic excision in right hemicolon cancer. Surg Endosc 28:477–483
10. Feng B, Sun J, Ling TL et al (2012) Laparoscopic complete mesocolic excision (CME) with medial access for right-hemi colon cancer: feasibility and technical strategies. Surg Endosc 26:3669–3675
11. Gouvas N, Pechlivanides G, Zervakis N et al (2012) Complete mesocolic excision in colon cancer surgery: a comparison between open and laparoscopic approach. Colorectal Dis 14:1357–1364
12. Shin JW, Amar AH, Kim SH et al (2014) Complete mesocolic excision with D3 lymph node dissection in laparoscopic colectomy for stages II and III colon cancer: long-term oncologic outcomes in 168 patients. Tech Coloproctol [Epub ahead of print]
13. Kang J, Kim IK, Kang SI et al (2014) Laparoscopic right hemicolectomy with complete mesocolic excision. Surg Endosc 28:2747-2451
14. Storli KE, Sondenaa K, Furnes B, Eide GE (2013) Outcome after introduction of complete mesocolic excision for colon cancer is similar for open and laparoscopic surgical treatments. Digestive Surg 30:317–327
15. Park JS, Choi GS, Park SY et al (2012) Randomized clinical trial of robot-assisted versus standard laparoscopic right colectomy. Brit J Surg 99:1219–1226
16. Zimmern A, Prasad L, Desouza A (2010) Robotic colon and rectal surgery: a series of 131 cases. World J Surg 34:1954–1958
17. Trastulli S, Desiderio J, Farinacci F et al (2013) Robotic right colectomy for cancer with intracorporeal anastomosis: short-term outcomes from a single institution. Int journal J Colorect Dis 28:807–814
18. D'Annibale A, Pernazza G, Morpurgo E et al (2010) Robotic right colon resection: evaluation of first 50 consecutive cases for malignant disease. Ann Surg Oncol 17:2856–2862
19. Shin JY (2012) Comparison of short-term surgical outcomes between a robotic colectomy and a laparoscopic colectomy during early experience. J Korean Soc Coloproctol 28:19–26
20. de Souza AL, Prasad LM, Park JJ et al (2010) Robotic assistance in right hemicolectomy: is there a role? Dis Colon Rectum 53:1000–1006
21. Casillas MA Jr, Leichtle SW, Wahl WL et al (2014) Improved perioperative and short-term outcomes of robotic versus conventional laparoscopic colorectal operations. Am J Surg 208:33–40

Left Colectomy and Segmental Resections for Cancer

14

Paolo Pietro Bianchi, Igor Monsellato, and Wanda Petz

14.1 Introduction

One of the goals of surgical oncology is to attempt to reduce the invasiveness of surgery while maintaining or further improving the outcomes of traditional open surgery. Therefore minimally invasive techniques have been applied to oncologic surgery since the end of 90s, on the basis of the good clinical results obtained by laparoscopic surgery in some benign diseases. The diffusion of laparoscopic colonic surgery has increased in recent years thanks to specific educational and training programs, but mainly in academic and high-volume hospitals [1]. The most frequently-performed procedures are the less difficult, such as sigmoidectomy for benign diseases and right colectomies with extracorporeal anastomosis [2]. Despite the improvement of technology some disadvantages of standard laparoscopy are still present, such as poor ergonomics, the difficulty to perform intracorporeal sutures and the problem of the assistant being able to hold the camera stable. Robotic surgery is an emerging technique that seems to overcome some difficulties of the standard laparoscopic approach, and its use in colorectal cancer is increasing quickly [3]. In this chapter, the technical details of robotic left colectomy and segmental colonic resections are reported.

P. P. Bianchi (✉)
Minimally Invasive Surgery Unit, European Institute of Oncology, Milan, Italy
e-mail: paolo.bianchi@ieo.it

G. Spinoglio (Ed), *Robotic Surgery: Current Applications and New Trends*, Updates in Surgery
DOI: 10.1007/978-88-470-5714-2_14, © Springer-Verlag Italia 2015

14.2 Left Colectomy

14.2.1 Patient Positioning and Docking

The patient is placed in a supine position with arms alongside the trunk and legs abducted. A slight Trendelenburg position and a right tilt are maintained in order to expose the operative field from the ileal loops. The procedure starts with the insertion of the Veress needle in the left hypochondrium through which a 12-mmHg pneumoperitoneum is induced. A 12-mm standard laparoscopic trocar is placed 2 cm right of the midline along an ideal line passing through the left anterosuperior iliac spine and right hypochondrium. The procedure is performed with a five-trocar technique: three 8-mm robotic trocars and two 12-mm standard laparoscopic trocars (Fig. 14.1a). The robotic cart approaches the operative table from the left side of the patient and the robotic arms are connected to the trocars, starting from the camera. Arm 1 is connected to the trocar in the right iliac fossa, arm 3 is connected to the trocar in the right hypochondrium, arm 2 is connected to the trocar in left iliac fossa (Fig. 14.1b). The initial instrument positions are configured as follows: the robotic monopolar hook/scissors are mounted on arm 1, the robotic grasper on arm 2 and the robotic bipolar grasper on arm 3.

14.2.2 Step-by-Step Review of Critical Elements of the Procedure

14.2.2.1 Left Colectomy and Sigmoidectomy

A laparoscopic exploration of the abdominal cavity and an intraoperative ultrasonography of the liver are systematically carried out in order to complete the staging of the disease. The laparoscopic exploration can be performed with the robotic camera or with a standard laparoscope. The standard laparoscope has the advantage of easy manoeuvrability compared to the manual use of the robotic camera, particularly when some adhesions must be removed before the full placement of the trocars. The site of the tumor is localized and the surgical procedure is usually planned with a complete mobilization of the splenic flexure.

14.2.2.2 Splenic Flexure Mobilization

The inferior mesenteric vein (IMV) is individuated at the level of the inferior border of the pancreas and a left retromesocolic dissection is carried out. A stable retraction of the left mesocolon is provided by the robotic grasper on arm 2, enhancing the saliency of the IMV. The bipolar grasper on arm 3 lifts the vein up and an incision in the peritoneum is performed below the vein by the robotic monopolar hook or scissors on arm 1; the virtual avascular plane between the two folds of the Toldt's fascia is opened. A sharp dissection is carried out in a medial-to-lateral way along the avascular plane. The root of the transverse mesocolon, exposed by the assistant by a laparoscopic grasper, is sectioned by

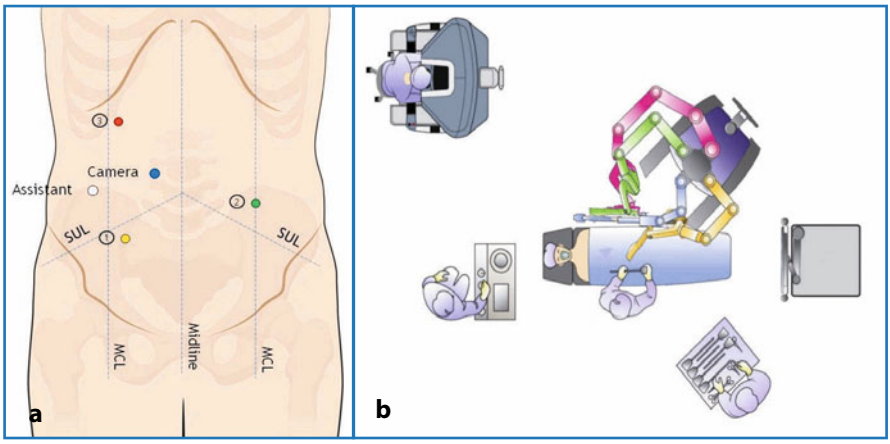

Fig. 14.1 Robotic left colectomy/splenic flefure resection. **a** Trocar positioning. *1*, monopolar robotic cautery device (hook or scissors); *2*, robotic grasper (Cadiere forceps); *3*, robotic bipolar grasper. **b** OR setup. (© 2014 Intuitive Surgical, Inc.)

the robotic monopolar hook on arm 1; the bipolar grasper on arm 3 helps this surgical step by granting a stable tension on the root. This maneuver allows the opening of the lesser sac, anterior to the pancreas (Fig. 14.2a). The IMV is freed from the peritoneal envelope by the robotic monopolar hook on arm 1 and sectioned between clips positioned by the assistant or by a robotic clip applier on arm 1. Medial dissection is carried out to the end of the pancreatic tail; a gauze may be positioned under the left mesocolon as a marker of the plane of dissection. Thereafter, the descending colon is retracted medially by the robotic grasper on arm 1 and by the assistant with a grasper. Lateral mobilization of the descending colon is achieved by the dissection of the parietocolic ligament performed by the robotic monopolar hook on arm 2. During this step, robotic arm 3 is not utilized. The left colon is then freed laterally in the caudocranial pathway up to the splenic flexure. The phrenocolic and splenocolic ligament, as well as the sustentaculum lienis, are sectioned by the robotic monopolar hook on arm 1 and bipolar coagulation. The robotic grasper on arm 3 gently retracts the spleen laterally with a gauze. Complete mobilization of the splenic flexure is obtained by dissection of the coloepiploic ligament. Then the transverse colon is retracted inferiorly by the grasper on arm 1 and by the assistant; the bipolar grasper on arm 3 lifts the coloepiploic ligament cranially, which is dissected by the robotic scissors on arm 2.

14.2.2.3 Inferior Mesenteric Artery Dissection with Locoregional Lymphadenectomy

The assistant pulls upward the dissected IMV with a grasper, while the arch of the inferior mesenteric artery (IMA) is lifted up and downward by the bipolar

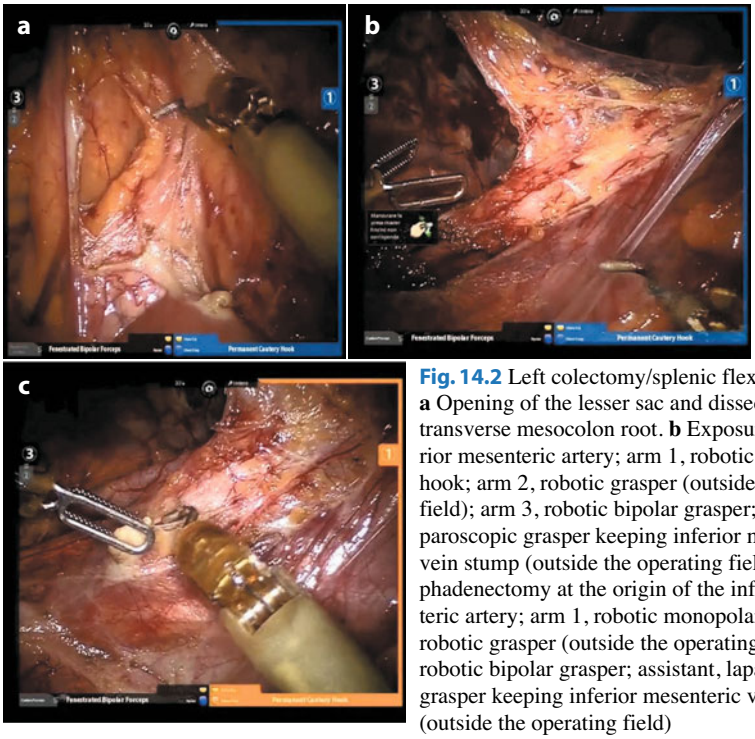

Fig. 14.2 Left colectomy/splenic flexure resection. **a** Opening of the lesser sac and dissection of the transverse mesocolon root. **b** Exposure of the inferior mesenteric artery; arm 1, robotic monopolar hook; arm 2, robotic grasper (outside the operating field); arm 3, robotic bipolar grasper; assistant, laparoscopic grasper keeping inferior mesenteric vein stump (outside the operating field). **c** Lymphadenectomy at the origin of the inferior mesenteric artery; arm 1, robotic monopolar hook; arm 2, robotic grasper (outside the operating field); arm 3 robotic bipolar grasper; assistant, laparoscopic grasper keeping inferior mesenteric vein stump (outside the operating field)

grasper on arm 3, enhancing the shape of the IMA (Fig. 14.2b). The angle between the IMA and the aorta is opened. This maneuver helps the surgeon to identify the paraaortic nerves, which lie over the preaortic plane, the surgical field is clear because of the stable retraction of the IMA by the locked robotic grasper. A careful dissection of the IMA and a locoregional lymphadenectomy is carried out preserving the paraortic nerves and the superior hypogastric plexus. This step is performed with the robotic monopolar hook on arm 1 and bipolar grasper on arm 3, which work synergically. The articulated tip of the robotic monopolar hook facilitates dissection of the IMA, which is freed by the surrounding lymphatic tissue, providing an optimal locoregional lymphadenectomy (Fig. 14.2c). As for the IMV, the IMA is isolated between clips positioned by the assistant or by robotic clip applier and then sectioned by the robotic scissors on arm 1 or by the assistant.

14.2.2.4 Distal Transection of the Colon

The site of distal transection is localized about 3 cm below the promontory, the proximal rectum is retracted superiorly and laterally by the robotic grasper (arm 2) and the wall of the rectum is cleaned with bipolar coagulation of the superi-

or mesorectal fat. The proximal rectum is sectioned with a linear stapler controlled by the assistant. This step can also be performed by a robotic stapler on arm 1, if available. The anastomosis is fashioned according to the Knight & Griffen technique. A minilaparotomy is created in the left iliac fossa or suprapubically. The descending colon is extracted through the protected incision and transected proximally. The anvil of a circular stapler is inserted into the colon stump and fixed by a manual purse-string suture. The colon is then reintroduced into the abdomen and the minilaparotomy is closed. A laparoscopy is carried out to perform the transanal end-to-end mechanical colorectal anastomosis. During this step the robot is undocked, but not deactivated, as it could be useful to perform additional sutures in the case of weak anastomosis.

14.3 Splenic Flexure Resection

14.3.1 Procedure Overview

Splenic flexure resection is a challenging procedure in minimally invasive surgery, both for anatomical and technical aspects [4]. The splenic flexure (SF) is joined strictly to the spleen by means of the splenocolic ligament and sustentaculum lienis. This anatomical connection requires colic manipulation to be performed gently in order to avoid any trauma or bleeding of the spleen, which is associated to an increased risk of postoperative morbidity. Moreover, there are some anatomical variables of the SF, such as the so-called "high" or "bulky" splenic flexure, which are demanding both in laparoscopic and in open surgery. Another challenging technical aspect in SF resection is vessel and lymph node dissection. Vascular supply to the SF is carried out by the left colic artery, originating from the IMA, and the middle colic artery, originating from the superior mesenteric artery (SMA). Individuation of the two vessels is considered technically difficult in traditional laparoscopy and depends on the surgeon's experience [5]. Lymphadenectomy involves all the nodes around these vessels and care should be taken in manipulating the transverse mesocolon during dissection around the middle colic vein to avoid venous bleeding. The anastomosis when performed intracorporeally is another demanding step, which requires extensive experience in minimally invasive surgery. Robotic assistance is helpful because it provides a stable three-dimensional vision of the anatomy, a fine vascular dissection and an easy fashioning of the intracorporeal anastomosis.

14.3.2 Patient Positioning and Docking

The patient is placed in the supine position with arms alongside the trunk. A slight anti-Trendelenburg position with a 10° right tilt are maintained in order to

expose the operative field from the ileal loops. The positioning of trocars, OR setup, and instruments are the same as for coloctomy (Fig. 14.1a, b).

14.3.3 Step-by-Step Review of Critical Elements of the Procedure

14.3.3.1 Splenic Flexure Mobilization

The procedure starts with the dissection of the IMV and IMA and identification of the left colic vein (LCV) and artery (LCA). The stable retraction of the left mesocolon provided by the robotic grasper on arm 2 and by an assistant grasper makes it easy to identify the origin of the IMA and then that of the LCA. Even though it is possible to section only the ascending branch of the LCA, it is preferable to section the entire artery, as the arterial vascular supply for the remnant descending colon and of the sigmoid is granted by the sigmoid vessels, i.e., branches of the IMA. In anatomic favorable patients, IMV can be preserved by dissecting and sectioning only the LCV, otherwise the IMV is dissected and sectioned as described in the left colectomy procedure. Left colic vessels are clipped by the assistant or by the robotic clip applier and sectioned by the assistant or by the robotic scissors on arm 1. After vascular dissection the descending colon and the splenic flexure are completely mobilized following the same steps described in left colectomy. The mobilization of the left colon is performed up to the sigmoid loop, as far as possible, in order to avoid any tension of the anastomosis. At this step, robotic arm 2 is not utilized.

14.3.3.2 Dissection of the Left Branch of the Middle Colic Vessels and Locoregional Lymphadenectomy

During this phase robotic arm 2 is turned upward and the robotic grasper maintains the distal transverse colon retracted, exposing the transverse mesocolon and facilitating vascular dissection. The assistant pulls the transverse colon upward providing tension on the root of the transverse colon. The identification of the middle colic vessels (MCV) starts at the level of the origin from the superior mesenteric axis near the inferior margin of the pancreas. The bipolar grasper on arm 3 provides a stable tension of the middle colic vessels and a precise isolation of the left branch of the MCV is performed by the robotic electrocautery hook on arm 1. The vessels are clipped by the assistant or by the robotic clip applier and sectioned by the robotic scissors on arm 1.

14.3.3.3 Transection of the Transverse and Descending Colon and Anastomosis

Once the SF has been mobilized and vascular dissection has been performed, the transverse colon and the left colon are transected by the assistant with a laparo-

scopic linear stapler. The use of both laparoscopic and robotic instruments permits a wider angle of motion and allows an easy transection of both the descending and transverse colon. After transection a stitch is placed to join together the colonic stumps; the wide articulation of the tip of the robotic needle-holder facilitates the intraoperative knotting, reproducing precise movements as in open surgery (Fig. 14.3a). The robotic bipolar gasper on arm 3 holds the descending colon stump while a colotomy is performed at the level of the tenia, with the robotic monopolar hook on arm 1. Then the assistant holds the transverse colon stump and a second incision is perfomed at the level of the tenia of the transverse colon stump, again with the robotic monopolar hook on arm 1. The laparoscopic linear stapler is introduced by the assistant through the trocar in the right flank and the surgeon at the console helps the introduction of the two branches of the stapler inside the colonic stumps with the robotic grasper on arm 1 and 3. A colo-colic side-to-side mechanical anastomosis is then performed (Fig. 14.3b). The vascular perfusion of the site of the colic transection can be evaluated by the use of indocyanine fluorescence and near-infrared image, if available, in order to reduce the risk of an ischemic anastomotic damage [6] (Fig. 14.3c). Thereafter, the entry hole of the stapler is closed by two running sutures starting from the opposite angles. The robotic grasper on arm 2 pulls the tail of the upper suture up favoring a stable position of the anastomosis, thus facilitating the closure of the defect. The first running suture is performed from the inferior angle upward. The tail of the upper suture and the inferior suture are tied together. After completing the first layer, the second suture is performed from the upper angle downward. As for the first layer, the upper suture is tied with the tail of the inferior suture; the wide articulation of the robotic needle-holder facilitates knot-tying (Fig. 14.3d). Then the robot is disconnected from the patient and a suprapubic minilaparotomy is performed through which the specimen is extracted inside a bag and with the placement of a wound protector.

14.4 Transverse Colon Resection

14.4.1 Patient Positioning and Docking

The patient is placed in anti-Trendelenburg position with the arms along the trunk and the legs abducted with a slight tilt to the right, which allows the small bowel to roll off the operative field (Fig. 14.4a).

The procedure starts with the insertion of the Veress needle in the left hypochondrium through which a 12-mmHg pneumoperitoneum is induced. A 12-mm standard laparoscopic trocar is placed 2 cm right of the midline along an ideal line passing through the left anterosuperior iliac spine and the right hypochondrium. The procedure is performed with a five-trocar technique: three 8-mm robotic trocars and two 12-mm laparoscopic trocars. Three 8-mm trocars

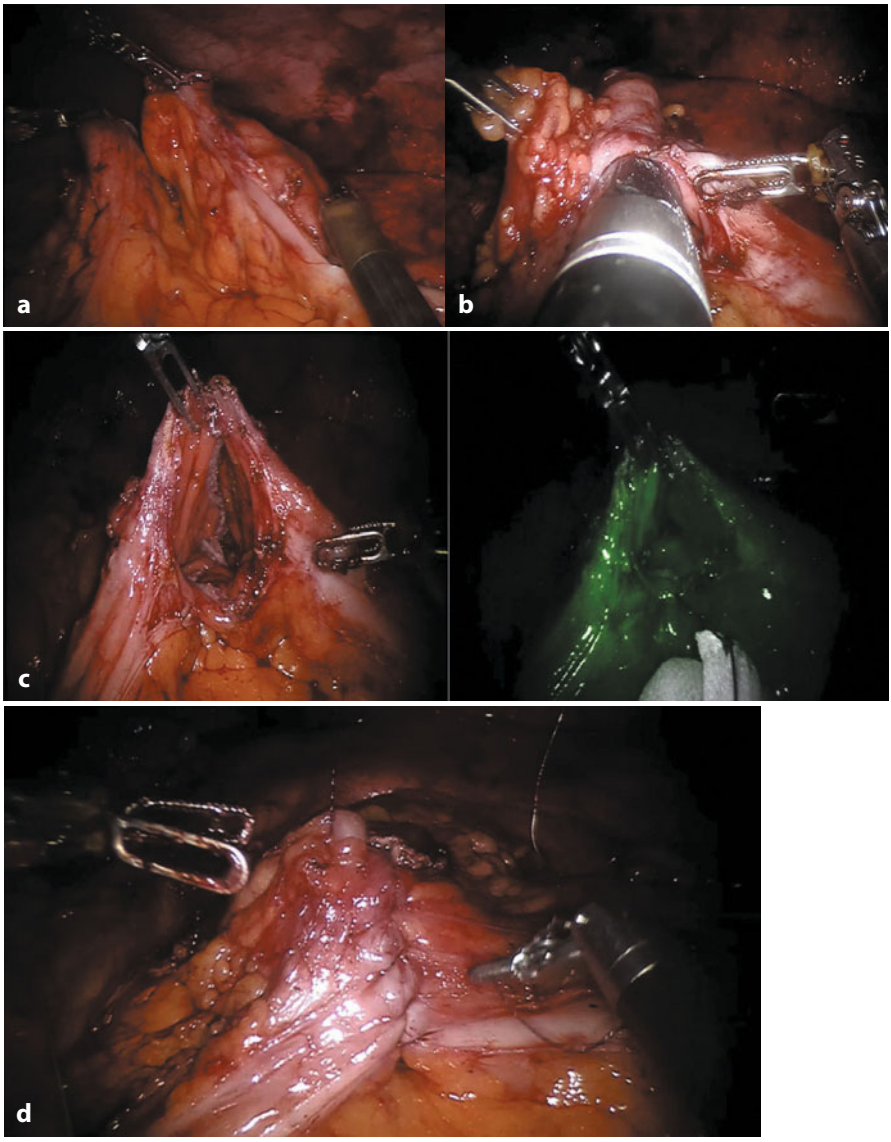

Fig. 14.3 Splenic flexure resection. **a** Approach of the transverse and descending colonic stumps by a stitch. **b** Fashioning of a side-to-side colo-colonic anastomosis by linear stapler. **c** Evaluation of colo-colonic anastomosis perfusion by fluorescence and near-infrared imaging. **d** Robotic suture of the service hole, after stapler colo-colonic side-to-side anastomosis

are placed in the left and right hypochondrium, and in the right flank, respectively. A 12-mm trocar is placed in the left flank for the assistant. The robotic cart approaches the operative table from the patient's head and the robotic arms are

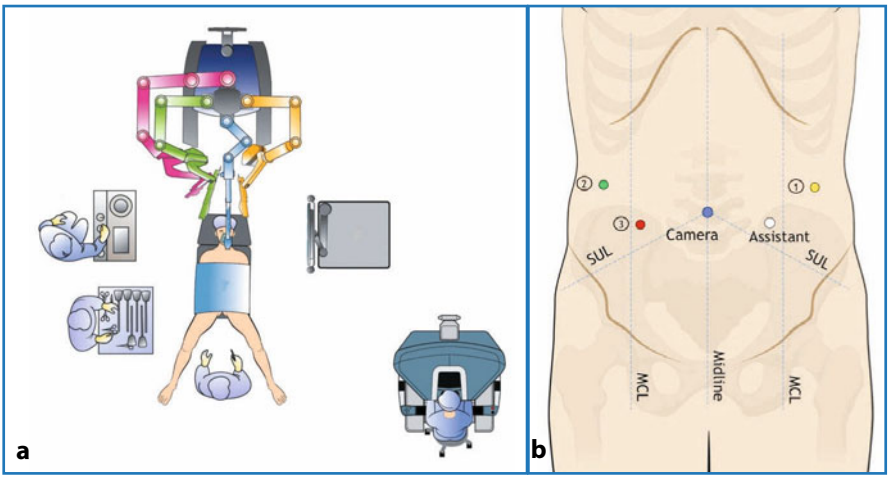

Fig. 14.4 Robotic transverse colonic resection. **a** OR setup. **b** Trocar positions. *1*, monopolar robotic cautery device (hook or scissors); *2*, robotic grasper (Cadiere forceps); *3*, robotic bipolar grasper. (© 2014 Intuitive Surgical, Inc.)

connected to the trocars, starting from the camera. Arm 1 is connected to the trocar in the left hypochondrium, arm 2 is connected to the trocar in the right hypochondrium, while arm 3 is connected to the trocar in the right flank (Fig. 14.4b). The initial instrument positions are configured as follows: the monopolar hook/scissors are mounted on arm 1, the robotic grasper on arm 2 and the robotic bipolar grasper on arm 3.

14.4.1.1 Dissection of the Middle Colic Vessels and Locoregional Lymphadenectomy

The greater omentum is pulled up by the surgeon with the robotic graspers on arms 1 and 2, helped by the assistant with a laparoscopic grasper, to expose the transverse colon and to identify the correct site of the tumor. The transverse colon is pulled up by the robotic grasper on arm 2, thus enhancing the middle colic vessels and exposing the ligament of Treitz and the root of the transverse colon. The latter is incised by the robotic monopolar hook on arm 1 at the origin of the main trunk of the middle colic vessels toward the end of the pancreatic tail. The lesser sac is opened. The bipolar grasper on arm 3 gently provides a stable tension on the vessels, facilitating the dissection and locoregional lymphadenectomy. The robotic monopolar hook on arm 1 allows circumferential isolation of the main trunk of the middle colic vein, which is clipped by the assistant or by the robotic clip applier and sectioned by the assistant or by the robotic scissors on arm 1. Dissection of the transverse mesocolon continues in a medial-to-lateral pathway. The robotic grasper on arm 2 grants a stable tension on the transverse colon and mesocolon; the robot-

ic bipolar grasper on arm 3 pulls up the mesocolon while the robotic monopolar hook or scissors on arm 1 perform a dissection of the transverse mesocolon from the posterior peritoneal layer toward the right colic flexure. Dissection of the transverse mesocolon is now achieved, resembling a V-shape with the base on the transverse colon, which is now pulled down.

14.4.1.2 Mobilization of the Left and Right Colic Flexures and of the Transverse Colon

The assistant provides a medial retraction of the proximal part of the descending colon and of the splenic flexure, as well as the bipolar grasper on arm 2, while the parietocolic ligament is sectioned by the robotic monopolar hook up to the left colic flexure. The phrenocolic and splenocolic ligament, as well as the sustentaculum lienis, are sectioned by a robotic monopolar hook on arm 1. The assistant now pulls the transverse colon down with a grasper, while the robotic bipolar grasper on arm 2 lifts up the proximal side of the gastrocolic ligament. The ligament is then dissected below the gastroepiploic vessels by the robotic monopolar hook on arm 1 up to the right flexure. The right colon is then retracted medially by the assistant by a laparoscopic grasper and by the robotic grasper on arm 3, allowing the dissection of the right parietocolic ligament, performed by the robotic monopolar hook on arm 2. Total mobilization of both the right and left colic flexures and of the transverse colon is completed without changing the docking of the robot.

14.4.1.3 Transection of the Transverse Colon and Anastomosis

The assistant transects the transverse colon with a laparoscopic linear stapler on both left and right side. The right and the left colon are joined by the robotic graspers on arms 1 and 2. Both the two colonic stumps are opened at the distal part by robotic scissors on arm 1 and an intracorporeal colo-colonic end-to-end anastomosis is performed with a double running suture (Fig. 14.5). The robotic grasper on arm 3 holds the right colon and the assistant holds the left colon with a grasper during this step. The articulation of the tip of the robotic needle-holders is an advantage in fashioning intracorporeal manual end-to-end anastomoses, as well as the three-dimensional view provided by the robotic system.

14.4.2 Advantages, Limitations and Relative Contraindications

The first robot-assisted colectomy was reported by Weber et al. in 2002 [6]. Since then several reports on robotic colorectal surgery have been published, but originating mainly from single-center experiences. In Table 14.1, the results are reported of the studies with more than 10 cases of robotic colonic resections. In all of these studies the main significant data was that robotic surgery resulted in a lower percentage of conversion to open surgery, compared to the laparoscopic

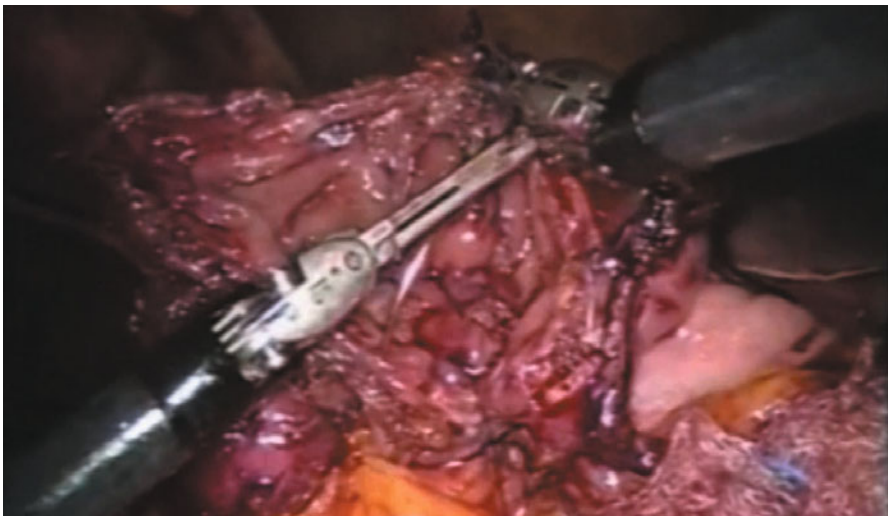

Fig. 14.5 Robotic transverse colonic resection. Robotic sewing end-to-end colo-colonic anastomosis

groups. Regarding short-term clinical and oncologic outcomes, no significant differences were found between laparoscopy and robotic surgery (Table 14.1) [7–15]. Advantages of robotic assistance in mobilizing the left colic flexure have been reported [11]. In the case of a high splenic flexure, the focused three-dimensional vision allows the correct identification of the flexure borders and its relation to the spleen, while a gentle traction on the spleen is granted by the robotic arm, avoiding the risk of splenic rupture or laceration. The improved dexterity of the instruments favors a precise tissue dissection and facilitates the intracorporeal fashioning of the anastomosis. The operative time was longer than those of laparoscopy, especially, in the first experiences, ranging from 162 to 383 minutes. Most of the authors reported that the docking/setup time was the main cause of longer operative time, beside the time spent for the learning curve, which has been demonstrated, however, to be shorter than the laparoscopic technique. Multiquadrant procedures have been claimed to be challenging if performed by robotic assistance, but if a redocking of the robot was necessary in the early experiences, to date, several multiquadrant surgeries have been carried out by switching one or more robotic arms without the need to redock the robot, with a reduction in the overall operative time.

One of the main concerns about robotic technology is the high cost of the purchase and maintenance of the equipment. Baek et al. [16] showed increased costs in robotic rectal resection compared to those in the standard laparoscopic procedure, with a significantly lower hospital profit in the robotic group.

Another emerging problem is the appropriate use of the technology by low-volume centers/surgeons, in fact a higher number of complications are reported

Table 14.1 Published and personal series on robotic colonic surgery with more than 10 cases

Year	Study [Reference]	Type of study	Total No. of patients	Mean operative time (min)	Postoperative complications n (%)	Conversion n (%)	Mortality n (%)	Type of procedure
2004	D'Annibale [7]	Comparative	53	240	4	0	0	17 LC, 11 SC
2006	DeNoto [8]	Case Series	11	197	2	1	0	11 SC
2006	Rawlings [9]	Case Series	30	225	6	2 (LPT)	0	13 SC
2008	Soravia [10]	Case Series	40	162	3	5 (3 LPS, 2 LPT)	0	28 SC
2008	Spinoglio [11]	Comparative	50	383	7	2 (1 LPS, 1 LPT)	0	10 LC
2009	Luca [12]	Case Series	55	290	12	0	0	27 LC
2011	Huettner [13]	Case Series	102	229.7	19	0	0	43 SC
2011	Patel [14]	Comparative	30	247	4	0	0	23 SC
2013	Helvind [15]	Comparative	101	243	22	5	1	12 LC, 34 SC
2013	Bianchi (unpublished data)	Case Series	31	270	2	0	0	11 LC, 6 SF, 1 TCR, 13 SC
Total			**503**	**248**	**81 (16)**	**15 (2.9)**	**1 (0.2)**	**66 LC, 150 SC**

LC, left colectomies; *SC*, sigmoidectomies; *TCR*, transverse colon resection; *LPT*, laparotomy; *LPS*, laparoscopy; *SF*, splenic flexure resection

by Keller et al. [17] in the low volume users when compared to middle- and high-volume centers and surgeons.

Although the results available on robotic surgery are still few, robotic assistance seems to reduce the percentage of conversions to open surgery among expert surgeons and is promising as a method to attenuate the learning curve of more difficult procedures, such as segmental and splenic flexure resections with intracorporeal anastomosis. At the moment, the robotic system has higher costs than laparoscopy and its use should be planned within the remit of a clearly-defined educational program, preferably in a hospital conducting middle/high volumes of minimally invasive surgery and colorectal procedures, in order to avoid an increase in complication rates.

References

1. Kang CY, Halabi WJ, Luo R et al (2012) Laparoscopic colorectal surgery. A better look to the latest trends. Arch Surg 147:724–731
2. The Surgical Care and Outcomes Assessment Program (SCOAP) Collaborative, Kwon S, Billingham R, Farrokhi E, Florence M, Herzig D, Horvath K, Rogers T, Steele S, Symons, Thirlby S, Whiteford M, Flum D (2012) Adoption of laparoscopy for elective colorectal resection: a report from surgical care and outcomes assessment program. J Am Coll Surg 214:909–918
3. Bianchi PP, Pigazzi A, Choi GS (2014) Clinical Robotic Surgery Association Fifth Worldwide Congress, Washington DC, 3–5 October 2013: Robotic Colorectal Surgery. Ecancermedicalscience 8:385
4. Schlachta CM, Mamazza J, Poulin EC (2007) Are transverse colon cancers suitable for laparoscopic resection? Surg Endosc 21:396–399
5. Kim HJ, Lee IK, Lee YS et al (2009) A comparative study on the short-term clinicopathologic outcomes of laparoscopic surgery versus conventional open surgery for transverse colon cancer. Surg Endosc 23:1812–1817
6. Weber PA, Merola S, Wasielevski A, Ballantyne GH (2002) Telerobotic-assisted laparoscopic right and sigmoid colectomies for benign disease. Dis Colon Rectum 45:1689–1694
7. D'Annibale A, Morpurgo E, Fiscon V et al (2004) Robotic and laparoscopic surgery for treatment of colorectal diseases. Dis Colon Rectum 47:2162–2168
8. DeNoto G, Rubach E, Ravikumar TS (2006) A standardized technique for robotically performed sigmoid colectomy. J Laparoendosc Adv Surg Tech A. 16:551–556
9. Rawlings AL, Woodland JH, Crawford DL (2006) Telerobotic surgery for right and sigmoid colectomies: 30 consecutive cases. Surg Endosc 20:1713–1718
10. Soravia C, Schwieger I, Witzig JA et al (2008) Laparoscopic robotic-assisted gastrointestinal surgery: the Geneva experience. J Robotic Surg 1:291–295
11. Spinoglio G, Summa M, Priora F et al (2008) Robotic colorectal surgery: first 50 cases experience. Dis Colon Rectum 51:1627–1632
12. Luca F, Cenciarelli S, Valvo M et al (2009) Full robotic left colon and rectal cancer resection: technique and early outcome. Ann Surg Oncol 16:1274–1278
13. Huettner F, Pacheco PE, Doubet JL et al (2011) One hundred and two consecutive robotic-assisted minimally invasive colectomies—an outcome and technical update. J Gastrointest Surg 15:1195–1204
14. Patel CB, Ragupathi M, Ramos-Valadez DI, Haas EM (2011) A three-arm (laparoscopic, hand-assisted, and robotic) matched-case analysis of intraoperative and postoperative outcomes in minimally invasive colorectal surgery. Dis Colon Rectum 54:144–150

15. Helvind NM, Eriksen JR, Mogensen A et al (2013) No differences in short-term morbidity and mortality after robot-assisted laparoscopic versus laparoscopic resection for colonic cancer: a case-control study of 263 patients. Surg Endosc 27:2575–2580
16. Baek SJ, Kim SH, Cho JS et al (2012) Robotic versus conventional laparoscopic surgery for rectal cancer: a cost analysis from a single institute in Korea. World J Surg 36:2722–2729
17. Keller DS, Hashemi L, Lu M, Delaney CP (2013) Short-term outcomes for robotic colorectal surgery by provider volume. J Am Coll Surg 217:1063–1069

Hybrid Robotic Technique for Rectal Cancer: Low Anterior Resection and Perineal Resection

15

Timothy F. Feldmann, Raul M. Bosio, and Alessio Pigazzi

15.1 Introduction

Colorectal cancer is the third most commonly diagnosed cancer with over 1.4 million new cases each year [1]. As surgical technology has evolved so has the treatment for this disease. Rectal cancer resection is complicated by the anatomic configuration of the pelvis and the proximity of these tumors to the anus. Evolving optics have allowed for the increased use of laparoscopy to allow for better visualization during pelvic surgery however its use was not implemented initially. Both the technical challenge of laparoscopic rectal surgery and the concern over oncological outcome have made its widespread adoption limited. As more surgeons gain comfort with advanced laparoscopic techniques the only concern is of the oncologic benefit [2–4]. The Conventional vs. Laparoscopic-Assisted Surgery in Colorectal Cancer (CLASICC) trial examined oncologic outcomes between laparoscopic and open rectal resections. Laparoscopic resection was associated with a higher rate of positive circumferential margin; however this did not translate into an increase in local recurrence when compared to the open procedures [5]. Long-term follow-up from the CLASICC trial has continued to provide support for the safe use of laparoscopy in colon and rectal cancer. The overall survival at 5 years after a low anterior resection was 56.7% in the open group and 62.8% in the laparoscopic one; abdominal perineal resection showed similar results with an overall survival of 41.8% in open cases and 53.2% in laparoscopic cases [6]. The Colorectal cancer Laparoscopic or Open Resection (COLOR II) trial has also advanced the use of laparoscopy and helped to show similarity in the completeness of mesorectal resection with a

A. Pigazzi (✉)
Department of Surgery, University of California Irvine,
Irvine, CA, USA
e-mail: apigazzi@uci.edu

G. Spinoglio (Ed), *Robotic Surgery: Current Applications and New Trends*,
Updates in Surgery
DOI: 10.1007/978-88-470-5714-2_15, © Springer-Verlag Italia 2015

10% rate of positive circumferential resection margin independent of the technique when specimens from patients randomly assigned to laparoscopy or open resection were analyzed [7].

Robotic surgery is still an evolving field but multiple factors make its use in rectal surgery appealing. The bony confines of the pelvis can lead to many difficulties including the inability to visualize structures or perform standard maneuvers used frequently in other body cavities. Patient factors such as obesity, large tumors, or a narrow male pelvis can make resection complex. The robotic platform allows for improved visualization especially as a result of the three-dimensional optics. Furthermore, surgical precision in these locations can be enhanced with the "wrist–like" functions that provide multiple degrees of freedom in instrument movement thus facilitating dissection. Robotic rectal resections have tended toward lower conversion rates than similar laparoscopic cases. Conversion rates from laparoscopic series have ranged from 1–17% but usually falling in the 10–15% range [10]. Results from previously published series show robotic resection to be feasible with adequate mesorectal excision [8–10]. Further randomized studies such as the Robotic versus Laparoscopic Resection for Rectal cancer (ROLARR) trial are underway to examine the use of robotics in an oncologic setting with a primary endpoint of determining conversion rates, as well as secondary endpoints regarding completeness of the mesorectal resection, genitourinary function and oncologic adequacy.

15.2 Procedures Overview

Rectal cancer resections at our institution are now commonly undertaken with a hybrid laparoscopic and robotic approach. The procedure is initiated with laparoscopic mobilization of the left colon, usually with takedown of the splenic flexure. This portion of the procedure can be accomplished robotically but we feel that this does not allow for the most effective use of resources, as operating room time may be prolonged when compared to performing this part of the operation laparoscopically. Laparoscopy allows for table positioning changes which may aid in the dissection of the descending colon and takedown of the splenic flexure. Single docking robotic procedures are feasible [11, 12] however they may not place the trocars in ideal positions for difficult pelvic dissection or be used on every patient. With surgeons unfamiliar with this technique, it may lead to repeated robotic docking procedures which increase operative time. It must also be stressed that prolonged Trendelenburg positioning is undesirable as it has been associated with several potential adverse consequences including lower extremity compartment syndrome and blindness. Following mobilization of the left colon and division of the inferior mesenteric artery (IMA) and vein (IMV), the robotic platform is docked and proctectomy is undertaken. Depending on the

patient's factors (i.e., incontinence) and tumor location, low anterior or abdominal perineal resection can be completed after total mesorectal excision has been performed. The robot is then undocked and the perineal or reconstructive portion of the operation may be accomplished. We outline the basic steps in our approach below.

15.3 Patient Selection and Preoperative Factors

The operating surgeon must be prepared for multiple challenges based on each patient he or she encounters. Preoperative discussion of the possible outcomes including type of procedure, the possibility of conversion, and surgical risks must be undertaken. Early discussions about temporary or permanent ostomy placement and future rectal function will allow patients to better understand the changes that they may undergo. Tumor location and staging is essential; endorectal ultrasound and/or pelvic MRI should be considered as part of the staging studies. Preoperative chemoradiation is indicated for lymph node positive disease and/or selected T3 or higher disease. We advocate the surgeon to perform his or her own evaluation with either digital rectal exam or endoscopy (flexible or rigid). This can help identify unforeseen technical challenges, such as the need for a partial or total trans-sphincteric resection, and can assist in operative planning.

15.4 OR Setup and Patient Positioning

Preoperative setup of the operating theater will help with facilitating an easy transition from laparoscopy to robotic surgery. The patient should be positioned in the center of the room on the operating table. The patient will need to be in a modified lithotomy position in a movable stirrup with adequate padding of the extremities. The right arm must be tucked at side to allow room for the operating surgeon; we prefer to tuck both arms at side during these operations to provide more space. We recommend the use of high density foam that is strapped to the operating room table to prevent the patient from sliding during steep positioning. A strap across the chest is also needed to prevent lateral sliding. Ideally a room with multiple integrated monitors should be available with a monitor placed on each side of the operating table. The laparoscopic equipment along with electrocautery devices and suction should be positioned at the patient's left shoulder. The scrub technician and instrument table will be set back off the patient's right side and right shoulder. The robotic equipment and tower should be to the side of the patient's right leg. The robot itself should be sterilely draped and available to be docked at the patient's left hip. The robotic console can be placed at the surgeon's preference (Fig. 15.1).

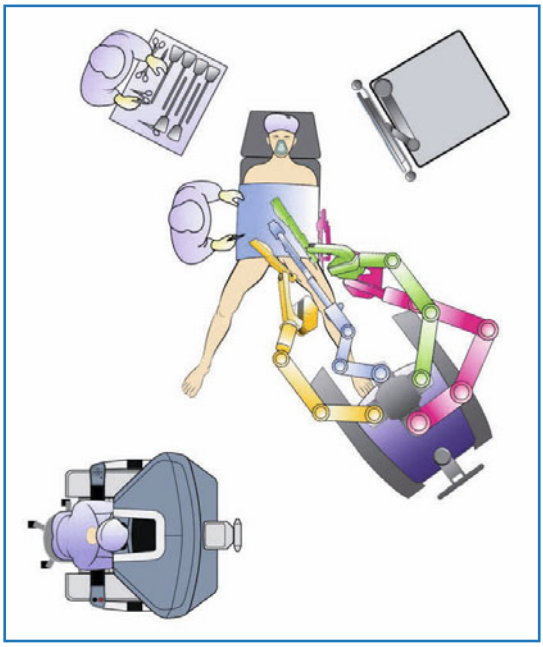

Fig. 15.1 OR setup for hybrid robotic rectal resection. (© 2014 Intuitive Surgical, Inc.)

15.5 Port Placement

The abdomen is then entered in the surgeon's standard fashion for laparoscopy. We prefer a single small incision at Palmer's point in the left upper quadrant. The abdomen is insufflated through a Veress needle to 15 mmHg and an initial 12-mm camera port is placed. This should ideally be placed halfway between the xyphoid and the pubic symphysis in the midline. Preference should be given to lower placement at about 20 cm above the pubis in patients with longer torsos. This allows for better visualization deep in the pelvis without disturbance from the sacrum. After camera placement the robotic and assistant trocars are then placed under direct vision.

Anatomic landmarks are then identified and marked with a surgical marker. The right and left anterior superior iliac spines (ASIS) are identified. An oblique line should be drawn from the camera port to each ASIS bilaterally. This will create two equal sides of a triangle. The port for arm 1 on the robot (R1) should be placed at least 8–10 cm (four finger breadths) away from the camera port on the line connecting the camera port to the right-sided ASIS. This port can be kept closer to the midline to allow for dissection within the pelvis without losing mobility on the pelvic sidewall. A 12-mm trocar should be placed to allow for future placement of a laparoscopic stapling device if needed. If robotic stapling technique is used, a 15-mm trocar is placed instead. When docking the robot, an 8-mm robotic trocar is placed within this trocar (trocar in trocar technique) to

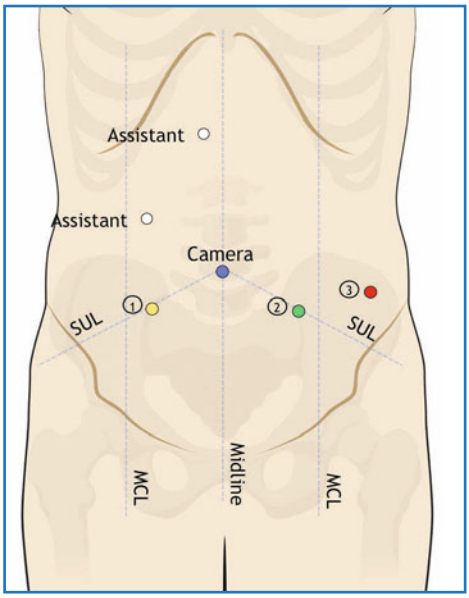

Fig. 15.2 Placement of ports: an oblique line should be drawn from the camera port to each ASIS bilaterally. The R1-port is placed at least 8–10 cm (four finger widths) away from the camera port on the line previously described. R2-port is in a mirror position to R1, on the left. R3 is placed 8–10 cm (four finger widths) lateral to R2. Two 5 mm laparoscopic assistant ports are placed as shown. (© 2014 Intuitive Surgical, Inc.)

allow for docking of the robotic arm.

Robotic arm 2 (R2) is placed in an identical fashion on the left side of the abdomen. The line connecting the camera port and the left ASIS should be used as a guide to place this port and as with the first port it should be located at least 8–10 cm away from the camera port. An 8-mm robotic port is placed at this site.

Robotic arm 3 (R3) is also placed along the left side of the abdomen. The site is chosen directly lateral to R2 at least 8–10 cm away. This will be located above the left ASIS and not on the previously made guidance line. Another 8-mm robotic port is placed at this location.

R2 and R3 are not necessary during the laparoscopic portion of the procedure but can allow for extra access points for retraction and dissection if placed at this time.

Two laparoscopic assistant ports are then placed, which will be used for both portions of the procedure. The first laparoscopic port (L1) is placed in the right abdomen. Positioning should be approximately 10–12 cm lateral to the camera port and a similar distance superior to the R1 port. The second laparoscopic port is placed just off of the midline (either right or left) high in the epigastric region. This should be at least 8–10 cm away from all other laparoscopic ports (Fig. 15.2).

15.6 Laparoscopic Mobilization of the Left Colon and Splenic Flexure

After visual inspection of the abdomen, attention is turned to the left colon. A medial-to-lateral approach is used to mobilize this region. Either the inferior

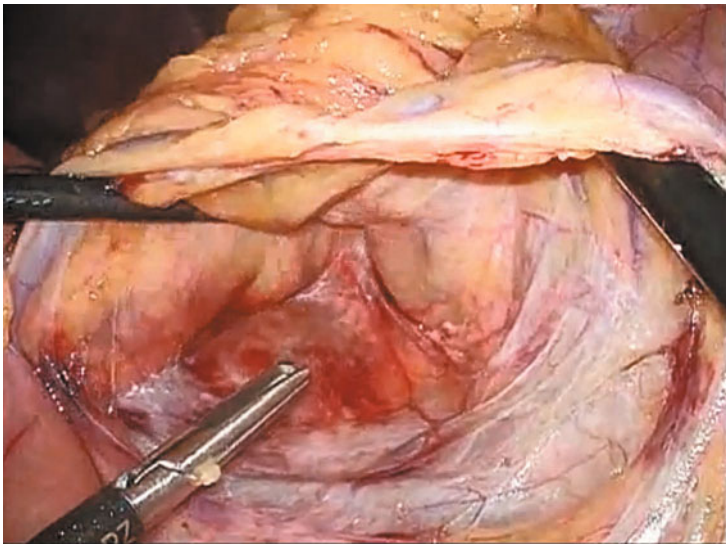

Fig. 15.3 Dissection plane beneath the inferior mesenteric vein. The pancreas is visible at the left edge of the picture. The inferior mesenteric artery will be found as dissection is carried toward the right edge of the picture

mesenteric vein (IMV) or the inferior mesenteric artery (IMA) can be isolated first and patient positioning should be changed as needed to allow for visualization. We find that identification of the IMV near the ligament of Treitz allows for development of the appropriate plane between the mesocolon and the retroperitoneum. The vein is identified lateral to the ligament of Treitz and the peritoneum below it is incised. Blunt dissection is carried laterally and inferiorly until the IMA is encountered. This dissection plane will be bordered anteriorly by the IMV and colonic mesentery, posteriorly by the retroperitoneum, superiorly by the pancreas, and inferiorly by the takeoff of the IMA (Fig. 15.3). Dissection is carried out within this space. Care should be taken if the dissection plane is continued superiorly as the natural dissection plane will continue underneath the pancreas. If this course is chosen then the surgeon will need to "step up" over the pancreas to avoid injury to the splenic vessels. Dissection over the pancreas can be accomplished later and therefore we recommend that blunt dissection be continued laterally and inferiorly until the IMA is reached. Mobilization of the splenic flexure will be completed once the lateral attachments have been divided. The IMV can be ligated at any point during the dissection through a variety of means (clips, staplers, bipolar cautery devices). Traction must be avoided on the vein and earlier division can avoid an avulsion injury. Once the superior aspect of the IMA is identified, the sigmoid colon is grasped and retracted toward the anterior abdominal wall. The superior rectal artery should be seen coursing through the mesenteric plane. Opening the peritoneum underlying this pedicle will allow for blunt dissection of the mesocolon once

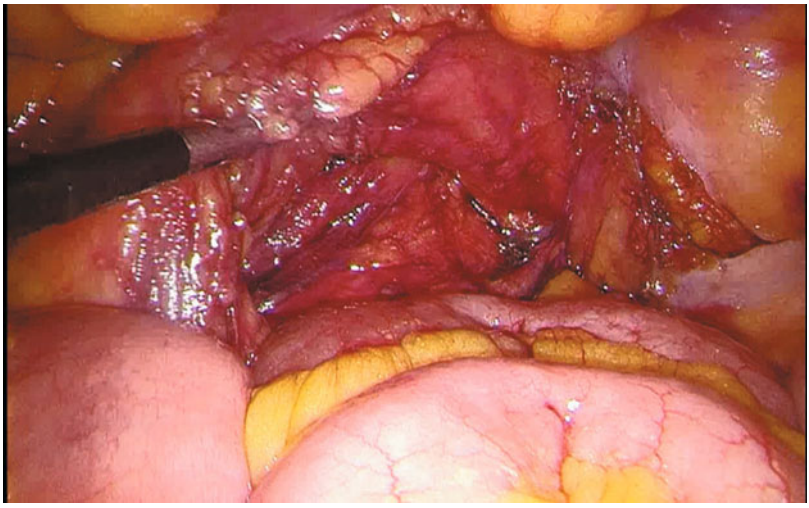

Fig. 15.4 Dissection plane beneath the superior hemorrhoidal artery. To the left of the picture is the pedicle of the inferior mesenteric artery. The ureter is coursing directly through the middle of the retroperitoneal plane

again. This dissection is again taken laterally and identification of the ureter and gonadal vessels is paramount. These structures should be kept on the retroperitoneal side of the dissection. Visualization of the psoas muscle tendon often implies a "deep" dissection and the ureter may have been swept into the tissue of the mesocolon. Once this plane has been fully developed it should expose the origin of the IMA and its branch point into the left colic and superior rectal artery. This dissection plane will now be bordered superiorly by the IMA pedicle, inferiorly by the mesorectum, anteriorly by the superior rectal artery and mesocolon, and posteriorly by the retroperitoneum (Fig. 15.4). The ureter and gonadal vessels travel in a crania-caudal direction within this area of the retroperitoneum. In order to allow optimal mobilization of the left colon, as well as to provide appropriate oncologic resection, the IMA should be taken at its origin. A classic view in the shape of a "T" should be seen at this point (Fig. 15.5). The IMA will be the body of the T with the left colic artery as the left branch and the superior rectal artery as the right branch. These structures should be free of the retroperitoneum so that the ureter is not taken with the artery. Just as with the IMV, the IMA can be taken using the surgeon's preferred method.

Once the mesocolon has been dissected from the medial side, the lateral colonic attachments must be taken down. The white line of Toldt is incised and carried superiorly toward the splenic flexure. The omental attachments to the descending colon should be taken as well. Dissection can continue from this direction or it may also be approached from the transverse colon. This allows mobilization of the omentum off of the colon and then entrance into the lesser

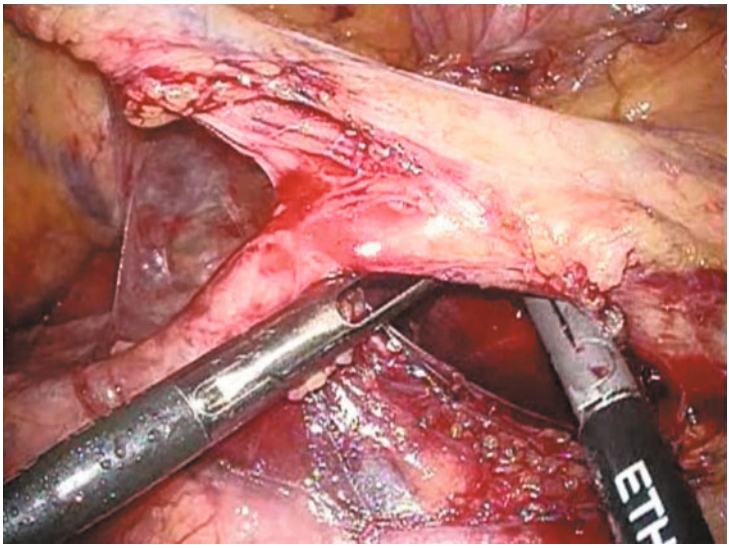

Fig. 15.5 Classic view of "T". The inferior mesenteric artery branches into the left colic (*left side*) and the superior hemorrhoidal artery (*right side*). Both previous dissection planes can be visualized

sac. The colon is retracted toward the midline and the splenocolic ligament is taken down to allow for full mobilization of the flexure. This step will ensure adequate colonic length to construct a tension free anastomosis once the resection is completed. After the mobilization is completed the patient is prepared for docking of the robot.

15.7 Robotic Rectal Resection

Prior to docking, the patient must be placed in the appropriate position. Once the robot is in place, rotation of the table is not possible. The patient should be placed in the Trendelenburg position with the left side up. This will allow the small bowel to fall out of the pelvis and not interfere with the rectal dissection. If adhesions are present and are fixing the small bowel to the lateral pelvic wall, the surgeon should divide them prior to docking to avoid small bowel injury by the robotic arms. An 8-mm trocar should be placed inside the 12 mm R1 port to prepare for docking. The robot is brought in from the patient's left side. Aligning the central column, with the ASIS and right shoulder should allow for optimal docking and adequate spacing between robotic arms. The robotic arms are then docked and a 0° camera is placed through the camera port. The remaining robotic instruments are then inserted under direct visualization and directed toward the pelvis. A typical instruments setup is as follows:

- R1 – monopolar scissors
- R2 – bipolar fenestrated grasper
- R3 – ProGrasp™ grasper
- L1 – suction irrigation device
- L2 – locking grasper (i.e., Davis & Geck)

The laparoscopic instruments will be used by the assistant, who will stay at the patient's right side. The operating surgeon should now proceed to the robotic console. The assistant should grasp the upper rectum with the locking grasper to allow for retraction throughout this part of the procedure.

Dissection of the mesorectum is then undertaken. Care should be taken to stay in the avascular plane that exists between the endopelvic visceral fascia and endopelvic parietal fascia. This will help to avoid the hypogastric nerve plexus and sacral venous plexus located deep in the parietal layer within the presacral space. R2 is used during this portion to provide upward traction on the mesorectum while the assistant places countertraction with the suction device when able. This allows for dissection to be carried out in the avascular plane posteriorly. Frequent repositioning of R2 to maintain adequate countertraction will allow the dissection plane to be continued to the level of the pelvic floor and for the lateral stalks to be identified. R2 should be used with the wrist joint in an L shape to allow for a larger surface area of retraction. The lateral stalks are then subsequently taken and dissection is carried onto the anterior surface of the rectum. Here the vagina or the seminal vesicles and prostate are dissected free and protected. R3 should be used as a static retractor to move these structures anteriorly using a similar wrist configuration as used previously with R2. As the middle rectal vessels are encountered they can be taken with bipolar cautery. The autonomic nerves lie laterally on the pelvic sidewalls and should be kept free of the dissection plane. The mesorectal excision continues downward in a cylindrical fashion until past the level of the lesion. If no margin is feasible then dissection should be carried as far as possible to allow for an easier perineal dissection. As the plane below the mesorectum is reached (bare rectum area) further dissection will lead to the intersphincteric plane. If a margin is obtainable, the rectum is divided using a 45-mm stapler in either an anterior-posterior or right-to-left fashion. Ideally, one or two loads are required. Once the rectum is free it is grasped with the locking grasper at the site of the staple line and the robot can be removed.

15.8 Anastomosis and Reconstruction

If a distal margin is obtained then the specimen must be extracted.

- **Abdominal extraction:** If the rectum has been divided under robotic visualization then our preferred extraction site is through a mini Pfannenstiel incision. This is performed in a muscle sparing fashion and a wound protector is then placed. The specimen is brought out and transected extracorporeally. A

purse-string suture is placed in the remaining portion and an anvil inserted. This is then returned to the abdomen and the Pfannenstiel incision is closed in multiple layers. If desired, certain wound protectors allow for reinsufflation of the abdomen without the need to close the incision. This allows for prompt reentry should the need arise. A standard end-to-end anastomosis (EEA) is then performed. If adequate colonic length is present, a colonic J-pouch can be constructed.

- **Transanal extraction:** In selected cases, consideration can be taken for transanal extraction. If an intersphincteric approach is planned, we usually perform this part of the operation first with the patient in the prone position. The rectum is divided circumferentially and then the suture closed to avoid spillage. Dissection is continued in the posterior plane toward the lower coccyx. A sponge is then placed in this location and will be encountered during the abdominal portion of the procedure. A decision to proceed with a transanal extraction can also be made after the robotic portion has been completed. In this case, the rectum is divided transanally after placement of a Lonestar™ retractor. A hand-sewn coloanal anastomosis can then be performed.
- A circular anastomosis can also be created if enough distal rectum is present. A purse-string suture is placed and an anvil inserted in the proximal colon and then it is returned to the abdomen. A second purse-string is then created in the distal rectum and secured around the pin of the EEA circular stapler. An end-to-end or colonic J-pouch to distal rectal anastomosis is then constructed under laparoscopic guidance.

It is our standard practice to perform a leak test with a flexible endoscope after any pelvic anastomosis. This allows for both air testing as well as visualization of the site. In selected cases, fluorescein angiography is performed to ensure adequate blood supply. If there is concern over the connection there must be consideration for the anastomosis to be undertaken again. We also perform a diverting ileostomy in all high-risk patients or those with an anastomosis within 7–8 cm of the anal verge. The R1 port site is enlarged and a loop of ileum is brought out with laparoscopic assistance. A pelvic drain may be placed through any of the other port sites in the lower abdomen if the surgeon desires. The laparoscopic ports are closed and the ileostomy is matured in standard Brooke fashion.

15.9 Perineal Resection

Once mobilization of the colon is completed, the bowel is divided intracorporeally using Endostaplers. It is important to have adequate mobilization so that the colon can be divided in such a fashion that the origin of the IMA is included in

the specimen side and an end colostomy can be constructed without tension. Once the abdominal portion of the procedure is completed, and the focus shifts to the perineal resection, two options are available from a patient positioning standpoint. The choice can be made based on surgeon preference; however location of the tumor may assist in decision making. Tumors located in the posterior portion of the rectum may be more easily approached from the lithotomy position while anterior or lateral lesions may be more amenable to prone positioning.

- If a decision is made to continue the operation in the lithotomy position. The legs are raised and a perineal incision outside the external sphincters is performed circumferentially. Dissection is carried superiorly and the levator ani divided. Starting the dissection posteriorly, toward the coccyx, allows for discovery of the superior plane of dissection. The rectum is then cleared circumferentially. Once free, the specimen can be extracted through the perineal incision. Closure of the perineal wound can then be performed, ideally in multiple layers. If preferred, tissue flaps, such as a vertical rectus abdominus myocutaneous (VRAM) flap, gluteal flap, or a gracilis flap can be transposed for reinforcement. The defect is closed and an end colostomy is brought out laparoscopically. The R2 port can be upsized into a permanent colostomy site with maturation in standard fashion after the laparoscopic sites are closed.
- The second option involves repositioning into the prone position for the perineal resection. Some studies would suggest this provides a better circumferential resection margin as opposed to lithotomy [13, 14]. In this case, and as mentioned above, laparoscopic or robotic stapling is used to transect the colon at the desired location and is then brought out through the R2 site as an end colostomy prior to changing to a prone position. Ports are then removed and the incisions closed and dressed prior to maturation of the colostomy. After the abdominal portion is complete the patient is then repositioned into a prone jackknife position. Again a circumferential incision is made outside the level of the external sphincter and dissection is carried down in an extralevator fashion until the dissection planes are joined. The specimen can then be extracted and the wound closed as per the surgeon's preference.

15.10 Conclusions

Robotic platforms have created new opportunities for rectal surgery. Through our experience we have found a hybrid laparoscopic and robotic approach that is safe, feasible, and efficacious. This technique allows us to tailor our approach for each patient and the location of the tumor. As technology moves forward and further research emerges, robotic rectal cancer surgery will allow for excellent cosmetic, oncologic, and overall outcomes.

References

1. Ferlay J, Soerjomataram I, Ervik M, Dikshit R, Eser S, Mathers C, Rebelo M, Parkin DM, Forman D, Bray F. GLOBOCAN 2012, Cancer Incidence and Mortality Worldwide: IARC CancerBase No. 11 [Internet]. Lyon, France: International Agency for Research on Cancer; 2013. Available from: http://globocan.iarc.fr, accessed on 3/20/14
2. Clinical Outcomes of Surgical Therapy Study Group (2004) A comparison of laparoscopically assisted and open colectomy for colon cancer. N Engl J Med 350:2050–2059
3. Colon Cancer Laparoscopic or Open Resection Study Group, Buunen M, Veldkamp R, Hop WC, Kuhry E, Jeekel J et al (2009) Survival after laparoscopic surgery versus open surgery for colon cancer: long-term outcome of a randomised clinical trial. Lancet Oncol 10:44–52
4. Veldkamp R, Kuhry E, Hop WC et al (2005) Laparoscopic surgery versus open surgery for colon cancer: short-term outcomes of a randomised trial. Lancet Oncol 6:477–484
5. Jayne DG, Guillou PJ, Thorpe H et al (2007) Randomized trial of laparoscopic-assisted resection of colorectal carcinoma: 3-year results of the UK MRC CLASICC Trial Group. J Clin Oncol 25:306–308
6. Jayne DG, Thorpe HC, Copeland J et al (2010) Five-year follow-up of the Medical Research Council CLASICC trial of laparoscopically assisted versus open surgery for colorectal cancer. Br J Surg 97:1638–1645
7. van der Pas MH, Haglind E, Cuesta MA et al (2013) Laparoscopic versus open surgery for rectal cancer (COLOR II): short-term outcomes of a randomized, phase 3 trial. Lancet Oncol 14:210–218
8. Baik SH, Ko YT, Kang CM et al (2008) Robotic tumor-specific mesorectal excision of rectal cancer: short-term outcome of a pilot randomized trial. Surg Endosc 22:1601–1608
9. Pigazzi A, Ellenhorn JD, Ballantyne GH, Paz IB (2006) Robotic-assisted laparoscopic low anterior resection with total mesorectal excision for rectal cancer. Surg Endosc 20:1521–1525
10. Dalton RS, Smart NJ, Edwards TJ et al (2012) Short-term outcomes of the prone perineal approach for extra-levator abdomino-perineal excision (elAPE). Surgeon 10:342–346
11. Bianchi PP, Luca F, Petz W et al (2013) The role of the robotic technique in minimally invasive surgery in rectal cancer. Ecancermedicalscience 7:357
12. Obias V, Sanchez C, Nam A et al (2011) Totally robotic single-position 'flip' arm technique for splenic flexure mobilizations and low anterior resections. Int J Med Robot 7:123–126
13. Hellan M, Stein H, Pigazzi A (2009) Totally robotic low anterior resection with total mesorectal excision and splenic flexure mobilization. Surg Endosc 23:447–451
14. Stelzner S, Hellmich G, Schubert C et al (2011) Short-term outcome of extra-levator abdominoperineal excision for rectal cancer. Int J Colorectal Dis 26:919–925

Full-robotic Technique for Rectal Cancer

16

Giuseppe Spinoglio, Giampaolo Formisano, Luca Matteo Lenti, Fabio Melandro, and Alessandra Marano

16.1 Introduction

Since the first robotic total mesorectal excision (TME) was reported in 2006 [1], two main methods for robotic rectal surgery, hybrid versus totally robotic technique, have been described.

In the hybrid technique [2, 3], the surgeon performs a splenic flexure mobilization laparoscopically and in almost all cases the vascular handling, while the robotic approach is reserved for pelvic dissection. Among the totally robotic procedures, there are the single and dual docking strategies with several subtypes, according to redocking of robotic arms and reorientation of the robotic cart (or patient table) during surgery [4–8].

Since the introduction of the da Vinci® Si™ system at our institution in 2010, we have developed a full-robotic single-docking technique for rectal anterior resection with TME. In this chapter we outline each step of our surgical strategy; the indications have already been discussed in Chapter 15.

16.2 Procedure Overview

The key steps for robotic rectal anterior resection (R-RAR) with TME are as follows:

1. Splenic flexure takedown
2. Primary vascular control, medial-to-lateral mobilization of descending colon/sigmoid and section of the mesocolon

G. Spinoglio (✉)
Department of General and Oncologic Surgery,
"Ss. Antonio e Biagio" Hospital,
Alessandria, Italy
e-mail: giuseppe.spinoglio@gmail.com

G. Spinoglio (Ed), *Robotic Surgery: Current Applications and New Trends*,
Updates in Surgery
DOI: 10.1007/978-88-470-5714-2_16, © Springer-Verlag Italia 2015

3. TME and rectal resection
4. Specimen removal and anastomosis

Our technique for RAR is so-called "single-docking" because it does not involve a change of the position of the robotic cart, but only of the robotic arms (except for robotic arm 1), during the above-mentioned surgical steps. The initial exposure and the anastomosis fashioning are usually performed laparoscopically.

16.3 Patient Positioning

After the induction of general anesthesia, the patient is placed supine in a modified lithotomy position. Legs are abducted with flexed knees (the left leg is less abducted compared to the right one so as not to interfere with the robotic arms) and are positioned in adjustable stirrups; arms are alongside the body. The patient is carefully secured with shoulder supports on both sides of the neck and with a safety band on the chest to prevent sliding.

The preparation is concluded by the insertion of a Foley catheter and an orogastric tube and by the application of a body warmer and a compression device for deep venous thrombosis prophylaxis. Antibiotics are injected according to the guidelines.

16.4 OR Setup

First assistant is on the patient's right side. The scrub nurse is at the lower right side of the table and the assistant's monitor is located at the patient's left shoulder. The cart is placed at the patient's left side and is docked from the left lower quadrant over the left hip, at approximately 45° to the perpendicular to the patient (Fig. 16.1).

16.5 Trocar Placement

A 12-mmHg pneumoperitoneum is achieved with a Veress needle and ports are introduced as follows:

- one 12-mm laparoscopic trocar for the 30° down endoscope through an incision 1–2 cm lateral and 3 cm above the umbilicus;
- one 8-mm robotic trocar (robotic arm 1, R1) on the right lower quadrant at the intersection between spino umbilical line (SUL) and the midclavicular line (MCL);
- one 8-mm robotic port robotic arm 2/3, R2/R3) in the right upper quadrant, slightly lateral to the right MCL, 3–4 cm below the 12th rib;
- one 8-mm robotic port robotic arm 2/3, R2/R3) in the left upper quadrant, 7–8 cm below the 12th rib and 5 cm lateral to the midline;

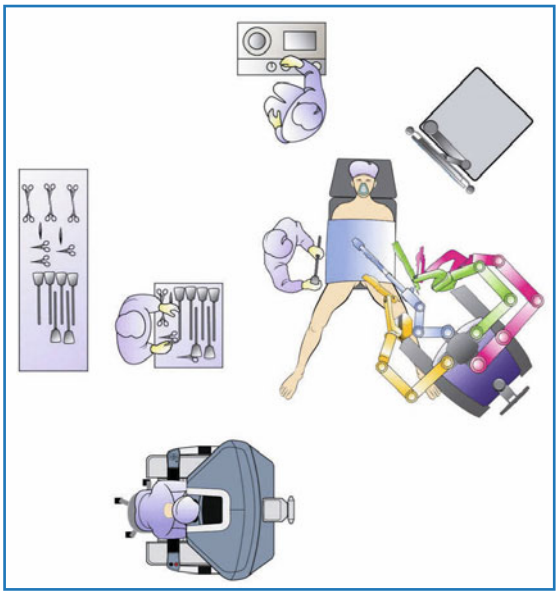

Fig. 16.1 OR setup for full-robotic single-docking rectal anterior resection. (© 2014 Intuitive Surgical, Inc.)

- one 8-mm robotic port (robotic arm 2, R2) in the left lower quadrant, 2 cm lateral to the MCL and 16–18 cm to the pelvis;
- one 12-mm laparoscopic port, in the right flank area, 2 cm lateral to the MCL.

16.6 Robot Positioning and Docking

Once the camera port is inserted, an assessment of the entire abdomen is performed and all trocar are placed at their optimal sites. The greater omentum and the small bowel loops are retracted out of the pelvic area into the right upper quadrant by means of laparoscopic graspers inserted through the robotic ports. If present, adhesions are freed.

At this time, the patient is placed in a 25° Trendelenburg position with a 20° right tilt. The robotic cart is brought into the left lower quadrant.

In order to define the correct position of the robotic cart, we need to pinpoint the best position for the camera arm. To adjust the positioning correctly, the following steps are as carried out:

1. Align the camera arm with the center column
2. Position setup joint 2 in the "sweet spot" by placing the blue arrow on the camera arm in the middle of the blue bar located on the camera arm setup joint
3. Move the cart to the patient so that a straight line passes through the center

column, the camera arm, the left anterior superior iliac spine and the camera trocar

4. When the camera arm joins the camera trocar, the robotic cart is in the correct position and does not require further adjustments.

This method of positioning and docking the robot is the best one for the TME step that is the core for the whole surgery.

Next, the patient is placed in a 15° reverse-Trendelenburg position and tilted completely to the right side. Robotic arms are now docked to the trocar.

16.7 Step-by-Step Review of Critical Elements of the Procedure

16.7.1 Step 1: Splenic Flexure Takedown

- The patient is placed in a 15° reverse-Trendelenburg position tilted down on the right side.
- Only robotic arm 1 and 2 are docked to minimize external collision (Fig. 16.2):
  - R1: Hot Shears™ (monopolar curved scissors) or cautery hook
  - R2: Bipolar forceps
- The assistant port is used for tissue retraction, suction/irrigation or clipping of vessels

The splenic flexure takedown can be performed in two ways:

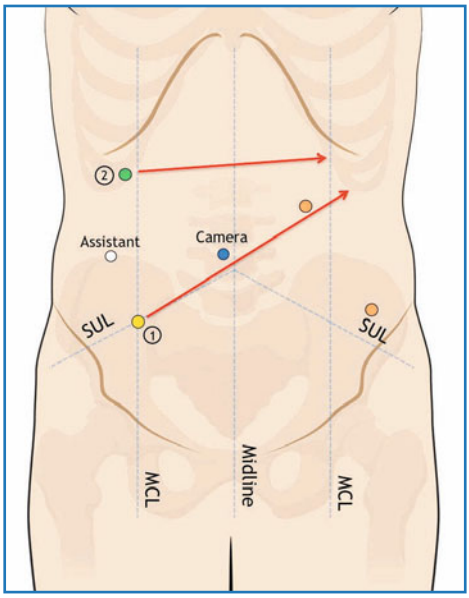

Fig. 16.2 Trocar layout for splenic flexure takedown (Step 1). (© 2014 Intuitive Surgical, Inc.)

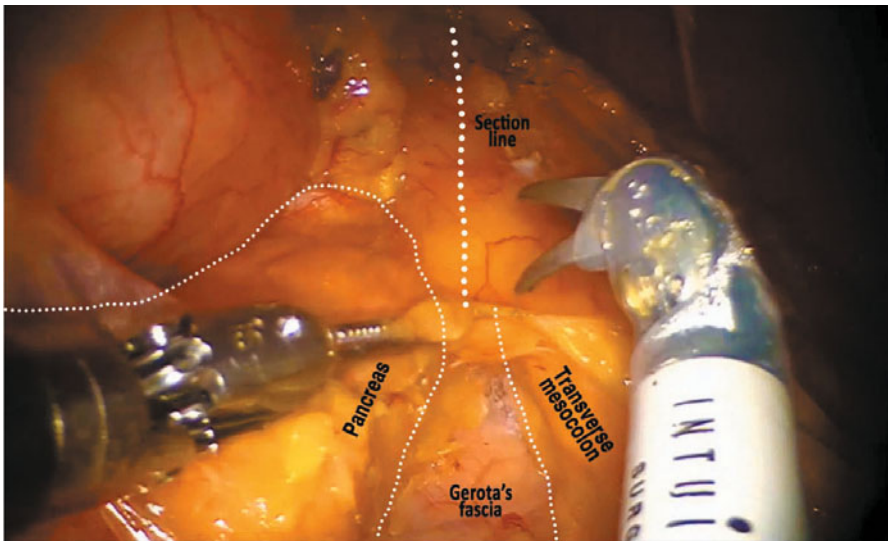

Fig. 16.3 Splenic flexure takedown from top-to-bottom

1. From top-to-bottom

The assistant grasps the omentum and pulls it down while the robotic instrument in R2 lifts the stomach up. The gastrocolic ligament is incised in its more translucent portion (the so-called Bouchet's area): a section from the right to the left side of the patient is progressively carried out considering the inferior splenic pole as a landmark. Once the gastrocolic ligament is sectioned, the posterior peritoneal layer of the lesser sac is incised 1 cm caudal to the inferior border of the pancreas in order to expose the Gerota's fascia.

The tranverse mesocolon is separated from the inferior border of the pancreas and the dissection proceeds in order to fully mobilize the splenic flexure and a portion of the descending colon, separating the Gerota's fascia from the Toldt's one or the two layers of the Toldt's fascia (Fig. 16.3).

2. From bottom-to-top (after primary vascular control step)

After having pulled up the greater omentum, the transverse mesocolon is opened from its inferior aspect just above the body of the pancreas to enter the lesser sac. Dissection of the transverse mesocolon continues toward the distal transverse colon and the base of the descending colon. The omentum, attached to the transverse colon, is then dissected in the avascular plane, beginning from the middle third of the transverse colon: the renocolic and splenocolic ligaments are divided and the splenic flexure is fully mobilized.

Our standardized technique involves the splenic flexure takedown from the top to the bottom for the following reasons:

- This strategy allows easy access to the avascular plane between the Toldt and Gerota's fascia (or the two layers of the Toldt's fascia) since the largest space between these two layers is at the level of the inferior border of the pancreas.

We believe that a dissection starting from this area is easier than the other one;

- In the case of the splenic flexure being in a high position, its takedown is easier to perform (also when an adhesiolysis is needed) and is safer since the spleen is always under visual control;
- The anatomical plane created after the splenic flexure mobilization from the top to the bottom makes the dissection easy to be implemented after the division of the inferior mesenteric vein (IMV).

16.7.2 Step 2 - Primary Vascular Control, Medial-to-Lateral Mobilization of Descending Colon/Sigmoid, Section of the Mesocolon

- The patient is placed in a steep Trendelenburg position with the right side down.
- The arm setup is shown in Fig. 16.4:
  - R1: Hot Shears™ (monopolar curved scissors) or cautery hook, Hem-o-lok® clip applier
  - R2: ProGrasp™ forceps
  - R3: Bipolar forceps
- The assistant port is used for tissue retraction, suction/irrigation or clipping of vessels.

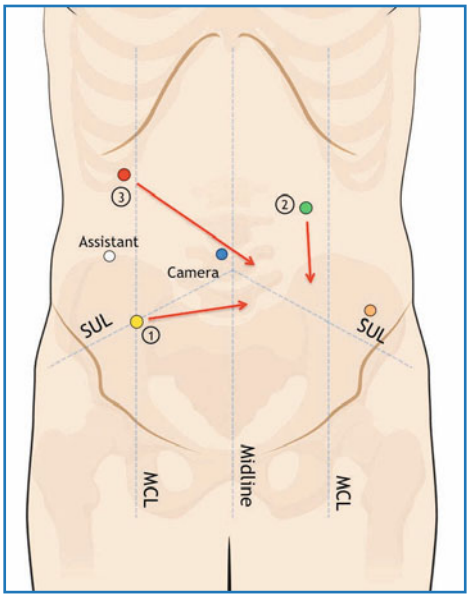

Fig. 16.4 Trocar layout for primary vascular control, medial-to-lateral mobilization and section of the mesocolon (Step 2). (© 2014 Intuitive Surgical, Inc.)

Transverse mesocolon is pulled up to expose the Treitz angle. The IMV is identified and divided close to the inferior border of the pancreas: the IMV transection allows easy entry into the space created during the splenic flexure mobilization and so the dissection can be carried out downward.

The sigmoid colon and upper rectum are lifted anteriorly and laterally by the assistant grasper and the robotic instrument in R2 to expose the base of the sigmoid mesocolon and the upper mesorectum. The peritoneum is then incised at the level of the sacral promontory with the Hot Shears™ in R1 and the inferior mesenteric artery (IMA) is identified, dissected at its origin and divided with Hem-o-lok® clips (Weck Teleflex Medical Europe Ltd).

A medial-to-lateral dissection is carried out posteriorly to the superior rectal artery thus joining the previous superior dissection below the IMV, until all the left colon is separated from the retroperitoneum preserving the left gonadal vessels and the left ureter. Lateral detachment is implemented along the white line of Toldt and continues cephalad to the middle portion of the descending colon while the sigmoid colon is retracted medially by the assistant. The dissection is extended inferiorly up to the psoas muscle where the ureter crosses the iliac vessels.

A complete intracorporeal division of the proximal mesocolon is also performed up to the chosen transection point in the left colon: the assessment of bowel stump perfusion will be carried out with the indocyanine green (ICG) fluorescence imaging system (see Chapter 19).

16.7.3 Step 3 - TME and Rectal Resection

- The patient positioning is the same as in step 2.
- The arm layout is shown in Fig. 16.5.
  - R1: Hot Shears™ (monopolar curved scissors) or cautery hook, Hem-o-lok® clip applier
  - R2: ProGrasp™ forceps
  - R3: Bipolar forceps
- The assistant uses both ports in the right flank for tissue retraction, suction/irrigation, clipping of vessels and stapler introduction in order to maximize the assistance.

TME is carried out according to Heald's principles [9] and this step has been already described in detail by Pigazzi et al. in Chapter 15, with the only difference being that, in our surgical strategy, instruments armed in R1 and R3 are the operative ones while R2 is used to expose the anatomical field (Fig. 16.6).

Additionally, we routinely perform an assessment of the bowel perfusion with the ICG fluorescence imaging system (see Chapter 19), before rectal resection (Fig. 16.7). At the end of this step, the robotic system is undocked if the anastomosis is fashioned laparoscopically.

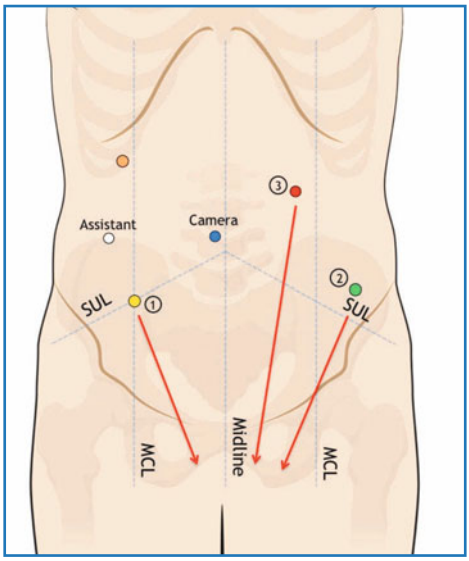

Fig. 16.5 Trocar layout for total mesorectal excision and rectal resection (Step 3). (© 2014 Intuitive Surgical, Inc.)

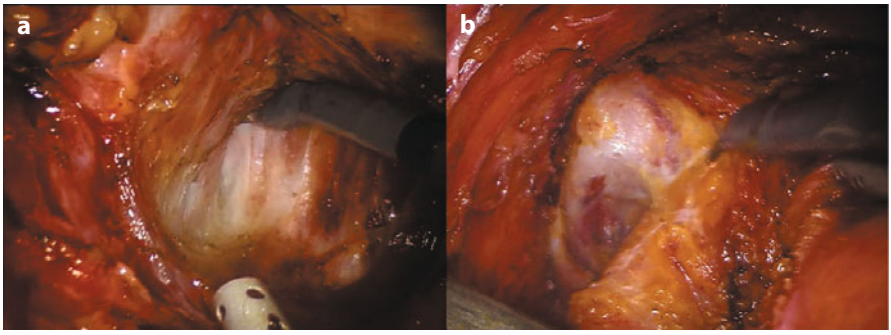

Fig. 16.6 Total mesorectal excision. **a** Posterior aspect. **b** Lateral aspect

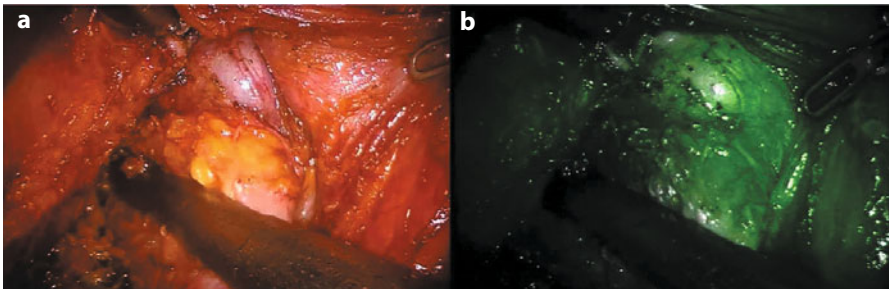

Fig. 16.7 White light (**a**) and NIR-fluorescent view (**b**) of rectal transection

16.7.4 Step 4 - Specimen Removal and Anastomosis

The diseased colorectal segment is extracted through a nearly 5 cm suprapubic Pfannenstiel incision, protected with a wound shield. The proximal colon is transected, the anvil is inserted into the proximal stump and the colon is dropped back into the abdomen. The Pfannenstiel incision is closed and pneumoperitoneum is re-established.

An end-to-end or side-to-end circular stapled anastomosis is fashioned intracorporeally or a handsewn coloanal anastomosis is used after intersphincteric resection. A diverting ileostomy is selectively fashioned in cases of incomplete donuts, preoperative radiation, coloanal anastomosis and ultralow RAR. Finally, the trocar are removed under direct vision, a drain is placed and laparoscopic fascial sites are closed as usual.

16.8 Advantages and Limitations of Full-robotic Technique for Rectal Cancer

The technical advantages of the da Vinci® four-arms system encouraged our team to develop a new surgical setting to exploit, as best, the robotic technology. Thus, after our first experience with the first-generation da Vinci® system [10], we have adopted a standardized setup for RAR with TME, a full-robotic single-docking technique and we trained each member of our group. Two fundamental steps are necessary: the tailoring of port placement after induction of pneumoperitoneum, and testing of the movement of the arms before introduction of the instruments, in order to adjust the positioning of the elbow of the arms and to facilitate their movement without conflicts.

Our strategy, also described with some variations by other authors [5, 8, 11, 12], offers potential distinct advantages in comparison with the multiple stage and hybrid technique. We believe that the fixed position of the robotic cart decreases the overall operating time and makes the surgery more on-going and coordinated, making use of the benefits of robotic technology. All abdominal quadrants can be reached easily by the robotic arms with correct port placement; moreover, the splenic flexure takedown can be implemented effortlessly, in particular in the case of its high positioning as previously described.

Potential criticisms of the full-robotic procedure such as higher cost, a longer operative time and a higher learning curve than those related to the hybrid technique are commonly reported [13], even if our personal feeling and experience are different. Indeed, as already reported by other authors [5], if we exclude the time for the robotic setup and disengagement, the operating time of our robotic series (341 min) is similar to that of our laparoscopic series (unpublished data) and is acceptable compared with that of the hybrid technique, which ranges from 217–383 minutes [2, 3].

Table 16.1 Our personal experience of full-robotic single-docking anterior resection

Variable	Robotic group (n=114)
Sex, M/F	68/46
Age (years), mean ± SD, (range)	67.6±10 (37–86)
BMI (kg/m^2), mean ± SD(range)	25.1±3.1 (18–32)
ASA 1/2/3/4	12/76/26/0
AJCC staging 0/1/2/3/4 n, (%)	18(16)/30(26)/25(22)/31(27)/10(9)
Upper/mild/inferior rectum n	46/24/44
Neoadjuvant chemoradiotherapy n, (%)	59 (51.8)
Anastomosis n, (%)	
Knight-Griffen	91 (80)
Coloanal	23 (20)
Ileostomy n, (%)	90 (78.9)
Conversion n, (%)	
Total /to open/to laparoscopy	5(4.4)/4 (3.5)/1(0.9)
Operative time (min), mean ± SD, (range)	341± 98.6 (175–723)
First flatus (days), mean ± SD (range)	1.5± 0.9 (1–6)
Oral re-intake (days) mean ± SD, (range)	1.3±0.8 (1–5)
Complications[a] n, (%)	
Total number /I-II /III-IV	17(14.9)/9(7.9)[b]/8(7)[c]
LOS (days) mean ± SD,(range)	9.9 ± 6.1 (4–40)
Retrieved LNs (n)mean ±SD	20.1± 8
Specimen length (cm) mean ±SD,(range)	23.4 ± 7.7 (11–78)
Size tumor (cm) mean ±SD, (range)	2.9 ±1.9 (0.3–10)
Distal resection margin (cm) mean ±SD, (range)	3.7±2.3 (0.5–12)
CRM positivity n, (%)	4(3.5)

LOS, length of stay; *LN*, lymph node; *CRM*, circumferential resection margin. [a]According to Clavien-Dindo Classification; [b]4 urinary retentions, 2 prolonged ileus, 2 pneumonias, 1 anastomotic fistula conservatively treated; [c]3 bowel obstructions, 1 descending colon ischemia, 1 anastomotic leakage, 1 ureteral injury, 1 parastomal hernia repair, 1 anastomotic bleeding

Our personal experience includes 114 RAR with TME performed from March 2010 to May 2014. The patient demographic and perioperative data are shown in Table 16.1. The procedure has been successfully performed in 109 out of 114 patients (conversion rate: 4.4%) with a mean operative time of 341 ± 98.6 minutes (range: 175–723 minutes, including loop ileostomy fashioning).

No intraoperative complications were observed. Bowel continuity was restored with transanal stapled end-to-end or end-to-side anastomosis in 91 patients and with manual coloanal anastomosis for ultralow anterior resections in 23 patients. A diverting loop ileostomy was matured in 90 patients (78.9%).

No positive distal resection margin was reported and the number of harvested lymph nodes was 20.1 ± 8. Four specimens (3.5%) showed circumferential

resection margin (CRM) involvement (defined as a CRM ≤1 mm); in three patients, who underwent neoadjuvant radiotherapy, the evaluation of the mesorectum quality showed a Grade 3 – Good. In the last patient, who did not receive a preoperative radiotherapy, the specimen showed a T_4N_0 at the final histological evaluation.

All patients were submitted to a perioperative fast-track program. Recovery of bowel function, oral re-intake and length of stay was on day 1.5 ± 0.9 (range: 1–6), 1.3 ± 0.8 (range: 1–5) and 9.9 ± 6.2 days (range: 4–40 days), respectively. The overall complication rate on the basis of the Clavien-Dindo classifications was 14%.

References

1. Pigazzi A, Ellenhorn JD, Ballantyne GH et al (2006) Robotic-assisted laparoscopic low anterior resection with total mesorectal excision for rectal cancer. Surg Endosc 20:1521–1525
2. Hellan M, Anderson C, Ellenhorn JD et al (2007) Short-term outcomes after robotic-assisted total mesorectal excision for rectal cancer. Ann Surg Oncol 14:3168–3173
3. Baik SH, Lee WJ, Rha KH et al (2008) Robotic total mesorectal excision for rectal cancer using four robotic arms. Surg Endosc 22:792–797
4. Hellan M, Stein H, Pigazzi A (2009) Totally robotic low anterior resection with total mesorectal excision and splenic flexure mobilization. Surg Endosc 23:447–451
5. Choi DJ, Kim SH, Lee PJ et al (2009) Single-stage totally robotic dissection for rectal cancer surgery: technique and short-term outcome in 50 consecutive patients. Dis Colon Rectum 52:1824–1830
6. Park YA, Kim JM, Kim SA et al (2010) Totally robotic surgery for rectal cancer: from splenic flexure to pelvic floor in one setup. Surg Endosc 24:715–720
7. Obias V, Sanchez C, Nam A et al (2011) Totally robotic single-position 'flip' arm technique for splenic flexure mobilizations and low anterior resections. Int J Med Robot 7:123–126
8. Bianchi PP, Ceriani C, Locatelli A et al (2010) Robotic versus laparoscopic total mesorectal excision for rectal cancer: a comparative analysis of oncological safety and short-term outcomes. Surg Endosc 24:2888–2894
9. Heald RJ (1988) The 'Holy Plane' of rectal surgery. J Royal Soc Med 81:503–508
10. Spinoglio G, Summa M, Priora F et al (2008) Robotic colorectal surgery: first 50 cases experience. Dis Colon Rectum 51:1627–1632
11. Kim SH, Kwak JM (2013) Robotic total mesorectal excision: operative technique and review of the literature. Tech Coloproctol 17 Suppl 1:S47–53
12. D'annibale A, Pernazza G, Monsellato I et al (2013) Total mesorectal excision: a comparison of oncological and functional outcomes between robotic and laparoscopic surgery for rectal cancer. Surg Endosc 27:1887–1895
13. Alasari S, Min BS (2012) Robotic colorectal surgery: a systematic review. ISRN Surg 2012:293894

Robotic Surgery for Complicated Diverticulitis

17

Giuseppe Spinoglio, Giampaolo Formisano, Francesca Pagliardi, Ferruccio Ravazzoni, and Alessandra Marano

17.1 Introduction

The severity of complicated diverticulitis includes a broad spectrum of diseases and is classified according to the Hinchey classification system [1]:

- Stage I: pericolic abscess, confined to the mesentery of the colon, usually responsive to conservative management, with a radiological drainage in the case of an abscess larger than 5 cm;
- Stage II: distant abscess amenable to percutaneous drainage (Stage IIa) or complex and multiple abscesses with or without a digestive fistula (Stage IIb);
- Stage III: diffuse purulent peritonitis;
- Stage IV: diffuse fecal peritonitis;

Hinchey Stage I and II are amenable to laparoscopic lavage-drainage, when percutaneous drainage has failed or in the case of clinical deterioration, which may spare the patient from major emergency colorectal surgery or postpone an elective delayed resection. Hinchey III diverticulitis represents a controversial stage: a broad spectrum of surgical options is considered, which range from a lavage-drainage to a major resection. An ongoing randomized trial (LADIES, NTR2037) is expected to provide further recommendations [2, 3]. In the case of Hinchey Stage IV, sigmoid resection with a primary anastomosis with or without a diverting loop ileostomy can be performed [3]; however this stage represents the major indication for Hartmann's procedure [2].

The laparoscopic approach for colorectal resection has been shown to be feasible and safe in an emergency setting if performed by experienced surgeons

G. Spinoglio (✉)
Department of General and Oncologic Surgery,
"Ss. Antonio e Biagio" Hospital,
Alessandria, Italy
e-mail: giuseppe.spinoglio@gmail.com

G. Spinoglio (Ed), *Robotic Surgery: Current Applications and New Trends*,
Updates in Surgery
DOI: 10.1007/978-88-470-5714-2_17, © Springer-Verlag Italia 2015

[4, 5] but to date, due to the weak evidence, no recommendation can be made. In elective settings, this minimally invasive technique provides a reduction in postoperative pain, systemic analgesia requirements, hospital stay, overall postoperative morbidity, total hospital cost and improved quality of life [6, 7]. However, the laparoscopic management is associated with a conversion rate of up to 65% due to the presence of bulky mesenteric tissue and ill-defined planes of dissection [8].

The robotic technique has been recently applied to the treatment of complicated diverticular diseases in elective settings. Thanks to its technology, the da Vinci® application seems to be promising and might overcome some limitations of the laparoscopic approach. This chapter deals with our experience of robotic delayed sigmoidectomy for complicated diverticulitis.

17.2 Procedure Overview

17.2.1 Patient and Trocar Positioning, OR Setup, and Docking

The details for this procedure are the same as those for our personal technique for rectal anterior resection (See Chapter 16).

17.2.2 Critical Elements of the Procedure

The key steps for our technique of single-docking full-robotic sigmoidectomy are listed as follows:

1. Splenic flexure takedown
2. Vascular control
3. Medial-to-lateral mobilization of descending colon/sigmoid
4. Final mobilization of sigmoid/upper rectum and distal resection
5. Specimen removal and anastomosis

This strategy is similar to that which we follow for single docking robotic anterior resection with some obvious differences related to the oncologic aspects. However, it is worth explaining in more detail certain issues of each step.

17.2.2.1 Step 1 - Splenic Flexure Takedown

We routinely mobilize the splenic flexure in order to prevent any further tension. In fact, Western patients have a higher incidence of diverticulitis compared to the Eastern ones; moreover, they have a relatively short sigmoid colon so that the mobilization of left colon splenic flexure is a routine procedure in most cases.

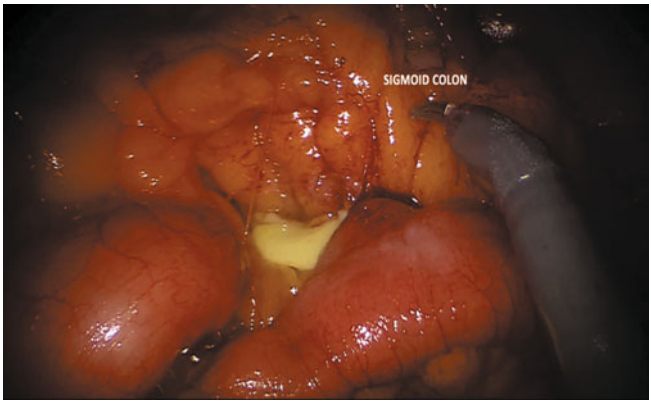

Fig. 17.1 Pericolic abscess involving a small bowel loop

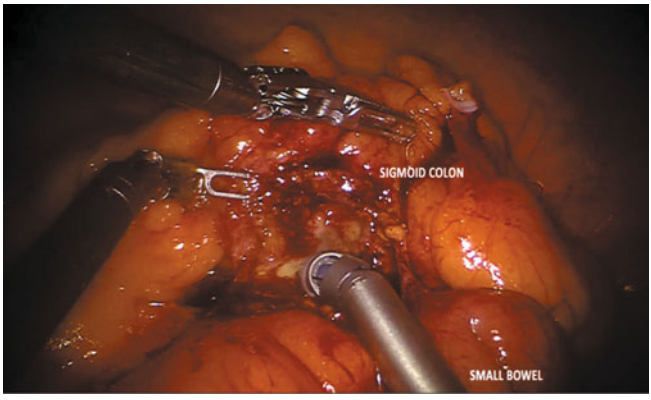

Fig. 17.2 Blunt dissection of the small bowel loop involved in the inflammatory process

17.2.2.2 Step 2 - Vascular Control

Two vascular ligation options can be considered during a delayed sigmoidectomy: a central one and a peripheral one.

Indeed, complicated diverticulitis can be characterized by the presence of intense inflammatory processes (Figs. 17.1 and 17.2) and by the involvement of the mesosigmoid and of the left ureteral posterior plane. If this occurs, the inferior mesenteric artery (IMA) division at its origin, preserving the hypogastric nerve plexus, can be recommended since it is easier and safer to perform compared to a more distal ligation. Following this strategy, a gentle dissection in the avascular retroperitoneal plane between Gerota's and Toldt's fascia can be progressively implemented, even if abscesses or adhesions are still present. The peripheral ligation, in this particular case, would be associated with a high risk of directly enter into the inflammatory process, losing the anatomical landmarks and eventually causing ureteral and vascular injuries.

Otherwise, in the case of less inflammatory settings or when abscesses are located in other sites such as in the pelvis, the section of the sigmoid arteries at their origin, preserving the superior hemorrhoidal artery has to be considered in order to guarantee a better rectal stump perfusion.

17.2.2.3 Step 3 - Medial-to-Lateral Mobilization of Descending Colon/Sigmoid

A medial-to-lateral dissection should be carried out until the left colon is separated from the retroperitoneum to avoid initial dissection into the inflammatory process and to facilitate the identification and preservation of the left gonadal vessels and the left ureter. As we routinely performed, the complete intracorporeal division of the proximal mesocolon is carried out to the chosen transection point in the left/sigmoid colon.

17.2.2.4 Step 4 - Final Mobilization of Sigmoid/Upper Rectum and Distal Resection

Following our standardized technique, the colonic mobilization proceeds down to the sacral promontory until the upper rectum is completely freed. At this level, the overlying peritoneum is laterally incised while the limit of the anterior dissection is represented by the absence of the anterior tenia on the rectal segment, close to the peritoneal reflection. During this step, the sequelae of the inflammatory process that may involve other organs, such as small bowel, bladder, uterus and especially left adnexa, are also treated.

Once the mobilization is completed, the mesorectum is dissected and the rectum, selected for distal stapler location, is skeletonized. The rectum is thus divided using an articulating linear endostapler via the assistant port, after having assessed the bowel perfusion with the indocyanine green fluorescence imaging system (see Chapter 19).

17.2.2.5 Step 5 - Anastomosis

An end-to-end or side-to-end circular stapled anastomosis, according to the surgeon's preference and the anatomical setting, is performed intracorporeally, usually without a temporary loop ileostomy since the anastomosis is fashioned at a safe colonic segment.

17.3 Advantages, Review of the Literature and Personal Outcomes

In recent decades, the surgical management of complicated diverticulitis is quickly moving toward less invasive procedures than previously. Even though a strong specific recommendation is not yet present [3], the laparoscopic approach for colonic resection can be adopted and to date the published literature reports potential benefits of this technique to improve patient outcomes. However, in the

case of significant inflammatory diverticular masses, the limits of visualization and dissection related to the laparoscopic approach have been associated with a significant conversion rate [9, 10] that consequently reduced the benefits of minimally invasive surgery [11].

The robotic technology, benefiting from its intrinsic technical advantages, has been recently applied for the treatment of complicated diverticular disease. It is worth specifying that at present the available data are poor. However, excluding case reports, the first experience of robotic sigmoidectomy for complicated diverticulitis was reported in 2011 [8]: data on nine enrolled patients showed no conversion and promising outcomes in terms of length of hospital stay (4.2 ± 4 days).

Recently, a study comparing laparoscopic (55 patients) versus robotic (20 patients) left colectomy for colovesical fistula was published [10]. The robotic group had shorter hospital stays, a lower complication rate and no conversions compared to the laparoscopic group (0% vs. 14.55%, $p = 0.001$). Even considering the small robotic sample size, the authors conclude that the advantages of robotic surgery might be of clinical significance in complicated, "high-risk-of-conversion" cases, such as fistulized diverticular disease.

In unpublished series, 25 robotic delayed sigmoidectomies with primary anastomosis have been performed at our institution. Demographic data, disease stratification and perioperative outcomes are shown in Table 17.1. There were neither intraoperative complications nor conversions to the open or laparoscopic approach; the mean hospital stay was 6.5 days (range = 3–13) and 3 out of 25 patients (12%) presented with a minor complication that was medically treated.

A retrospective analysis was conducted on prospectively collected data of a series of 46 patients whom underwent delayed laparoscopic sigmoidectomy for

Table 17.1 Personal experience of robotic delayed sigmoidectomy for complicated diverticulitis

Variable	Robotic sigmoidectomy group, n=25 pts
Sex (F/M)	11/14
Mean age, yrs (range)	60 (32–85)
Mean BMI, kg/m^2 (range)	27.3 (18.7–33)
Hinchey I, n(%)	10 (40%)
Hinchey II, n(%)	14 (56%)
Stenosis, n(%)	1 (4%)
Conversion rate %, (n)	0% (0/25)
Central/peripheral vascular ligation (n)	16/9
Mean OT, min (range)	327 (200–515)
Mean LOS, days (range)	6.6 (3–13)
Intraoperative complications rate %	0%
Postoperative complications rate %, (n)	12% (3/25); 1 perianastomotic collection; 1 pulmonary embolism; 1 proctorrhage

OT, operative time; *LOS*, length of stay

complicated diverticulitis; this group was comparable to the robotic one in terms of demographic characteristics and Hinchey disease stratification. A statistically significant reduction in conversion rate (0% vs. 17.4%, $p=0.027$) was observed in favor of the robotic group, with comparable operating room times (282 min vs. 255 min; $p=0.167$). No statistically significant differences were observed regarding hospital stay or 30-day postoperative morbidity between the compared groups.

Our results support the robotic approach as a safe and effective tool in maximizing the advantages of minimally invasive surgery in the management of complicated diverticular diseases. The 3DHD vision and the Endowristed technology make the robotic approach particularly useful during surgery performed in these settings. The dissection of hard and severely inflamed tissue in the abdomen (and also in a narrow pelvis) and the identification of the proper plane are likely to be the areas that benefit from this technology mainly.

References

1. Hinchey EJ, Schaal PG, Richards GK (1978) Treatment of perforated diverticular disease of the colon. Adv Surg 12:85–109
2. Mutter D, Marescaux J (2013) Appendicitis/diverticulitis: minimally invasive surgery. Dig Dis 31:76–82
3. Agresta F, Ansaloni L, Baiocchi GL et al (2012) Laparoscopic approach to acute abdomen from the Consensus Development Conference of the Societa Italiana di Chirurgia Endoscopica e nuove tecnologie (SICE), Associazione Chirurghi Ospedalieri Italiani (ACOI), Societa Italiana di Chirurgia (SIC), Societa Italiana di Chirurgia d'Urgenza e del Trauma (SICUT), Societa Italiana di Chirurgia nell'Ospedalita Privata (SICOP), and the European Association for Endoscopic Surgery (EAES). Surg Endosc 26:2134–2164
4. Zdichavsky M, Granderath FA, Blumenstock G et al (2010) Acute laparoscopic intervention for diverticular disease (AIDD): a feasible approach. Langenbecks Arch Surg 395:41–48
5. Cirocchi R, Cochetti G, Randolph J et al (2014) Laparoscopic treatment of colovesical fistulas due to complicated colonic diverticular disease: a systematic review. Tech Coloproctol doi:10.1007/s10151-014-1157-5
6. Klarenbeek BR, Veenhof AA, Bergamaschi R et al (2009) Laparoscopic sigmoid resection for diverticulitis decreases major morbidity rates: a randomized control trial: short-term results of the Sigma Trial. Ann Surg 249:39–44
7. Alves A, Panis Y, Slim K et al (2005) French multicentre prospective observational study of laparoscopic versus open colectomy for sigmoid diverticular disease. Br J Surg 92:1520–1525
8. Ragupathi M, Ramos-Valadez DI, Patel CB et al (2011) Robotic-assisted laparoscopic surgery for recurrent diverticulitis: experience in consecutive cases and a review of the literature. Surg Endosc 25:199–206
9. Purkayastha S, Constantinides VA, Tekkis PP et al (2006) Laparoscopic vs. open surgery for diverticular disease: a meta-analysis of nonrandomized studies. Dis Colon Rectum 49:446–463
10. Maciel V, Lujan HJ, Plasencia G et al (2014) Diverticular disease complicated with colovesical fistula: laparoscopic versus robotic management. Int Surg 99:203–210
11. Guillou PJ, Quirke P, Thorpe H et al (2005) Short-term endpoints of conventional versus laparoscopic-assisted surgery in patients with colorectal cancer (MRC CLASICC trial): multicentre, randomised controlled trial. Lancet 365:1718–1726

Part V

New Technologies in Robotic Platform

Single-Site™ Surgery

18

Giuseppe Spinoglio, Giampaolo Formisano,
Luca Matteo Lenti, Fabio Priora, and Alessandra Marano

18.1 Introduction

The Single-Site™ platform was primarily designed to work in a narrow operative field and with a specific anatomical target. To date, the most consistent published experiences are regarding the use of this technology to perform cholecystectomy [1–9] but, recently, it has been applied in other fields of general surgery [10–12]. This chapter will focus on its current application in performing cholecystectomy and right colectomy.

18.2 Single-Site™ Robotic Cholecystectomy (SSRC)

18.2.1 Patient and Robot Positioning

Under general anesthesia, the patient is secured in a supine position with both arms tucked at sides. The robotic cart should approach the patient at 45° (from perpendicular) over the right shoulder ensuring that the target anatomy is in-line with the center column, umbilicus and arrow on the port. The assistant and the scrub nurse are positioned at the patient's left side and at the patient's feet, respectively; the main assistant monitor is located at the right of the patient in the line of vision of the assistant (Fig. 18.1a).

G. Spinoglio (✉)
Department of General and Oncologic Surgery,
"Ss. Antonio e Biagio" Hospital,
Alessandria, Italy
e-mail: giuseppe.spinoglio@gmail.com

G. Spinoglio (Ed), *Robotic Surgery: Current Applications and New Trends*,
Updates in Surgery
DOI: 10.1007/978-88-470-5714-2_18, © Springer-Verlag Italia 2015

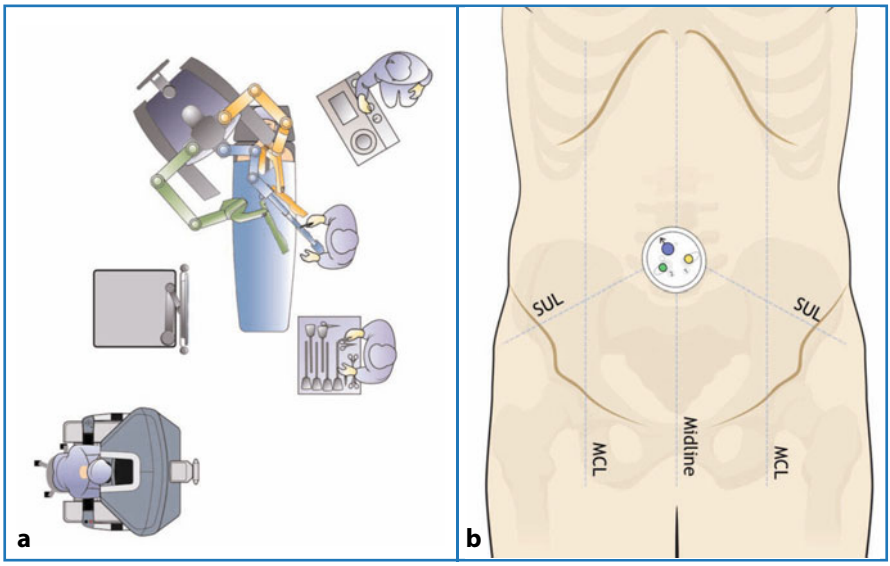

Fig. 18.1 **a** Overhead views of OR setup for Single-Site™ robotic cholecystectomy and Single-Site TM robotic right colectomy. **b** Single-Site™ port placement for cholecystectomy. (© 2014 Intuitive Surgical, Inc.)

18.2.2 Single-Site™ Placement and Docking

Access to the peritoneal cavity is gained through a nearly 2.5 cm midline intraumbilical incision extended to the fascia and by means of transection of the umbilical stalk if necessary (Fig. 18.1b). In order to exclude the presence of adhesions, a digital exploration of the abdominal cavity is recommended and so it is suggested to slightly enlarge the fascial incision.

Subsequently, the Single-Site™ port, folded by the clamp technique or unfolded, is lubricated with a sterile solution, and is introduced with an atraumatic clamp just above its lower rim into the abdomen with a downward motion while countertraction is provided by retractors within the single incision. The right position of the port is achieved when the top port flanges lay flat against the abdominal wall and the arrow marking on the port is aligned with the theoretical anatomical target (gallbladder).

A 12-mmHg pneumoperitoneum is instilled and the 30° downscope and the accessory cannula are inserted. The table is placed at the minimum angle of reverse-Trendelenburg (10–15°) and is rolled to the left side (5°) for better exposure of the gallbladder. Diagnostic laparoscopy is so performed.

The assistant grasps and retracts the fundus of the gallbladder with a laparoscopic grasper to expose the infundibulum: this step is crucial to assess port alignment, to ensure an adequate working space for the cannulae and finally to choose the most appropriate length of these. The laparoscopic grasper, the endoscope and the accessory cannula are then removed. The patient cart is brought at

a 45° angle over the right shoulder ensuring that the target anatomy is in-line with the center column, umbilicus and arrow on the port.
For SSRC, only robotic arm 1 (R1) and arm 2 (R2) are used in addition to the camera arm:

- the camera arm has to be in line with the center of the column and bent at an angle of 45° (sweet spot);
- R1 is placed to the left of the patient and its instruments reach the surgical field from the right: Cadiere forceps (alternatively crocodile or Maryland grasper);
- R2 is placed to the right of the patient and its instruments reach the surgical field from the left: monopolar cautery with hook tip, Hem-o-lok® clip applier, curved scissors, suction/irrigator;
- accessory port: laparoscopic grasper.

It is worth pointing out that one of the main innovations is that the da Vinci® software restores the correct hand/instrument correlation: the surgeon uses the right hand to drive the instrument visualized on the right side of the operative screen, even if the instrument comes from the left and vice versa.

The endoscope is reinserted vertically; under direct vision the lubricated curved cannulae are inserted by sight to avoid visceral injury, in order that they cross inside the port keeping the remote center at the level of the abdominal wall. Then, the robot is docked.

18.2.3 Operative Technique

At the patient's bedside, the assistant grasps the fundus of the gallbladder and lifts up and toward the patient's right shoulder to expose the hepatoduodenal ligament. At the console, the da Vinci® software has automatically associated the surgeon's hand to the ipsilateral instrument tip: the surgeon retracts the scope, moves it under the grasper, and pushes it toward the gallbladder while the assistant lifts the grasper (and therefore the fundus of the gallbladder) upward. Finally, the surgeon can easily retract the gallbladder infundibulum laterally to open the Calot's triangle, as in multitrocar laparoscopy.

Dissection begins and follows the traditional steps until the critical view of safety is achieved. The peritoneum, close to the gallbladder neck, is incised with the monopolar hook by gentle dissection of the peritoneal elements. The cystic duct and artery are identified and skeletonized (Fig. 18.2). The ligation is performed with Hem-o-lok® ML clips (clip applier in R2) and the division is performed with curved scissors (R2).

The dissection of the gallbladder from the liver bed is carried out using the Cadiere forceps (R1) and monopolar cautery hook (R2). During this last step, the scope is repositioned above the grasper to lift the liver and expose the surgical field. Before completion of the dissection of the gallbladder from the liver, it is important to inspect the gallbladder bed and ducts for evidence of bleeding

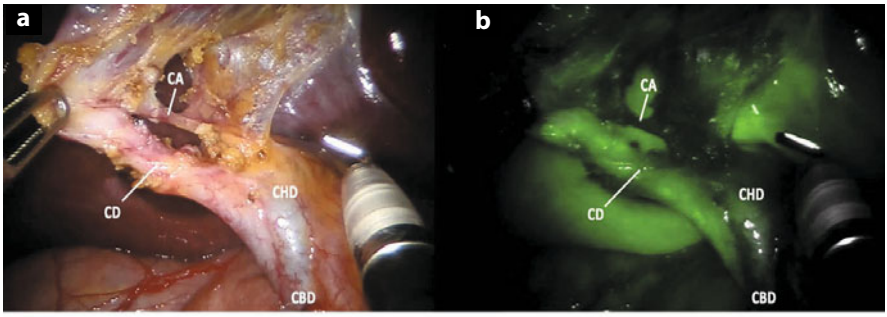

Fig. 18.2 Final view of cystic duct and cystic artery after Calot's dissection in white light (**a**) and near-infrared fluorescent (**b**) view. *CD*, cystic duct; *CA*, cystic artery; *CHD*, common hepatic duct; *CBD*, common bile duct

or bile leak: if required, the suction/irrigation instrument is inserted in R2 and later replaced with the previous energy instrument.

After complete dissection of the gallbladder from the liver bed, a lubricated 10-mm accessory cannula for the extraction bag replaces the 5-mm one. The gallbladder is then placed inside the retrieval bag and removed along with the Single-Site™ port after all instruments and cannulae have been withdrawn. The fascia is closed with absorbable suture, the umbilicus is restored to its physiological position and the skin is reapproximated with a running subcuticular closure.

When indicated, an intraoperative cholangiography can be performed using a percutaneous laparoscopic cholangiography set. The catheter is inserted percutaneously in the right upper quadrant, under visualization, and grasped by means of the robotic instruments per standard technique. During the procedure, the endoscope and all Single-Site™ instruments are removed, robotic cart is undocked from patient and the curved cannulae (left in port) are retracted back until an exposure of about 3 cm below the remote center is achieved.

At the end of the cholangiography, the robot is redocked. The balloon catheter is removed by sight. Finally, the surgery is completed as usual.

Another innovative tool is represented by the fluorescent cholangiography that can be routinely performed, during the surgery, to visualize in "real time" the biliary tree (see Chapter 19).

18.3 Discussion

18.3.1 Advantages

The robotic Single-Site™ platform offers distinct advantages:

- the lateral traction of the infundibulum, that is essential to open Calot's triangle and to reach the "critical view of safety" [13], is guaranteed;

- the correct triangulation of the target anatomy is restored by the rigid cannulae, crossing at the monoport and the robotic arm collisions are minimized;
- the bedside-assistant port enables dynamic retraction to perform a safe dissection;
- any internal clashing with other instruments are avoided because of the placement of the robotic camera in the middle of the curved cannulae zone (instead of being parallel as in SILS);
- the same-sided hand-eye control of the instruments is maintained by the da Vinci® intuitive software: "what is right is right and vice versa";
- the added benefits of the stable 3DHD view, the precision, the better ergonomic comfort and the intraoperative dynamic fluorescent cholangiography increase the safety and make the surgery easy to perform.

18.3.2 Limitations

The main drawbacks of the Single-Site™ system are:
- the absence of the EndoWrist® technology at the flexible instrument tips;
- the reduced intracorporeal range of motion of the robotic instruments;
- the interaction between the assistant instrument and the scope: since the assistant cannula can only be parallel to the camera one, it is very important to consider the close relationship between these two tools and especially that the assistant instrument can be moved by the camera controlled by the surgeon at the console.

18.3.3 Outcomes Overview

The most consistent experiences of SSRC are reported in Table 18.1. Nine articles evaluating over 600 SSRC with Single-Site™ kit have been published between 2011 and January 2014 [1–9]. Based on available data, the approach is safe and feasible and has been easily adopted by surgeons mainly of American and European origin.

SSRC was successfully carried out not only in the case of symptomatic cholelithiasis but also for cholecystitis with a conversion rate of about 3.8%. The mean length of hospital stay, derived from seven articles, was 30.2 hours and few early or late major complications have been reported. It is worth saying that no bile duct injuries occurred in any of the above mentioned papers.

Our single institutional experience consists of 151 patients whom underwent SSRC for symptomatic cholelithiasis (n = 139, 92%), cholecystitis (n = 8, 5.3%) and gallbladder polyposis (n = 4, 2.7%) from July 2011 to May 2014. The mean total operative time was 70.7 minutes; no conversions occurred and no additional port was required. With a mean hospital stay of 1.2 days, no major intraoper-

ative or early postoperative complications occurred, including bile duct injuries. At a mean follow-up of 26.3 months, two incisional hernias (1.3 %) were observed (Table 18.2).

18.4 Single-Site™ Robotic Right Colectomy (SSRRC)

18.4.1 Patient and Robot Positioning

The patient is placed in a partial Trendelenburg supine position with a slight roll to the left and the cart is on the patient's right shoulder. The assistant is at the patient's left side and the scrub nurse at the patient's feet. The main assistant monitor is located at the patient's right side (Fig. 18.1).

18.4.2 Single-Site™ Placement and Docking

The Single-Site™ port, grasped with an atraumatic clamp, is introduced through a nearly 2.5 cm left paramedian transverse sovrapubic incision (Fig. 18.3) and a 12-mmHg pneumoperitoneum is established. The 8.5-mm cannula for the 3DHD scope is lubricated and inserted; under direct vision, the other two robotic curved cannulae and the accessory cannula for the assistant are introduced as well. For right colectomy, our usual instruments are:

- R1: Cadiere grasper
- R2 : Curved scissors or alternatively monopolar cautery with hook tip, Hem-o-lok® clip applier, suction/irrigator, bipolar Maryland and curved needle driver (recently put on the market)
- Accessory port: laparoscopic grasper.

18.4.3 Step-by-Step Review of Single-Site™ Robotic Right Colectomy with Intracorporeal Anastomosis

The first surgical step is represented by the lateral retraction of the last ileocolic loop with the Cadiere grasper tenting up the ileocolic vessels; then, in order to create a window under these, the peritoneum is opened with the cautery hook to visualize the duodenum. The ileocolic vessels are clipped, sectioned (Fig. 18.5) and following the superior mesenteric vein (SMV) left anterior surface upward, the right branches of the middle colic vessels are clipped and sectioned too, as a result of the cephalad traction of the transverse mesocolon with the assistant's laparoscopic grasper. A medial-to-lateral colonic mobilization is performed in the avascular plane between Gerota's and Toldt's fasciae keeping the right ureter and the gonadic vessels down.

For malignant diseases, a complete mesocolic excision (CME), according to the principles of Hohenberger et al. [14], is carried out as we usually perform in

Table 18.1 Single-Site™ robotic cholecystectomy (SSRC): major clinical series of at least 25 cases

Study [Reference]	Study design	No. of patients (F/M)	Preoperative diagnosis	Age, years; BMI, kg/m^2; ASA score, (mean, SD)	Docking; console; total time, min. (mean, SD)	Conversion; adding port; n (%)	Incision, cm (mean)	LOS, hours (mean)	Major early; late complications, n (%)
Konstantinidis [1] (2012, Greece)	Case series	45 (22/23)	36 cholelithiasis; 5 cholecystitis; 4 other[1]	47 ± 12; 28.8 ± 4; 1.48 ± 1	5.8 ± 1.56; 43 ± 21.98; 84.5 ± 25.5	0(0); 3(6.7)	2	23.8	1(2.2); 0; 1 hemorrhage
Pietrabissa [2] (2012, Italy)	Prospective observational	100 (71/29)	100 cholelithiasis	53.4 ± 12.9; 24.4 ± 3.7; –	13 ± 6; 32 ± 13; 71 ± 19	2 to OC(2); 0	2	-	0; –
Spinoglio [3] (2012, Italy)	Retrospective comparative[a]	25 (20/5)	23 cholelithiasis; 2 other[1]	54.2 (19–78)*; 23.7(16.5–32.4)*; –	5.2 ± 1.1; 22.3 ± 10.9; 62.7 ± 16.6 [p]	0; 0	2.5	26.4	0;0
Angus [4] (2013, USA)	Case series	55 (34/21)	37 cholelithiasis; 18 other[3]	46.01± 4.25; 26.57± 4.25; –	11.34±3.74; 28.74±11.04; 61.84±14.66	0; 0	2	-	0;0
Gonzalez [5] (2013, USA)	Retrospective comparative[b]	166 (131/35)	127 cholelithiasis; 20 cholecystitis; 19 other[1,2,3]	51.6 ± 15.9; 29.4 ± 6.2; 1.84 ± 0.73	– ; – ; 63.0 ± 25.2 [p]	0; 3(1.8)	2.5	28.8	2(1.2); 0; 2 intrabdominal abscesses
Spinoglio [6] (2013, Italy)	Case series	45 (33/12)	45 cholelithiasis	48(23–76)*; 24.7(19–43)*; –	– ; 24.1 (7.3–59.3)*; 67(35–110)*	0; 0	-	26.4	0; –
Uras [7] (2013, Turkey)	Case series	36 (31/5)	36 cholelithiasis	40.1(21–64)*; – ; –	9.8 (4–30)*; 24.9 (7–60)*; 61.8 (34–110)*	0; 1(2.7)	2.5	24	0; 1(2.7); 1 incisional hernia

(*cont.*) →

Table 18.1 (*continued*)

Study [Reference]	Study design	No. of patients (F/M)	Preoperative diagnosis	Age, years; BMI, kg/m^2; ASA score, (mean, SD)	Docking; console; total time, min. (mean, SD)	Conversion; adding port; n (%)	Incision, cm (mean)	LOS, hours (mean)	Major early; late complications, n (%)
Vidovszky [8] (2013, USA)	Prospective cohort study	95 (68/27)	80 cholelithiasis; 8 cholecystitis; 7 other[1,3,4]	45.2 ± 16.1; 30.1 ± 7.1; –	4.9 ± 3.0; 39.1 ± 15.3; 88.63 ± 32.0	7 (6 to LC, 1 to OC, 8.4)/ 0	2.5	24 (84%pts)	4(4.2); 0; 3 residual CBD lithiasis, 1 biloma
Morel [9] (2014, Switzerland)	Case series	82 (72/28)	82 cholelithiasis	48.74 ± 13.23; 26.33 ± 4.18; 1.73 ± 0.54	6.60 ± 7.58; 50.90 ± 23.25; 91.05 ±29.92	1 to OC(1.2); 2(2.4)	2.93	58.1	1(1.2); 1(1.2); 1 duodenal lesion/1 incisional hernia

[a]SSRC vs. Single-Incision Laparoscopic Cholecystectomy (SILC); [b]SSRC vs. SILC vs. SPIDER approach; [1] gallbladder polyps; [2] biliary pancreatitis; [3] biliary dyskinesia; [4] Recurrent pyogenic cholangitis; *median(range); [p] Value with statistical significance between compared group; *CBD*, common bile duct; *OC*, open cholecystectomy; *LC*, laparoscopic cholecystectomy; *LOS*, length of stay

Table 18.2 Demographics and perioperative outcomes of our series of Single-Site™ robotic cholecystectomy

Variable	Total No. of patients, n=151
Sex, n (F/M)	109/38
Age, years (mean ± SD)	49.4 ± 14.0
BMI, kg/m^2	
mean ± SD	24.5 ± 4.2
<25, n (%)	89 (58.9)
25–29.9, n (%)	46 (30.5)
>30, n (%)	16 (10.6)
Previous major abdominal surgery, n (%)	54 (37.2)
Preoperative diagnosis	
Symptomatic cholelithiasis, n (%)	139 (92)
Cholecystitits, n (%)	8 (5.3)
Gallbladder polyps, n (%)	4 (2.7)
Total operative time, min (mean ± SD)	70.7 ± 24.8
Conversion/adding ports, n (%)	0 (0)
IOC, n (%)	1 (0.7)
Major intraoperative complication, n (%)	0 (0)
Major early postoperative complication, n (%)	0 (0)
LOS (mean ± SD)	1.17 ± 0.5
Mean follow-up, months	26.3

IOC, intraoperative cholangiography; *LOS*, length of stay

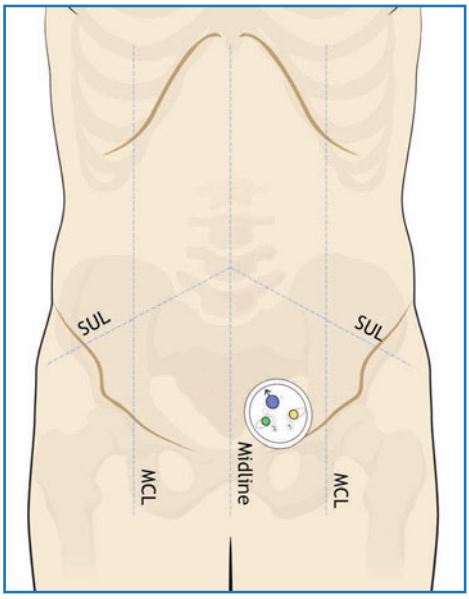

Fig. 18.3 Single-Site™ port placement for right colectomy. (© 2014 Intuitive Surgical, Inc.)

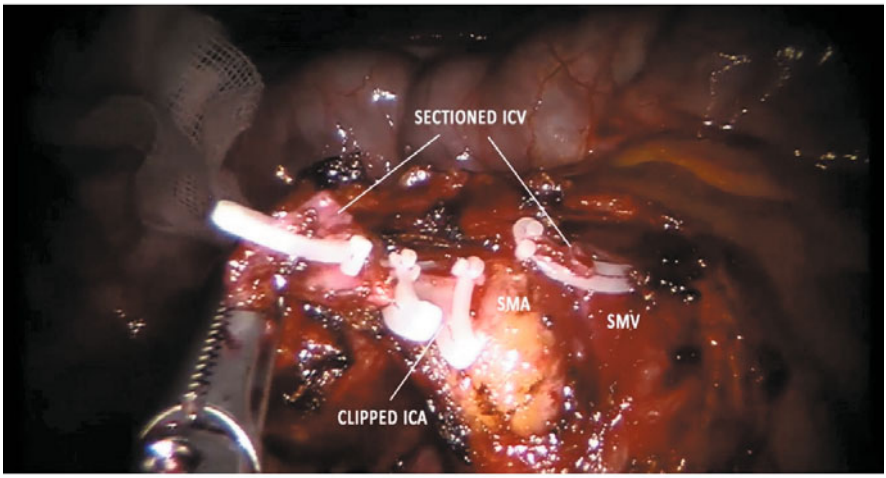

Fig. 18.5 Skeletonization and division of ileocolic vessels at their root. *ICA*, ileocolic artery; *ICV*, ileocolic vein; *SMA*, superior mesenteric artery; *SMV*, superior mesenteric vein

our laparoscopic or robotic multiport standardized technique. The segment of transverse colon chosen for the section is skeletonized and the gastrocolic ligament and the omentum are divided. The hepatic flexure is then mobilized and the detachment of the right colon is completed by the dissection of the right peritoneal groove. Finally, the segment of the terminal ileum is as well identified and prepared.

In order to perform an intracorporeal anastomosis and to insert the specimen into a 15 mm Endobag, we placed a 15-mm trocar on the right side of the single port, just enlarging the previous skin incision.

The ileum and the transverse colon are approximated side-to-side by a 3–0 absorbable monofilament suture, placed at their antimesenteric side. An enterotomy and a colotomy are made at the antimesenteric border. The two bowel stumps are vertically aligned with a traction on the stay suture in order to insert a 60 mm long flexible stapler (Echelon Flex™ Endopath®, blue cartridge) and to perform a side-to-side anisoperistaltic anastomosis.

Finally, the ileum and the transverse colon are mechanically transected with two stapler applications, including the remaining enterotomies (Fig. 18.6). Then, the specimen, inserted into an Endobag, is extracted through a Pfannenstiel minilaparotomy, resulting from the single port and 15-mm trocar incisions. Fascia and skin are sutured in standard fashion. Fluorescence imaging with indocyanine green (ICG), integrated into the da Vinci® system, can be used to verify bowel stump perfusion before bowel transaction (see Chapter 19).

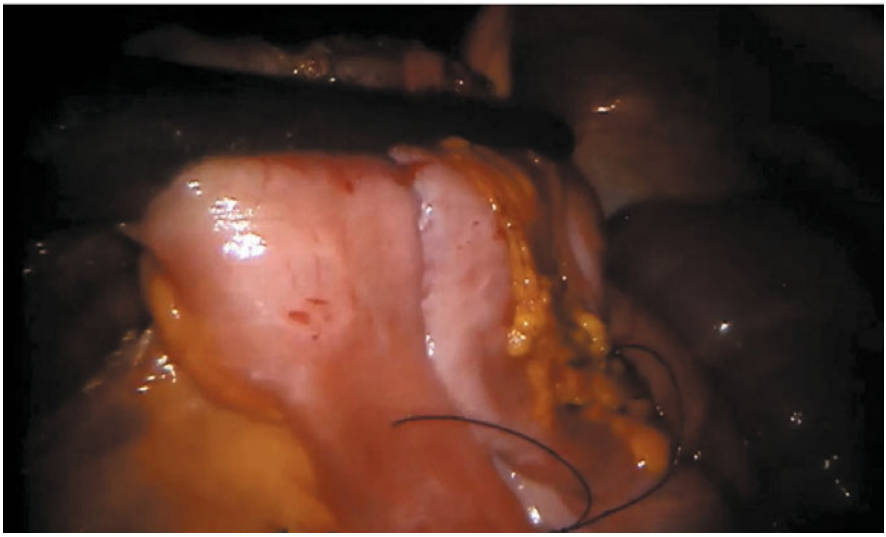

Fig. 18.6 The ileum and the transverse colon are mechanically transected with two stapler applications, including the remaining enterotomies, after having performed the side-to-side anisoperistaltic anastomosis

18.5 Discussion

18.5.1 Advantages

The robotic Single-Site™ platform provides some benefits in performing right colectomy compared to SILS:

- the correct triangulation is restored and internal and external instrument collision is minimized thanks to the curvature of the cannulae that increases the distance between the instrument tips allowing each to reach the target anatomy in a convergent way;
- the intuitive control is re-established by the da Vinci® software that automatically associates the surgeon's hands to the ipsilateral instrument tips;
- the stable 3D vision, the absence of tremor together with the recent introduction of new robotic Single-Site™ instruments (curved needle driver and bipolar Maryland) potentially allow performing a more accurate lymphadenectomy, an easier dissection and intracorporeal anastomosis compared to SILS.

In our opinion, the insertion of the monoport in the left transverse sovrapubic area rather than around or through the umbilicus provides a correct vision of the SMV, along all its length and on the left side: the entire medial to lateral dissection and an adequate CME can be easily performed. Furthermore, the left sovrapubic port insertion combines a good visualization of the superior mesen-

teric axis with the Pfannenstiel minilaparotomy. The extraction of the specimen through this incision is carried out in order to obtain an improved cosmesis, a decreased pain and a lower rate of incisional hernia compared to median supra and infraumbilical laparotomy.

Fluorescence imaging with indocyanine green (ICG), integrated into the da Vinci® system, can also be used to verify bowel stump perfusion before bowel transection.

18.5.2 Limitations

The main drawbacks of the Single-Site™ system are as follows:

- the absence of the EndoWrist® technology at the flexible instrument tips: the desired release of an Endowristed Single-Site™ needle driver in the near future could facilitate this procedure;
- in the case of intracorporeal anastomosis, the stapler for the bowel transection has to be introduced into the abdomen through an additional laparoscopic port: although this issue makes the single-incision technique lose its theoretical principle, its own value is preserved since the additional trocar is inserted into the same slightly enlarged skin incision used for specimen extraction.

18.5.3 Outcomes Overview

Up to date, one case of SSRRC has been published [11]. It was in a patient affected by a malignant polyp of the caecum and both resection and anastomosis have been carried out extracorporeally. The authors reported about the safety and feasibility of this procedure underlying the main technical benefits of this system.

Our experience consists of three full SSRRC with the robotic monoport inserted through a left sovrapubic transverse incision [12]. Overall SSRRC operative time was 218.3 ± 75.9 min. A side-to-side anisoperistaltic anastomosis was fashioned intracorporeally in two out of three cases. All patients were discharged within 5 days from surgery; oncological principles have been satisfied in both two candidates affected by colon cancer.

References

1. Konstantinidis KM, Hirides P, Hirides S et al (2012) Cholecystectomy using a novel Single-Site® robotic platform: early experience from 45 consecutive cases. Surg Endosc 26:2687–2694
2. Pietrabissa A, Sbrana F, Morelli L et al (2012) Overcoming the challenges of single-incision cholecystectomy with robotic single-site technology. Arch Surg (Chicago, Ill: 1960) 147:709–714

3. Spinoglio G, Lenti LM, Maglione V et al (2012) Single-site robotic cholecystectomy (SSRC) versus single-incision laparoscopic cholecystectomy (SILC): comparison of learning curves. First European experience. Surgical endoscopy 26:1648–1655
4. Angus AA, Sahi SL, McIntosh BB (2014) Learning curve and early clinical outcomes for a robotic surgery novice performing robotic single site cholecystectomy. Int J Med Robot 10:203–207
5. Gonzalez AM, Rabaza JR, Donkor C et al (2013) Single-incision cholecystectomy: a comparative study of standard laparoscopic, robotic, and SPIDER platforms. Surg Endosc 27:4524–4531
6. Spinoglio G, Priora F, Bianchi PP et al (2013) Real-time near-infrared (NIR) fluorescent cholangiography in single-site robotic cholecystectomy (SSRC): a single-institutional prospective study. Surg Endosc 27:2156–2162
7. Uras C, Böler DE, Erguner I, Hamzaoglu I (2013) Robotic single port cholecystectomy (R-LESS-C): Experience in 36 patients. Asian J Surg 37:115–119
8. Vidovszky TJ, Carr AD, Farinholt GN et al (2013) Single-site robotic cholecystectomy in a broadly inclusive patient population: A prospective study. Ann Surg 260:134–141
9. Morel P, Buchs NC, Iranmanesh P et al (2014) Robotic single-site cholecystectomy. J Hepatobiliary Pancreat Sci 21:18–25
10. Corcione F, Bracale U, Pirozzi F et al (2014) Robotic single-access splenectomy using the Da Vinci Single-Site(R) platform: a case report. Int J Med Robot 10:103–106
11. Morelli L, Guadagni S, Caprili G et al (2013) Robotic right colectomy using the Da Vinci Single-Site® platform: case report. Int J Med Robot 9:258–261
12. Spinoglio G, Lenti LM, Ravazzoni F et al (2014) Evaluation of technical feasibility and safety of Single-Site™ robotic right colectomy: three case reports. Int J Med Robot. DOI: 10.1002/rcs.1609
13. Strasberg SM, Brunt LM (2012) Rationale and use of the critical view of safety in laparoscopic cholecystectomy. J Am Coll Surg 211:132–138
14. Hohenberger W, Weber K, Matzel K et al (2009) Standardized surgery for colonic cancer: complete mesocolic excision and central ligation–technical notes and outcome. Colorectal Dis 11:354–364

ICG Fluorescence: Current and Future Applications

19

Giuseppe Spinoglio, Alessandra Marano, Luca Matteo Lenti, Fabio Priora, and Giampaolo Formisano

19.1 Introduction

The imaging technique based on indocyanine green (ICG) fluorescence has been widely used for more than forty years, especially to study blood flow and microcirculation. This method was first applied in general surgery to perform sentinel lymph node (SLN) biopsies in patients affected by breast and colorectal cancer. In 2010, a near-infrared (NIR) laser light system was integrated with the da Vinci® Si™ HD robotic system (Intuitive Surgical Inc., Sunnyvale, CA, USA). This imaging system is able to provide both white light and near-infrared light images through dedicated endoscopic illuminators and filters by simply pressing a pedal on the surgical console, thus allowing real-time fluorescence-guided surgery. There are many fields of application of ICG fluorescence in robotic general surgery, some experimental and still evolving, that include:

- intraoperative (IO) fluorescent cholangiography to assess biliary anatomy;
- evaluation of bowel stump perfusion;
- lymph node (LN) mapping and the SLN biopsy in colorectal cancer surgery;
- colorectal tattoing.

In this chapter, we describe our nearly 3-year experience with fluorescence-guided robotic general surgery.

G. Spinoglio (✉)
Department of General and Oncologic Surgery,
"Ss. Antonio e Biagio" Hospital,
Alessandria, Italy
e-mail: giuseppe.spinoglio@gmail.com

G. Spinoglio (Ed), *Robotic Surgery: Current Applications and New Trends*,
Updates in Surgery
DOI: 10.1007/978-88-470-5714-2_19, © Springer-Verlag Italia 2015

19.2 Fluorescent Cholangiography (FC) during Single-Site Robotic Cholecystectomy

19.2.1 Procedure Overview

Bile duct injury (BDI) is a rare but serious and feared complication of cholecystectomy and in the current era of laparoscopy the incidence of these lesions increased to 0.2–0.5% [1] when compared to open surgery (0.1–0.2%) [2]. Moreover, single-incision laparoscopic cholecystectomies may be associated with an even higher rate of BDI (0.7–0.8%) [3] due to the loss of the linchpins of conventional laparoscopy, such as triangulation and respect of optimal working angles. A "misperception" of the biliary anatomy is considered the primary cause of BDI rather than the lack of skill or knowledge and the use of a routinely intraoperative cholangiography (IOC) has been emphasized recently [4]. While recognizing the importance of IOC, it has several disadvantages, such as the interruption of the regular workflow with increased operative time, requirement for a multidisciplinary team and equipment, patient and staff exposure to radiation and the necessity to cannulate the cystic duct. Moreover, it provides static images that are often difficult to interpret. As already mentioned by some authors, there is a need for a "simpler method of locating the course of the ductal system during the operation, something simpler than cholangiography or ultrasonography" [5].

Single-Site™ robotic cholecystectomy (SSRC) certainly allows easier and safer surgical procedures than single-incision laparoscopy to be performed by overcoming its inherent technical limitations; however, the difficulty in visualizing the biliary structures can still remain. The use of the da Vinci® NIR-fluorescence imaging system could be a valid solution to allow real-time view of the anatomy of the extrahepatic biliary tract and a time-efficient dissection of Calot's triangle, thus further increasing safety during single-site surgery.

19.2.2 Technique

A dose of 2.5 mg of ICG is injected intravenously during induction of general anesthesia, about 30–45 minutes before surgery. If fluorescence is not detected after 60 minutes, an additional dose of 2.5 mg ICG can be administered. The SSRC procedure has already been described in detail in Chapter 18. Once the exposure of Calot's triangle is achieved, the imaging system is switched to fluorescence mode for an initial attempt to identify the biliary anatomy (Fig. 19.1). Subsequently, the dissection of Calot's triangle is performed as usual according to the principles of the "critical view of safety" of Strasberg, alternately switching from white to NIR light and allowing visualization of the fluorescent bile ducts in real time. In this way, the surgeon can follow a road map for a safe dissection of the cystic duct and the cystic artery (Fig. 19.2), especially in the presence of accessory structures and/or anatomical variations. The cystic duct may be clipped under fluorescence before sectioning, especially if it is very short and if there are problems in the bil-

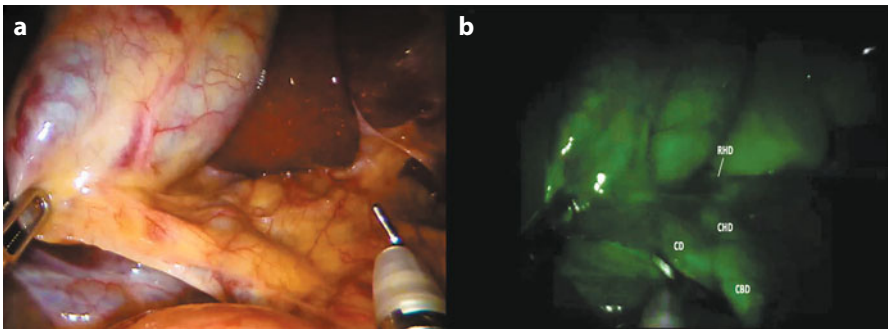

Fig. 19.1 White light (**a**) and near-infrared view (**b**) of biliary anatomy prior to Calot's dissection. *CD*, cystic duct; *CBD*, common bile duct; *CHD*, common hepatic duct; *RHD*, right hepatic duct

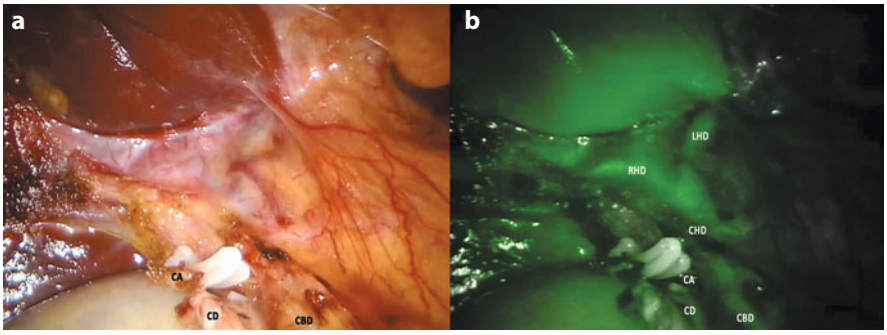

Fig. 19.2 White light (**a**) and near-infrared view (**b**) of biliary anatomy after Calot's dissection. *CD*, cystic duct; *CA*, cystic artery; *CBD*, common bile duct; *CHD*, common hepatic duct; *RHD*, right hepatic duct; *LHD*, left hepatic duct

iary confluence. If there are concerns with the vascular anatomy, it is possible to proceed with a further injection of 2.5 mg of ICG: after 10–20 seconds, hepatic and cystic arteries can be visualized to avoid any damage to both main and anomalous branches, especially the branch to the sixth hepatic segment. During the detachment of the gallbladder from the liver bed, the use of fluorescence is useful to define the limit between the gallbladder and liver bed (especially in cases of a thin or intrahepatic gallbladder) and to visualize any aberrant Luschka ducts. At the end of the procedure, a final fluorescent view of the operative field may be prudent.

19.2.3 Advantages, Limitations and Relative Contraindications (Personal Experience and Literature Outcomes)

19.2.3.1 Advantages

The advantages of FC over standard IOC are numerous:

- no interruption of the regular workflow: the surgeon operates both in white and fluorescent light;

- real-time interpretation of the images, in contrast to the traditional IOC that provides static information;
- control of the cystic duct section with a clear distinction of its confluence with the common bile duct;
- real-time detection of any aberrant Luschka ducts and bile leaks;
- identification of the vascular anatomy of the hepatic and cystic arteries, if necessary.

19.2.3.2 Limitations

The main limitations of FC are obesity and inflammation since fluorescent NIR light has a limited tissue penetration (5–10 mm). The ability of NIR light to reach deeper, inflamed and edematous tissues must be further investigated. Moreover, the capability of this method to recognize common bile duct stones or other obstructions is low and, of course, IOC remains the best method to assess choledocholithiasis.

19.2.3.3 Personal Experience and Literature Outcomes

FC during SSRC allows safe real-time evaluation of the biliary tract anatomy and is an additional helpful tool to prevent BDI during the procedure. First Ishizawa and then Buchs demonstrated the technical feasibility of this approach during multiport laparoscopic cholecystectomy [6], SILC [7] and SSRC [8]; also our initial experience has already been published [9]. Recently, Daskalaki et al. [10] reported their series of 184 robotic cholecystectomy (112 multiport and 72 Single-Site™): ICG fluorescence allowed visualization of at least one biliary structure in 99% of cases (182/184 patients), with promising results even in the setting of acute cholecystitis and obesity (BMI >30).

From July 2011 to May 2014, 120 patients (31 male / 89 female) underwent SSRC with FC for symptomatic cholelithiasis and gallbladder polyposis. Eight out of 120 patients suffered from acute cholecystitis (6.6%); the mean age was 48 ys and the mean BMI was 24.7 kg/m^2; the mean operative time and mean console time were 71 and 30 minutes, respectively. No statistically significant differences in operative times between standard SSRC (our previous experience) and SSRC with FC were observed, thus confirming that no additional time is needed. There were no conversions, BDIs, intra- or postoperative complications or adverse events; the mean hospital stay was 1.2 days. At a medium follow-up of 21 months, no patients presented with an incisional hernia.

Calot's dissection is defined as the skeletonization to at least 1 cm of the cystic duct and artery [9]. The rates of visualization of the cystic duct , the common hepatic duct and the common bile duct were 95%, 76.6 %, 79.2 % prior to Calot's dissection, respectively, and 99.2%, 92.5%, 96.6% after Calot's dissection, respectively. At least one biliary structure was visualized in 100% of cases after Calot's dissection, and in 116 out of 120 patients (96.6%) before Calot's dissection (Table 19.1). Our results are comparable to those reported by the more consistent series regarding the application of FC during conventional laparoscopic cholecystectomy [6].

Table 19.1 Visualization of fluorescent biliary ducts prior to and after Calot's dissection

	No. of visualization/total procedures	%
Before Calot's dissection		
Cystic duct	114/120	95
CHD	92/120	76.6
CBD	95/120	79.2
At least one duct	116/120	96.6
After Calot's dissection		
Cystic duct	119/120	99.2
CHD	111/120	92.5
CBD	116/120	96.6
At least one duct	120/120	100

CHD, common hepatic duct; *CBD*, common bile duct

We can conclude that FC is a simple, fast, safe and effective procedure. It allows clear real-time identification of extrahepatic biliary anatomy in almost all patients, thus implementing the well-known advantages of SSRC over the traditional single-incision laparoscopic approach.

19.3 Evaluation of Bowel Stump Perfusion

19.3.1 Procedure Overview

The anastomotic leakage is one of the most feared complications in colorectal surgery occurring in 1.2–19.2% of all operations, with rates reaching 39% for rectal cancer cases requiring low or ultralow anastomosis.

The underlying pathogenic mechanism has not yet been fully clarified and is thought to be a multifactorial problem: adequate exposure and access, correct surgical technique and gentle handling of the bowel, adequate hemostasis, absence of tension at anastomosis, avoidance of fecal contamination and approximation of well-vascularized bowel are all cornerstones to safely performing an intestinal anastomosis and have historically been considered as "good practice" by the surgical community.

Besides technical aspects, adequate bowel perfusion is certainly the main factor in ensuring the integrity of an anastomosis: it has been traditionally based on subjective parameters such as the presence of active bleeding from the section line, pulsatility of the mesenteric vessels, as well as peristalsis and the lack of discoloration of bowel segments. The clinical judgment alone, however, could represent an inaccurate method to evaluate the risk of anastomotic leakage, with limited predictive accuracy [11].

Though many different solutions have been proposed [12–14], the da Vinci® NIR-fluorescence imaging system represents the latest innovation in the field: it

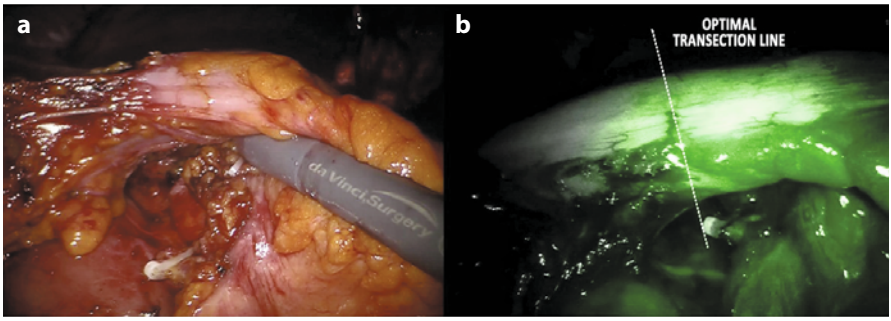

Fig. 19.3 White light (**a**) and near-infrared view (**b**) for evaluation of bowel stump perfusion

can be used to assess in real time both macroscopic vascular anatomy and perfusion of intestinal stumps thus supporting surgeons in choosing the correct section point during colorectal resections. Moreover, it can be extremely useful in nonstandardized colonic procedures (i.e., transverse colon, splenic flexure), since vascular abnormalities can strongly impair blood supply.

19.3.2 Technique

Surgery is performed with the da Vinci® Si™ HD surgical system according to the usual technique of vascular control and mesenteric division to prepare the intestinal segments. Afterward, the optimal transection line is evaluated by the surgeon with white light and a dose of 0.1 mg/kg of ICG is administered intravenously: after approximately 15–30 seconds, the surgeon switches to fluorescent vision (Fig. 19.3). If the site chosen for the section does not appear to be sufficiently perfused, the section line may be revised and the stapler can be moved to a more proximal/distal location according to the best fluorescence point reflected. In case of doubt, the test can be repeated after waiting for a few minutes to allow the dye to washout. However, depending on the tissue, the green fluorescent intensity appears different and at different times.

Regarding the colonic stumps, the vessels of the epiploic appendices and mesentery turn green first, then the green spreads across the intestinal wall. The antimesenteric border of the descending and transverse colon is always a little paler, because the vascularization of the tenia is less intense due to the thickness of muscle tissue. The perfused segments gradually become green until they assume a bright green color, in contrast with the gray segments that are not well vascularized. Further checks may be carried out before and after performing the anastomosis.

With regard to the rectal stump, the pelvic wall turns green first (as does the uterus in women), because it is highly vascularized. After a few seconds, the rectal stump colors up allowing the assessment of perfusion at the selected point. The ends of the section lines of the rectum in a Knight-Griffen anastomosis or of the colon in a laterolateral anastomosis are often referred to as critical points of leak-

age for their potential minor irroration: particular attention should be paid to their perfusion.

19.3.3 Advantages, Limitations and Relative Contraindications (Personal Experience and Literature Outcomes)

19.3.3.1 Advantages

Visual inspection and caution are often sufficient to choose a well-vascularized intestinal stump for anastomosis, especially for experienced surgeons. However there are difficult cases, both for patient conditions (such as obesity, diabetes, inflammatory disease, etc) and for the type of anastomosis (i.e., ultralow anterior rectal resection, splenic flexure resection, right colectomy), in which the evaluation of perfusion is important, even if only as confirmation, especially in the presence of a thick mesocolon and short mesentery. Moreover, this application might clearly be useful during minimally invasive surgery where there is a loss of tactile feedback.

19.3.3.2 Limitations

A limitation of this method can be represented by the fluorescence of the peritoneum due to an accidental spillage in the course of injection for tattoo or LN mapping. In this case, it may be difficult to appreciate the fluorescence of the stump tied to the perfusion, as distinct from the one linked to impregnation of the tissue.

Unfortunately, at present it remains a linear-graded result that requires subjective interpretation as to the cutoff point between sufficient and insufficient perfusion. However, in our opinion, there is a very clear visible cutoff in fluorescence mode between not perfused and perfused bowel during the first seconds after ICG administration. Quantitative real-time analysis of the fluorescence image would be desirable but is currently not available on the robotic system.

19.3.3.3 Personal Experience and Literature Outcomes

The first study to use fluorescence imaging for colorectal surgery was published in 2010 [12] with interesting results. This retrospective study compared 201 patients with laser fluorescence angiography (LFA) to a control group. The authors reported an overall reduction of revision due to anastomotic leaks by 4% in the LFA group (3.5% LFA vs. 7.5% control). In 13.9% of patients, the use of LFA resulted in a change in the initially planned transection line.

To date, only limited clinical data can be found in the literature regarding bowel perfusion assessment using the da Vinci® NIR-fluorescence imaging system.

Jafari et al. [15] have recently analyzed the effectiveness of fluorescence in reducing the rate of anastomotic leak after robotic-assisted low anterior resection (LAR) for rectal cancer in a retrospective case-control study. They compared LAR with and without fluorescence imaging and reported a change in the proximal transection point in 3 out of 16 patients (19%) and a reduced leak rate of 6% when compared to 18% for the control group.

Promising outcomes have also been reported by Bae et al. [16] in three case reports. The authors applied the ICG fluorescence during robotic LAR for cancer to better demark the ischemic area in the distal rectum so that the surgeon was helped to define the distal resection margin.

A prospective multicenter study [17] has recently evaluated the impact of fluorescence imaging on visualization of perfusion and subsequent change of transection point during left-sided robotic colorectal surgery. Fluorescence imaging was applied on 40 patients and resulted in a change of the proximal transection location in 40% (16/40) of the candidates: two patients (5%) with a change in transection line developed an anastomotic leak at postoperative days 15 and 40. The authors concluded that fluorescence imaging during colorectal procedures provides important additional information about bowel perfusion at the transection site; this may eventually help to decrease leaks caused by hypoperfusion.

From September 2011 to May 2014, we have performed bowel stump evaluation with fluorescence imaging system in 128 full-robotic multiport colorectal resections for benign and malignant diseases (unpublished data), which included: 51 right colectomies, 39 low and ultralow anterior rectal resections, 32 left colectomies and 6 splenic flexure resections. We routinely choose the transection line, after mesenteric section and bowel preparation, according to intestinal perfusion as shown by fluorescence imaging system. There were no intraoperative or anesthetic complications associated with the injection of ICG dye and the fluorescence bowel assessment was easily accomplished in real-time in 100% of cases with no additional operative time.

We registered one case of anastomotic leak (0.8%) in a 78-year-old obese male patient affected by sigmoid cancer. He presented a Grade C anastomotic leakage on postoperative day 4 and therefore he underwent emergency laparoscopic surgery with toilette and endoscopic clip placement.

To conclude, considering both promising published outcomes and our large experience, ICG fluorescence imaging is an effective and not time-consuming method to evaluate bowel stump perfusion. Whether this will eventually translate into decreased leakage rates, if compared to standard subjective parameters, remains to be definitively proven by large and well-conducted randomized trials. Integrated software to quantify the fluorescent signal could be useful.

19.4 Sentinel Lymph Node (SLN) Biopsy in Colon Cancer

19.4.1 Procedure Overview

The concept of the SLN biopsy is based on the premise that drainage from a solid organ tumor occurs in an orderly and near linear manner via lymphatics to regional LNs. Identification of SLNs during surgery through dedicated tracers would identify the “proper nodes” for pathologic examination. The promise of an accurate nodal staging with reduced surgical trauma and morbidity pushed the development

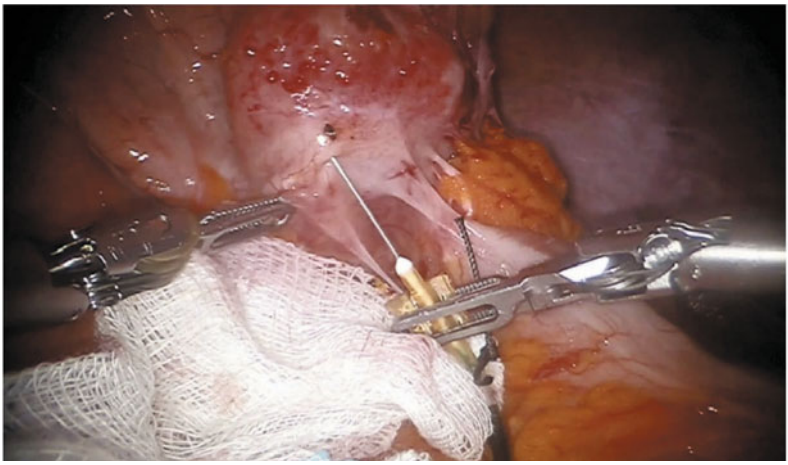

Fig. 19.4 Intraoperative subserosal injection of indocyanine green for sentinel lymph node biopsy for caecal cancer

of the SLN biopsy for melanoma and breast cancer in 1992 and 1994, respectively.

When compared with breast cancer or melanoma, however, SLN biopsy in colon cancer is used primarily for improving the accuracy of staging since typically it does not determine a more limited surgical resection, which remains clearly investigational because of the still high rate of false-negative SLNs.

Therefore, although its clinical value in colon cancer is far from being fully established, the aim is to upstage tumors (stage I and II) by providing the pathologist with one to three lymph nodes for detailed immunohistochemical evaluation. A reliable sentinel node harvesting technique may eventually alter the management in colon cancer treatment (i.e., adjuvant chemotherapy) where nodal micrometastases or isolated tumor cells would remain undetected by conventional pathological examination.

19.4.2 Technique

The dye (1.5–2.5 mg) is injected intraoperatively into the subserosa, by the insertion, through the assistant trocar, of a butterfly infusion set (Fig. 19.4). About 10–20 minutes after the injection, from one to three fluorescent LNs are displayed (Fig. 19.5). SLNs are removed selectively with a "berry picking" technique or marked with clips for ex vivo identification: each SLN will be stained with H&E and if no metastases are identified, the pathologist will select from each SLN a superficial, intermediate and deep section, respectively, that will be immunostained for cytokeratin (AE-1/AE-3).

Removed tissues are labeled according to anatomical location and sent separately for pathological evaluation.

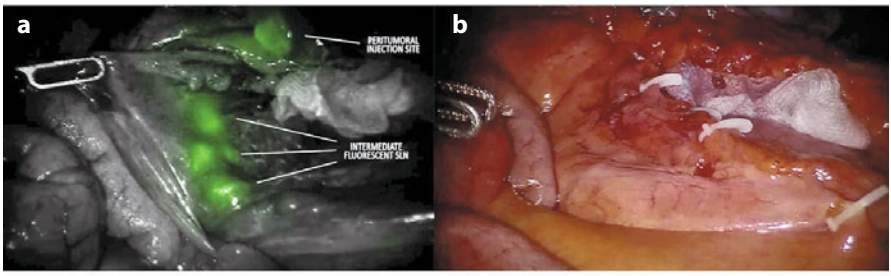

Fig. 19.5 Near-infrared view of sentinel lymph nodes (**a**). Final white light view of clipped sentinel lymph nodes (**b**)

19.4.3 Discussion

Published results on identifying SLNs in CRC with radioguided or blue-dye injection show variable success rates ranging from 58% to 100%. Consequently, there is ample room for investigation.

The feasibility of NIR-fluorescence SLN identification during open and laparoscopic colonic resections has already been demonstrated by some studies [18–22], with a detection rate ranging from 88.5% to 100%. This technique with a robotic fluorescent imaging system was first investigated for gynecological cancers in both preclinical and clinical settings, reporting a SLN detection rate of 95% [23].

To the best of our knowledge, no published reports exist about ICG SLN biopsy in robotic colonic surgery.

To date, we have performed 14 SLN biopsies at our institution for stage I and II colonic cancer, by using the da Vinci® NIR-fluorescence imaging system. The overall detection rate (number of successful attempts to retrieve LNs/number of attempts to retrieve LNs) was 92.8%. No aberrant lymphatic drainage was observed, unlike previous studies have reported [19, 24].

Our preliminary experience showed some shortcomings. The subserosal butterfly needle injection for SLN biopsy can be difficult and often remains too superficial and spreads the dye into the peritoneum. An important caveat in the removal of fluorescent LN with the "berry picking" technique is to gently manipulate them since, even without fractures, the dye can easily spread staining the robotic forceps and, consequently, the surrounding tissues. Additionally, the dose of the dye was progressively reduced over time: this can help surgeons to improve the accuracy of detection.

Recently, a study protocol for SLN identification using the robotic NIR fluorescent imaging system has been approved by the Ethical Committee of our institution. The objectives of the study are to establish the feasibility and accuracy of this method in "real-time" identification of SLN in patients affected by stage I/II colon cancer and to histologically evaluate by immunohistochemistry the SLN harvested for micrometastasis. Further studies should then highlight the prognostic significance of upstaging and consequences for adjuvant therapy in this subgroup of patients; a Dutch randomized prospective trial is currently recruiting patients (EnRoute Trial – ClinicalTrials.gov Identifier: NCT01097265).

19.5 Lymph Node (LN) Mapping in Rectal Cancer

19.5.1 Procedure Overview

The prognosis and quality of life of patients affected by colorectal cancer depends on the extent of the tumor (i.e., stage), its biological features (i.e., differentiation grade) and characteristics of onset. Complete surgical removal with en-bloc regional lymphadenectomy is pivotal for patient oncological outcomes and correct staging. Nevertheless, concerns about lymphatic spread in rectal cancer still exist.

Examples of involved nodal basins, which are not usually removed through a standard lymphadenectomy, are represented by lateral pelvic and periaortic LNs in rectal cancer, that typically have a variable drainage pattern. Although more radical surgical treatments (such as lateral pelvic lymphadenectomy in Japan) have been advocated over the years, surgical oncology is evolving toward less aggressive approaches: in this scenario, LN mapping with ICG might be considered a valid tool in performing a "tailored" surgery, eventually changing the operative strategy by performing an extended but selective lymphadenectomy according to the lymphatic migration of the fluorescent dye. The aim of LN mapping in rectal cancer is to potentially improve the staging process without higher morbidity figures if compared to standard resections.

19.5.2 Technique

From 1.5 to 2.5 mg of ICG solution are injected endoscopically around the tumor in the submucosa from 3 to 24 hours before surgery. Within 10–15 minutes, it reaches the first LN, one or two hours later it reaches the regional LNs where it remains for about 24–48 hours. Operating in NIR light, the LNs, from where the ICG has been drained, are highlighted during dissection. The LNs are removed en bloc if present in typical sites, whilst they are removed with a "berry picking" technique when present in unusual locations after LN mapping (i.e., periaortic, pericaval and lateral pelvic nodes, Fig. 19.6).

19.5.3 Discussion

To date, no studies about ICG lymph node mapping in robotic rectal surgery have been reported.

We have performed 19 LN mappings for rectal cancer, at our institution, to evaluate the feasibility of using the da Vinci® NIR-fluorescence imaging system. The overall detection rate was 78.9%. LN mapping was not successful in 4 out of 19 patients: two patients underwent preoperative radiochemotheraphy, which could compromise the detection rate by obliteration of lymphatic channels or by sclerosing of LNs draining the primary tumor. An overdose of ICG was administered in

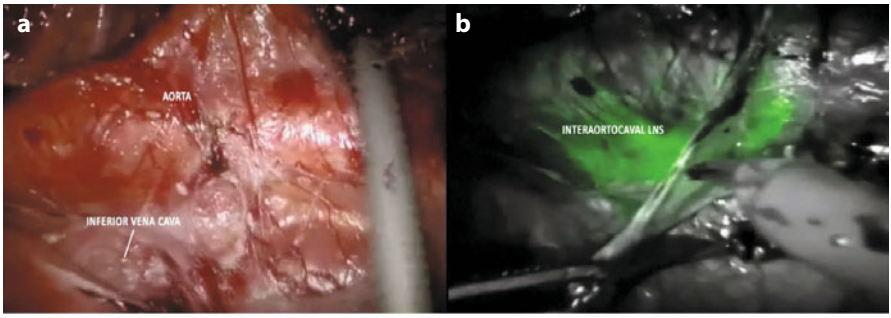

Fig. 19.6 White light (**a**) and near-infrared view (**b**) of interaortocaval lymph nodes following submucosal indocyanine green injection for rectal cancer

the remaining two cases, making the surgical field appear completely green in the fluorescent view.

Important caveats in LN mapping are the same as for the SLN biopsy, and include gentle manipulation of fluorescent LNs to avoid inadvertent staining of the surrounding tissues and ICG dose.

The ICG fluorescence imaging system during robotic colorectal surgery is a novel and challenging procedure: it may represent an additional tool to perform LN mapping and SLN biopsies. Our experience is still at a feasibility stage and we hope that our on-going study on SLN biopsy could provide useful information.

19.6 Colorectal Tattooing

To date, Indian ink is the most common agent used for perioperative colorectal tumor localization in the case of small or flat lesions. However, the use of this tattooing agent has been associated with complications [25, 26]. Therefore, some authors have proposed the use of ICG for endoscopic tattooing and have demonstrated the feasibility of the technique without adverse events [27].

A preoperative endoscopic tattooing with a dose of 2.5 mg ICG can be performed in order to identify, in real time, the tumor during robotic colorectal resections.

The use of ICG fluorescent imaging may be safe and useful for perioperative colorectal tumor localization; nevertheless, the peritumoral injection of the ICG before the surgery may cause an excessive or inadequate diffusion of the fluorescent dye around the tumor, spreading the ICG inside the abdominal cavity.

References

1. Connor S, Garden OJ (2006) Bile duct injury in the era of laparoscopic cholecystectomy. Brit J Surg 93:158–168

2. Rowe CK, Franco FB, Barbosa JA et al (2012) A novel method of evaluating ureteropelvic junction obstruction: dynamic near infrared fluorescence imaging compared to standard modalities to assess urinary obstruction in a Swine model. J Urol 188:1978–1985
3. Joseph M, Phillips MR, Farrell TM, Rupp CC (2012) Single incision laparoscopic cholecystectomy is associated with a higher bile duct injury rate: a review and a word of caution. Ann Surg 256:1–6
4. Berci G, Hunter J, Morgenstern L et al (2013) Laparoscopic cholecystectomy: first, do no harm; second, take care of bile duct stones. Surgical endoscopy 27:1051–1054
5. Way LW, Stewart L, Gantert W et al (2003) Causes and prevention of laparoscopic bile duct injuries: analysis of 252 cases from a human factors and cognitive psychology perspective. Ann Surg 237:460–469
6. Ishizawa T, Bandai Y, Ijichi M (2010) Fluorescent cholangiography illuminating the biliary tree during laparoscopic cholecystectomy. Brit J Surg 97:1369–1377
7. Ishizawa T, Kaneko J, Inoue Y et al (2011) Application of fluorescent cholangiography to single-incision laparoscopic cholecystectomy. Surg Endosc 25:2631–2636
8. Buchs NC, Hagen ME, Pugin F et al (2012) Intra-operative fluorescent cholangiography using indocyanin green during robotic single site cholecystectomy. Int J Med Robot Comput Assist Surg 8:436–440
9. Spinoglio G, Priora F, Bianchi PP et al (2013) Real-time near-infrared (NIR) fluorescent cholangiography in single-site robotic cholecystectomy (SSRC): a single-institutional prospective study. Surg Endosc 27:2156–2162
10. Daskalaki D, Fernandes E, Wang X et al (2014) Indocyanine Green (ICG) fluorescent cholangiography during robotic cholecystectomy: results of 184 consecutive cases in a single institution. Surg Innov. doi: 10.1177/1553350614524839
11. Karliczek A, Harlaar NJ, Zeebregts CJ (2009) Surgeons lack predictive accuracy for anastomotic leakage in gastrointestinal surgery. Int J Colorectal Dis 24:569–576
12. Kudszus S, Roesel C, Schachtrupp A, Hoer JJ (2010) Intraoperative laser fluorescence angiography in colorectal surgery: a noninvasive analysis to reduce the rate of anastomotic leakage. Langenbeck's Arch Surgery 395:1025–1030
13. Sherwinter DA, Gallagher J, Donkar T (2013) Intra-operative transanal near infrared imaging of colorectal anastomotic perfusion: a feasibility study. Colorectal Dis 15:91–96
14. Ris F, Hompes R, Cunningham C et al(2014)Near-infrared (NIR) perfusion angiography in minimally invasive colorectal surgery. Surg Endosc 28:2221-2226
15. Jafari MD, Lee KH, Halabi WJ et al (2013) The use of indocyanine green fluorescence to assess anastomotic perfusion during robotic assisted laparoscopic rectal surgery. Surg Endosc 27:3003–3008
16. Bae SU, Baek SJ, Hur H et al (2013) Intraoperative near infrared fluorescence imaging in robotic low anterior resection: three case reports. Yonsei Med J 54:1066–1069
17. Hellan M, Spinoglio G, Pigazzi A, Lagares-Garcia JA (2014) The influence of fluorescence imaging on the location of bowel transection during robotic left-sided colorectal surgery. Surg Endosc 28:1695–1702
18. Hirche C, Mohr Z, Kneif S et al (2012) Ultrastaging of colon cancer by sentinel node biopsy using fluorescence navigation with indocyanine green. Int J Colorectal Dis 27:319–224
19. Cahill RA, Anderson M, Wang LM et al (2012) Near-infrared (NIR) laparoscopy for intraoperative lymphatic road-mapping and sentinel node identification during definitive surgical resection of early-stage colorectal neoplasia. Surg Endosc 26:197–204
20. Kusano M, Tajima Y, Yamazaki K et al (2008) Sentinel node mapping guided by indocyanine green fluorescence imaging: a new method for sentinel node navigation surgery in gastrointestinal cancer. Digestive surgery 25:103–108
21. Nagata K, Endo S, Hidaka E et al (2006) Laparoscopic sentinel node mapping for colorectal cancer using infrared ray laparoscopy. Anticancer Res 26:2307–2311
22. Hutteman M, Choi HS, Mieog JS et al (2011) Clinical translation of ex vivo sentinel lymph node mapping for colorectal cancer using invisible near-infrared fluorescence light. Ann Surg Oncol 18:1006–1014

23. Jewell EL, Huang JJ, Abu-Rustum N et al (2014) Detection of sentinel lymph nodes in minimally invasive surgery using indocyanine green and near-infrared fluorescence imaging for uterine and cervical malignancies. Gynecol Oncol 132:274–277
24. Saha S, Johnston G, Korant A et al (2013) Aberrant drainage of sentinel lymph nodes in colon cancer and its impact on staging and extent of operation. Am J Surg 205:302–305
25. Yano H, Okada K, Monden T (2003) Adhesion ileus caused by tattoo-marking: unusual complication after laparoscopic surgery for early colorectal cancer. Dis Colon Rectum 46:987
26. Gianom D, Hollinger A, Wirth HP (2003) Intestinal perforation after preoperative colonic tattooing with India ink. Swiss Sur 9:307–310
27. Miyoshi N, Ohue M, Noura S et al (2009) Surgical usefulness of indocyanine green as an alternative to India ink for endoscopic marking. Surg Endosc 23:347–351

Part VI

Miscellany

Splenectomy and Hemisplenectomy

20

Giuseppe Spinoglio, Alessandra Marano,
Luca Matteo Lenti, Francesca Pagliardi,
and Giampaolo Formisano

20.1 Splenectomy

20.1.1 Procedure Overview

Minimally invasive splenectomy has become an established standard of care in general surgery for nontraumatic splenic lesions. Since laparoscopic splenectomy was first reported in 1991 by Delaitre et al. [1], subsequent literature has clearly shown that this approach dramatically improves short-term perioperative outcomes and provides enhanced cosmesis [2].

However, standard laparoscopy has some drawbacks, including an unstable two-dimensional vision and rigid instrumentation: these inherent limitations could make the procedure difficult to perform in the case of massive splenomegaly and fragile parenchyma.

The robotic system, thanks to its technological advantages, may potentially be a valid tool in performing splenectomy in these challenging situations [3, 4]. Moreover, the meticulous hilar dissection achieved with endowristed instruments may allow to easily perform partial splenectomies as well [3, 5, 6].

20.1.2 Patient and Robot Positioning

The patient is positioned in a right-lateral supine position (left side up by approximately 60–70°) and legs closed. Arms are secured with belts and appropriate supports to avoid injuries. The operating table is then flexed, lowering the

G. Spinoglio (✉)
Department of General and Oncologic Surgery, "Ss. Antonio e Biagio" Hospital, Alessandria, Italy
e-mail: giuseppe.spinoglio@gmail.com

G. Spinoglio (Ed), *Robotic Surgery: Current Applications and New Trends*, Updates in Surgery
DOI: 10.1007/978-88-470-5714-2_20, © Springer-Verlag Italia 2015

legs and the thorax, with the umbilicus above the pivoting point of the table. This position widens the space between the costal margin and anterior superior iliac spine for introducing trocars. A mild reverse-Trendelenburg tilt is applied to improve exposure of the operative field.

The robot is brought to the table from the left shoulder with a 45° angle and docked (Fig. 20.1a).

20.1.3 Trocar placement

Five trocars are placed after induction of 12 mmHg pneumoperitoneum by the Veress needle. A 12-mm camera port is introduced in the middle point between the left costal margin and the umbilicus; a 30° downscope is used.

Under direct visualization, trocars are inserted as follows (Fig. 20.1b):

- One 8-mm robotic trocar (R1) is placed on the transverse umbilical line, 5–6 cm left paraumbilical, for Hot Shears™ (monopolar curved scissors), cautery hook or robotic clip applier. We do not routinely use an ultrasonic scalpel in case of splenectomy;
- One 8-mm robotic trocar (R2) is placed in the epigastric area, 2–3 cm left paramedian, for bipolar forceps. Harmonic scissors are mounted on R2 for parenchymal transection during hemisplenectomy;
- One 8-mm robotic trocar (R3) in the left flank for the ProGrasp™ forceps or Cadiere forceps, used for upward traction on the splenic parenchyma or downward traction on the left colonic flexure to achieve exposure;
- One 15-mm assistant's trocar is placed between R1 and R3 for suction/irrigation, clip application (if necessary) or other maneuvers to achieve optimal exposure of the splenic hilum.

A thorough inspection of the peritoneal cavity for gross pathology and accessory spleen is performed. If identified, the accessory spleen should be removed.

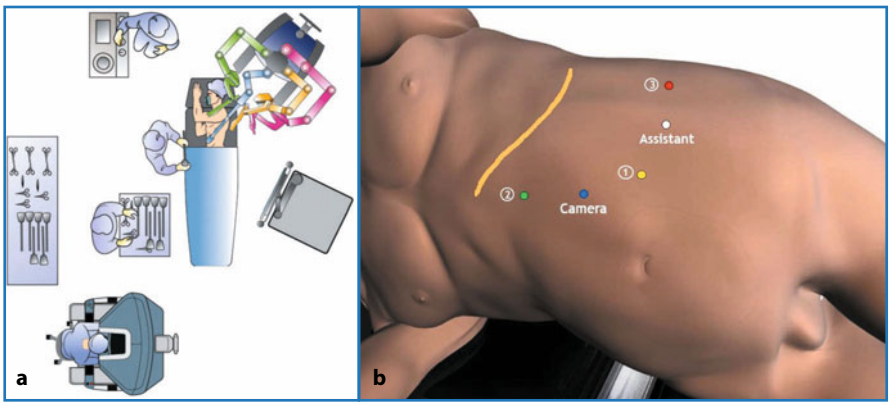

Fig. 20.1 Splenectomy and hemisplenectomy. **a** OR setup. **b** Trocar layout. (© 2014 Intuitive Surgical, Inc.)

20.1.4 Step-by-Step Review of Critical Elements of the Procedure

20.1.4.1 Step 1 - Access to the Lesser Sac and Splenic Hilum Exposure

Robotic Splenectomy (RS) is performed with an anterior approach (i.e., vessel division without a posterior mobilization of the spleen). The stomach is retracted medially by the assistant's grasper and a gentle and constant lateral traction on the spleen is applied with the fenestrated grasper in R3. Gastrocolic and gastrosplenic ligaments, within which short gastric vessels lie, are opened with the bipolar forceps in R2 and the cautery hook/monopolar scissors in R1; clips may be applied if required.

There are two vascular patterns of the splenic pedicle: the magistral type, in which the main splenic artery enters the splenic hilum as a compact structure without branching; and the distributed type, which is the most common pattern, in which multiple arterial branches arise from the main splenic artery 2–3 cm from the hilum. Indeed, two or three lobar arteries can be found in the majority of cases (86% and 12%, respectively) [7].

20.1. 4.2 Step 2 - Vascular Dissection

This step of the operation is carried out with the cautery hook in R1 and bipolar forceps in R2. The monopolar scissors, clip applier and large needle driver can be mounted on R1 when necessary.

The pancreatic tail is exposed and the splenic artery may be thus easily identified along its superior border. The splenic artery is dissected circumferentially and passed under with a loop as distally as possible for vascular inflow control. The splenic artery can be ligated or clipped along its main trunk (Fig. 20.2) but, if it gives off long lobar or segmental branches, they can be dissected separately and divided between self-locking nonabsorbable clips.

Finally, the splenic vein is dissected (Fig. 20.3), ligated and divided. It is important that the length of the prepared vessels is optimal to allow both double proximal and a distal ligature: an important advantage provided by the robotic system is the possibility to easily and safely ligate splenic vessels with traditional knots, if required. Venous branches usually overlay arterial vessels at the splenic hilum: if this dissection is challenging, the main trunk of the splenic artery can be clipped thus reducing splenic vascular inflow and allowing a safer control of the splenic vein.

20.1.4.3 Step 3 - Spleen Mobilization

The spleen is pulled cranially and laterally with the grasper in R3, while the assistant gently stretches the Gerota's fascia caudally with the suction/irrigator to maintain the operative field clean. The cautery hook in R1 and bipolar forceps in R2 are used to dissect the posterior attachments in a caudal-to-cephalad direction. Care should be taken to avoid any parenchymal fracture in neoplastic diseases.

20.1.4.4 Step 4 - Specimen Extraction

An endobag is inserted through the assistant trocar for specimen extraction and the robot is undocked. The spleen is removed for morcellation by slightly

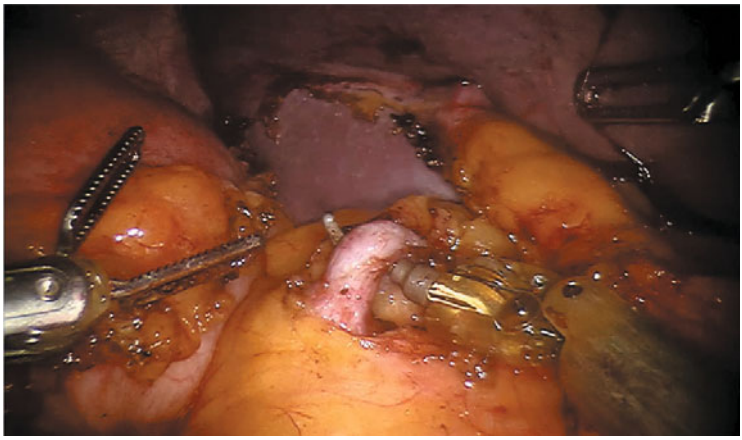

Fig. 20.2 Dissection of the main trunk of the splenic artery

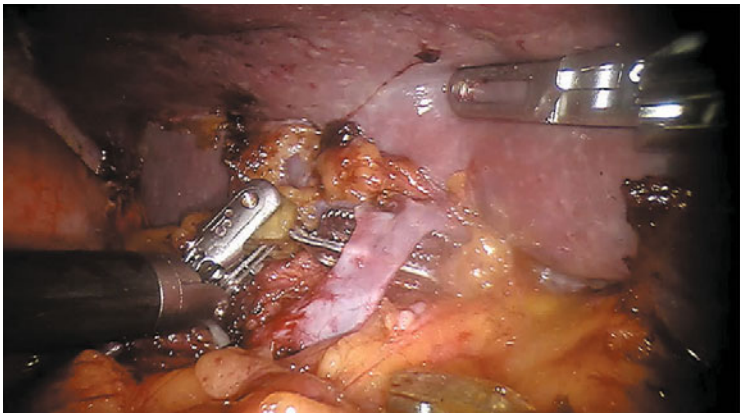

Fig. 20.3 After arterial control, the vein is fully dissected and divided

enlarging a trocar site, otherwise through a Pfannenstiel laparotomy if larger specimens cannot be morcellated because of the underlying pathology. After a final laparoscopic check of the operative field, a suction drain is routinely left in place and trocars are removed under direct vision.

20.2 Hemisplenectomy

20.2.1 Procedure Overview

The value in performing partial splenectomy for selected benign diseases has been well demonstrated in preserving the immune function, particularly in young patients.

The robotic assisted approach may be the most indicated for hemisplenectomy because it theoretically allows a more meticulous dissection of small arterial branches if compared to laparoscopy. However, to date, different studies have shown laparoscopic partial splenectomy to be feasible and safe with good clinical results [8–16] and only few robotic series have directly addressed this issue [3, 5, 6].

20.2.2 Step-by-Step Review of Critical Elements of the Procedure

Patient and robot positioning, trocar placement and splenic hilum exposure are the same as previously described for total splenectomy, except for an extensive division of the more cranial short gastric vessels in the case of lesions located at the lower pole of the spleen.

The splenic artery is dissected first and passed under with a loop as distally as possible for bleeding control, if necessary, during hilar and parenchymal dissection. The hilar dissection is then undertaken and all arterial branches are identified and progressively dissected free, depending on the vascular pattern. Any arterial or venous branches to be preserved are identified, while the other vessels are clipped proximally and distally or ligated with absorbable sutures (Fig. 20.4). The cautery hook in R1 guarantees for precise dissection of even small branches of the splenic vessels.

The demarcation line is then identified in white light or through the integrated fluorescence imaging system after the intravenous administration of 0.1 mg/kg of indocyanine green (ICG); also arterial vascular branching can be assessed in real-time during the procedure. The spleen is divided using the

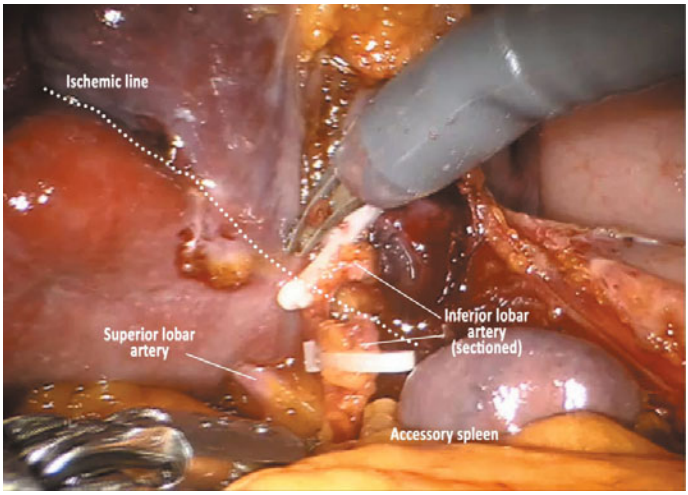

Fig. 20.4 Dissection and ligation of the inferior lobar artery during hemisplenectomy. The demarcation line is clearly visible

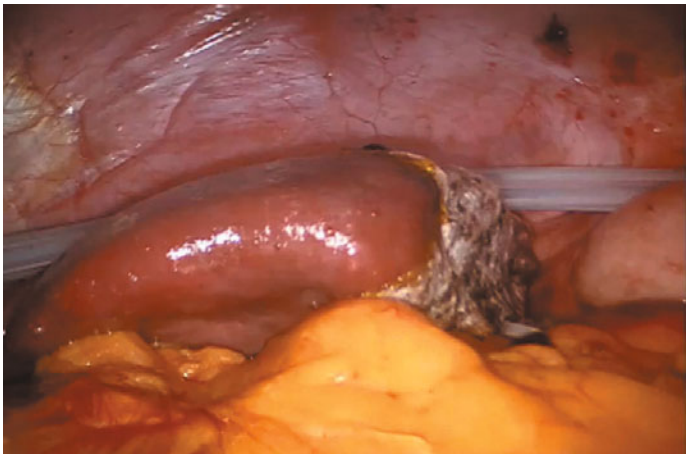

Fig. 20.5 Final view after hemisplenectomy. An absorbable fibrin sealant patch is applied on the transected splenic parenchyma

Harmonic scalpel on R2 or the bipolar forceps and retrieved in an endobag. During this step, small median vessels (subsegmental arteries and veins or their branches) may be encountered, gently skeletonized and selectively clipped as a result of the technological features of the robotic system. Hemostasis of the remaining splenic parenchyma can be refined through bipolar coagulation or dedicated hemostatic materials (Fig. 20.5). A suction drain is routinely left in place, robot is undocked and trocars are removed.

20.3 Advantages and Personal Experience

Minimally invasive splenectomy is considered a well-accepted approach for a variety of conditions, including auto-immune or congenital hematological disorders, lymphoproliferative diseases, focal lesions, cysts, abscesses and tuberculosis.

To date, comparative studies did not show any significant advantages of RS over standard laparoscopy. From a technical point of view, the choice of whether to use the robotic or laparoscopic approach for the hilar dissection should be considered on a case-by-case basis and is dependent on various factors, including anatomy of the pancreatic tail, anatomy of the splenic vessels, and volume and consistency of the spleen.

It seems reasonable to advocate a laparoscopic approach in the case of a small and compact spleen associated with a short pancreatic tail, allowing for safe stapling of the pedicle.

However, the endowristed instruments together with the magnified 3DHD vision may give advantageous results in the case of (3, 4, 6):

- multiple and short arterial and venous branches of the splenic vessels;
- bulky or “intrasplenic” pancreatic tail;

- fragile parenchyma and huge spleen volume, which is the main predictor for conversion to open surgery in the case of laparoscopic splenectomy;
- previous radiotherapy with extensive fibrosis and adhesions;
- hemisplenectomy, for selective small vessel ligation, parenchymal transection and parenchymal sparing.

In the case of hemisplenectomy, different methods of parenchymal transection can be used [6]; however, we do not routinely oversew the remaining splenic parenchyma with pledgets as described by other authors [3]. Moreover, Vasilescu et al. [6] have demonstrated lower blood loss and vascular dissection time during robotic subtotal splenectomy if compared to the laparoscopic approach.

To date, we performed 15 total splenectomies and 5 hemisplenectomies. There were 9 men (45%) and 11 (55%) women, with a mean age of 45.2 years. Indications for surgery with total splenectomies included hematological disorders (8 pts), lymphoproloferative diseases (5 pts) and voluminous cysts (2 pts); the mean spleen size for total splenectomy was 13.2 cm. Hemisplenectomies were performed for benign focal lesions. The mean operative times were 229 min and 260 min for total and partial splenectomy, respectively. Overall, there were no conversions to open surgery and no intraoperative complications or major postoperative complications were observed.

In conclusion, our series and previous studies report RS as safe and feasible; it provides a valid alternative to laparoscopic splenectomy, especially in more challenging cases and during hemisplenectomy.

References

1. Delaitre B, Maignien B (1991) Splenectomy by the laparoscopic approach. Report of a case. Presse Med 20:2263
2. Gamme G, Birch DW, Karmali S (2013) Minimally invasive splenectomy: an update and review. Can J Surg 56:280–285
3. Giulianotti PC, Buchs NC, Addeo P (2011) Robot-assisted partial and total splenectomy. Int J Med Robot Comput Assist Surg 7:482–488
4. Gelmini R, Franzoni C, Spaziani A (2011) Laparoscopic splenectomy: conventional versus robotic approach–a comparative study. J Laparoendosc Adv Surg Tech A 21:393–398
5. Vasilescu C, Tudor S, Popa M (2010) Robotic partial splenectomy for hydatid cyst of the spleen. Langenbeck's Arch Surg 395:1169–1174
6. Vasilescu C, Stanciulea O, Tudor S (2012) Laparoscopic versus robotic subtotal splenectomy in hereditary spherocytosis. Potential advantages and limits of an expensive approach. Surg Endosc 26:2802–2809
7. Liu DL, Xia S, Xu W et al (1996) Anatomy of vasculature of 850 spleen specimens and its application in partial splenectomy. Surgery 119:27–33
8. Seims AD, Breckler FD, Hardacker KD, Rescorla FJ (2013) Partial vs total splenectomy in children with hereditary spherocytosis. Surgery 154:849–853
9. Zhang Y, Chen XM, Sun DL, Yang C (2014) Treatment of hemolymphangioma of the spleen by laparoscopic partial splenectomy: a case report. W J Surg Oncol 12:60
10. Slater BJ, Chan FP, Davis K, Dutta S (2010) Institutional experience with laparoscopic partial splenectomy for hereditary spherocytosis. J Ped Surg 45:1682–1686

11. Morinis J, Dutta S, Blanchette V et al (2008) Laparoscopic partial vs total splenectomy in children with hereditary spherocytosis. J Ped Surg 43:1649–1652
12. Hery G, Becmeur F, Mefat L et al (2008) Laparoscopic partial splenectomy: indications and results of a multicenter retrospective study. Surg Endosc 22:45–49
13. Breitenstein S, Scholz T, Schafer M (2007) Laparoscopic partial splenectomy. J Am Coll Surg 204:179–181
14. Uranues S, Grossman D, Ludwig L, Bergamaschi R (2007) Laparoscopic partial splenectomy. Surg Endosc 21:57–60
15. Rescorla FJ, West KW, Engum SA, Grosfeld JL (2007) Laparoscopic splenic procedures in children: experience in 231 children. Ann Surg 246:683–687
16. Dutta S, Price VE, Blanchette V, Langer JC (2006) A laparoscopic approach to partial splenectomy for children with hereditary spherocytosis. Surg Endosc 20:1719–1724

Transperitoneal Adrenalectomy

21

Giuseppe Spinoglio, Alessandra Marano, Ferruccio Ravazzoni, Francesca Pagliardi, and Giampaolo Formisano

21.1 Procedure Overview

Laparoscopic transperitoneal adrenalectomy was first reported in 1992 by Gagner et al. [1]. During the last decade, it has largely replaced the open approach as the standard of care for adrenal gland removal, especially for benign tumors, given the well-known advantages of minimally invasive surgery. Nevertheless, laparoscopy is recognized as associated with a steep learning curve and has some technical constraints. Robotic surgery can potentially provide a solution to these drawbacks.

In 1999, Piazza et al. [2] described the first robotic adrenalectomy case series using the AESOP 2000, which was the commercially available robotic platform in Europe at that time. With the introduction of the da Vinci® system (Intuitive Surgical, Sunnyvale, CA, USA), different series of robotic adrenalectomy have been reported [3–13], showing the safety and feasibility of the procedure as well as potential advantages over laparoscopy because of its unique technological features. The first report of robotic transperitoneal adrenalectomy with the da Vinci® system dates back to the 2001 [14].

In 1996, Walz et al. [15] first described a posterior retroperitoneoscopic approach for adrenal masses: though comparative studies of transperitoneal and retroperitoneal laparoscopic adrenalectomy demonstrate heterogeneous results, retroperitoneal techniques may offer less postoperative pain, faster recovery and an easier bleeding control by simply increasing the CO_2 pressure up to 28 mmHg in a confined space. Disadvantages include the smaller working space, and the requirement for the surgeon to learn a new "reverse angle"

G. Spinoglio (✉)
Department of General and Oncologic Surgery, "Ss. Antonio e Biagio" Hospital, Alessandria, Italy
e-mail: giuseppe.spinoglio@gmail.com

G. Spinoglio (Ed), *Robotic Surgery: Current Applications and New Trends*, Updates in Surgery
DOI: 10.1007/978-88-470-5714-2_21, © Springer-Verlag Italia 2015

anatomic perspective. In 2010, the robotic posterior approach was also reported by Berber et al. [16].

In this chapter, we will focus on the robotic lateral transperitoneal approach for adrenal gland tumors.

21.2 Patient and Robot Positioning

After administration of general anesthesia, the patient is placed in a lateral right or left decubitus position, according to the side of the tumor, with legs closed.

Arms are secured with belts and appropriate supports to avoid injuries. The operating table is then flexed, lowering the legs and the thorax, with the umbilicus above the pivoting point of the table. A mild reverse-Trendelenburg tilt is applied to improve exposure of the operative field.

The robot is brought to the table from the shoulder with a 45° angle and is docked (Fig. 21.1).

21.3 Trocar Placement

For left adrenalectomy, five trocars are placed after induction of 12 mmHg pneumoperitoneum by the Veress needle in the left subcostal space. A 12-mm camera port is introduced in the middle point between the left costal margin and the umbilicus. A 30° downscope is used.

Under direct visualization, trocars are inserted as follows (Fig. 21.2):

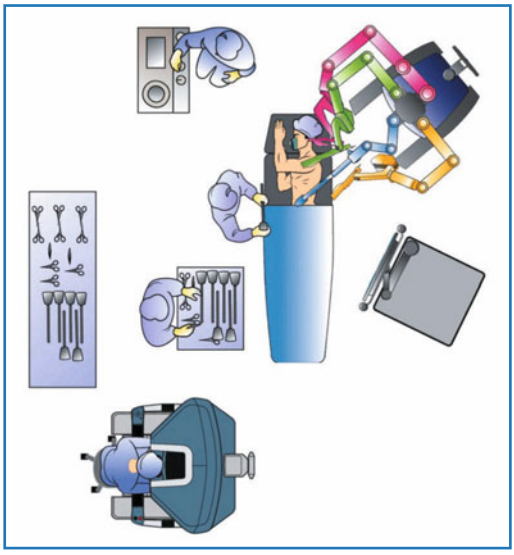

Fig. 21.1 OR setup for left adrenalectomy. For right adrenalectomy the cart is brought to the table from the opposite side. (© 2014 Intuitive Surgical, Inc.)

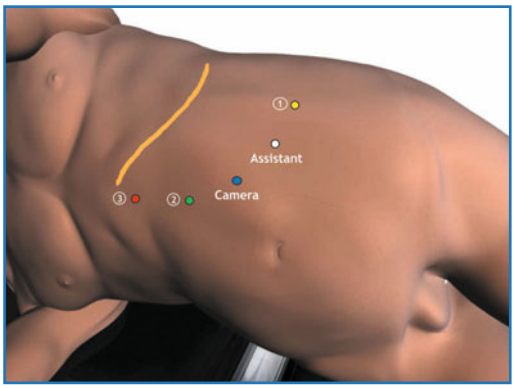

Fig. 21.2 Trocar layout for left adrenalectomy. (© 2014 Intuitive Surgical, Inc.)

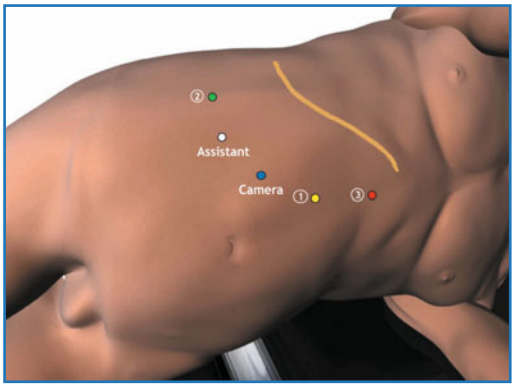

Fig. 21.3 Trocar layout for right adrenalectomy. (© 2014 Intuitive Surgical, Inc.)

- One 8-mm robotic trocar (R1) is placed in the left flank for Hot Shears™ (monopolar curved scissors), cautery hook or robotic clip applier. We do not routinely use an ultrasonic scalpel;
- One 8-mm robotic trocar (R2) is placed in the epigastric area, 2–3 cm left paramedian, for bipolar forceps;
- One 8-mm robotic trocar (R3) is placed cranially to R2, a few centimeters below the xyphoid process, for the ProGrasp™ forceps or Cadiere forceps; they are used for traction on the adrenal gland or on the splenic parenchyma along with the pancreatic tail;
- One 12-mm assistant's trocar is placed between R1 and the camera ports for suction/irrigation, clip application (if necessary) or other maneuvers to achieve optimal exposure of the adrenal gland.

Trocars are placed in a mirror image for right-sided adrenal masses, with R1 in the epigastric area and R2 in the right flank (Fig. 21.3).

We perform a totally robotic approach, though a hybrid technique with laparoscopic mobilization of the liver or of the splenopancreatic block has been described.

21.4 Step-by-Step Review of Critical Elements of the Procedure

21.4.1 Right Adrenalectomy

It is not necessary to divide the triangular and coronary ligaments with the robotic approach, whilst this maneuver is required in laparoscopic surgery. The liver is retracted upward with the fenestrated grasper in R3 and the inferior caval vein (ICV) is identified.

The peritoneum and the Gerota's fascia are opened along the right border of the ICV; the dissection is continued upward along the inferior surface of the liver and then counterclockwise to gain access to the right margin of the superior renal pole. Once the peritoneum has been incised, the liver can be further mobilized and pulled cranially with the grasp in R3 without any risk of capsular tears because of the stable and constant traction exerted by the robotic instruments.

The inferior part of the right border of the caval vein and the superior aspect of the right renal vein are fully exposed to gain access to the posterior muscular plane. We separate the adipose capsule from the posterior abdominal wall opening a wide dihedral angle that represents our first working space and allows the control of the right middle adrenal vein more easily and safely, as a result of an anterior and posterior access. If present, upper polar renal arteries must be identified and preserved. Attention should be paid to a small accessory hepatic vein (Fig. 21.4).The middle adrenal vein is dissected and clipped with laparoscopic or robotic nonabsorbable self-locking clips (Hem-o-lok®, Weck-Teleflex Europe Ltd.) and divided (Fig. 21.5). This maneuver is a crucial step of the operation, especially in the case of a large and short adrenal vein: the robotic clip applier should be used in these situations because of the advantages offered by the EndoWrist® technology.

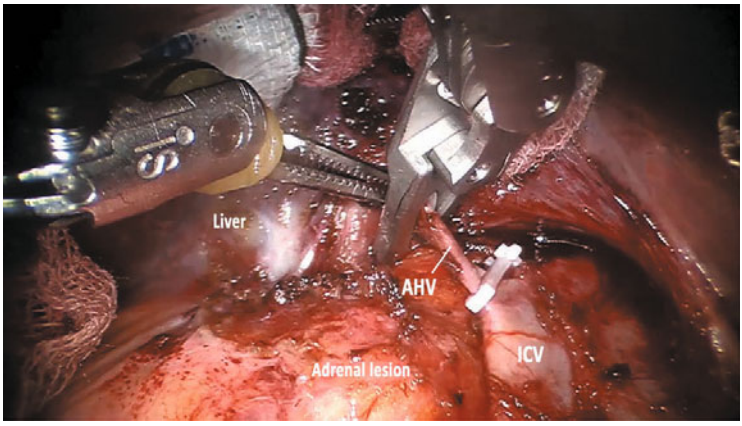

Fig. 21.4 An accessory hepatic vein (*AHV*), crossing the upper pole of the adrenal gland is clipped and divided. *ICV*, inferior caval vein

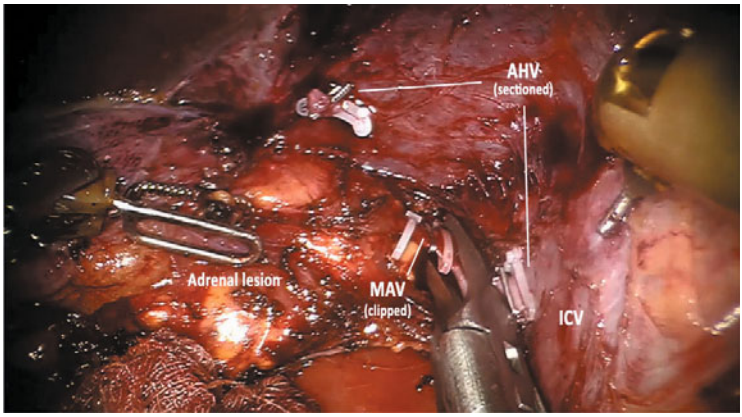

Fig. 21.5 Medial dissection during right adrenalectomy. *MAV*, middle adrenal vein; *ICV*, inferior caval vein; *AHV*, accessory hepatic vein

Other small venous or arterial branches are usually controlled with bipolar energy and are divided. The adrenal gland is dissected completely free along with the surrounding epinephric fat, with complete respect for oncological principles.

The robot is undocked and the lesion is removed in a specimen retrieval bag by slightly enlarging a trocar site. A suprapubic minilaparotomy can be performed in the case of larger masses.

21.4.2 Left Adrenalectomy

The Toldt's white line is incised starting from the proximal descending colon in a caudal-to-cephalad direction, thus gaining access to the avascular plane and exposing the lateral aspect of the Gerota's fascia. The peritoneum is incised up to the greater curvature of the stomach behind the spleen by the division of the splenophrenic ligament; the dissection is carried out progressively upward and the splenopancreatic block, together with the splenic flexure, is fully mobilized and can be retracted medially to expose the adrenal gland.

The Gerota's fascia is then incised along the medial aspect of the adrenal gland thus entering into the epinephric fat. The left renal vein is identified as a landmark for medial dissection and isolation of the middle adrenal vein, paying great attention not to damage the spermatic vessels, as well as the underlying renal artery. If present, upper polar renal arteries must be identified and preserved. The middle adrenal vein is dissected free and clipped with laparoscopic or robotic nonabsorbable self-locking clips (Hem-o-lok®, Weck-Teleflex Europe Ltd.) and divided. A small superior adrenal artery, arising from the inferior phrenic artery, may be found; it can be controlled with bipolar energy or clips. Once the specimen is completely freed, the procedure continues as already described.

21.5 Advantages, Limitations and Relative Contraindications (Personal Experience and Literature Outcomes)

To date, there is not indisputable proof that robotic adrenalectomy is superior to laparoscopic adrenalectomy, both with the transabdominal and posterior retroperitoneal approach. Although there are several case reports describing the laparoscopic techniques, robotic adrenalectomy is, to date, the subject of a still limited number of studies in the literature.

The only available randomized prospective trial comparing laparoscopic approach to the robotic counterpart was reported by Morino et al. [12] in 2004. There were 20 patients randomized to either the laparoscopic or robotic approach. The operative time was longer in the robotic group (169 vs. 115 min) and conversion to laparoscopy was required in 40% of patients in the robotic group. The morbidity rate (20% vs. 0%) and the costs ($3.467 vs. $2,737) were significantly higher in the robotic series. The authors concluded that laparoscopic adrenalectomy was superior to robotic adrenalectomy in terms of feasibility, morbidity and costs. However, this study has a small patient sample and neither the power of the study nor the randomization method are described in detail. Additionally, the procedures were conducted at the beginning of the learning curve with the old three-arm da Vinci® System: an updated high-quality evaluation should be considered.

In a prospective study of 100 patients who underwent robotic transperitoneal unilateral adrenalectomy, Brunaud et al. [8] achieved no mortality and a 10% morbidity rate. Their conversion rates were 4% to laparoscopy and 1% to open surgery. The mean operative time was 99 min, which decreased by 1 min for every 10 cases: surgeon's experience, first assistant's level, and tumor size were found to be independent predictors of operative time. The cost of the robotic procedure was 2.3 times more than the lateral transperitoneal laparoscopic adrenalectomy (€4,102 vs. €1,799). Despite its costs, Brunaud et al. and associates suggested that the robotic procedure was preferable owing to better vision quality and surgeon comfort.

Adrenalectomy in obese patients may be challenging due to the difficult exposure. However, though Brunaud et al. [17] and Giulianotti et al. [10] have shown that the robotic approach may be a valid option for patients with a BMI of 30 kg/m^2, results from Aksoy et al. [5] have suggested that the robotic approach does not provide significant benefits because of the difficulties in maintaining adequate exposure and dissection. Postoperative outcomes and operative times were similar between the laparoscopic and the robotic group.

Karabulut et al. [18] have recently published their comparative study of robotic vs laparoscopic adrenalectomy, both with transperitoneal and posterior approach. Operative time was comparable between the two groups with both the transperitoneal and posterior approach. However, the robotic procedures were more favorable because of a lower morbidity and shorter hospital stay over the laparoscopic counterpart. Once experience has been gained, robotic posterior adrenalectomy could shorten the operative time compared to the laparoscopic posterior approach.

The same group compared the robotic vs. standard laparoscopic technique in the surgical treatment of large adrenal tumors >5 cm [3]. The operative time and conversion rate were lower in the robotic group (159 min vs. 187 min, and 4% vs. 11%, respectively). Additionally, the length of hospital stay was shorter in the robotic vs. laparoscopic group (1.4 vs. 1.9 days). These results suggest that the robotic platform could potentially facilitate the resection of large adrenal tumors.

An additional benefit of the robotic approach may be glimpsed in partial adrenalectomy for patients requiring bilateral adrenalectomy and therefore lifelong steroid supplementation. Few cases, however, have been reported in the literature [19–21].

Recently, a metanalysis has been published by Brandao et al. [22] to critically analyze the available evidence of studies comparing laparoscopic and robotic adrenalectomy. Studies with both the transperitoneal and posterior approach have been included. Authors showed that the robot-assisted adrenalectomy can be performed safely and effectively with operative times and complication rates similar to laparoscopic adrenalectomy and it can provide the potential advantage of a shorter hospital stay and less blood loss.

To date, we have performed 14 robotic adrenalectomy (unpublished data), mainly for right-sided adrenal tumors (12 out of 14). The indications for surgery were five nonfunctional adenomas, four pheochromocytomas, three metastasis and two Cushing syndromes. Mean BMI was 25 kg/m^2. The mean tumor size was 5.2 cm and the mean operative time was 180 min. Neither intraoperative nor early postoperative complications were recorded, and there were no conversions to laparoscopic or open surgery.

Our experience, even though limited, confirms the feasibility and safety of robotic adrenalectomy with the transperitoneal approach. The technological properties of the da Vinci® system strongly improve the dissection during adrenal surgery, especially in the case of large right-sided tumors (>6 cm) posterior to the caval vein. The stable platform and the EndoWrist™ technology also enables the surgeon to safely control and divide large and short right adrenal veins at the caval confluence.

Future studies involving larger case series and randomized trials with adequate power will determine the exact role of robotics in adrenal surgery with both the anterior and posterior approach. Moreover, the experience with minimally invasive surgery is limited and therefore controversial in the case of malignant lesions.

References

1. Gagner M, Lacroix A, Bolte E (1992) Laparoscopic adrenalectomy in Cushing's syndrome and pheochromocytoma. N Engl J Med 327:1033
2. Piazza L, Caragliano P, Scardilli M et al (1999) Laparoscopic robot-assisted right adrenalectomy and left ovariectomy (case reports). Chirurgia Italiana 51:465–466

3. Agcaoglu O, Aliyev S, Karabulut K et al (2012) Robotic versus laparoscopic resection of large adrenal tumors. Ann Surg Oncol 19:2288–2294
4. Agcaoglu O, Aliyev S, Karabulut K et al (2012) Robotic vs. laparoscopic posterior retroperitoneal adrenalectomy. Arch Surg 147:272–275
5. Aksoy E, Taskin HE, Aliyev S et al (2013) Robotic versus laparoscopic adrenalectomy in obese patients. Surg Endosc 27:1233–1236
6. Aliyev S, Karabulut K, Agcaoglu O et al (2013) Robotic versus laparoscopic adrenalectomy for pheochromocytoma. Ann Surg Oncol 20:4190–4194
7. Brandao LF, Autorino R, Zargar H et al (2014) Robot-assisted laparoscopic adrenalectomy: step-by-step technique and comparative outcomes. Eur Urol. doi: 10.1016/j.eururo.2014.04.003
8. Brunaud L, Ayav A, Zarnegar R et al (2008) Prospective evaluation of 100 robotic-assisted unilateral adrenalectomies. Surgery 144:995–1001
9. D'Annibale A, Lucandri G, Monsellato I et al (2012) Robotic adrenalectomy: technical aspects, early results and learning curve. Int J Med Robot Comput Assist Surg 8:483–490
10. Giulianotti PC, Buchs NC, Addeo P et al (2011) Robot-assisted adrenalectomy: a technical option for the surgeon? Int J Med Robot Comput Assist Surg 7:27–32
11. Ludwig AT, Wagner KR, Lowry PS (2010) Robot-assisted posterior retroperitoneoscopic adrenalectomy. J Endourol 24:1307–1314
12. Morino M, Beninca G, Giraudo G et al (2004) Robot-assisted vs. laparoscopic adrenalectomy: a prospective randomized controlled trial. Surg Endosc 18:1742–1746
13. Pineda-Solis K, Medina-Franco H, Heslin MJ (2013) Robotic versus laparoscopic adrenalectomy: a comparative study in a high-volume center. Surg Endosc 27:599–602
14. Horgan S, Vanuno D (2001) Robots in laparoscopic surgery. J Laparoendosc Adv Surg Tech A 11:415–519
15. Walz MK, Peitgen K, Hoermann R et al (1996) Posterior retroperitoneoscopy as a new minimally invasive approach for adrenalectomy: results of 30 adrenalectomies in 27 patients. World J Surg 20:769–774
16. Berber E, Mitchell J, Milas M, Siperstein A (2010) Robotic posterior retroperitoneal adrenalectomy: operative technique. Arch Surg 145:781–784
17. Brunaud L, Bresler L, Ayav A et al (2008) Robotic-assisted adrenalectomy: what advantages compared to lateral transperitoneal laparoscopic adrenalectomy? Am J Surg 195:433–438
18. Karabulut K, Agcaoglu O, Aliyev S (2012) Comparison of intraoperative time use and perioperative outcomes for robotic versus laparoscopic adrenalectomy. Surgery 151:537–542
19. Asher KP, Gupta GN, Boris RS et al (2011) Robot-assisted laparoscopic partial adrenalectomy for pheochromocytoma: the National Cancer Institute technique. Eur Urol 60:118–124
20. Boris RS, Gupta G, Linehan WM et al (2011) Robot-assisted laparoscopic partial adrenalectomy: initial experience. Urology 77:775–780
21. St Julien J, Ball D, Schulick R (2006) Robot-assisted cortical-sparing adrenalectomy in a patient with Von Hippel-Lindau disease and bilateral pheochromocytomas separated by 9 years. J Laparoendosc Adv Surg Tech A 16:473–477
22. Brandao LF, Autorino R, Laydner H et al (2014) Robotic versus laparoscopic adrenalectomy: a systematic review and meta-analysis. Eur Urol 65:1154–1161

Robotic-assisted Organ Transplantation

22

Raquel Garcia-Roca, Ivo Tzvetanov, Hoonbaen Jeon, Jose Oberholzer, and Enrico Benedetti

22.1 Introduction

The da Vinci® Robotic Surgical System (Intuitive Surgical, Sunnyvale, CA) is the only robotic system approved by the Food and Drugs Administration (FDA) for use in humans. It offers several advantages over laparoscopic surgery, such as: efficient microsuturing through the ports, three-dimensional high-definition view, and wristed instruments with seven degrees of freedom. However, the greatest limitations of the current robotic system are high cost and lack of haptic feedback.

The da Vinci® surgical system has enabled surgeons to complete complex major surgical procedures in a minimally invasive fashion expanding into those fields of surgery that were never considered before. Robotic surgery has been successfully used in kidney transplantation [1, 2], and in a lesser proportion in pancreas transplantation [3] and donor hepatectomy for living donor liver transplantation [4].

22.2 Living Donor Robotic-assisted Nephrectomy

Living donation is an elective procedure compared to deceased donation. This offers the advantage of having kidney grafts of excellent quality and the option to perform the procedure when the recipient is in optimal condition. In addition, wait time until transplantation and dialysis duration can be minimized. The main obstacle for living donation is the exposure of a healthy individual to the

R. Garcia-Roca (✉)
Department of Surgery, Division of Transplantation, University of Illinois Hospital and Health Sciences System, Chicago, IL, USA
e-mail: garciarr@uic.edu

G. Spinoglio (Ed), *Robotic Surgery: Current Applications and New Trends*, Updates in Surgery
DOI: 10.1007/978-88-470-5714-2_22, © Springer-Verlag Italia 2015

inherent risk of a surgical intervention without a direct health benefit. The availability of a minimally invasive, laparoscopic surgical technique greatly enhanced living donation rates by reducing postoperative pain, achieving faster recovery and minimizing the surgical incisions. The da Vinci® Surgical System has been used in living donor nephrectomy as a logical extension of the widely adapted laparoscopic approach. To date there are no randomized trials comparing robotic versus laparoscopic donor nephrectomy. Intuitively, with the expanded range of movements, it simplifies complicated procedures in the presence of multiple renal arteries or other vascular anomalies. The first worldwide transabdominal hand-assisted robotic donor nephrectomy was performed successfully at the University of Illinois at Chicago Hospital in 2000 [5]. Since then, our institution has performed over 800 robotic donor nephrectomies with excellent outcomes.

Potential donors are evaluated by a multidisciplinary transplant team, which includes a surgeon, pharmacist, social worker, nutritionist, financial counselor and nurse coordinator. The medical screening involves assessment of immunologic compatibility, the renal function and the current medical status of the patient to exclude conditions that can be transmitted to the recipient or jeopardize the donor health. The decision regarding which kidney to be harvested is based on the function and anatomy of the kidneys determined by a 3D reconstruction from an abdominal CT scan with arterial contrast. Usually the left kidney is procured, due to its favorable anatomy (longer left renal vein) and the lower complexity of the left nephrectomy, even in the presence of multiple arteries on that side.

22.2.1 Step-by-Step Review of Surgical Procedure

For a left nephrectomy, the patient is rolled into the right lateral decubitus position with a cushioned beanbag and axillary roll, and the table is flexed. The patient should be secured to the operative table, because any instability after docking the robotic system could jeopardize the safety. The table should be in the Trendelenburg position to avoid injury of the arm and shoulder from the left robotic arm (Fig. 22.1a).

22.2.1.1 Step 1 - Incision and Trocar Placement

Robotic-assisted donor nephrectomy is a transabdominal procedure through four laparoscopic-robotic ports. Additionally, a 7-cm access incision, longitudinal or transverse, is required in the lower abdomen for extraction of the kidney. In our practice the assistant's hand, previously wrapped with protective, sterile Ioband™ (3M, USA) around the wrist and forearm is inserted directly through the incision. This maneuver does not interfere with the maintenance of pneumoperitoneum and, according to our observation, significantly decreases the incidence of wound infections.

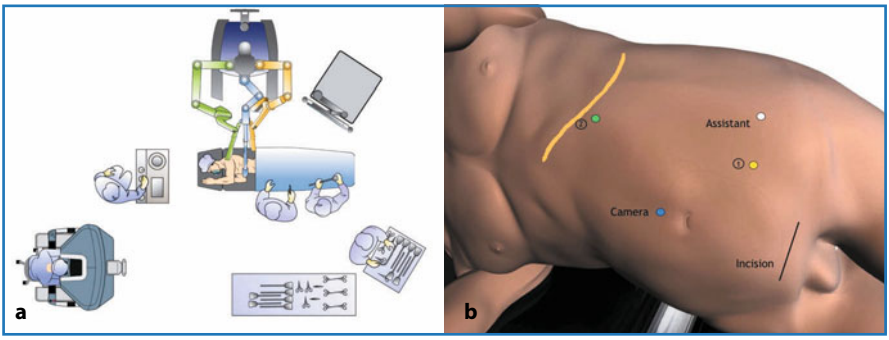

Fig. 22.1 Living donor nephrectomy. **a** OR setup. **b** Trocar placement. (© 2014 Intuitive Surgical, Inc.)

The kidney to be harvested is palpated to identify the position of the hilum. Under hand control from inside the abdomen, a 12-mm laparoscopic port is placed above the umbilicus, close to the midline, at the level of the renal hilum. This port is required for the 30° robotic camera system. To achieve good triangulations, the two 8-mm robotic working ports are placed along the left mid clavicular line. They are located proximal and distal, 10 to 12 cm apart from camera port. Last, 12-mm port is placed in left lower quadrant to assist with suction, clipping, stapling, and cutting (Fig. 22.1b). The robotic system is docked and integrated to the ports and pneumoperitoneum is achieved. To obtain additional working space, the robotic arms are used to give additional lift on the ports.

22.2.1.2 Step 2 - Exposure of the Retroperitoneum and Identification of the Ureter

The assisting surgeon medially retracts the descending colon; the lateral peritoneal attachments are divided with cautery, exposing the left paracolic gutter and fully mobilizing the sigmoid colon. The splenocolic ligament is transected and the anterior surface of the left kidney is exposed following the plane between the mesentery of the left colon and the Gerota's fascia. Dissection in this plane permits a bloodless exposure even in cases with significant intraabdominal adiposity.

In the lower quadrant, the assisting surgeon retracts the mobilized left colon medially; the ureter is circumferentially dissected and mobilized distally to the point where it crosses the iliac vessels. Minimal dissection is advised to preserve its blood supply. A short Penrose drain is secured with laparoscopic Hem-o-lok® around the ureter allowing atraumatic retraction by the assisting surgeon. With lateral light retraction of the ureter, the posterior and inferior aspects of the kidney are mobilized.

22.2.1.3 Step 3 - Identification of Renal Hilum

The gonadal vein is identified medial to the ureter and dissected toward its junction with the left renal vein where it is transected between two robotic Hem-o-

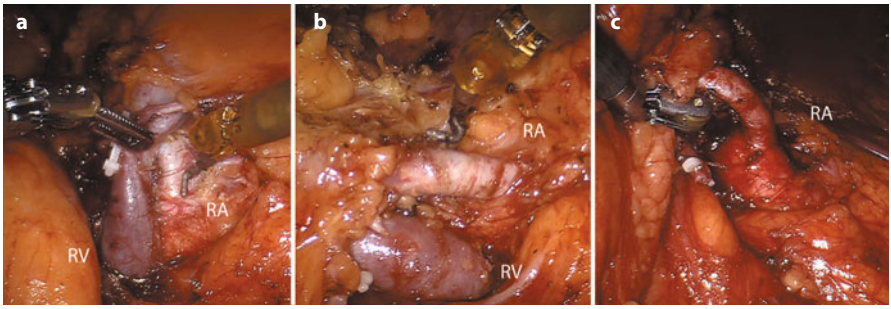

Fig. 22.2 **a** Anterior dissection of the artery. **b** Posterior exposure of the artery and transection of lymphatic tissue. **c** The left robotic arm gently retracts the artery to facilitate introduction of the stapling device. *RV*, renal vein; *RA*, renal artery

lok® clips. Along the upper border of the renal vein, the left adrenal vein is also dissected and transected between robotic clips. In most of the cases at least one lumbar vein will be joining the left renal vein and should be similarly transected. In these cases the articulating skills of the robotic system and the 3D vision give significant advantage over conventional laparoscopic instruments.

In the dissection plane between the upper pole of the kidney and the adrenal gland lies the adrenal artery, which originates from the left renal artery and should be divided between clips whenever present. The upper pole of the kidney is then fully mobilized close to the renal capsule, leaving behind Gerota's fascia and fat. With the kidney in the anatomical position, the artery can be found just behind the renal vein, the lymphatic tissue surrounding the artery is transected with the hook forceps.

The previously mobilized ureter is clipped with two robotic Hem-o-lok® clips at the pelvic rim and sharply transected proximal to them. The posterior attachments of the kidney are divided with the help of the assisting surgeon, exposing the renal hilum posteriorly. At this point the orientation of the kidney should be maintained anatomical avoiding twisting of the vessels. This could potentially result in ischemia of the kidney, or worse, intimal dissection of the renal artery. Additionally, the robotic surgeon may injure the renal artery if the anatomy is distorted due to torsion. With the kidney in the medial position, the ganglionic and lymphatic tissue surrounding the renal artery needs to be transected. The vessel needs to be circumferentially dissected at the level of its origin from the aorta (Fig. 22.2). If multiple arteries are present, every vessel has to be dissected free as described. If a lower polar artery, originating from distal abdominal aorta, is present, this vessel needs to be identified and exposed carefully, because its unintentional injury would deprive the ureter from blood supply.

22.2.1.4 Step 4 - Vascular Exclusion and Kidney Graft Extraction

As the kidney is now completely dissected, the surgeon at the console is prepared with a robotic clip on the right arm. The assistant surgeon maintains the mobilization of the kidney medially, exposing the renal artery posteriorly.

Intravenous heparin (5000 IU) is administered to avoid parenchymal thrombosis after arterial occlusion. The second assistant surgeon advances the Endo TA™ stapler, with vascular load, through the 12-mm left lower quadrant port and the renal artery is stapled on its origin from the aorta. Utilization of a Endo TA™ stapler allows the additional length of the artery to facilitate the implantation of the graft. After checking the proper deployment of the stapling line, the robotic clip is placed to enhance hemostasis. The artery is sharply divided with robotic scissors at least 3–4 mm distal from the stapler line. If multiple arteries are present, they are sequentially stapled and transected in a similar fashion.

The kidney is now placed in an anatomical position and the renal vein exposed. The operating surgeon exercises gentle lift and traction to the hilum, thus straightening the vein. The vessel is divided with an Endo-GIA™ vascular stapler, inserted by the second assist surgeon through the left lower quadrant assisting port. Care should be taken not to engage previously placed plastic clips into the stapler line.

The kidney graft is rapidly removed from the abdominal cavity and placed in a container with cold solution with the temperature below 4° C, the staple line in the renal vein is transected and the kidney is flushed with cold preservation solution through the renal artery.

The abdominal cavity is inspected for bleeding. The arterial and venous stumps are visualized, and the condition of the stapler line is verified. The field should be cautiously examined for the presence of lymphatic leak, which, if present, can be controlled with suture ligation. The robotic system is disengaged and the ports removed. Closure of the 12-mm port sides is not mandatory, but is recommended. The 7-cm assist incision is closed in layers anatomically. Skin incisions are closed cosmetically.

22.2.1.5 Special Considerations

Right donor nephrectomy: The anatomical features of the right kidney make it less preferred for harvesting, mostly because the shorter length and greater fragility of the right renal vein. The right renal artery is commonly found directly posterior to the short right renal vein, requiring increased intraoperative manipulation raising the potential for vasospasm and iatrogenic vascular injury. The main indication for harvesting the right kidney is the presence of anatomical defects compatible with transplantation in the right kidney or significant difference in function between both kidneys. For robotic-assisted right donor nephrectomy the patient is placed in a left decubitus position and the robotic tower docks from the right side of the patient. The 7-cm incision is performed in the same way, while the port sites are placed in mirror image locations. Occasionally, one additional port is placed in the left upper quadrant for liver retraction. After medial mobilization of the right colon, the ureter is identified and the IVC is exposed. Following the gonadal vein the dissection continues superiorly to the renal vein. Additional Kocher maneuver may be necessary to fully expose the IVC. The right renal vein is identified and circumferentially dis-

sected free. The renal artery is localized after posterior mobilization and medial retraction of the kidney. The right renal artery may bifurcate behind the vena cava; ligation of lumbar veins may become necessary to medially rotate the IVC adequately exposing the renal artery. The rest of the procedure follows the same steps as described for left nephrectomy.

Multiple vessels: The transplant team at our institution prefers to remove the left kidney even in the presence of multiple arteries. In the hands of experienced surgeons, reconstruction of multiple vessels has similar outcomes in terms of graft function and risk of graft loss [6]. The surgeon needs to evaluate the 3D reconstructions of the computerized tomography to visualize the relationship between the arteries and renal vein. Lower polar arteries should be preserved in every case, as they are the sole blood supply of the ureter. Upper polar arteries may be sacrificed if they are small and do not feed to a large portion of the renal parenchyma. This can only be assessed once the kidney is removed and flushed in the back table through the main renal artery, as it will demarcate the area dependent on the upper polar artery better. Vascular reconstruction is necessary if the area is significant.

Arteries need to be fully dissected individually; this is better done from the posterior aspect of the kidney. The arterial occlusion is performed in a similar fashion as when there is a single artery, they are sequentially clipped and transected from the lower polar to the upper one.

Retroaortic and circumaortic renal vein: The reported incidence of circumaortic and retroaortic left renal vein is 9 to 14%, this common variant has been considered a relative contraindication for left donor nephrectomy due to the potential for inadvertent venous injury. Evaluation of the renal anatomy preoperatively via computerized tomography and 3D reconstructions provides superior details of the renal vascular anatomy including the location, size and spatial interrelationship of the renal, adrenal, gonadal, and lumbar veins.

Left donor nephrectomy was efficaciously performed in the presence of left renal venous anomaly, with surgical outcomes comparable to patients with a normal left renal vein. Importantly, the warm ischemia time and harvested length of the left renal artery and vein were similar [7]. The two components of the circumaortic renal vein are meticulously dissected. In most situations, the posterior component of the circumaortic renal vein can be safely ligated, similar to a larger lumbar vein.

In the presence of a retroaortic renal vein, the aorta limits the posterior dissection and the vein will be significantly shortened. This should not compromise the transplant procedure and in our experience, it has never required backbench repair or extension patch prior to implantation.

22.3 Robotic Kidney Transplantation

We consider the robotic-assisted surgical approach to be applicable to all medically suitable patients with a body mass index (BMI) >30 kg/m^2. In the United

States, obesity is a common comorbidity among waitlisted patients, causing increased waiting times for kidney transplantation compared to nonobese candidates. Presumably, due to more technically demanding case and increased surgical complication rates compromising graft outcomes.

Recent studies suggest that a BMI >30 kg/m^2 is an independent risk factor for surgical site infection (SSI), which is directly correlated to decreased graft survival [8]. However, obese recipients who avoid SSI have similar outcomes to nonobese recipients [9], thus, we draw the conclusion that in order to obtain similar outcomes in obese recipients, we need to devise a technique that minimizes incision to dramatically reduce the risk of infection.

The experience acquired using the robotic system for different procedures was essential in the development of the robotic-assisted kidney transplant procedure. One of the goals with this new surgical approach was to offer a similar opportunity to obese patients with end-stage renal disease to access kidney transplantation as leaner patients at similar complication risk, by reducing SSI risk and in turn, optimizing graft outcomes. Robotic kidney transplantation uses a 7-cm incision located in the upper abdomen in addition to the access robotic-laparoscopic ports. The location of the incision in the epigastric area is more favorable, as the thickness of the subcutaneous tissue is lower and the length of the incision is significantly reduced. In addition, the epigastrium is generally more visible to patients and less likely to remain moist due to sweat. These are contributing factors to a lower infection rate in this location.

Over the last four years at the University of Illinois at Chicago Hospital, we performed over 80 kidney transplants on obese recipients using the da Vinci® robotic surgical system. Initial results showed the advantages and feasibility of the robotic-assisted procedure [10].

22.3.1 Step-by-Step Review of the Surgical Technique

22.3.1.1 Step 1 - Graft Preparation

Backbench preparation for robotic implantation has some specific steps, regardless of the kidney graft originating from a living or deceased donor. The purpose is to facilitate orientation of the organ and minimize bleeding after the implantation. The adipose capsule is meticulously ligated with 3-0 silk during excision. The renal vein and artery are dissected toward the hilum and marked for orientation, depending on the site of implantation, right or left. Lastly, the ureter is appropriately shortened, vessels ligated and the end is spatulated.

22.3.1.2 Step 2 - Patient Positioning and Trocar Placement

The patient will be in the Trendelenburg position during most of the surgical procedure; to assure safety, they should be secured by using shoulder block and tape over the hips to avoid sliding of the patient during the operation. In larger patients, we have been using a beanbag to add additional support, as they might

be wider than the operating table. After proper preparation and draping, a 7-cm midline incision approximately 5 cm below the xyphoid process is made for the placement of the hand access device.

Port placement can be done under direct laparoscopic visualization through a 5-mm port inserted through the epigastric incision. The position of the laparoscopic ports are as follows:

- A 12-mm long laparoscopic port for the 30° robotic scope is inserted just above the umbilicus;
- Two 7-mm robotic ports are inserted triangulating to the target vessels in the pelvis, one is placed in the right flank and the other in the left lower quadrant (or mirror image in the case of left implantation);
- Another 12-mm assistant laparoscopic long port is placed to the left of the camera one (Fig. 22.3a).

The patient is placed in a 45° Trendelenburg position and the table is rotated to the left (for implantation to the right external iliac vessels). This positioning uses gravity to retract the bowels away from the surgical field. The robot system is docked into position parallel to the patient's right leg and slightly diagonal to the body (Fig. 22.3b).

22.3.1.3 Step 3 - Vascular Exposure

The right colon is mobilized medially exposing the right external iliac vessels and ureter. The iliac vessels are dissected free and lymphatic tissue is excised. In order to facilitate the exposure and the dissection around the external iliac vein, the vessel loop is used to retract the artery upward and it may be fixed to the abdominal wall with a Hem-o-lok® clip, maintaining exposure during vascular anastomosis. Another vessel loop is placed around the iliac vein to allow the dissection on the posterior surface of the vein; the loop serves as a handle for retraction (Fig. 22.4). Any collateral vessels found during the dissection will need to be suture ligated with Prolene 5-0 and transected.

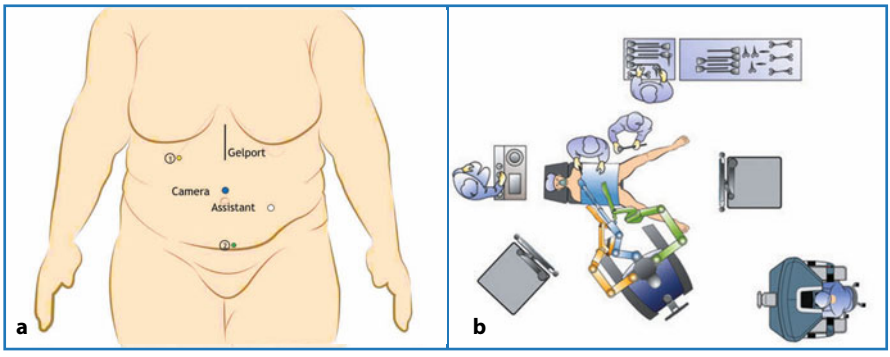

Fig. 22.3 Kidney transplantation in obese patients. **a** Trocar placement. **b** OR setup. (© 2014 Intuitive Surgical. Inc.)

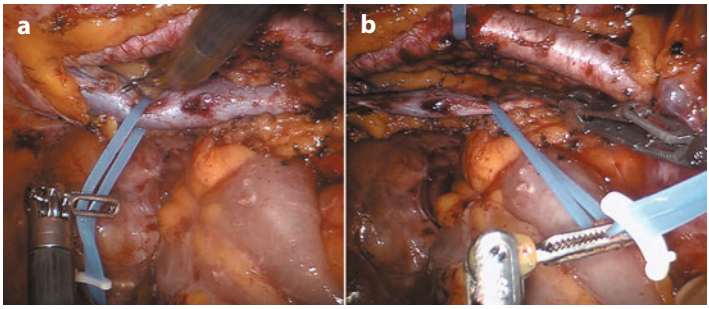

Fig. 22.4 Dissection of the iliac vein: (**a**) using vessel loop for retraction; (**b**) application of robotic vascular clamps on the iliac vein

22.3.1.4 Step 4 - Graft Implantation and Reperfusion

Once the external iliac vessels are dissected completely free, two robotic bulldog clamps are used to clamp the external iliac vein. Robotic Potts scissors are used to create a venotomy to about 15-mm in length. For the vascular anastomosis we use a double needle Gore-Tex 5-0 suture, this needs to be prepared beforehand, measure length at twelve centimeters and knotted in the middle leaving each needle at equal length. Kidney graft is inserted in the abdominal cavity by the assisting surgeon making sure the ureters is positioned toward the pelvis and the vessels facing those of the recipient, the vascular markings prepared earlier will now be useful to find the proper orientation. Veno-venous anastomosis is completed in an end-to-side fashion with running sutures (Fig. 22.5). If needed, interrupted stitches of 5-0 Prolene are used to reinforce the anastomosis.

The external iliac artery is then clamped between double robotic bulldogs and an oval-shaped window is made in the anterior wall of the artery using robotic scissors. The arterial anastomosis is completed in an end-to-side fashion with 12-cm double needle 6-0 Gore-Tex suture with a knot in the middle prepared similar to the one used for the venous anastomosis (Fig. 22.6).

Once the reconstruction is completed venous clamps are removed first, followed by immediate removal of the arterial clamps. The reperfusion of the organ and hemostasis are additionally verified and bleeding points secured with 6-0 Prolene suture. At this point the pressure of the pneumoperitoneum is decreased to minimize possible negative effect of high intraabdominal pressure on the graft perfusion.

22.3.1.5 Step 5 - Neocystoureterostomy

The bladder is distended with diluted methylene blue solution in order to facilitate its identification; this can be possible by infusion on the third port of the Foley catheter. The ureter is anastomosed to the bladder mucosa with running 5-0 Monocryl sutures, and the bladder muscular layer is approximated with interrupted 3-0 Vicryl sutures to create an antireflux mechanism. Utilization of a ureteral stent is optional.

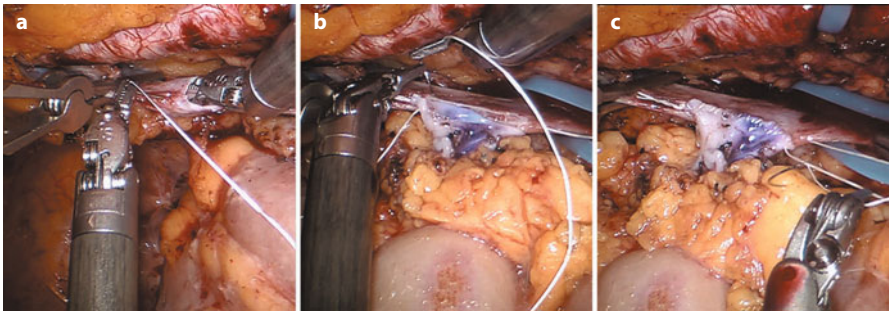

Fig. 22.5 **a** Placing corner stitch, 5-0 Gore-Tex 12-cm double needle tied ends. **b** Posterior wall running suture. **c** Completion of anastomosis

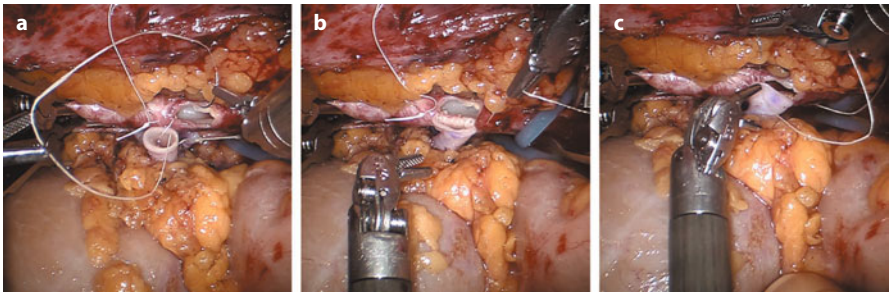

Fig. 22.6 **a** Corner stitch made with 6-0 Gore-Tex. **b** Posterior wall with running suture. **c** Followed with anterior wall running suture

At the end of the procedure the minilaparotomy is closed with running 0 PDS and the two 12-mm port sites are closed laparoscopic visualization with 0 Vicryl suture.

22.3.2 Discussion

In the last four years, we have used this technique and performed more than 80 robotic-assisted kidney transplants in obese recipients. We include any patient with a BMI >30 kg/m^2, without an upper limit. The mean BMI of the group was 45 kg/m^2. We have not observed any SSI within the first 30 post-transplant days. High immunologic risk or multiple previous surgeries were not considered contraindications for the procedure. The only exclusion criteria were severe atherosclerosis in the iliac vessels of the recipient or in the graft vessels of kidney coming from a deceased donor. To evaluate our initial hypothesis of improving wound complications with the robotic approach, we performed a case-control study comparing our first 28 robotic-assisted kidney transplants to a matched retrospective cohort of obese recipients who underwent kidney transplantation

by open technique. We observed no wound complications occurring in the sample of robotic-assisted kidney transplanted obese recipients as compared to 28% in the control group, and up to 40% in previous published studies [9]. In addition to the proven advantages of minimally invasive surgery, such as early mobilization and patient satisfaction, we have observed excellent graft function possibly related to the minimization of wound complications [10].

Based on the experience in our institution, we can state that the robotic-assisted kidney transplantation for obese recipients is a safe and effective procedure. By achieving excellent kidney graft function and minimizing surgical complications this surgical technique gives the opportunity to the disadvantaged group of obese patients with ESRD to have more realistic access to transplantation. A surgeon attempting this procedure requires the expertise in robotic surgery including advanced vascular suture techniques.

22.4 Application in Pancreas Transplantation

Despite the advantages in surgical technique, pancreas transplantation has the highest rate of surgical complications among solid organ transplantation. Therefore, the introduction of innovating surgical techniques to achieve a reduction of post-transplant morbidity in these patients is needed.

Living donor pancreas transplantation is seldom used due to the morbidity of the procedure, some think the increased risk of complications, such as pancreatitis, leak and diabetes due to low islet mass results in excess morbidity to the donor [11]. Distal pancreatectomy in the presence of pathology carries a morbimortality rate, this might be an unacceptable risk for most surgeons to take in healthy individuals. Nevertheless, living donor pancreatectomy has been performed in the past, using open surgical approach in most cases [12], with promising outcomes for the recipient. If we could minimize the morbidity to the donor, it may become a more popular approach to treat diabetes outside the deceased donor list. The only case reported worldwide of robotic distal pancreatectomy and nephrectomy for living donor transplantation was performed in 2006 at the University of Illinois at Chicago.

Nephrectomy was completed first as previously described. Subsequently, the patient required repositioning to a supine position, and the procedure continued laparoscopically in order to takedown the gastrocolic ligament and retract the stomach to ensure a good exposure of the pancreas. The gastroepiploic pedicle was handled carefully to preserve the left gastroepiploic artery as the sole supply to the spleen. The short gastric vessels were spared as well.

The da Vinci® Surgical System was again brought to the field from the patient's head. The splenic artery and vein were isolated and divided close to the hilum in the extrapancreatic portion at the tail of the pancreas. The spleen remained viable after vascular division. The body and tail of the pancreas is mobilized medially to expose the celiac trunk. At the neck of the pancreas, dis-

section of the splenic vein is performed at the confluence with the mesenteric vein. The splenic artery was dissected from the celiac trunk.

The parenchymal transection was performed at the junction between the body and the head of the pancreas with a robotic UltraCision device. After systemic heparinization, the splenic artery was stapled at the take-off with a TA vascular stapler and then sharply divided with a robotic scissor. Finally the splenic vein was divided with a GIA vascular stapler and the pancreas immediately retrieved through the midline incision.

During the recipient's operation, the renal graft was anastomosed to the left external iliac vessels and the pancreas graft to the right external iliac artery and vein. The exocrine secretions were drained to the bladder via pancreaticocystostomy. The allografts became functional immediately on transplantation into the recipient.

The potential postoperative complications for the donor include pancreatitis, pancreatic leak, pseudocyst formation and splenic infarction. But a more devastating long-term complication is the development of diabetes in the donor. In 2005, Tan et al. [11] reported their first initial experience with five hand-assisted laparoscopic donor pancreatectomies. The donor and recipient survival rate was 100% at up to 3 years of follow-up. None of these donors have had complications or required antidiabetic medications. More recent publications acknowledge the risk of diabetes in the donor but support the procedure in selected cases of highly-sensitized recipients, owing to long waiting times for deceased pancreas donors [12].

In reference to the future of minimally invasive pancreas transplantation, Boggi et al. reported the first three whole pancreas transplants performed with the assistance of the da Vinci® Surgical System [3]. The mean warm and cold ischemia times were 30 minutes and 7.3 hours, respectively. Hemorrhage that required intervention occurred in the third pancreas graft; however, it was controlled successfully using the robotic system. None of the recipients needed blood transfusions. Their experience proves the feasibility of robotic-assisted laparoscopic surgery in pancreas transplantation. However, further studies are necessary and larger series for it to become an alternative approach to the conventional open technique.

22.5 Application in Liver Transplantation

Living donation for liver transplantation offers excellent results with minimal complication to the donor. The procedure is complex and results in long incisions and prolonged hospital stay for them. Recently, complete laparoscopic left and right donor hepatectomy have been reported [13, 14]. The goal is to improve recovery and cosmetic results on the donors without compromising on the safety. There are many barriers before the standardization of such procedures but in selected cases, it is a valid and feasible option. Our institution is a major refer-

ral center for robotic liver procedures, such experience in combination with living donation expertise made possible the first robotic right donor hepatectomy.

Our first case was conducted in a 53-year-old healthy man, donating the right lobe to his brother who had hepatocellular carcinoma, which was complicating his hepatitis C cirrhosis [4]. The entire procedure was performed using the da Vinci® Robotic Surgical System. After the laparoscopic trocars were placed and the robotic system was installed, a cholecystectomy was performed. The hepatic artery and the right portal vein were dissected free, followed by isolation and transection of the right hepatic duct. The right lobe was completely mobilized exposing the retrohepatic cava upward from the caudate lobe. Consequently, parenchyma transection was performed with the robotic Harmonic scalpel while preserving vascularization of the lobe. The vascular transsection was performed using Endo-GIA™ vascular stapler, first to the right hepatic artery, then the right portal vein and lastly the right hepatic vein. The graft was rapidly removed through a lower abdominal incision. The operative time was approximately 8 hours, with an estimated blood loss of 350 mL and no transfusion requirements. His postoperative course was uneventful and he was discharged home on the fifth postoperative day.

Besides facilitating the vascular and biliary dissection, the robotic technology also offers the possibility of identifying biliary structures using Indocyanine Green, minimizing dissection around the biliary tree, and thus reducing the chances of ischemic injury of the biliary anastomosis [13]. The lower incision provides better pulmonary care and minimizes analgesic requirements, thus facilitating early mobilization. This incision decreases the pain and risk of pulmonary complications associated with an upper midline incision. However, living donor hepatectomy should only be undertaken by experienced surgical teams, due to the significant morbidity and mortality associated to this procedure for donor and recipient.

References

1. Giulianotti P, Gorodner V, Sbrana F et al (2010) Robotic transabdominal kidney transplantation in a morbidly obese patient. Am J Transplant 10:1478–1478
2. Boggi U, Vistoli F, Signori S et al (2011) Robotic renal transplantation: first European case. Transpl Int 24:213–218
3. Boggi U, Signori S, Vistoli F et al (2012) Laparoscopic robot-assisted pancreas transplantation: first world experience. Transplantation 93:201–206
4. Giulianotti PC, Tzevetanov I, Jeon H et al (2012) Robot-assisted right lobe donor hepatectomy. Transpl Int 25:e5–9
5. Horgan S, Vanuno D, Sileri P et al (2002) Robotic-assisted laparoscopic donor nephrectomy for kidney transplantation. Transplantation 73:1474–1479
6. Kay MD, Brook N, Kaushir M et al (2006) Comparison of right and left laparoscopic live donor nephrectomy. BJU Int 98:843–844
7. Lin CHSteinberg AP, Ramani AP et al (2004) Laparoscopic live donor nephrectomy in the presence of circumaortic or retroaortic left renal vein. J Urol 171:44–46

8. Aalten J, Christriaans MH, de Filter H et al (2006) The influence of obesity on short- and long-term graft and patient survival after renal transplantation. Transpl Int 19:901–907
9. Lynch RJ, Ranney DN, Shijine C et al (2009) Obesity, surgical site infection, and outcome following renal transplantation. Ann Surg 250:1014–1020
10. Oberholzer J, Giulianotti P, Danielson KK et al (2013) Minimally invasive robotic kidney transplantation for obese patients previously denied access to transplantation. Am J Transplant 13:721–728
11. Tan M, Kandaswamy R, Sutherland DE, Gruessner RW (2005) Laparoscopic donor distal pancreatectomy for living donor pancreas and pancreas-kidney transplantation. Am J Transplant 5:1966–1970
12. Sutherland DE, Radosevich D, Gruessner RW et al (2012) Pushing the envelope: living donor pancreas transplantation. Curr Opin Organ Transplant 17:106–115
13. Rotellar F, Pardo F, Benito A (2013) Totally laparoscopic right-lobe hepatectomy for adult living donor liver transplantation: useful strategies to enhance safety. Am J Transplant 13:3269–3273
14. Samstein B, Cherqui D, Rotellar F (2013) Totally laparoscopic full left hepatectomy for living donor liver transplantation in adolescents and adults. Am J Transplant 13:2462–2456